

# REVIEWS OF MODERN PHYSICS

VOLUME 13

APRIL, 1941

NUMBER 2

## Electronic Spectra of Polyatomic Molecules

H. SPONER, *Duke University, Durham, North Carolina*

AND

E. TELLER, *The George Washington University, Washington, D. C.*

### TABLE OF CONTENTS

	PAGE
Introduction . . . . .	76
<b>Part I. Theoretical Considerations</b>	
a. Electronic States and Selection Rules . . . . .	77
<i>Linear Molecules</i> . . . . .	77
<i>Other Axial Molecules</i> . . . . .	80
<i>Cubic Molecules</i> . . . . .	82
b. Vibrations and Franck-Condon Principle . . . . .	85
c. Coupling between Vibration and Electronic Motion . . . . .	90
<i>Splitting of Degenerate Electronic States</i> . . . . .	90
<i>Violation of Selection Rules</i> . . . . .	96
d. Anharmonicity and Predissociation . . . . .	99
e. Rotational Structure . . . . .	102
<i>Linear Molecules</i> . . . . .	103
<i>Spherical Top Molecules</i> . . . . .	103
<i>Symmetrical Top Molecules</i> . . . . .	104
<i>Asymmetrical Top Molecules</i> . . . . .	105
f. Isotopic Effect . . . . .	105
<b>Part II. Applications to Observed Spectra</b>	
a. Linear Molecules . . . . .	106
<i>Mercury Halides</i> . . . . .	106
<i>C<sub>2</sub>N<sub>2</sub></i> . . . . .	108
<i>N<sub>2</sub>O</i> . . . . .	109
b. Tetrahedral Molecules . . . . .	110
<i>OsO<sub>4</sub>, RuO<sub>4</sub></i> . . . . .	110
c. Methane Derivatives . . . . .	110
<i>CH<sub>3</sub>I</i> . . . . .	110
<i>H<sub>2</sub>CO</i> . . . . .	113
<i>CH<sub>3</sub>NH<sub>2</sub></i> . . . . .	114

<b>d. Benzene and Derivatives</b> .....	115
<i>The Near Ultraviolet Absorption System of Benzene</i> .....	115
<i>The Near Ultraviolet Absorption System of Substituted Benzenes</i> .....	118
<i>Other Absorption Systems of Benzene in the Farther Ultraviolet</i> .....	122
<i>Furan</i> .....	123
<b>Appendix; Tables A-I</b> .....	124
<b>Literature References to Appendix, Tables A-I</b> .....	166

### Introduction

IN recent years the experimental study of electronic spectra of polyatomic molecules has attracted increasing attention. But in spite of much work done, spectroscopy of polyatomic molecules is still in the exploring state. The reasons that band spectra of polyatomic molecules have not yet proved as valuable in the study of molecular structural problems as those of diatomic molecules are well known. The variety of vibrational and rotational frequencies associated with electronic jumps is greater for polyatomic than for diatomic molecules. Furthermore, the anharmonicity of the vibrations does not produce a simple convergence of the bands; it can change their vibrational structure in complicated ways, especially at large amplitudes. Also, vibrations can interact with rotation in various ways, so that distinction between vibrational and rotational structure of the spectrum becomes difficult. Finally, a polyatomic molecule possesses more possibilities of dissociation than a diatomic one and many of its excited states will be unstable. Instability results in continuous or at least diffuse band spectra, which are less valuable for an analysis than discrete spectra. The purpose of the present article is to discuss the theoretical basis for an analysis of polyatomic spectra. Since a different general appearance of the spectrum is associated with different electronic states, a complete analysis should explain not only the structure and appearance of the bands but should also

give information about the atomic configurations and symmetry properties of the electronic states involved. Consequently a brief treatment of these states will be given here; we shall not attempt, however, to present the theory of electronic structure of molecules in a systematic way since the extensive work<sup>1</sup> in this field would necessitate a separate article. We shall also restrict ourselves almost exclusively to gas molecules in order to avoid complications arising from intermolecular forces.

In the first part of this paper we shall discuss general properties of the electronic states. Particular emphasis will be put on symmetry properties and selection rules. Next, the motions of heavier masses within the molecule will be treated. As the most striking structure of a polyatomic spectrum is caused by the vibrations, they will receive special consideration. The rotational structure of polyatomic spectra has so far proved to be of minor importance, in most cases on account of insufficient resolution, but promising progress has been made recently (p. 102).

In the second part of this article the theory will be applied to typical examples.

<sup>1</sup> See especially papers by E. Hückel, F. Hund, J. E. Lennard-Jones, R. S. Mulliken, L. Pauling, J. C. Slater. For references compare E. Hückel, *Zeits. f. Elektrochemie* **43**, 752, 827 (1937); R. S. Mulliken, Series on "Electronic Structures of Polyatomic Molecules" in *Phys. Rev.* and *J. Chem. Phys.* (1932-1935); L. Pauling, *Nature of the Chemical Bond* (Cornell University Press, 1940).

### Part I. Theoretical Considerations

#### a. Electronic States and Selection Rules

The first general classification of electronic states of polyatomic molecules concerns their multiplicity and leads, in exact analogy to atomic spectra, to singlet, doublet, triplet terms, etc. In analogy to spectra of atoms and diatomic molecules the multiplicity is indicated in the term symbol by a superscript in the left upper corner. As in the case of atoms we have, in first approximation, the selection rule that only states of the same multiplicity combine with each other. Intercombinations may occur with appreciable intensity only if the molecule contains some heavier atoms. Most molecules which are chemically stable have singlet terms in their normal states. Hence we expect in absorption and fluorescence mainly the occurrence of singlet terms.

Further classification of electronic states is based upon symmetry properties. Though the electrons in a polyatomic molecule do not move in a spherical field as in an atom, or in a cylindrical field as in a diatomic molecule, the potential field may still be left unchanged during certain rotations and reflections characteristic of the molecular symmetry. The electronic wave functions will transform according to definite laws when such symmetry operations are performed. It is impossible to obtain exact expressions for the electronic eigenfunctions; the mathematical difficulties are too great. The only exact statements concern symmetry properties or are based upon such. The most important results are the selection rules. In order that electronic terms combine, they must satisfy certain transformation properties; otherwise the relevant matrix elements vanish.

Symmetrical configuration of nuclei is, of course, required for the classification. In the molecules this is realized in general only for equilibrium positions; small displacements usually destroy the symmetry.<sup>2</sup> Symmetry properties must be discussed separately for molecules belonging to different symmetry groups. In

<sup>2</sup> It is only for diatomic molecules that the vibration does not disturb any symmetry: for triatomic molecules at least one plane of symmetry (going through the three nuclei) is preserved during oscillations.

the following part of this section a brief survey is given of the rather extended system of molecular symmetries and corresponding electronic terms.

#### Linear Molecules

With all atoms in a straight line the same classification of electronic terms is applicable as in the case of diatomic molecules. The selection rules are also unaltered. Two symmetry classes have to be distinguished, which comprise molecules with a center of symmetry and those with no center of symmetry. The symbol for the first class is  $D_{\infty h}$ , for the second  $C_{\infty v}$ .<sup>3</sup> The notations for the electronic terms together with their behavior with respect to symmetry operations are summarized in Table I.<sup>4</sup> We first consider the table without the two rows added at the bottom. The first column contains the electronic term symbols of molecules belonging to symmetry class  $D_{\infty h}$ . The  $\Sigma$  terms are non-

TABLE I. Symmetry types of electronic terms of linear molecules.

$D_{\infty h}$	$C_{\infty v}$		$C_{\infty}$	$\sigma_v$	$C_2$	$\sigma_h$	$i$
$\Sigma^+_g$	$\Sigma^+$		+	+	+	+	+
$\Sigma^-_g$	$\Sigma^-$	$R_z$	+	-	-	+	+
$\Sigma^+_u$	$\Sigma^+$	$T_z$	+	+	-	-	-
$\Sigma^-_u$	$\Sigma^-$		+	-	+	-	-
$\Pi_g$	$\Pi$	$R_x R_y$	$e^{\pm i\varphi}$	*	*	-	+
$\Pi_u$	$\Pi$	$T_x T_y$	$e^{\mp i\varphi}$	*	*	+	-
$\Delta_g$	$\Delta$		$e^{\pm 2i\varphi}$	*	*	+	+
$\Delta_u$	$\Delta$		$e^{\mp 2i\varphi}$	*	*	-	-
		$D_{\infty h}$	•	•	•	•	•
		$C_{\infty v}$	•	•			

<sup>3</sup>  $C_{\infty}$  signifies the existence of a symmetry axis with the property that any rotation (i.e., infinitely many rotations) about this axis leaves the molecule unchanged. A linear molecule remains also unchanged by reflection in a plane containing the symmetry axis and this is indicated by the subscript  $v$ . If the molecule has in addition a center of symmetry, then twofold axes through the center occur which are perpendicular to the original axis ( $D_{\infty}$ ). At the same time a plane of symmetry passes through the center in a direction perpendicular to the infinite-fold axis ( $D_{\infty h}$ ).

<sup>4</sup> This table and some of the next ones are similar to those given in G. Placzek, *Handbuch der Radiologie*, Vol. 6, No. 2 (1934), pp. 293-297.

degenerate, all other terms are twofold degenerate. It is well known from the theory of diatomic spectra that  $\Pi$  and  $\Delta$  terms have angular momenta about the figure axis of amount  $h/2\pi$  and  $2 \times h/2\pi$ , the degeneracy arising from the two possible directions of rotation. Electronic terms with higher momenta  $3 \times h/2\pi$  and  $4 \times h/2\pi$  are not included in Table I; they are denoted by  $\Phi$  and  $\Gamma$  terms.<sup>5</sup> The subscripts  $g$  and  $u$  refer to symmetrical and antisymmetrical behavior of the electronic eigenfunctions with respect to the center of symmetry. The second column gives the corresponding notations of the symmetry group  $C_{\infty v}$ . Since in this case we have no center of symmetry the subscripts  $g$  and  $u$  become meaningless. Thus in this column every symbol occurs twice. When, in a molecule with center of symmetry, this center is destroyed by some perturbation (for instance by vibration), then its electronic states represented in column 1 transform into the corresponding ones in column 2. In the third column is indicated when an electronic term has the same symmetry properties as a translation ( $T$ ) or a rotation ( $R$ ). We have chosen the  $z$  axis to coincide with the figure axis. Thus  $T_z$  means a translation along the axis joining the nuclei and  $R_z$  a rotation about the same axis. The following columns explain the behavior of the electronic eigenfunctions with respect to the various symmetry operations.  $C_\infty$  refers to rotations about the figure axis. The  $+$  signs in this column indicate that the  $\Sigma$  terms remain unchanged during such rotations. The twofold degenerate electronic wave functions with momenta  $\Lambda h/2\pi$  will transform like  $e^{+i\Lambda\varphi}$  and  $e^{-i\Lambda\varphi}$ , respectively, as shown in column 4.  $\sigma_v$  symbolizes planes through the figure axis. Here  $+$  and  $-$  signs denote symmetrical and antisymmetrical behavior with regard to reflections in these planes. They correspond to  $\Sigma^+$  and  $\Sigma^-$  terms. The  $\Pi$  and  $\Delta$  functions transform into their conjugate complex values or into multiples thereof, which is indicated by an asterisk. The last column exhibits the behavior of the eigenfunctions with respect to an inversion through the center.  $+$  and  $-$  signs

<sup>5</sup>  $\Phi$  and  $\Gamma$  terms have not yet been observed with certainty.

correspond to the subscripts  $g$  and  $u$  of the first column. The sixth and seventh column refer to rotations by  $180^\circ$  about twofold axes through the center perpendicular to the figure axis and to a reflection in the plane through the center and perpendicular to the figure axis. The behavior with regard to  $C_2$  and  $\sigma_h$  is already determined by the transformation properties described in the other columns. Columns 6 and 7 have been included here only for the sake of completeness. It can be checked easily that, for instance, the translation  $T_z$  remains unchanged during rotations about the figure axis  $C_\infty$  and during reflections in the planes  $\sigma_v$ , and changes its sign, i.e., reverses the direction, during the operations connected with the elements  $C_2$ ,  $\sigma_h$  and  $i$ . A somewhat more complicated situation prevails for  $T_x$  and  $T_y$  which may be transformed into each other by operations corresponding to the symmetry elements  $C_\infty$ ,  $\sigma_v$  and  $C_2$ . The transformation properties given in the table refer to the behavior of the linear combinations  $T_x + iT_y$  and  $T_x - iT_y$ . It can also be seen that  $R_z$  remains unchanged when the system is rotated about the figure axis and changes to the opposite rotation when reflected in  $\sigma_v$ .

Some of the transformation properties given in Table I are significant only for symmetry group  $D_{\infty h}$  as the corresponding symmetry elements are absent in  $C_{\infty v}$ . At the bottom of the table is indicated which symmetry elements occur in the two groups, respectively. The dots in the first of the two added rows signify that all symmetry elements are present in  $D_{\infty h}$  while the dots in the second row show that in  $C_{\infty v}$  only  $C_\infty$  and  $\sigma_v$  occur. Thus, when the table is used for  $C_{\infty v}$  the last three columns of the upper part have to be omitted.

By means of Table I we can also discover the transformation properties resulting when some symmetry elements are destroyed by atomic displacements. Removal of the symmetry center has already been treated. As another example may be considered the case where the infinite-fold axis is destroyed while one of the planes  $\sigma_v$  is preserved. The terms retain then their character of being symmetrical and antisymmetrical with respect to  $\sigma_v$  wherever  $+$  and  $-$  signs are found in the column  $\sigma_v$ . The degenerate



TABLE II. *Direct products for  $D_{\infty h}$ .*

$\Sigma^+_g$	$\Sigma^-_g$	$\Sigma^+_u$	$\Sigma^-_u$	$\Pi_g$	$\Pi_u$	$\Delta_g$	$\Delta_u$	
$\Sigma^+_g$	$\Sigma^-_g$	$(\Sigma^+_u)$	$\Sigma^-_u$	$\Pi_g$	$(\Pi_u)$	$\Delta_g$	$\Delta_u$	$\Sigma^+_g$
	$\Sigma^+_g$	$\Sigma^-_u$	$(\Sigma^+_u)$	$\Pi_g$	$(\Pi_u)$	$\Delta_g$	$\Delta_u$	$\Sigma^-_g$
		$\Sigma^+_g$	$\Sigma^-_g$	$(\Pi_u)$	$\Pi_g$	$\Delta_u$	$\Delta_g$	$\Sigma^+_u$
			$\Sigma^+_g$	$(\Pi_u)$	$\Pi_g$	$\Delta_u$	$\Delta_g$	$\Sigma^-_u$
				$\Sigma^+_g, \Sigma^-_g,$ $\Delta_g$	$(\Sigma^+_u), \Sigma^-_u,$ $\Delta_u$	$\Pi_g, \Phi_g$	$(\Pi_u), \Phi_u$	$\Pi_g$
					$\Sigma^+_g, \Sigma^-_g,$ $\Delta_g$	$(\Pi_u), \Phi_u$	$\Pi_g, \Phi_g$	$\Pi_u$
						$\Sigma^+_g, \Sigma^-_g,$ $\Gamma_g$	$(\Sigma^+_u), \Sigma^-_u,$ $\Gamma_u$	$\Delta_g$
							$\Sigma^+_g, \Sigma^-_g,$ $\Gamma_g$	$\Delta_u$

terms will be split into a symmetrical and an antisymmetrical state.

According to group theoretical rules<sup>6</sup> the symbols for the electronic terms and the transformation properties designated by them can be multiplied with each other. The process is called formation of the direct product. The result of this multiplication is again a term symbol, or when two degenerate terms are multiplied, several term symbols. The direct products of the electronic terms of linear molecules are listed in Table II. The term symbols represent the direct product of the term on top of the column and at the end of the row. Thus,  $\Sigma^-_u \times \Delta_g$  gives  $\Delta_u$  and  $\Pi_g \times \Delta_u$  gives  $\Pi_u$  and  $\Phi_u$ . Table II applies in the form presented to group  $D_{\infty h}$ . The direct products for  $C_{\infty v}$  can be readily obtained by omitting the subscripts  $g$  and  $u$ . Table II will be useful in many ways, for example for the derivation of selection rules.

Electronic transition probabilities are determined by the matrix elements of the dipole moment  $\int \psi'^*_{e1} M \psi''_{e1} d\tau_{e1}$ . Here  $\psi'_{e1}$  and  $\psi''_{e1}$  are the electronic eigenfunctions in the upper and lower states; the asterisk ( $\psi'^*$ ) indicates the conjugate complex value.  $M$  is the dipole moment of the system of nuclei and electrons for a definite electronic configuration. The integration must be carried out over all configurations of the electrons (symbolically indicated by the volume

element  $d\tau_{e1}$ ). The nuclei are held in fixed positions during the integration. For our present purpose this configuration is symmetrical, more specifically it is the equilibrium position of the nuclei. Now it can be shown that the integral vanishes if the integrand transforms in a non-totally symmetrical way. As an illustration the proof will be indicated for antisymmetrical integrands. The only effect which symmetry operations can have on the integration is to change the order of integration, which should not affect the result. Now if, for instance, a symmetry operation changes the sign of the integrand, it also changes the sign of the integral and since according to the above argument, it must at the same time leave the integral unaltered, the only conclusion left is that the integral vanishes. A general group theoretical argument shows that  $\int \psi'^*_{e1} M \psi''_{e1} d\tau_{e1}$  can be different from zero only if the direct product of the transformation properties of the separate factors contains a totally symmetrical term (i.e., one that remains unchanged during all symmetry operations). One can prove moreover that the above condition is equivalent to the requirement that the direct product of the term symbols belonging to  $\psi'_{e1}$  and  $\psi''_{e1}$  should contain a term with the transformation properties of  $M$ . The latter transforms in the same way as a translation. Therefore the following general statement can be made: *A combination between two states is allowed if their direct product contains a term which transforms like one of the translations  $T_x$ ,  $T_y$  or  $T_z$ . The direction of this translation*

<sup>6</sup> In this article merely the results of group theory are used. For derivations and detailed discussions see E. Wigner, *Gruppentheorie* (Vieweg und Sohn, Braunschweig, 1931).

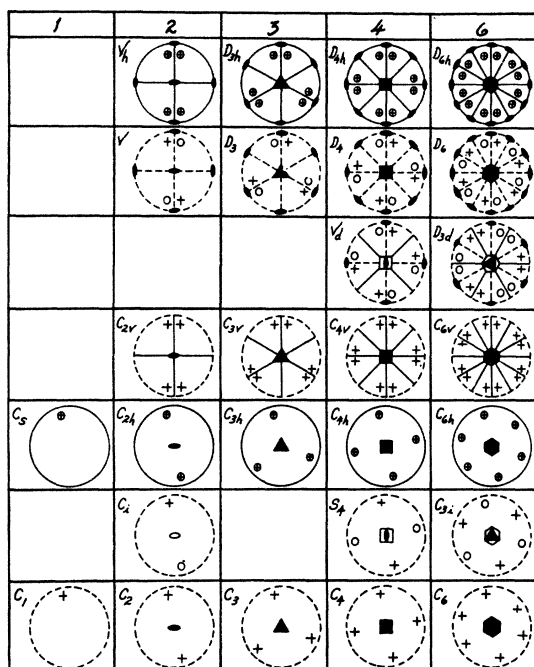


FIG. 1. Stereographic projections of axial symmetry classes.

determines the direction of the dipole moment connected with the transition (transition moment). Thus  $\Sigma^+_g$  and  $\Sigma^+_u$  combine with each other since their product  $\Sigma^+_u$  transforms like  $T_z$  according to Table I. The transition moment lies in the  $z$  axis and gives rise to parallel bands.  $\Pi_u$  and  $\Delta_g$  combine also and give rise to perpendicular bands because the direct product contains  $\Pi_u$  which transforms like  $T_x, T_y$ . On the other hand,  $\Sigma^+_u$  and  $\Delta_g$  obviously do not combine. To facilitate the use of Table II those symbols appear in parentheses which correspond to allowed transitions.

When trying to find the selection rules for  $C_{\infty v}$  from Table II we encounter an ambiguity since the same symbol, for instance  $\Sigma^+$  is obtained from  $\Sigma^+_g$  and  $\Sigma^+_u$ . In such cases the transition will be allowed whenever there is at least one way in which Table II allows it. For instance  $\Sigma^+$  will combine with  $\Sigma^+$  because Table II allows the combination of  $\Sigma^+_g$  with  $\Sigma^+_u$ . On the other hand,  $\Sigma^+$  and  $\Sigma^-$  do not combine because none of the transitions  $\Sigma^+_g \rightarrow \Sigma^-_g$ ,  $\Sigma^+_g \rightarrow \Sigma^-_u$ ,  $\Sigma^+_u \rightarrow \Sigma^-_g$  and  $\Sigma^+_u \rightarrow \Sigma^-_u$  is allowed according to Table II.

### Other Axial Molecules

Under this heading molecules will be discussed which possess at least one axis that remains unchanged during all symmetry operations. Linear molecules have already been discussed and are omitted now. The symmetry classes in question are represented in Fig. 1.<sup>7</sup> It exhibits stereographic projections on a plane perpendicular to the figure axis. If the symmetry of the molecule includes reflections across a plane perpendicular to the figure axis, then this plane will coincide with the plane of projection. Likewise, if a center of symmetry exists, the plane of projection will contain this center. A cross represents the position of an arbitrary point lying outside of all symmetry elements. Further crosses stand for other points obtained from the first one by rotation about the figure axis or reflections across planes containing the figure axis. Thus all crosses lie in the same level above the plane of projection. Circles represent points below the plane of projection, their distance from this plane being the same as that of the crosses. The circles are obtained from the crosses by reflections across the plane of projection, by inversion through the center or by rotary reflection. The positions of crosses and circles determine the symmetry group. In addition, Fig. 1 shows the different symmetry elements of each group. They are described as follows:

Full and dotted large circles, respectively, represent that the system has one or no plane of symmetry in the plane of projection.

Full lines show intersections of vertical symmetry planes with plane of projection.

Dotted lines indicate twofold axes of symmetry  $C$  in plane of projection.

Solid ellipses, triangles, squares and hexagons are end-points of twofold, threefold, fourfold and sixfold axes, respectively; such signs in center of figures represent  $p$ -fold axes  $C_p$  in  $z$  direction, i.e.,  $\perp$  to plane of projection. The ellipses at the end of full lines in plane of projection indicate that intersection of  $\sigma_v$  with  $\sigma_h$  is also a  $C_2$  axis.

Open ellipses, squares and hexagons are end points of twofold, fourfold and sixfold axes of rotary reflection  $S_p$ , respectively. (In a rotary reflection one has to rotate the system about an axis and at the same time reflect across a plane  $\perp$  to that axis. A twofold axis of rotary reflection is identical with a center of symmetry  $i$ .)

<sup>7</sup> This figure has been taken, with slight modifications, from K. W. F. Kohlrusch, *Der Smekal-Raman-Effekt* (Julius Springer, Berlin, 1938), p. 42.

The symbols of the symmetry groups in Fig. 1 are those introduced by A. Schoenflies. Symbols more closely related to actual symmetry properties have been proposed by C. Hermann and Ch. Mauguin. Since these symbols are frequently used, we include a list of the latter with the corresponding Schoenflies symbols below them:<sup>8</sup>

$\begin{vmatrix} 1 \\ C_1 \end{vmatrix}$	$\begin{vmatrix} \bar{1} \\ C_i \end{vmatrix}$	$\begin{vmatrix} m \\ C_s \end{vmatrix}$	$\begin{vmatrix} 2 \\ C_2 \end{vmatrix}$	$\begin{vmatrix} 2/m \\ C_{2h} \end{vmatrix}$	$\begin{vmatrix} 2 & m & m \\ C_{2v} \end{vmatrix}$	$\begin{vmatrix} 2 & 2 & 2 \\ V \end{vmatrix}$
$\begin{vmatrix} 2/m & 2/m & 2/m \\ V_h \end{vmatrix}$	$\begin{vmatrix} \bar{4} \\ S_4 \end{vmatrix}$	$\begin{vmatrix} 4 \\ C_4 \end{vmatrix}$	$\begin{vmatrix} \bar{4} & 2 & m \\ V_d \end{vmatrix}$	$\begin{vmatrix} 4 & m & m \\ C_{4v} \end{vmatrix}$		
$\begin{vmatrix} 4 & 2 & 2 \\ D_4 \end{vmatrix}$	$\begin{vmatrix} 4/m & 2/m & 2/m \\ D_{4h} \end{vmatrix}$	$\begin{vmatrix} 3 \\ C_3 \end{vmatrix}$	$\begin{vmatrix} \bar{3} \\ C_{3i} \end{vmatrix}$	$\begin{vmatrix} 3 & m \\ C_{3v} \end{vmatrix}$		
$\begin{vmatrix} 3 & 2 \\ D_3 \end{vmatrix}$	$\begin{vmatrix} \bar{3} & 2/m \\ D_{3d} \end{vmatrix}$	$\begin{vmatrix} \bar{6} \\ C_{3h} \end{vmatrix}$	$\begin{vmatrix} 6 \\ C_6 \end{vmatrix}$	$\begin{vmatrix} 6/m \\ C_{6h} \end{vmatrix}$	$\begin{vmatrix} \bar{6} & 2 & m \\ D_{3h} \end{vmatrix}$	
$\begin{vmatrix} 6 & m & m \\ C_{6v} \end{vmatrix}$	$\begin{vmatrix} 6 & 2 & 2 \\ D_6 \end{vmatrix}$	$\begin{vmatrix} 6/m & 2/m & 2/m \\ D_{6h} \end{vmatrix}$	In discus-			

sions of molecular structure the Schoenflies symbols are generally used.<sup>9</sup>

Table III contains the symbols and transformation properties of electronic terms belonging to the symmetry groups of columns 1 and 2 in Fig. 1. These groups are members of the triclinic ( $C_i$  and  $C_1$ ), monoclinic ( $C_{2h}$ ,  $C_2$  and  $C_s$ ) and rhombic ( $V_h$ ,  $V$  and  $C_{2v}$ ) symmetry classes. In all three classes several axes are found which remain unchanged during all symmetry operations. In the triclinic system any axis has this property, in the monoclinic system the figure axis and any axis perpendicular to it, and in the rhombic system three mutually perpendicular axes have this characteristic. The choice of the principal axis is arbitrary in the triclinic and rhombic systems; in the first any axis can be chosen, in the second one of the three mutually perpendicular axes. It is evident that in the monoclinic system the principal axis has to be the twofold axis of symmetry or, in the absence

of such, an axis perpendicular to the plane of reflection. In Tables III, V and VII the principal axis lies in the  $z$  direction. The general scheme of these tables is similar to that of Table I. The meaning of the symbols for the different groups can be found with the help of Fig. 1.  $C_2^z$  and  $C_2^y$  are twofold axes in the  $z$  and  $y$  directions;  $\sigma_h$  and  $\sigma_v^y$  are planes of reflection perpendicular to these directions;  $i$  denotes the center of symmetry. All electronic terms, denoted by  $A$  and  $B$ , are non-degenerate. They are symmetrical and anti-symmetrical with respect to the different symmetry elements, as is indicated on the right side of Table III.

The symbol  $A$  in Table III is used for terms symmetrical to all twofold axes,  $B$  for the remaining terms.  $g$  and  $u$  refer to symmetric and anti-symmetric behavior with regard to the center, primes and double primes with regard to  $\sigma_h$ . The subscripts 1 and 2 differentiate between the remaining terms. Column 9 and the lower right-hand part of Table III have the same significance as the corresponding parts of Table I. Only for the group  $V_h$  are all last five columns of Table III significant. For the group  $C_{2h}$ , for instance, only the columns with headings  $C_2^z$ ,  $\sigma_h$  and  $i$  must be considered, as is indicated by the dots in the  $C_{2h}$  row of the lower right-hand part of the table.

Table III can be used to find out what becomes of an electronic term if the symmetry is reduced. Thus, if in  $V_h$  the symmetries of reflection are destroyed, the group  $V$  is obtained and the term

TABLE III. Types of electronic terms for triclinic, monoclinic and rhombic symmetries.

$V_h$	$V$	$C_{2v}$	$C_{2h}$	$C_2$	$C_s$	$C_i$	$C_1$	$C_2^z$	$C_2^y$	$\sigma_v^y$	$\sigma_h$	$i$
$A_{1g}$	$A_1$	$A_1$	$A_g$	$A$	$A'$	$A_g$	$A$	+	+	+	+	+
$A_{1u}$	$A_1$	$A_2$	$A_u$	$A$	$A''$	$A_u$	$A$	+	+	-	-	-
$B_{1g}$	$B_1$	$A_2$	$A_g$	$A$	$A'$	$A_g$	$A$	$R_z$	+	-	-	+
$B_{1u}$	$B_1$	$A_1$	$A_u$	$A$	$A''$	$A_u$	$A$	$T_z$	+	+	+	-
$B_{2g}$	$B_2$	$B_1$	$B_g$	$B$	$A''$	$A_g$	$A$	$R_y$	-	+	+	-
$B_{2u}$	$B_2$	$B_2$	$B_u$	$B$	$A'$	$A_u$	$A$	$T_y$	-	+	-	+
$B_{3g}$	$B_3$	$B_2$	$B_g$	$B$	$A''$	$A_g$	$A$	$R_x$	-	-	-	+
$B_{3u}$	$B_3$	$B_1$	$B_u$	$B$	$A'$	$A_u$	$A$	$T_x$	-	-	+	-
								$V_h$	•	•	•	•
								$V$	•	•		
								$C_{2v}$	•			
								$C_{2h}$	•		•	•
								$C_2$	•			
								$C_s$			•	
								$C_i$				•
								$C_1$				

<sup>8</sup> In the Hermann-Mauguin symbols 1, 2, 3 ... stand for one-, two-, threefold symmetry axes; a bar indicates a rotary reflection axis;  $m$  stands for a plane of symmetry and a line separating  $m$  from the symbol of an axis shows that the two elements are perpendicular to each other.

<sup>9</sup> R. S. Mulliken, Phys. Rev. **43**, 279 (1933); G. Placzek, *Handbuch der Radiologie*, Vol. 6, No. 2 (1934), p. 205; J. E. Rosenthal and G. M. Murphy, Rev. Mod. Phys. **8**, 317 (1936); L. Tisza, Zeits. f. Physik **82**, 48 (1933).

TABLE IV. *Direct products for  $V_h$ .*

$A_{1g}$	$A_{1u}$	$B_{1g}$	$B_{1u}$	$B_{2g}$	$B_{2u}$	$B_{3g}$	$B_{3u}$	
$A_{1g}$	$A_{1u}$	$B_{1g}$	<b><math>B_{1u}</math></b>	$B_{2g}$	<b><math>B_{2u}</math></b>	$B_{3g}$	<b><math>B_{3u}</math></b>	$A_{1g}$
	$A_{1g}$	<b><math>B_{1u}</math></b>	$B_{1g}$	<b><math>B_{2u}</math></b>	$B_{2g}$	<b><math>B_{3u}</math></b>	$B_{3g}$	$A_{1u}$
		$A_{1g}$	$A_{1u}$	$B_{3g}$	<b><math>B_{3u}</math></b>	$B_{2g}$	<b><math>B_{2u}</math></b>	$B_{1g}$
			$A_{1g}$	<b><math>B_{3u}</math></b>	$B_{3g}$	<b><math>B_{2u}</math></b>	$B_{2g}$	$B_{1u}$
				$A_{1g}$	$A_{1u}$	$B_{1g}$	<b><math>B_{1u}</math></b>	$B_{2g}$
					$A_{1g}$	<b><math>B_{1u}</math></b>	$B_{1g}$	$B_{2u}$
						$A_{1g}$	$A_{1u}$	$B_{3g}$
							$A_{1g}$	$B_{3u}$

$B_{3g}$ , for instance, is reduced to  $B_3$ . Correlations between the terms of Tables I and III are given by Mulliken.<sup>10</sup>

Table IV gives the direct products for the group  $V_h$ . The arrangement is the same as in Table II. Transition between two electronic states is permitted if the symbol found in the intersecting square of the corresponding row and column appears in heavy print. Table IV can also be used for the other groups represented in Table III. The term symbols for  $V_h$  have then to be replaced by symbols which appear in the same row in Table III. Transitions in groups different from  $V_h$  will be permitted if there is at least one symbol in heavy print in a column and row of the terms in question.

In Table V are collected the electronic terms for the axial groups containing a fourfold axis. The arrangement is the same as in Tables I and III. The states  $A$  and  $B$  are again non-degenerate.  $A$  is symmetric and  $B$  antisymmetric to rotation by  $90^\circ$  about the fourfold axis  $C_4$ . The terms  $E$  are twofold degenerate. They are somewhat analogous to the  $\Pi$  terms of Table I as shown by the transformation properties under  $C_4$ ,  $\sigma_v$  and  $C_2$ .  $g$  and  $u$  have the same significance as before. 1 and 2 mean symmetric and antisymmetric with regard to the twofold axis  $C_2$ . In the absence of this axis, 1 and 2 mean symmetric and antisymmetric to  $\sigma_v$  or  $S_4$ .

Table VI gives the direct products for  $D_{4h}$  and has to be used for this and the other groups of Table V in a fashion similar to that of Tables I and III.

Table VII contains the electronic terms for axial systems with a trigonal axis. The term

symbols are again in analogy to those in previous tables.  $A$  and  $B$  mean symmetric and antisymmetric with respect to the twofold axis  $C_2$ . The superscripts  $+$  and  $-$  sometimes attached to the symbols  $E$  signify symmetric and antisymmetric to the same axis. If the group has both the elements  $C_2$  and  $C_3$ , this corresponds to an axis  $C_6$ . The transformation properties of  $E^+$  with respect to rotations about  $C_6$  can be represented by  $e^{\pm 2i\varphi}$ , those of  $E^-$  by  $e^{\pm i\varphi}$ . Thus,  $E^+$  and  $E^-$  are analogous to the  $\Delta$  and  $\Pi$  terms of Table I.

In Table VIII the direct products for  $D_{6h}$  are collected. Their use is as described before.

Tables III, V and VII include all non-linear axial groups encountered in the actual molecules. They are the only axial groups which occur in crystallography. Other groups, for instance those with a fivefold axis, are therefore not discussed.

### Cubic Molecules

Molecules of cubic symmetry possess at least four threefold symmetry axes which can be visualized as pointing from the center of a regular tetrahedron towards its corners. The symmetry groups belonging to the cubic system are illustrated in Fig. 2. This figure is similar to

TABLE V. *Types of electronic terms for tetragonal symmetry.*

$D_{4h}$	$D_4$	$C_{4v}$	$C_{4h}$	$C_4$	$V_d$	$S_4$		$C_4$	$S_4$	$\sigma_v$	$C_2$	$i$
$A_{1g}$	$A_1$	$A_1$	$A_g$	$A$	$A_1$	$A$		+	+	+	+	+
$A_{1u}$	$A_1$	$A_2$	$A_u$	$A$	$B_1$	$B$		+	-	-	+	-
$A_{2g}$	$A_2$	$A_2$	$A_g$	$A$	$A_2$	$A$	$R_z$	+	+	-	-	+
$A_{2u}$	$A_2$	$A_1$	$A_u$	$A$	$B_2$	$B$	$T_z$	+	-	+	-	-
$B_{1g}$	$B_1$	$B_1$	$B_g$	$B$	$B_1$	$B$		-	-	+	+	+
$B_{1u}$	$B_1$	$B_2$	$B_u$	$B$	$A_1$	$A$		-	+	-	+	-
$B_{2g}$	$B_2$	$B_2$	$B_g$	$B$	$B_2$	$B$		-	-	-	-	+
$B_{2u}$	$B_2$	$B_1$	$B_u$	$B$	$A_2$	$A$		-	+	+	-	-
$E_g$	$E$	$E$	$E_g$	$E$	$E$	$E$	$R_x R_y$	$e^{\pm i\varphi}$	$e^{\mp i\varphi}$	*	*	+
$E_u$	$E$	$E$	$E_u$	$E$	$E$	$E$	$T_x T_y$	$e^{\pm i\varphi}$	$e^{\pm i\varphi}$	*	*	-
							$D_{4h}$	•	•	•	•	•
							$D_4$	•			•	
							$C_{4v}$	•		•		
							$C_{4h}$	•	•			•
							$C_4$	•				
							$V_d$		•		•	
							$S_4$		•			

<sup>10</sup> R. S. Mulliken, Phys. Rev. **43**, 279 (1933).

TABLE VI. *Direct products for  $D_{4h}$ .*

$A_{1g}$	$A_{1u}$	$A_{2g}$	$A_{2u}$	$B_{1g}$	$B_{1u}$	$B_{2g}$	$B_{2u}$	$E_g$	$E_u$	
$A_{1g}$	$A_{1u}$	$A_{2g}$	$A_{2u}$	$B_{1g}$	$B_{1u}$	$B_{2g}$	$B_{2u}$	$E_g$	$E_u$	$A_{1g}$
	$A_{1g}$	$A_{2u}$	$A_{2g}$	$B_{1u}$	$B_{1g}$	$B_{2u}$	$B_{2g}$	$E_u$	$E_g$	$A_{1u}$
		$A_{1g}$	$A_{1u}$	$B_{2g}$	$B_{2u}$	$B_{1g}$	$B_{1u}$	$E_g$	$E_u$	$A_{2g}$
			$A_{1g}$	$B_{2u}$	$B_{2g}$	$B_{1u}$	$B_{1g}$	$E_u$	$E_g$	$A_{2u}$
				$A_{1g}$	$A_{1u}$	$A_{2g}$	$A_{2u}$	$E_g$	$E_u$	$B_{1g}$
					$A_{1g}$	$A_{2u}$	$A_{2g}$	$E_u$	$E_g$	$B_{1u}$
						$A_{1g}$	$A_{1u}$	$E_g$	$E_u$	$B_{2g}$
							$A_{1g}$	$E_u$	$E_g$	$B_{2u}$
								$A_{1g} A_{2g}$ $B_{1g} B_{2g}$	$A_{1u} A_{2u}$ $B_{1u} B_{2u}$	$E_g$
								$A_{1g} A_{2g}$ $B_{1g} B_{2g}$	$A_{1u} A_{2u}$ $B_{1u} B_{2u}$	$E_u$

TABLE VII. *Types of electronic terms for hexagonal and trigonal symmetry.*

$D_{6h}$	$D_6$	$C_{6v}$	$C_{6h}$	$C_6$	$D_{3h}$	$C_{3h}$	$D_{3d}$	$D_3$	$C_{3v}$	$S_6$	$C_3$		$C_3$	$C_{2'}$	$C_{2''}$	$\sigma_h$	$\sigma_v$	$i$
$A_{1g}$	$A_1$	$A_1$	$A_g$	$A$	$A'_1$	$A'$	$A_{1g}$	$A_1$	$A_1$	$A_g$	$A$		+	+	+	+	+	+
$A_{1u}$	$A_1$	$A_2$	$A_u$	$A$	$A''_1$	$A''$	$A_{1u}$	$A_1$	$A_2$	$A_u$	$A$		+	+	+	-	-	-
$A_{2g}$	$A_2$	$A_2$	$A_g$	$A$	$A'_2$	$A'$	$A_{2g}$	$A_2$	$A_2$	$A_g$	$A$	$R_z$	+	+	-	+	-	+
$A_{2u}$	$A_2$	$A_1$	$A_u$	$A$	$A''_2$	$A''$	$A_{2u}$	$A_2$	$A_1$	$A_u$	$A$	$T_z$	+	+	-	-	+	-
$B_{1g}$	$B_1$	$B_1$	$B_g$	$B$	$A''_1$	$A''$	$A_{1g}$	$A_1$	$A_1$	$A_g$	$A$		+	-	+	-	+	+
$B_{1u}$	$B_1$	$B_2$	$B_u$	$B$	$A'_1$	$A'$	$A_{1u}$	$A_1$	$A_2$	$A_u$	$A$		+	-	+	+	-	-
$B_{2g}$	$B_2$	$B_2$	$B_g$	$B$	$A''_2$	$A''$	$A_{2g}$	$A_2$	$A_2$	$A_g$	$A$		+	-	-	-	-	+
$B_{2u}$	$B_2$	$B_1$	$B_u$	$B$	$A'_2$	$A'$	$A_{2u}$	$A_2$	$A_1$	$A_u$	$A$		+	-	-	+	+	-
$E^+_{1g}$	$E^+$	$E^+$	$E^+_{1g}$	$E^+$	$E'$	$E'$	$E_g$	$E$	$E$	$E_g$	$E$		$e^{\pm i\varphi}$	+	*	+	*	+
$E^+_{1u}$	$E^+$	$E^+$	$E^+_{1u}$	$E^+$	$E''$	$E''$	$E_u$	$E$	$E$	$E_u$	$E$		$e^{\pm i\varphi}$	+	*	-	*	-
$E^-_{2g}$	$E^-$	$E^-$	$E^-_{2g}$	$E^-$	$E''$	$E''$	$E_g$	$E$	$E$	$E_g$	$E$	$R_x R_y$	$e^{\pm i\varphi}$	-	*	-	*	+
$E^-_{2u}$	$E^-$	$E^-$	$E^-_{2u}$	$E^-$	$E'$	$E'$	$E_u$	$E$	$E$	$E_u$	$E$	$T_x T_y$	$e^{\pm i\varphi}$	-	*	+	*	-
												$D_{6h}$	•	•	•	•	•	•
												$D_6$	•	•	•			
												$C_{6v}$	•	•			•	
												$C_{6h}$	•	•		•		•
												$C_6$	•	•				
												$D_{3h}$	•		•	•		
												$C_{3h}$	•			•		
												$D_{3d}$	•		•		•	
												$D_3$	•		•			
												$C_{3v}$	•				•	
												$S_6$	•					•
												$C_3$	•					

TABLE VIII. *Direct products for  $D_{6h}$ .*

$A_{1g}$	$A_{1u}$	$A_{2g}$	$A_{2u}$	$B_{1g}$	$B_{1u}$	$B_{2g}$	$B_{2u}$	$E_g^+$	$E_u^+$	$E_g^-$	$E_u^-$	
$A_{1g}$	$A_{1u}$	$A_{2g}$	$A_{2u}$	$B_{1g}$	$B_{1u}$	$B_{2g}$	$B_{2u}$	$E_g^+$	$E_u^+$	$E_g^-$	$E_u^-$	$A_{1g}$
	$A_{1g}$	$A_{2u}$	$A_{2g}$	$B_{1u}$	$B_{1g}$	$B_{2u}$	$B_{2g}$	$E_u^+$	$E_g^+$	$E_u^-$	$E_g^-$	$A_{1u}$
		$A_{1g}$	$A_{1u}$	$B_{2g}$	$B_{2u}$	$B_{1g}$	$B_{1u}$	$E_g^+$	$E_u^+$	$E_g^-$	$E_u^-$	$A_{2g}$
			$A_{1g}$	$B_{2u}$	$B_{2g}$	$B_{1u}$	$B_{1g}$	$E_u^+$	$E_g^+$	$E_u^-$	$E_g^-$	$A_{2u}$
				$A_{1g}$	$A_{1u}$	$A_{2g}$	$A_{2u}$	$E_g^-$	$E_u^-$	$E_g^+$	$E_u^+$	$B_{1g}$
					$A_{1g}$	$A_{2u}$	$A_{2g}$	$E_u^-$	$E_g^-$	$E_u^+$	$E_g^+$	$B_{1u}$
						$A_{1g}$	$A_{1u}$	$E_g^-$	$E_u^-$	$E_g^+$	$E_u^+$	$B_{2g}$
							$A_{1g}$	$E_u^-$	$E_g^-$	$E_u^+$	$E_g^+$	$B_{2u}$
								$A_{1g} A_{2g}$	$A_{1u} A_{2u}$	$B_{1g} B_{2g}$	$B_{1u} B_{2u}$	$E_g^+$
								$E_g^+$	$E_u^+$	$E_g^-$	$E_u^-$	$E_u^+$
									$A_{1g} A_{2g}$	$B_{1u} B_{2u}$	$B_{1g} B_{2g}$	$E_g^-$
									$E_g^+$	$E_u^-$	$E_g^-$	$E_g^-$
										$A_{1g} A_{2g}$	$A_{1u} A_{2u}$	$E_u^-$
										$E_g^+$	$E_u^+$	$E_u^-$
											$A_{1g} A_{2g}$	$E_g^+$

Fig. 1, but, while in the axial case all points obtained by symmetry operations from one point are lying in one or two planes, we encounter in cubic molecules a set of points lying on a sphere. The intersection of this sphere with the plane of projection is indicated by full or broken circles. Again crosses and small circles are used to denote points above and below the plane of projection. The positions of the points in space are determined by their perpendicular projection shown in the figure and by the fact that they lie on the sphere mentioned above. The point sets characterize the symmetry of the group but, for completeness, positions of symmetry elements are also shown. Axes of symmetry including axes of rotary reflection are indicated in the same way as in Fig. 1. Their positions are the projections of the intercepts of the axes and the sphere. Full lines, ellipses and circles are projections of the circles in which planes of reflection intersect the spheres. Broken lines, broken ellipses and broken circles indicate the absence of the corresponding symmetry elements. Schoenflies symbols are again used in the figure. The Hermann-Mauguin symbols together with the corresponding Schoenflies symbols are given in the following list:

$2\ 3$	$2/m\ \bar{3}$	$\bar{4}\ 3\ m$	$4\ 3\ 2$	$4/m\ \bar{3}\ 2/m$
$T$	$T_h$	$T_d$	$O$	$O_h$

Table IX contains the electronic terms for cubic symmetry. In addition to symbols which have been used in previous tables, the notation  $F$  occurs. It stands for threefold degenerate electronic eigenfunctions. The letter  $c$  found in the  $F$  rows means that the transformation properties of the term during the symmetry operation in question are the same as the trans-

TABLE IX. *Types of electronic terms for cubic symmetry.*

$O_h$	$T_h$	$O$	$T_d$	$T$	$C_{2v}$	$C_{2v}$	$C_3$	$S_4$	$C_4$	$i$
$A_{1g}$	$A_g$	$A_1$	$A_1$	$A$	+	+	+	+	+	+
$A_{1u}$	$A_u$	$A_1$	$A_2$	$A$	+	+	+	-	+	-
$A_{2g}$	$A_g$	$A_2$	$A_2$	$A$	+	+	+	-	-	+
$A_{2u}$	$A_u$	$A_2$	$A_1$	$A$	+	+	+	+	-	-
$E_g$	$E_g$	$E$	$E$	$E$	+	+	$e^{\pm i\varphi}$	*	*	+
$E_u$	$E_u$	$E$	$E$	$E$	+	+	$e^{\pm i\varphi}$	*	*	-
$F_{1g}$	$F_g$	$F_1$	$F_1$	$F$	$R$	$c$	$c$	$-c$	$c$	+
$F_{1u}$	$F_u$	$F_1$	$F_2$	$F$	$T$	$c$	$c$	$c$	$c$	-
$F_{2g}$	$F_g$	$F_2$	$F_2$	$F$		$c$	$c$	$c$	$-c$	+
$F_{2u}$	$F_u$	$F_2$	$F_1$	$F$		$c$	$c$	$-c$	$-c$	-
$O_h$					$O_h$	.	.	.	.	.
$T_h$					$T_h$	.	.	.	.	.
$O$					$O$	.	.	.	.	.
$T_d$					$T_d$	.	.	.	.	.
$T$					$T$	.	.	.	.	.

formation properties of coordinates  $x$ ,  $y$ ,  $z$  of a point. The term  $F_{1u}$  of the group  $O_h$  always transforms like the coordinate or like translations as denoted by  $T$  appearing in this row.  $-c$  is used if the transformation of the term differs from that of the coordinates in sign.

The direct products and selection rules for  $O_h$  are given in Table X. In addition to the groups discussed, molecules belonging to one more symmetry class, the icosaeader class, may occur according to group theory.<sup>11</sup> No representative molecules are known. Nor is it probable that such molecules should be found except perhaps complex ions in solutions. The electronic terms of the icosaeader group are therefore not discussed here.

### b. Vibrations and Franck-Condon Principle

The vibrations<sup>12</sup> of a polyatomic molecule can be classified according to their symmetries in a similar way as the electronic states. The vibrational motion is considered as being a superposition of normal vibrations, the total vibrational energy being the sum of the energies belonging to the individual vibrations. In a normal mode of vibration coordinates corresponding to all degrees of freedom oscillate harmonically with the same frequency. The corresponding energy levels are equidistant with spacing  $h\nu$ . We distinguish non-degenerate and degenerate vibrations. In non-degenerate vibrations the atoms of a molecule move along straight lines and all are in phase. These vibrations are symmetrical or antisymmetrical with respect to the various symmetry operations, that means they remain unchanged during such operations or reverse their direction. If they preserve the symmetry during all symmetry operations, they are called totally symmetric; if certain symmetries are not maintained they are called non-totally symmetric. One speaks of degenerate

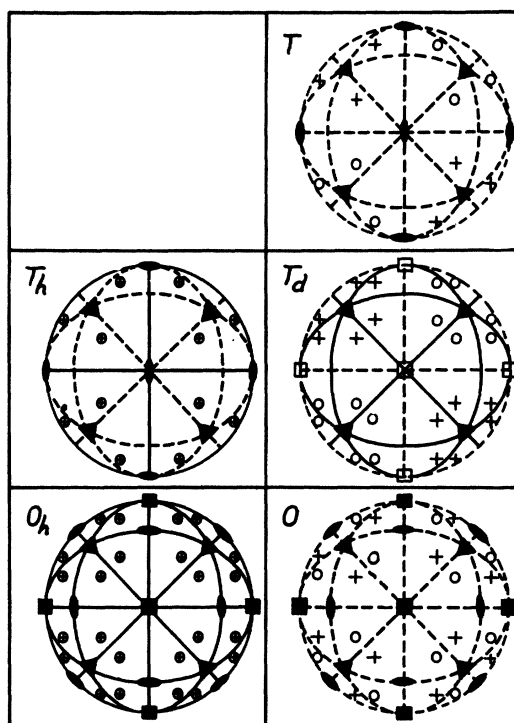


FIG. 2. Stereographic projections of cubic symmetry classes.

vibrations when several independent motions can be found with the same frequency. In general, exact degeneracy is caused by symmetry. One calls this necessary degeneracy while in other cases the degeneracy is called accidental. Degenerate vibrations may be symmetric or antisymmetric to some symmetry operations, but other symmetry operations will cause the several degenerate modes to transform into each other. The transformation properties of both non-degenerate and degenerate vibrations are the same as those of the corresponding electronic terms. Actually, the symbols given in Tables III, V, VII, IX for non-linear molecules have been used for electronic eigenfunctions and also for vibrations. But, in order to distinguish between the electronic wave functions and the purely classical vibrations we prefer to use small Greek letters for indicating the latter's symmetry character. Thus,  $\alpha$  and  $\beta$  replace  $A$  and  $B$ , while  $\epsilon$  and  $\varphi$  correspond to  $E$  and  $F$  terms. In all other respects the symmetry symbols remain the same and Tables III–X can also be used for vibrations. In the case of linear molecules we

<sup>11</sup> L. Tisza, *Zeits. f. Physik* **82**, 48 (1933).

<sup>12</sup> For more detailed discussion of vibrations of polyatomic molecules see D. M. Dennison, *Rev. Mod. Phys.* **3**, 280 (1931); **12**, 175 (1940); E. Teller, *Hand- und Jahrbuch der chemischen Physik*, Vol. 9, No. 2 (1934), p. 13; K. W. F. Kohlrausch, *Der Smekal-Raman-Effekt* (Julius Springer, Berlin, 1931 and 1938); H. A. Stuart, *Molekülstruktur* (Julius Springer, Berlin, 1934); H. Sponer, *Molekülspektren und ihre Anwendung auf chemische Probleme*, Vol. 2 (Julius Springer, Berlin, 1936); Ta-You Wu, *Vibrational Spectra and Structure of Polyatomic Molecules* (National University, Peking, 1939).

TABLE X. *Direct products for  $O_h$ .*

$A_{1g}$	$A_{1u}$	$A_{2g}$	$A_{2u}$	$E_g$	$E_u$	$F_{1g}$	$F_{1u}$	$F_{2g}$	$F_{2u}$	
$A_{1g}$	$A_{1u}$	$A_{2g}$	$A_{2u}$	$E_g$	$E_u$	$F_{1g}$	$\mathbf{F}_{1u}$	$F_{2g}$	$F_{2u}$	$A_{1g}$
	$A_{1g}$	$A_{2u}$	$A_{2g}$	$E_u$	$E_g$	$\mathbf{F}_{1u}$	$F_{1g}$	$F_{2u}$	$F_{2g}$	$A_{1u}$
		$A_{1g}$	$A_{1u}$	$E_g$	$E_u$	$F_{2g}$	$F_{2u}$	$F_{1g}$	$\mathbf{F}_{1u}$	$A_{2g}$
			$A_{1g}$	$E_u$	$E_g$	$F_{2u}$	$F_{2g}$	$\mathbf{F}_{1u}$	$F_{1g}$	$A_{2u}$
				$A_{1g}, A_{2g}$	$A_{1u}, A_{2u}$	$F_{1g}, F_{2g}$	$\mathbf{F}_{1u}, F_{2u}$	$F_{1g}, F_{2g}$	$\mathbf{F}_{1u}, F_{2u}$	$E_g$
				$E_g$	$E_u$					$E_u$
					$A_{1g}, A_{2g}$	$\mathbf{F}_{1u}, F_{2u}$	$F_{1g}, F_{2g}$	$\mathbf{F}_{1u}, F_{2u}$	$F_{1g}, F_{2g}$	$F_{1g}$
					$E_g$					$F_{1u}$
						$A_{1g}, E_g$	$A_{1u}, E_u$	$A_{2g}, E_g$	$A_{2u}, E_u$	$F_{2g}$
						$F_{1g}, F_{2g}$	$\mathbf{F}_{1u}, F_{2u}$	$F_{1g}, F_{2g}$	$\mathbf{F}_{1u}, F_{2u}$	$F_{2u}$
							$A_{1g}, E_g$	$A_{2u}, E_u$	$A_{2g}, E_g$	
							$F_{1g}, F_{2g}$	$\mathbf{F}_{1u}, F_{2u}$	$F_{1g}, F_{2g}$	
								$A_{1g}, E_g$	$A_{1u}, E_u$	
								$F_{1g}, F_{2g}$	$\mathbf{F}_{1u}, F_{2u}$	
									$A_{1g}, E_g$	
									$F_{1g}, F_{2g}$	

shall use the symbol  $\alpha$  for non-degenerate vibrations and  $\epsilon$  for degenerate vibrations. Here  $\alpha$  corresponds to  $\Sigma$  terms and  $\epsilon$  to  $\Pi$  terms.  $\Delta$  and higher terms do not have analogs for vibrations.

The vibrational wave functions of a molecule are classified in the same way as the electronic functions. They will be denoted by Greek letters in heavy print. But the symmetry character of a vibration and its vibrational wave function is in general not the same. The lowest vibrational state is always totally symmetric, i.e., it remains unchanged during all symmetry operations. It is therefore an  $\alpha_{1g}$ ,  $\alpha_1$ ,  $\alpha_g$ ,  $\alpha'$  or  $\alpha$  state according to the group in question. With only one vibration excited to its first level the symmetries of this vibration and its vibrational eigenfunction are the same. When a non-degenerate vibration is excited with  $n$  quanta (with no excitation of other vibrations), then the symmetry characters of vibration and vibrational function are identical if  $n$  is odd (the wave function is an odd function of the displacement) and the vibrational function is totally symmetric if  $n$  is even (the wave function is an even function of the displacement). When a degenerate vibration is excited, the degree of degeneracy increases with increasing number of quanta. This higher degree of degeneracy is not caused by symmetry alone but also by the harmonic nature of the forces. In the presence of anharmonic forces the highly degenerate level splits into several levels which transform according to Tables III, V, VII and

IX. If the degenerate vibration is excited with an even number of quanta then at least one of the levels arising from the splitting is totally symmetrical. A detailed description of which terms arise by splitting from degenerate levels is given by Tisza.<sup>11</sup> If two different normal vibrations are excited, the symmetry of the resulting vibrational levels is obtained by taking the direct product of the terms belonging to the separate normal vibrations. Thus, if a molecule has the symmetry  $V_h$  and an  $\alpha_{1u}$  and a  $\beta_{2u}$  vibration are excited each with one quantum, one obtains, according to Table IV,  $\beta_{2g}$  for the resulting vibrational term. Again, if the molecule belongs to  $C_4$  and two different  $\epsilon$  vibrations are excited with one quantum, the two twofold degenerate vibrations will give a fourfold degenerate level. Anharmonicity splits this degeneracy into two  $\alpha$  and two  $\beta$  terms as can be checked from Table VI. If more than two vibrations are excited, the direct products of all vibrations involved can be found by applying the tables several times. For example, if in a molecule with symmetry  $C_{6h}$  vibrations  $\beta_{1u}$ ,  $\epsilon^+_{1g}$  and  $\epsilon^+_{2u}$  are excited, each with one quantum, the procedure is as follows: from Table VIII the direct product of  $\beta_{1u}$  and  $\epsilon^+_{1g}$  is  $\epsilon^-_{2u}$ . This multiplied by  $\epsilon^+_{2u}$  gives  $\beta_{1g}$ ,  $\beta_{2g}$  and an  $\epsilon^-_{2g}$  vibrational term. The result would have been the same if the formation of the direct products were carried out in different order.

The vibrational eigenfunction must be com-



bined with the electronic function to obtain a complete description of that part of the molecular motion  $\psi_{\text{rel}}$  which arises from the relative movement of the constituents.<sup>13</sup> Finally,  $\psi_{\text{rel}}$  has to be multiplied with  $\psi_{\text{rot}}$  to include the orientation of the molecule in space. This simple scheme is, however, only correct for non-linear molecules with non-degenerate functions  $\psi_{\text{rel}}$ . In linear molecules  $\psi_{\text{rot}}$  depends only on the orientation of the figure axis, while  $\psi_{\text{rel}}$  includes all other degrees of freedom. Further complications arise when a degenerate  $\psi_{\text{rel}}$  is coupled with  $\psi_{\text{rot}}$ . In the present section we shall give consideration to  $\psi_{\text{rel}}$  only.

It is customary<sup>14</sup> to write  $\psi_{\text{rel}}$  in the form of a product  $\psi_{\text{rel}} = \psi_{\text{el}} \cdot \psi_{\text{vib}}$ . The first factor  $\psi_{\text{el}}$  does not depend on the electrons alone but includes the nuclear positions as parameters. The second factor is the vibrational eigenfunction depending on the relative positions of the nuclei. This factor as well as the potential field in which the nuclei move is different for different electronic states. The product representation is an approximation the validity of which will be treated in the following section.

The symmetry properties of  $\psi_{\text{rel}}$  (vibronic state) are again described in Tables III, V, VII, IX. When the term symbols of these tables are used for  $\psi_{\text{rel}}$  a bar will be written over the symbol. To determine the symmetry of  $\psi_{\text{rel}}$  the direct products of the symmetry symbols for  $\psi_{\text{el}}$  and  $\psi_{\text{vib}}$  must be formed. This is readily done by means of Tables IV, VI, VIII and X. Suppose the molecule has the symmetry  $O_h$ ,  $\psi_{\text{el}}$  has the symmetry  $A_{1u}$  and  $\psi_{\text{vib}}$  the symmetry  $\epsilon_g$ . Then the symmetry of  $\psi_{\text{rel}}$  is described by the symbol  $\bar{E}_u$ . The exact selection rules for transitions between upper and lower states  $\psi'_{\text{rel}}$  and  $\psi''_{\text{rel}}$  are also contained in Tables IV, VI, VIII and X, the transition being allowed if the direct product of the two term symbols belonging to  $\psi'_{\text{rel}}$  and  $\psi''_{\text{rel}}$  contains a term with the transformation properties of a translation.<sup>15</sup>

<sup>13</sup> The corresponding state is called by Mulliken vibronic (abbreviation for vibrational-electronic) state.

<sup>14</sup> M. Born and R. Oppenheimer, *Ann. d. Physik* **84**, 457 (1927). A detailed discussion is found on page 93.

<sup>15</sup> This follows from a discussion of the integral  $\int \psi'^*_{\text{rel}} M \psi''_{\text{rel}} d\tau_{\text{rel}}$  which proceeds along the same line as the discussion of  $\int \psi'^*_{\text{el}} M \psi''_{\text{el}} d\tau_{\text{el}}$  (p. 79).

This exact selection rule is of no great practical importance as it still allows a large number of transitions many of which are weak on account of approximately valid selection rules. It is more useful to consider the electronic and vibrational parts separately. The strongest bands appear when the transition between  $\psi'_{\text{el}}$  and  $\psi''_{\text{el}}$  is allowed. This is in fact the selection rule already discussed in the preceding section. The gross features of the vibrational structure can be obtained by applying the Franck-Condon principle to polyatomic molecules.<sup>16</sup>

According to the simple principle of Franck<sup>17</sup> the nuclear positions and velocities do not change during the electronic jump. If in the beginning the molecule is at rest, the equilibrium positions of the nuclei in the initial state become turning points of the vibration in the final state. Therefore, if we assume that the symmetry of the equilibrium position is the same in both the initial and final states, then only those vibrations will be strongly excited which preserve the symmetry (totally symmetrical vibrations). The same holds if totally symmetrical vibrations are excited in the initial state. Besides totally symmetrical vibrations there can also occur non-totally symmetrical vibrations. If, as assumed before, the symmetry is the same in both electronic states, then the equilibrium configurations for non-totally symmetrical vibrations, i.e., the symmetrical nuclear configurations, will also be the same in the initial and final states. From this follows that the potential surfaces for all non-totally symmetrical vibrations will have their minima directly above one another. Franck's principle implies that the  $0-0$ ,  $1-1$ ,  $\dots v-v$  transitions are intense unless they are weakened too much by Boltzmann factors.

If the symmetry is different in both states, then all those vibrations will be excited which preserve the symmetry properties common to the states concerned. This suggests that only symmetry elements common to both states need be considered which in fact is the case for vibrational selection rules. For electronic selection rules, however, all symmetry elements of the

<sup>16</sup> G. Herzberg and E. Teller, *Zeits. f. physik. Chemie* **B21**, 410 (1933).

<sup>17</sup> J. Franck, *Trans. Faraday Soc.* **21**, part 3 (1925).

initial state must be considered. In fact, according to the Franck-Condon principle the electronic transition first leads to a state with unaltered nuclear positions and the symmetry is changed only later by vibrations in the excited state, a process which is not directly related with the electronic jump.

The superposition of the vibrational frequency on the electronic frequency can be understood by means of the following classical picture.<sup>18</sup> Suppose that  $\nu_e$  is the electronic frequency for the equilibrium position of the nuclei, that  $\pm\delta\nu_e$  is the change of electronic frequency which occurs for the maximum elongation of nuclear vibrations and that the electronic frequency shall vary linearly with the nuclear displacement. Let  $\nu_v$  be the vibrational frequency. Then the instantaneous electronic frequency is given by  $\nu_e + \delta\nu_e \sin 2\pi\nu_v t$ . The time dependent oscillating dipole moment  $\mathfrak{M}(t)$  which corresponds to the electronic transition satisfies the differential equation

$$d\mathfrak{M}(t)/dt = \mathfrak{M}(t) 2\pi i (\nu_e + \delta\nu_e \sin 2\pi\nu_v t).$$

The general solution of the equation is

$$\mathfrak{M}(t) = \mathfrak{M} \exp[i\{2\pi\nu_e t - (\delta\nu_e/\nu_v) \cos 2\pi\nu_v t\}].$$

Here  $\mathfrak{M}$  is the amplitude of the vibrating dipole.

To obtain the frequencies which can occur in emission or absorption we have to take the Fourier analysis of  $\mathfrak{M}(t)$ . Explicit expressions for the intensities contain Bessel functions. One can see, however, in a simple way that the only frequencies occurring in the Fourier analysis are  $\nu_e \pm$  integer multiples of  $\nu_v$ . Indeed

$$\begin{aligned} \mathfrak{M}(t) \exp[-2\pi i \nu_e t] \\ = \mathfrak{M} \exp[-i(\delta\nu_e/\nu_v) \cos 2\pi\nu_v t] \end{aligned}$$

is a periodic function of  $t$  with the period  $1/\nu_v$ . One can also see easily that the strongest Fourier components belong to frequencies between  $\nu_e - \delta\nu_e$  and  $\nu_e + \delta\nu_e$ .

Essentially the same results are obtained from the Franck-Condon principle except for the fact that both the vibrational frequencies in the upper and lower states may be superposed on the electronic frequency. In addition, non-linear variation of the electronic frequency with nuclear displacements and the detailed behavior

of the wave function cause an intensity distribution in the band system which differs from the intensities obtained by the classical method.

In an antisymmetrical vibration of a polyatomic molecule the frequency is an even function of the displacement. For small amplitudes the frequency change will vary quadratically with the displacement and one obtains for the oscillating dipole

$$d\mathfrak{M}(t)/dt = \mathfrak{M}(t) 2\pi i [\nu_e + \delta\nu_e \sin^2 2\pi\nu_v t].$$

The  $\sin^2$  term in the bracket can be transformed according to the relation

$$\sin^2 \alpha = \frac{1}{2}(1 - \cos 2\alpha)$$

so that  $\mathfrak{M}(t)$  becomes

$$\mathfrak{M}(t) = \mathfrak{M} \exp[i\{2\pi\nu_e t + \pi\delta\nu_e t - (\delta\nu_e/4\nu_v) \sin 4\pi\nu_v t\}].$$

If we multiply  $\mathfrak{M}(t)$  with  $\exp[-2\pi i(\nu_e + \frac{1}{2}\delta\nu_e)t]$  a periodic function of  $t$  is obtained with the period  $1/2\nu_v$ . Therefore only multiples of  $2\nu_v$  will be superimposed on the electronic frequency  $\nu_e$ . In quantum theory this corresponds to the statement that antisymmetrical vibrations may change only by multiples of two quanta.

For antisymmetrical vibrations of small amplitudes, only slight changes  $\delta\nu_e$  of the electronic frequencies take place. This is so because in these vibrations the rate of change of  $\nu_e$  with the nuclear displacement is zero for the equilibrium configuration. As a general rule  $\delta\nu_e$  for the zero-point vibration is small compared to  $2\nu_v$ . Therefore in the Fourier analysis of

$$\mathfrak{M} \exp[i\{2\pi\nu_e t + \pi\delta\nu_e t - (\delta\nu_e/4\nu_v) \sin 4\pi\nu_v t\}],$$

the term proportional to  $\exp[2\pi i(\nu_e + \frac{1}{2}\delta\nu_e)t]$  will have the greatest coefficient. All further terms appear with much smaller amplitudes. Thus the frequencies of antisymmetrical vibrations will in general not be superposed<sup>19</sup> on  $\nu_e$ .

The above statements about vibrations based upon a classical picture, can be made more precise by using the wave-mechanical procedure applied by Condon<sup>20</sup> to diatomic molecules. The

<sup>19</sup> This is valid with the exceptions of  $1-1$ ,  $2-2$ ,  $\dots$   $v-v$  transitions. In classical theory these transitions coincide with the  $0-0$  band because the difference in vibrational frequencies in the upper and lower states cannot be incorporated in the classical treatment.

<sup>20</sup> E. U. Condon, Phys. Rev. **32**, 858 (1928).

<sup>18</sup> W. Lenz, Zeits. f. Physik **25**, 299 (1924).

transition probabilities are proportional to the square of the matrix elements  $\int \psi'^*_{\text{rel}} M \psi''_{\text{rel}} d\tau_{\text{rel}} = \int \psi'^*_{\text{el}} \psi''_{\text{vib}} M \psi''_{\text{el}} \psi''_{\text{vib}} d\tau_{\text{el}} d\tau_{\text{nuc}}$ . Here  $d\tau_{\text{nuc}}$  means integration over the nuclear configurations. We shall first carry out the integration  $\int \psi'^*_{\text{el}} M \psi''_{\text{el}} d\tau_{\text{el}}$ . This integral, which we shall designate by  $\mathfrak{M}$ , depends on the nuclear configuration. Following the procedure customary for diatomic molecules we shall consider for the present  $\mathfrak{M}$  as a constant. This is justified to a certain extent for small amplitudes of nuclear vibrations. Then  $\mathfrak{M}$  will not vary greatly from its value in the equilibrium configuration. In the integral

$$\int \psi'^*_{\text{el}} M \psi''_{\text{el}} \psi'^*_{\text{vib}} \psi''_{\text{vib}} d\tau_{\text{el}} d\tau_{\text{nuc}} = \int \mathfrak{M} \psi'^*_{\text{vib}} \psi''_{\text{vib}} d\tau_{\text{nuc}}$$

the factor  $\mathfrak{M}$  can now be written before the integral  $\mathfrak{M} \int \psi'^*_{\text{vib}} \psi''_{\text{vib}} d\tau_{\text{nuc}}$ . In the transition probability which is proportional to

$$|\mathfrak{M}|^2 \left| \int \psi'^*_{\text{vib}} \psi''_{\text{vib}} d\tau_{\text{nuc}} \right|^2$$

the first factor  $|\mathfrak{M}|^2$  gives the electronic part of the transition probability, while the probability for changes in vibrational quantum numbers is given by the second factor. It can be shown, in fact, that when  $\left| \int \psi'^*_{\text{vib}} \psi''_{\text{vib}} d\tau_{\text{nuc}} \right|^2$  is summed over all states  $\psi''_{\text{vib}}$ , the result is unity, so that the sum of transition probabilities from one vibrational state of the initial electronic level to all vibrational states of the final level depends on the electronic transition probability alone.

The vibrational selection rules are obtained from the integral  $\int \psi'^*_{\text{vib}} \psi''_{\text{vib}} d\tau_{\text{nuc}}$ . The integral is different from zero only if the integrand is left unchanged by all symmetry operations. From this follows in turn that *the transition probability will be different from zero only if the vibrational eigenfunction has the same symmetry in the initial and final states*. This rule depends, of course, on the assumptions made before. We will discuss in the next section which changes must be introduced when these assumptions are dropped.

The general vibrational selection rule at which we have just arrived, together with the rules about symmetry properties of vibrational eigenfunctions, lead to the following specific statements. Totally symmetric vibrations may change by any number of quanta. Vibrations which are

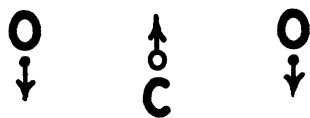
antisymmetric to some symmetry element may change by  $\Delta v = 0, 2, 4, \dots$ , where  $v$  is the vibrational quantum number. No transition can occur from a state in which only totally symmetrical vibrations are excited to several quanta to another state in which in addition one non-totally symmetrical vibration with one quantum is present.

Changes of quanta of totally symmetrical vibrations follow the rules known from the vibrational structure of diatomic spectra. If the equilibrium position differs greatly in the two electronic states (this means different internuclear distances in both states), then long series of the corresponding totally symmetrical vibration will occur. But when the equilibrium positions in the two combining states are much alike, then  $0-0, 1-1, \dots, v-v$  transitions of the totally symmetrical vibrations will be most probable.

As has been mentioned before, such transitions are always most probable for non-totally symmetrical vibrations as they behave like vibrations of diatomic molecules with the same equilibrium position in the two combining states. Thus, the transition  $0-2$ , although allowed by symmetry, will have a smaller intensity. If the potential for the nuclear oscillation is the same in both electronic states, then the vibrational quantum number will not change. In fact, the wave functions  $\psi'_{\text{vib}}$  and  $\psi''_{\text{vib}}$  will be solutions of the same Schrödinger equation in this case, and because of the orthogonality of the eigenfunctions,  $\int \psi'^*_{\text{vib}} \psi''_{\text{vib}} d\tau_{\text{nuc}}$  vanishes unless the quantum number is the same in  $\psi'_{\text{vib}}$  and  $\psi''_{\text{vib}}$ . If, on the other hand, the frequency of a non-totally symmetrical state is different in the two electronic levels the wave functions  $\psi'_{\text{vib}}$  and  $\psi''_{\text{vib}}$  will be different even if they agree in their quantum numbers. In this case  $\Delta v = 2, 4, \dots$  occurs in addition to  $\Delta v = 0$ . If the calculations are performed for purely harmonic vibrations, the following intensity ratio holds for the changes in the quanta of any non-totally symmetrical vibration  $V$ :

$$\frac{(\nu' \nu'')^{\frac{1}{2}}}{\frac{1}{2}(\nu' + \nu'')} = \frac{\text{intensity of band } 0-0 \text{ in } V}{\text{intensity of all bands } 0-v \text{ in } V};$$

$$v = 0, 2, 4, \dots$$

FIG. 3. Deformation vibration of  $\text{CO}_2$ .

where  $\nu'$  and  $\nu''$  are the frequencies in the two electronic states of  $V$ . This means, that even in the extreme case when the vibrational frequencies in the upper and lower states show a change of 1 : 2, the intensity of the 0-0 band amounts to 94.4 percent of the total intensity and only 5.6 percent is left for the bands  $\nu''=0$  and  $\nu' \neq 0$ . Hence bands due to transitions of non-totally symmetrical vibrations 0-2, 0-4, ... will be weak even when the frequencies change considerably. On the other hand, 1-3, 2-4, ... transitions have somewhat greater transition probabilities. For small vibrational frequency changes and small values of  $v$  the  $v \rightarrow v+2$  transition probability increases roughly with  $(v+1)^2$ . This will become important for low frequencies. ( $\approx 100 \text{ cm}^{-1}$ .)

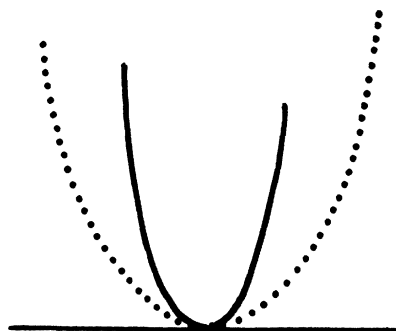
### c. Coupling Between Vibration and Electronic Motion

#### *Splitting of Degenerate Electronic States*

The influence of nuclear displacements on the behavior of the electrons is most important for degenerate electronic states. The reason for electronic degeneracy is the symmetry of the molecule and the degeneracy may split as soon as the nuclei occupy an asymmetric position. Two types of behavior are possible which will be illustrated by the following two examples.

We first consider a linear triatomic molecule, for instance  $\text{CO}_2$ . The molecule shall be in a  $\Pi$  state. The twofold degeneracy in the  $\Pi$  state is caused by cylindrical symmetry which is destroyed by the vibration shown in Fig. 3. During this vibration the electronic state splits into two terms, one being symmetrical, the other antisymmetrical to the plane through the three atoms. If only one  $\pi$  electron is present one can see this immediately since the nodal plane of the wave function may be either perpendicular to the  $\text{OCO}$  plane or it may be identical with that plane. But even in the case of a general  $\Pi$  function one can see that the sum and difference of the two

degenerate functions which transform like  $e^{i\varphi}$  and  $e^{-i\varphi}$  are symmetrical and antisymmetrical if  $\varphi$  is counted from the  $\text{OCO}$  plane. If the displacements shown in Fig. 3 are reversed, the symmetrical wave function stays symmetrical and the antisymmetrical function stays antisymmetrical. Furthermore it is obvious that the energies are the same for the original and the reversed configuration. Therefore, the energy is an even function of the displacements and the linear constellation corresponds to an extreme value of the energy. If the linear configuration of the nuclei represents a minimum for the symmetrical electronic function and the antisymmetrical as well, then and only then is the linear nuclear configuration stable. The potentials for the symmetrical and antisymmetrical wave functions  $U_s$  and  $U_a$  have, as a rule, the same value only for the linear configuration and may differ considerably for other positions. The dependence of the potential function upon the deformation displacement of Fig. 3 is illustrated in Fig. 4 for the case where the linear configuration corresponds to a stable minimum.

FIG. 4. Splitting of a  $\Pi$  state by a deformation vibration.

In a second example we consider the electronic wave function in the field of a plane square configuration of four identical nuclei. The configuration has the symmetry  $D_{4h}$  and we assume that the electronic term is  $E_g$ . The degeneracy shall be split by displacements of the nuclei as indicated in Fig. 5, I and II. The configurations may be regarded clearly as belonging to a positive and negative value of one and the same nuclear displacement. This nuclear displacement destroys the fourfold axial symmetry, replacing it by the twofold symmetry  $V_h$ . The degenerate state will split

into two terms  $B_{2g}$  and  $B_{3g}$ , the first having a node in the plane of symmetry  $\sigma_v^x$  and the second a node in the plane  $\sigma_v^y$ . The configuration I can be transformed into II by rotation through  $90^\circ$  which interchanges the two symmetry planes. Therefore the energy for  $B_{2g}$  in configuration I must be the same as the energy for  $B_{3g}$  in II. If  $U_2$  and  $U_3$  are the corresponding energies, we have the relations  $U_2(\text{I}) = U_3(\text{II})$  and  $U_2(\text{II}) = U_3(\text{I})$ . Thus the two energy levels cross at the undisplaced configuration (see Fig. 6). There is in this case no reason of symmetry which necessitates an extreme value of the energy for the undisplaced configuration. Therefore, the energy will, as a general rule, depend linearly upon nuclear displacements in the neighborhood of the square configuration and this configuration will not correspond to a stable equilibrium.

It can be shown that the behavior discussed in the second example is the usual one. Indeed, stable equilibrium is compatible with a degenerate electronic wave function only for molecules with all the atoms in a straight line. In all other molecules the splitting of degeneracy produces a linear dependence of the energy level on some nuclear displacement and therefore the symmetrical configuration does not correspond to a minimum energy. Since, on the other hand, orbital degeneracy is due to symmetry it may be said that *in a non-linear molecule no electronic degeneracy is to be expected in the stable equilibrium configuration*. Exceptions from this rule may, however, occur. For example, if the degenerate electronic orbits do not contribute appreciably to the molecular binding they will be perturbed but slightly by nuclear displacements. The equilibrium configuration will remain very nearly symmetrical in such cases; if the deviation from

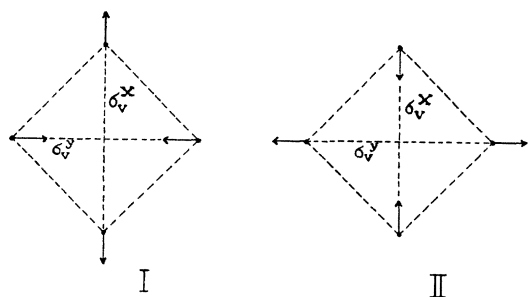


FIG. 5. Nuclear displacement in a tetragonal molecule.

symmetry is small compared to the zero-point amplitude of the vibrations, the molecule may be considered symmetrical for almost all practical purposes.

The statement made above may be proved by applying group theory to perturbation calculation.<sup>21</sup> The electronic energy levels of the dis-

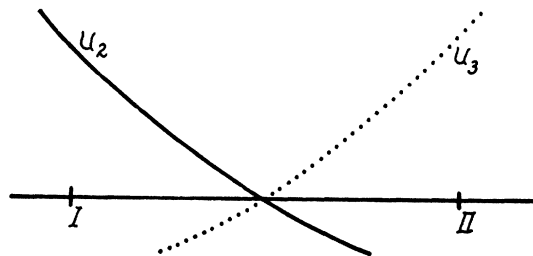


FIG. 6. Splitting of an  $E_g$  state. I and II on abscissae correspond to displacements as shown in Fig. 5, I and II.

placed configuration are the characteristic values of a perturbation matrix, the elements of which may be expressed in a power series of the nuclear displacements. Unless those perturbation matrix elements, which are linear in the nuclear displacements, all vanish, then at least one perturbed energy level will depend linearly upon a nuclear displacement. Now the matrix elements are invariant with respect to all symmetry operations of the molecule. Indeed, the matrix elements are integrals in which a symmetry operation merely causes a change in the order of integration. The integrands, on the other hand, are products whose transformation properties are determined by those of the degenerate wave functions and the nuclear displacements. The integral will be different from zero only if the direct product of the transformation properties of these factors contains a totally symmetrical term (i.e., one which is invariant to all symmetry operations). Now in all molecules in which not all atoms lie on a straight line, there exist displacements for which the direct product contains such a term. Therefore, a linear dependence of the energy on some nuclear displacement must be expected. On the other hand, one can show that in linear molecules the direct product never contains a totally symmetrical term. Hence all elements of the perturbation matrix vanish and

<sup>21</sup> The proof can be found in a paper by H. A. Jahn and E. Teller, Proc. Roy. Soc. A161, 220 (1937).

one obtains an extreme value of the energy in the equilibrium configuration.

The theorem discussed above leads to a practical conclusion about the spectra of molecules with cubic symmetry.<sup>22</sup> We mentioned before that a stable symmetrical configuration requires non-degenerate electronic wave functions in the initial state. Applying the selection rules for cubic molecules (Table X) we find that non-degenerate states combine only with degenerate ones and according to the above theorem the equilibrium configuration for the latter does not have the same symmetry as for the former. Therefore we shall expect for such a molecule that absorption takes place from a non-degenerate ground state to a degenerate higher level. Non-totally symmetrical vibrations will be excited simultaneously. The spectrum will have a rather complicated appearance. If, moreover, the equilibrium positions differ considerably in the two states, the number of bands may be increased so greatly that the spectrum looks continuous. It may even happen that there will be no equilibrium configuration in the final electronic state so that the molecule dissociates and a true continuum appears. We conclude that allowed electronic bands in cubic molecules must either have a complicated vibrational structure (possibly quasi-continuous) or that they are actually continuous. The same holds for molecules with axial symmetry if the transition moment is perpendicular to the figure axis, for in this case a non-degenerate electronic state may combine only with a degenerate one and the above argument may therefore be applied.

The above considerations are valid only for orbitally degenerate functions. If the influence of spin is considered there exists always at least a twofold degeneracy whenever the molecule possesses an odd number of electrons. This does not cause, however, any splitting or instability. Nor can the degeneracy be removed by any electric field<sup>23</sup> because the degeneracy is not due to symmetry in space but rather to the fact that the form of physical conditions remains un-

changed if the direction of time is reversed.<sup>24</sup> Magnetic fields, however, split such doublet states since one can consider the magnetic field as caused by a current, i.e., by a process which is changed in sign by reversing the time.

With this one exception of twofold spin degeneracy it remains true that symmetrical configurations of non-linear molecules are unstable in degenerate electronic states.<sup>25</sup> Thus, triplet states will split in the same way as orbitally degenerate states, but the splitting will be much smaller. This is caused by a weak coupling between spin and orbital motion, the latter being influenced by nuclear displacements. A quartet state will split into two twofold degenerate states which, however, will not split any further since they have the same properties as the spin doublets discussed before.

In molecules with non-degenerate orbital functions splitting due to spin is extremely small so that one will not expect spin degeneracy to impair the stability of symmetrical configurations to a noticeable extent. A greater effect of coupling between spin and orbit can occur only in orbitally degenerate levels. It causes a splitting into several levels of which the lowest may be non-degenerate. For this lowest level the symmetrical configuration may, of course, be stable. If in addition the lowest component lies sufficiently far away from the other levels of the multiplet, the stability of the lowest component may remain undisturbed by the higher levels.

In summarizing, we see that the influence of spin alone does not cause noticeable instability of symmetrical configurations, and the spin may stabilize the symmetrical state where the orbital function alone would destroy the symmetry. Effects of the last kind may be expected among molecules with heavy atoms and consequently with strong spin-orbit coupling.

In linear polyatomic molecules with degenerate electronic states nuclear displacements cause splitting of the degeneracy just as in non-linear molecules. But while in the latter the splitting produces instability of the symmetrical configuration, in the former the linear configuration

<sup>22</sup> E. Teller and O. R. Wulf, 1937. Report given at the Gibson Island Conference; H. Spöner, *Occas. Publ. A. A. S.* (1938), p. 108.

<sup>23</sup> H. A. Kramers, *Proc. Acad. Sci. Amst.* **33**, 959 (1930).

<sup>24</sup> E. Wigner, *Nach. Gött. Ges. Wiss.* (1932), p. 546.

<sup>25</sup> H. A. Jahn, *Proc. Roy. Soc. London*, **A164**, 117 (1938).

may remain the stable one as has been illustrated by the example on page 90. As shown in Fig. 4 two electronic levels exist for nuclear arrangements which deviate from the straight line whereas the two levels coincide for linear arrangement. The distance between the two electronic states is of the same order of magnitude as the potential energy of the nuclear vibration. Under these conditions the ordinary separation of the molecular wave function into an electronic and a nuclear part cannot be carried out because vibrational frequencies are no longer small as compared to all electronic frequencies. Therefore, we have to re-examine the customary separation into electronic and nuclear eigenfunctions.

The Schrödinger equation for the total molecular wave function can be written in the following form

$$\sum_{\kappa} \frac{h^2}{8\pi^2\mu} \Delta_{\kappa} \psi + \sum_k \frac{h^2}{8\pi^2 M_k} \Delta_k \psi + (E - U_{nn} - U_{ne} - U_{ee}) \psi = 0. \quad (1)$$

Here  $\sum_{\kappa}$  indicates summation over all electrons,  $\sum_k$  summation over the nuclei.  $\mu$  is the mass of the electron,  $M_k$  that of the  $k$ th nucleus,  $\Delta$  is the Laplacian operator with  $\Delta_{\kappa}$  and  $\Delta_k$  indicating differentiations with respect to the  $\kappa$ th electron and the  $k$ th nucleus.  $U_{nn}$ ,  $U_{ne}$  and  $U_{ee}$  are the Coulomb potentials between nuclei and nuclei, nuclei and electrons, electrons and electrons.  $E$  is the total energy of the molecule.

According to Born and Oppenheimer<sup>14</sup>  $\psi$  can be approximated by a product

$$\psi = \psi_{e1} \psi_n. \quad (2)$$

$\psi_{e1}$  is the wave function of the electrons moving in the field of nuclei kept in fixed positions

$$\sum_{\kappa} \frac{h^2}{8\pi^2\mu} \Delta_{\kappa} \psi_{e1} + (E_{e1} - U_{ne} - U_{ee}) \psi_{e1} = 0. \quad (3)$$

$E_{e1}$  is the eigenvalue of electronic motion in the field of fixed nuclei. Equation (3) contains the nuclear positions as parameters. Thus  $U_{ne}$  depends on both nuclear and electronic coordinates and because of the influence of this term  $\psi_{e1}$  too will contain the nuclear positions as parameters.  $E_{e1}$  also depends on the nuclear positions.

The function  $\psi_n$  depends on the nuclear posi-

tions alone. It satisfies the equation

$$\sum_k \frac{h^2}{8\pi^2 M_k} \Delta_k \psi_n + [E - (E_{e1} + U_{nn})] \psi_n = 0. \quad (4)$$

It is seen from (4) that the nuclei move in a potential  $U_{nn} + E_{e1}$ , which is the sum of electronic energy  $E_{e1}$  and Coulomb interaction of the nuclei  $U_{nn}$ . Both terms are, of course, dependent upon nuclear positions.  $E_{e1}$  takes different values for the various electronic states. The nuclei move therefore in different effective potential fields for each electronic state.

The validity of approximation (2) can be tested by multiplying (3) with  $\psi_n$ , (4) with  $\psi_{e1}$ , adding and comparing the result with the expression obtained when substituting (2) into (1). The agreement is exact with the exception of the dependence of  $\psi_{e1}$  on the nuclear positions. Because of this dependence the terms

$$\sum_k \frac{h^2}{4\pi^2 M_k} (\text{grad}_k \psi_n \cdot \text{grad}_k \psi_{e1}) \quad (5a)$$

and

$$\sum_k \frac{h^2}{8\pi^2 M_k} \psi_n \Delta_k \psi_{e1} \quad (5b)$$

appear when (2) is substituted into (1) and only if these terms are neglected does the product (2) satisfy the strict Schrödinger Eq. (1). (The symbol  $\text{grad}_k \psi$  stands for the vector whose components are the derivatives of  $\psi$  with regard to the  $x$ ,  $y$  and  $z$  coordinates of the  $k$ th nucleus. The product appearing in (5a) is a scalar product of the vectors  $\text{grad}_k \psi_n$  and  $\text{grad}_k \psi_{e1}$ .)

The neglected terms (5a) and (5b) are small as compared to the kinetic energy

$$\sum_k \frac{h^2}{8\pi^2 M_k} \psi_{e1} \Delta_k \psi_n$$

of the nuclei which in turn is, as a general rule, about 100 times smaller than the electronic energies. In fact, the nuclear wave function  $\psi_n$  changes more rapidly with the nuclear coordinates than  $\psi_{e1}$ , that means differentiation of the latter will give rise to a smaller term than differentiation of the former. The ratio of the two is approximately given by the breadth of one crest in the  $\psi_n$  wave divided by the extension of  $\psi_{e1}$  or by the ratio of electronic and nuclear

momenta  $p_{el}/p_n$ . Thus, (5a) is about  $p_{el}/p_n$  times smaller than the kinetic energy of the vibrations and (5b) is  $(p_{el}/p_n)^2$  times smaller than the same quantity. Remembering that vibrational energies divided by electronic energies are approximately equal to the square root of electronic mass to nuclear mass and that  $p_{el}/p_n$  is approximately equal to the fourth root of the same ratio, one sees that the neglected terms (5a) and (5b) are small indeed.

An exact solution of (1) can be obtained by taking a sum over terms of type (2) with  $\psi_{el}$  in the sum belonging to the different solutions of (3) and  $\psi_n$  representing approximate coefficients depending on nuclear positions alone. The sum can be obtained by starting from the single term given in (2) and introducing (5a) and (5b) as perturbations. If the perturbation is small new terms will appear with small coefficients.

In the case of a linear molecule in a degenerate state, however, the difference in electronic energies due to the splitting of degeneracy (see Fig. 4) is no longer small as compared to some terms in (5a) and (5b). The simple product function is therefore a poor approximation. One has to use two terms containing the electronic wave functions  $\psi_{el}^+$  and  $\psi_{el}^-$  into which the originally degenerate functions split

$$\psi = \psi_{el}^+ \psi_n^+ + \psi_{el}^- \psi_n^- \quad (6)$$

Here  $\psi_n^+$  and  $\psi_n^-$  are wave functions depending on nuclear positions alone. They have to be chosen in such a way as to make (6) a good approximation for the solution of (1).

In the following discussion<sup>26</sup> we shall restrict ourselves for the sake of simplicity to molecules of the  $\text{CO}_2$  type, i.e. to linear triatomic molecules with a center of symmetry.  $\psi_{el}^+$  and  $\psi_{el}^-$  will be symmetrical and antisymmetrical, respectively, to the plane determined by the three nuclei. We assume that the two originally degenerate levels transform like  $e^{+i\Lambda\varphi}$  and  $e^{-i\Lambda\varphi}$  when the electrons are rotated through an angle  $\varphi$ . ( $\Lambda$  has the same significance as on p. 78)  $\psi_{el}^+$  and  $\psi_{el}^-$  will then transform like  $\cos\Lambda(\varphi - \varphi_n)$  and  $\sin\Lambda(\varphi - \varphi_n)$  where  $\varphi_n$  is the angle enclosed by the plane through the three atoms and another plane fixed in space and passing through the equilibrium

configuration of the atoms. If (6) were substituted into (1) and differentiations of  $\psi_{el}^+$  and  $\psi_{el}^-$  with regard to coordinates of the nuclei were neglected, the usual Born-Oppenheimer approximation would be obtained. However, the derivatives of  $\psi_{el}^+$  and  $\psi_{el}^-$  with regard to  $\varphi_n$  are no longer small as compared to the derivatives of the  $\psi_n$  functions. Therefore, the terms (5a) and (5b) can be neglected only if the differentiations appearing in these expressions are not carried out with respect to  $\varphi_n$ . The latter give, because of the transformation properties of  $\psi_{el}^+$  and  $\psi_{el}^-$ ,

$$\begin{aligned} \frac{\partial \psi_{el}^+}{\partial \varphi_n} &= \Lambda \psi_{el}^-, & \frac{\partial \psi_{el}^-}{\partial \varphi_n} &= -\Lambda \psi_{el}^+; \\ \frac{\partial^2 \psi_{el}^+}{\partial \varphi_n^2} &= -\Lambda^2 \psi_{el}^+, & \frac{\partial^2 \psi_{el}^-}{\partial \varphi_n^2} &= -\Lambda^2 \psi_{el}^-. \end{aligned} \quad (7)$$

Since  $\psi_{el}^+$  and  $\psi_{el}^-$  satisfy differential equations

$$\begin{aligned} \sum_k \Delta_k \psi_{el}^+ + (E_{el}^+ - U_{ne} - U_{ee}) \psi_{el}^+ &= 0, \\ \sum_k \Delta_k \psi_{el}^- + (E_{el}^- - U_{ne} - U_{ee}) \psi_{el}^- &= 0, \end{aligned} \quad (8)$$

substitution of (6) into (1) gives terms in which the electronic dependence is contained either in a factor  $\psi_{el}^+$  or in  $\psi_{el}^-$ . Thus (1) will be satisfied if the factors of  $\psi_{el}^+$  and  $\psi_{el}^-$  are put equal to zero:

$$\begin{aligned} \sum_k \frac{h^2}{8\pi^2 M_k} \Delta_k \psi_n^+ - \Lambda \frac{h^2}{4\pi^2 \xi^2} \frac{\partial \psi_n^-}{\partial \varphi_n} - \Lambda^2 \frac{h^2}{8\pi^2 \xi^2} \psi_n^+ \\ + [E - (E_{el}^+ + U_{nn})] \psi_n^+ &= 0, \\ \sum_k \frac{h^2}{8\pi^2 M_k} \Delta_k \psi_n^- + \Lambda \frac{h^2}{4\pi^2 \xi^2} \frac{\partial \psi_n^+}{\partial \varphi_n} - \Lambda^2 \frac{h^2}{8\pi^2 \xi^2} \psi_n^- \\ + [E - (E_{el}^- + U_{nn})] \psi_n^- &= 0. \end{aligned} \quad (9)$$

The quantity  $\xi^2$  is the square of the distance of the central atom to the line joining the two outer atoms multiplied with the reduced mass of the central atom  $M_c$  and the two outer atoms  $M_0$ , i.e. with  $2M_c M_0 / (M_c + 2M_0)$ . The second terms in (9) correspond to (5a) and the third terms to (5b). The second terms couple the two Eqs. (9) which therefore must be solved simultaneously. The resulting eigenvalues  $E$  contain the customary vibrational contributions due to the normal vibrations taking place along the molecular axis (i.e., vibrations with transformation properties similar to those of  $\Sigma$  states). Deformation vibra-

<sup>26</sup> R. Renner, Zeits. f. Physik 92, 172, (1934).



tions, however, (transforming like  $\Pi$  states, see Fig. 3 for  $\text{CO}_2$ ), are coupled with the electronic motion intimately and no series of equidistant or nearly equidistant levels can be expected as for vibrations along the molecular axis. Only if one of the functions  $\psi^+_n$  and  $\psi^-_n$  is independent of  $\varphi$  will the other vanish. In this case simple equidistant or nearly equidistant series of vibrational levels are obtained. The eigenvalues of the deformation vibration in a molecule of the  $\text{CO}_2$  type coupled with a  $\Pi$  state are shown in Fig. 7.

The deviation from the simple harmonic level scheme is, of course, due to the splitting  $E^+_{e1} - E^-_{e1}$  of the electronic level. It is useful therefore, to write (9) in a form in which the splitting appears in a direct way. We put

$$\frac{1}{2}(E^+_{e1} + E^-_{e1}) = E_{e1}, \quad \frac{1}{2}(E^+_{e1} - E^-_{e1}) = \bar{\epsilon};$$

$$\psi^+_n + i\psi^-_n = \psi^i_n, \quad \psi^+_n - i\psi^-_n = \psi^{-i}_n$$

and obtain from (9) by adding  $+i$  and  $-i$  times the second equation to the first

$$\begin{aligned} \sum_k \frac{h^2}{8\pi^2 M_k} \Delta_k \psi^i_n + i\Lambda \frac{h^2}{4\pi^2 \xi^2} \frac{\partial \psi^i_n}{\partial \varphi_n} - \Lambda^2 \frac{h^2}{8\pi^2 \xi^2} \psi^i_n \\ + [E - (E_{e1} + U_{nn})] \psi^i_n - \bar{\epsilon} \psi^{-i}_n = 0, \\ \sum_k \frac{h^2}{8\pi^2 M_k} \Delta_k \psi^{-i}_n - i\Lambda \frac{h^2}{4\pi^2 \xi^2} \frac{\partial \psi^{-i}_n}{\partial \varphi_n} - \Lambda^2 \frac{h^2}{8\pi^2 \xi^2} \psi^{-i}_n \\ + [E - (E_{e1} + U_{nn})] \psi^{-i}_n - \bar{\epsilon} \psi^i_n = 0. \end{aligned} \quad (10)$$

Equations (10) are useful if the splitting is small. Then, in first approximation, the terms containing  $\bar{\epsilon}$  can be neglected and the two Eqs. (10) become independent of each other. They can be reduced to (4) by setting  $\psi^i_n = e^{-i\Lambda\varphi_n} \psi_n$  and  $\psi^{-i}_n = e^{i\Lambda\varphi_n} \psi_n$ . It is easy to verify that with these substitutions (6) reduces to (2). Thus we obtain the undisturbed vibrational levels as the eigenvalues of (9). The terms containing  $\bar{\epsilon}$  can then be reintroduced into (10) and their effect treated as a perturbation. The broken curves in Fig. 7 have been obtained by this method.

The dependence of the splitting  $E^+_{e1} - E^-_{e1}$  on the amplitude of the deformation vibration differs for the various electronic states. The effect of the nuclear displacement can be described by dipoles with their negative charge at the original nuclear position and their positive charge at the

new position. The mean value of the perturbation by such dipoles is zero for any electronic wave function. Thus the first-order perturbation vanishes and the splitting does not depend linearly on the nuclear displacements, a fact which has been mentioned before. Perturbation matrix elements exist, however, between  $\Sigma$  and  $\Pi$  states,  $\Pi$  and  $\Delta$  states and, in general, between states which differ by one unit in  $\Lambda$ . Therefore, only second-order perturbations due to the dipoles will be effective and the splitting will change quadratically with nuclear displacement. A further quadratic term in the splitting is obtained from the quadrupole associated with the nuclear displacement. This quadrupole causes a splitting by a first-order perturbation, but the quadrupole itself changes quadratically with the displacement. In general the splitting will be of the same order of magnitude as the potential energy of vibration.

In a  $\Delta$  state the two degenerate wave functions transform like  $e^{2i\varphi}$  and  $e^{-2i\varphi}$ . The mean value of the dipole perturbation is again zero. Dipole matrix elements exist between the  $e^{2i\varphi}$  wave function and  $\Pi$  states which transform like  $e^{i\varphi}$ ; also between the latter and  $\Sigma$  states, between  $\Sigma$  states and the  $e^{-i\varphi}$  parts of the  $\Pi$  functions; and finally between the  $e^{-i\varphi}$  functions and the  $e^{-2i\varphi}$  component of the original  $\Delta$  function. Thus four matrix elements establish the shortest conjunction between the two originally degenerate functions. It can be shown easily that a splitting of the two levels occurs only in fourth order and the splitting is, therefore, proportional to the fourth power of the displacement. The same result is obtained when the effects of quadrupole and higher-pole perturbations are considered. A similar argument shows that the splitting is proportional to the nuclear displacement into the  $2\Lambda$ th power if the original wave functions transform like  $e^{\pm i\Lambda\varphi}$ . In  $\Delta$  states as well as in states with higher  $\Lambda$  values the splitting will be small as compared to the vibrational energy at least as long as the vibrational amplitudes are not too great, because the vibrational energy increases with the second power of the amplitude and the splitting with a higher power. In these cases Eq. (10) will be used in preference to (9) and the terms containing  $\bar{\epsilon}$  can be taken into account as a perturbation.

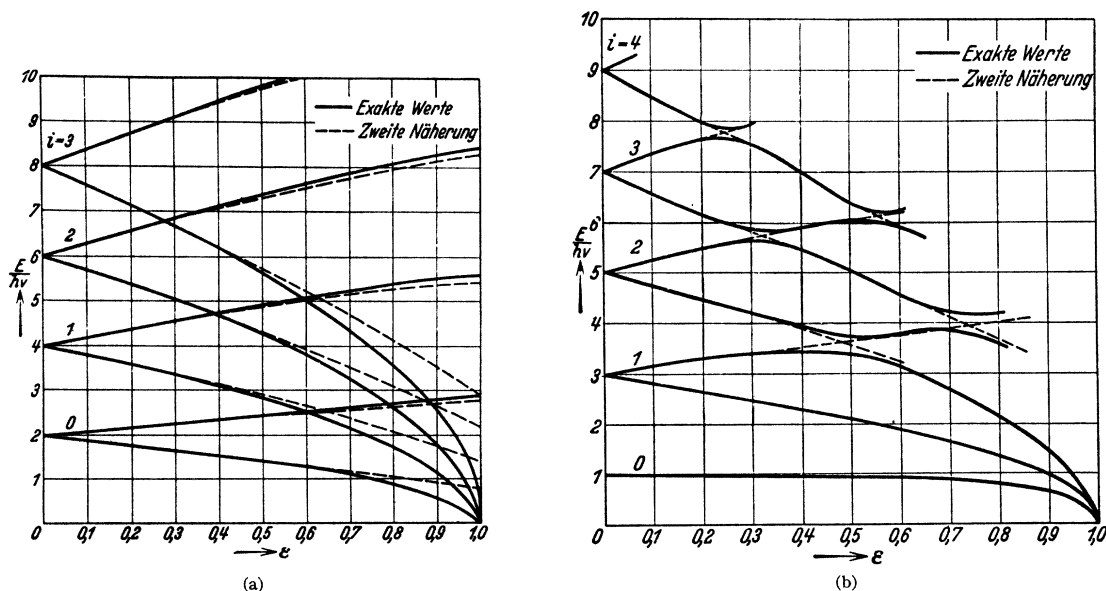


FIG. 7. (Taken from R. Renner, *Zeits. f. Physik* **92**, 186 and 190 (1934).) Eigenvalues of the deformation vibration in a  $\Pi$  term with the total angular momentum about the figure axis  $K=0$  (Fig. 7(a)) and  $|K|=1$  (Fig. 7(b)) as function of  $\epsilon$ . Here  $\epsilon = (E_{e1}^+ - E_{e1}^-) / (E_{e1}^+ + E_{e1}^-)$ . The unit in which the ordinate is measured is  $h\nu$  where  $\nu$  is the vibrational frequency for an oscillator with the potential energy  $\frac{1}{2}(E_{e1}^+ + E_{e1}^-)$ . In Fig. 7(a)  $i$  stands for  $2v$ , in 7(b) for  $2v+1$ . For  $v > 1$  the quantity  $|K|$  may be greater than one. No calculations exist for this case.

### Violation of Selection Rules

In diatomic molecules selection rules based upon symmetry of the electronic wave function are violated for two main reasons: collisions between molecules and coupling with rotation. The first reason may also cause violation of selection rules in polyatomic molecules. The effect of rotation is, as a general rule, somewhat less pronounced in polyatomic molecules because of their greater moments of inertia and smaller angular velocities. It is, moreover, rather unimportant, even for diatomic molecules.

In polyatomic molecules there exists a third reason for the breakdown of pure electronic selection rules: excitation of molecular vibrations. They may destroy the molecular symmetry while vibrations of diatomic molecules never have this effect. One important consequence is that forbidden transitions in polyatomic molecules may gain in intensity if the temperature is raised and as a result vibrations are excited. If of appropriate symmetry, they tend to make the formerly forbidden transition allowed.

A more detailed investigation of the influence of vibration reveals that the vibrational structure of an allowed band spectrum is different from the structure of a spectrum made allowed by the

effect of vibrations. As will be seen we can even make, with the help of the vibrational structure, definite statements about the symmetry of the combining electronic states. Thus, study of the vibrational structure plays to some extent the same rôle in polyatomic spectra as the analysis of rotational structure in diatomic spectra. This is fortunate because rotational lines in polyatomic spectra are frequently so closely spaced and have often such a complicated arrangement that it may become impractical to arrive from their study at electronic symmetries.

The classical treatment (p. 88) can be extended to cover those electronic transitions which are forbidden for the equilibrium state of the nuclei but become allowed if the nuclei are displaced in a non-symmetrical way. For the sake of simplicity we shall assume here that the electronic frequency does not change with the nuclear displacement. Since the transition is forbidden we have  $\mathfrak{M} = 0$  for the equilibrium configuration. For small vibrational amplitudes we assume that  $\mathfrak{M}$  varies linearly with the displacement reaching a maximum value of  $\mathfrak{M}_v$ . The expression for  $\mathfrak{M}(t)$  is then

$$\begin{aligned} \mathfrak{M}(t) &= \mathfrak{M} \exp[2\pi i \nu_e t] = \mathfrak{M}_v \cos 2\pi i \nu_v t \exp[2\pi i \nu_e t] \\ &= \frac{1}{2} \mathfrak{M}_v \exp[2\pi i (\nu_e + \nu_v) t] \\ &\quad + \frac{1}{2} \mathfrak{M}_v \exp[2\pi i (\nu_e - \nu_v) t]. \end{aligned}$$

From the last expression we see that the only frequencies to appear in the Fourier analysis are  $\nu_e + \nu_v$  and  $\nu_e - \nu_v$  while the simple electronic frequency is absent. The corresponding statement in quantum theory is that during the electronic transition the non-totally symmetrical vibration in question must change its energy by  $+$  or  $-$  one quantum. This is indeed the case if, as we have assumed, the electronic transition is made allowed only by the vibration in question.

It is easy to see that whenever several vibrations have the property of removing the selection rule, the frequencies of any one of them may appear added to or subtracted from  $\nu_e$ . This is valid if  $\mathfrak{M}$  is a homogeneous linear function of all nuclear displacements which make the transition allowed. Each vibration contributes then two terms to the Fourier expansion  $\nu_e \pm \nu_v$  in which the corresponding vibrational frequency  $\nu_v$  appears.

In the strict quantum-mechanical treatment the following statements about breakdown of selection rules do not affect the strict rule that the *total* wave functions must obey the selection rules contained in Tables II, IV, VI, VIII and X. This "strict" rule can be violated by collisions or by coupling with rotation or spin but not by excitation of vibrations. Only those rules need be restricted which concern electronic and vibrational functions separately.

One assumption on which the conclusions in section *b* have been based was that the electronic matrix element of the dipole moment  $\mathfrak{M} = \int \psi'^*_{el} M \psi''_{el} d\tau_{el}$  does not depend on the nuclear positions. In reality  $\mathfrak{M}$  does vary with displacements of nuclei.<sup>27</sup> If they are small  $\mathfrak{M}$  can be expanded into a power series in the displacements:

$$\mathfrak{M} = \mathfrak{M}_0 + \sum_i \mathfrak{M}_i \xi_i + \sum_{ik} \mathfrak{M}_{ik} \xi_i \xi_k + \dots \quad (11)$$

Here the  $\xi_i$  represent normal coordinates giving the magnitude of the displacements in the  $i$ th normal vibration.<sup>28</sup>  $\mathfrak{M}_0$ ,  $\mathfrak{M}_i$ ,  $\mathfrak{M}_{ik}$  are coefficients

<sup>27</sup> A. S. Coolidge, H. M. James and R. D. Present, J. Chem. Phys. **4**, 193 (1936).

<sup>28</sup> One may use the normal coordinates in any of the two combining levels or one can use any set of general coordinates describing the relative positions of nuclei. But to facilitate the derivation of selection rules it is of advantage to use coordinates with transformation properties as described in Tables I, III, V, VII, IX. Normal coordinates fulfill this condition.

in the expansion. Some of them may vanish for reasons of symmetry. If  $\mathfrak{M}$  consists only of the constant term  $\mathfrak{M}_0$  then we have simply the rules stated in the previous section. From the terms  $\mathfrak{M}_i \xi_i$  one obtains the contributions  $\mathfrak{M}_i \int \psi'^*_{vib} \xi_i \psi''_{vib} d\tau_{nuc}$  to the transition matrix element. According to rules of group theory the integral is different from zero when the direct product of the initial and final wave functions contains the transformation properties of  $\xi_i$ . If the  $i$ th vibration is totally symmetrical this condition is identical with the one obtained in the previous section. If the  $i$ th vibration is non-totally symmetrical new bands appear among which those are the strongest in which the initial and final states, apart from changes in totally symmetrical vibrations, differ only in one quantum of the  $i$ th vibration. Thus the rule of the previous section, that no transitions are possible from a state in which no non-totally symmetrical vibrations are excited to one in which only one of these vibrations is excited by one quantum, can be violated. This will happen only if the coefficient  $\mathfrak{M}_i$  is different from zero. It need not be discussed separately what the symmetry requirements are for  $\mathfrak{M}_i \neq 0$ , since they are fulfilled then and only then when the strict selection rule for the total eigenfunctions  $\psi_{rel} = \psi_{el} \psi_n$  is satisfied.

The transitions discussed above, in which one non-totally symmetrical vibration changes by one quantum, are always among the strongest transitions belonging to the term  $\mathfrak{M}_i \xi_i$ . Unless the potential surfaces differ very greatly all other additional transitions are of considerably smaller intensity. But even the strongest transitions caused by  $\mathfrak{M}_i \xi_i$  are weak as compared to the strongest bands due to  $\mathfrak{M}_0$ . Indeed one can show<sup>16</sup> that the intensity ratio of the bands caused by  $\mathfrak{M}_i \xi_i$  to the bands due to  $\mathfrak{M}_0$  is of the order of magnitude<sup>29</sup>

$$\left( \sum_{kp} \frac{Z^*_{ke^2} |\xi_{ik}|}{\Delta E_p r^2} \right)^2. \quad (12)$$

Here  $|\xi_{ik}|$  is the displacement of the  $k$ th nucleus

<sup>29</sup> In order to be accurate one should take sums of the kind appearing in (12) for both initial and final states and combine the results. Since, however, at best only rough estimates are possible we may restrict ourselves to that state which gives the greater value.

due to the  $i$ th normal vibration.  $Z_{ke}^*$  is the effective charge of that nucleus and  $e$  the charge of the electron.  $r$  is a length of the magnitude of the molecular dimension and  $\Delta E_p$  is the energy difference between one of the combining states and any other electronic level  $E_p$  with proper symmetry. An electronic eigenfunction  $\psi_{e1}$  has the proper symmetry if the direct product of  $\psi_{e1}$  and the original electronic function contains the transformation properties of the  $i$ th normal vibration. In  $|\xi_{ik}|$  only displacements which occur during vibrations in the initial state are counted. Although the molecule may vibrate violently after the transition and  $\psi_n$  of the final state may be spread out over a large region, the magnitude of  $\int \psi_n^* \xi_i \psi_n' d\tau_n$  and with it the sum over  $\xi_{ik}$  is determined by the less extended wave function which usually belongs to the initial state. If  $Z_{ke}^* \simeq 1$  and  $e^2/r$  is approximately equal to the smallest possible value of  $\Delta E_p$  (conditions fulfilled for the normal case) then the ratio of intensities will be  $|\xi_{ik}/r|^2$ , i.e., about  $10^{-2}$ – $10^{-4}$ . This means that the additional bands discussed in the present section are relatively weak. The same holds to an even greater extent for the bands obtained from higher terms in expansion (11). Therefore, they need not be discussed in detail particularly, since most of the selection rules which can be violated by vibrations will already break down under the influence of  $\mathfrak{M}_i \xi_i$ . A greater effect can be expected only for extremely small values of  $\Delta E_p$  (smaller than 1 ev). If an energy level  $E_p$  of proper symmetry lies close to one of the combining levels, then this level will be particularly easily polarizable and even small nuclear displacements may cause a breakdown of the selection rules obtained for the equilibrium configuration.

In spite of the usually small intensity of transitions due to the  $\mathfrak{M}_i \xi_i$  terms they become rather important if the main term  $\mathfrak{M}_0$  vanishes. This is the case for transitions which according to electronic selection rules alone are forbidden, but for which the electronic transition matrix element differs from zero as soon as the nuclei leave their equilibrium positions. In such "forbidden" electronic band systems the usually allowed vibrational transitions (in which  $\psi_n'$  and  $\psi_n''$  have the same symmetry properties) do not appear. Only the weak bands in which

non-totally symmetrical vibrations are excited will be present. Among them changes by one quantum number of a non-totally symmetrical vibration will be most frequent. The structure of such a forbidden electronic band system consists, therefore, of one or several non-totally symmetrical vibrational transitions which make the transition allowed; superimposed on each such transition should be found the whole vibrational structure typical for an allowed electronic band system.

We shall now discuss which transitions can be made allowed by a single vibration. Because of the normal displacement  $\xi_i$  each of the combining electronic levels will be disturbed by other levels  $E_p$  of proper symmetry. If  $\xi_i$  makes the transition allowed one of the combining electronic functions, say  $\psi_{e1}'$ , must be disturbed by a function  $\psi_{e1}^p$  which in turn combines according to the electronic selection rules with  $\psi_{e1}''$ . This means, that  $\psi_{e1}' \psi_{e1}^p$  and also  $\psi_{e1}^p \psi_{e1}''$  must contain a totally symmetrical term, or, according to group theory,  $\psi_{e1}' \xi_i \psi_{e1}''$  must contain a term which remains unchanged during all symmetry operations. Somewhat less exactly one may say that  $\xi_i$  will make the transition allowed if a level exists which combines with  $\psi_{e1}''$  and differs from  $\psi_{e1}'$  by the transformation properties of  $\xi_i$ . The same holds, of course, when the roles of  $\psi_{e1}'$  and  $\psi_{e1}''$  are interchanged.

The forbidden transition will have a considerable intensity only if  $E_p$  lies close to the level which it disturbs. In such cases a stronger allowed transition must lie close to the forbidden one. Their vibrational structures might easily overlap and the analysis may become difficult.

We are now in a position to obtain from the vibrational structure information about the symmetry of the combining states. If, for instance, we find that a transition is made allowed by a vibration with the displacement  $\xi_i$  we may conclude that  $\psi_{e1}' \xi_i \psi_{e1}''$  contains a totally symmetrical term, or we may say that  $\psi_{e1}' \psi_{e1}''$  contains the transformation properties of  $\xi_i$ .

The application of this rule is facilitated by the fact that most actual examples concern absorption spectra where the lower state  $\psi_{e1}''$  is totally symmetrical. Then the transformation properties of  $\xi_i$  must be contained in the product

$M\psi_{e1}$ . If for instance, we have a molecule of the symmetry  $V_h$  and if a forbidden absorption is made allowed by vibrations of the symmetries  $\alpha_{1u}$ ,  $\beta_{2u}$  and  $\beta_{3u}$  then one can conclude that  $\psi'_{e1}$  has the symmetry  $B_{1g}$ . Indeed, according to Table IV  $B_{1g}$  is the only state from which  $A_{1u}$ ,  $B_{2u}$  and  $B_{3u}$  are obtained, when multiplied with the transformation properties of the three components of  $M$ , i.e., with  $B_{1u}$ ,  $B_{2u}$  and  $B_{3u}$ .

The general law governing the symmetry properties of the displacement  $\xi_i$ , that makes the transition allowed, leads to another specific consequence. If the transition is forbidden because of the presence of a symmetry element with regard to which all wave functions show either symmetrical or antisymmetrical behavior,  $\xi_i$  must be antisymmetrical to that symmetry element. We may consider, for instance, a molecule with a center of symmetry. Just as in spectra of atoms or of diatomic molecules even-even ( $g-g$ ) and odd-odd ( $u-u$ ) combinations are forbidden. However, such transitions may be made permitted by vibrations which are antisymmetrical to the center.

Finally we should mention a second general reason for the breakdown of selection rules. In the foregoing we have made use of the Born-Oppenheimer product approximation Eq. (2) for the wave functions while the complete wave function is given by a sum of such products. The additional terms are due to the perturbations (5a) and (5b), the term (5a) usually being the more important one. The deviation from the Born-Oppenheimer approximation causes the appearance of new bands. Their intensity can be obtained by taking into account the perturbing influence of (5a). The ratio of their intensity to that of the allowed bands is approximately<sup>16</sup>

$$\left( \sum_{kp} \frac{h^2 Z_k^* e^2}{4\pi^2 M_k \Delta E_p^2 |\xi_{ik}^0| r^2} \right)^2. \quad (13)$$

Here  $\xi_{ik}^0$  is the zero-point amplitude of the  $k$ th nucleus in the  $i$ th normal vibration. The  $i$ th normal vibration and the perturbing levels  $E_p$  play the same rôle and obey the same symmetry rules as in the previous discussion. But the intensities according to (13) are small as compared to the intensities from (12) except for very small  $\Delta E_p$  values ( $\Delta E_p \lesssim 0.2$  ev).

Deviations from the Born-Oppenheimer approximation can also cause coupling between electronic motion and rotation. This coupling appears also in diatomic molecules.<sup>30</sup> The intensity ratio of bands due to coupling with rotation to the allowed transitions is approximately

$$\mu \omega^2 e^2 r / \Delta E_p^2, \quad (14)$$

where  $\omega$  is the angular velocity of the molecular rotation and  $\mu$  is the mass of the electron. Even for  $\Delta E_p = 0.1$  ev, expression (14) is smaller than  $10^{-3}$ . It will be extremely difficult to find experimental examples for violation of selection rules by rotation, because whenever  $\Delta E_p$  is not very small the intensity of the bands is negligible; and if  $\Delta E_p$  is very small the forbidden spectrum will be overlapped by an allowed one in which  $E_p$  will be one of the combining levels.

#### d. Anharmonicity and Predissociation

In the presence of harmonic forces the frequencies of the normal vibrations are independent of their amplitudes and, moreover, the individual vibrations are independent of each other. This is not strictly true for real molecules, because we encounter here always anharmonic forces. But it is a very good approximation for small amplitudes where the ratio of vibrational amplitude to the internuclear distances is very small. Because of the anharmonicity the vibrational levels are not strictly equidistant and the different normal vibrations are not simply additive. If, because of the anharmonicity, the potential energy increases less than quadratically at larger amplitudes, then the frequencies decrease with increasing amplitudes and the distances between succeeding levels become smaller with increasing energies. This behavior is the rule with diatomic molecules, but in polyatomic molecules also the opposite is possible.

Small anharmonicity should be expected for totally symmetrical vibrations. If such a vibration would lead to dissociation, then usually more than two particles will be the products of dissociation. For example, in benzene the excitation of the totally symmetrical  $C$  vibration of  $992 \text{ cm}^{-1}$  will lead in the limit to a dissociation

<sup>30</sup> R. de L. Kronig, Zeits. f. Physik 50, 347 (1928).

into six CH groups. From this follows that high dissociation energies correspond to such vibrations and that they converge very slowly.

Convergences of vibrational levels are expected in all cases when with increasing internuclear distance the potential curves become flatter than simple parabolas would be. Although this is the usual behavior also in polyatomic molecules, the anharmonicity may occasionally work in the opposite sense.

The effect of anharmonicity upon degenerate levels has been mentioned earlier (p. 86).

The main emphasis in this section will be laid upon predissociation phenomena in polyatomic spectra. The first indication of predissociation in an absorption spectrum is an incipient diffuseness of lines which gives the bands a fuzzy appearance.<sup>31</sup> The phenomenon is due to the fact that the molecule can pass from its stable excited state into a dissociated state. It can be described in terms of the uncertainty principle. According to this principle each level has a certain energy width  $b$  which is connected with the mean life  $\tau$  by the relationship  $b\tau = h/2\pi$ . The shortest observable lifetime is that of a half-vibration which is of the order of  $10^{-13}$  sec. For this time the width is of the same magnitude as the difference between two successive vibrational levels.

The occurrence of predissociation<sup>32</sup> can be most easily discussed by means of Fig. 8, which represents the crossing of two potential curves  $a$  and  $b$ . Absorption or emission of light may bring the molecule to the activated state  $a$  from which it can go over to  $b$  with subsequent dissociation. This happens only if at least point  $D$  is reached which has the same energy as the asymptote of  $b$ . In order that the radiationless transition should occur the two curves  $a$  and  $b$  must disturb each other. This perturbation must be moderate. If it is strong the two curves avoid each other in the indicated way (dotted), and

ordinary dissociation instead of predissociation takes place in the state belonging to the lower curve. If the interaction between curves  $a$  and  $b$  is very weak then the states are independent of each other and there is again no transition between them. Only in the case of moderate interaction when the curves repel each other slightly is there such a small deformation in the intersecting area that one can speak of a transi-

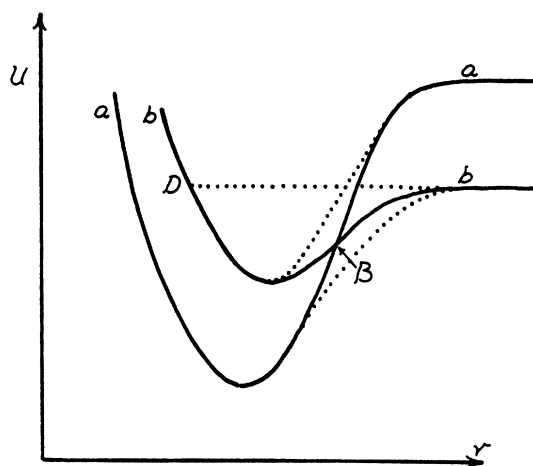


FIG. 8. Potential curves for predissociation.

tion from  $a$  to  $b$ . Now in diatomic molecules there is often too strong an interaction between terms with the same transformation properties and a too weak one between terms which differ in their transformation properties (only caused by rotation). But in polyatomic molecules levels, which for symmetrical nuclear configurations have different transformation properties and hence do not influence each other, may develop such an influence by the excitation of non-totally symmetrical vibrations. The transition probability for such cases is larger than when caused by rotation in diatomic molecules. This together with the fact that there exists a much larger variety of electronic levels in polyatomic than in diatomic molecules accounts for the experience that predissociation phenomena are more frequently observed in the former than in the latter. But while the diffuseness in diatomic spectra sets in more or less suddenly—the width of the diffuse region usually amounts to 10–30 Å and extends over 1 or 2 bands—its beginning can be

<sup>31</sup> V. Henri, *Structure des Molécules* (J. Hermann, Paris, 1925).

<sup>32</sup> For detailed discussion of predissociation in diatomic molecules see: R. de L. Kronig, *Band Spectra and Molecular Structure* (Cambridge University Press, 1930); G. Herzberg, *Ergeb. d. exakt. Naturwiss.* 10, 207 (1931); H. Sponer, *Molekülspektren und ihre Anwendung auf chemische Probleme*, Vol. II (Julius Springer, Berlin, 1936); G. Herzberg, *Molecular Spectra and Molecular Structure* (Prentice-Hall, New York, 1939).

very gradual in polyatomic molecules and can extend over several 100Å.

In polyatomic molecules radiationless transitions will be governed by selection rules which are analogous to Kronig's rules<sup>33</sup> for diatomic molecules and by the Franck-Condon principle. Kronig's first rule that there should be no change in the total angular momentum is valid for polyatomic as well as for diatomic molecules. This is not an important restriction, because the translational motion of the dissociating parts can carry off almost any required amount of angular momentum.

The second rule that the multiplicity is maintained (for small multiplet separations) can also be extended to polyatomic molecules.

The remaining three rules of Kronig concern symmetries of the electronic wave function. Their main contents can be summarized and applied to polyatomic molecules by requiring that the symmetry of the electronic function should remain unchanged during predissociation. In diatomic molecules exceptions of this rule occur on account of interaction between electronic motion and rotation so that transitions with  $\Delta\Lambda = \pm 1$  may take place with very small probability. Such transitions of small probability may also occur in polyatomic molecules. The symmetry properties of the wave functions before and after the radiationless transition will differ by transformation properties of the nuclear displacements produced by an infinitesimal rotation. But these transitions are less probable in polyatomic than in diatomic molecules because angular velocities are smaller for the former. More important are changes in the electronic wave functions caused by coupling between electronic and vibrational motion. The electronic eigenfunctions before and after predissociation will then differ by the transformation properties of a normal vibration. The transformation properties of the total (vibronic) wave function  $\psi_{el}\psi_n$  are, however, preserved. This is in close analogy to the rôle vibrations play in the violation of optical selection rules (p. 96).

If the symmetries of the electronic wave functions remain unaltered then the two potential

surfaces (replacing potential curves of diatomic molecules) may repel each other so strongly that the observed process is a dissociation rather than a predissociation. (See the corresponding relations in a diatomic molecule in Fig. 8.) On the other hand, the coupling between the two electronic states may be weak due to change in multiplicity or because the excitation is localized in molecular regions which are very different in the two combining states. Of course, other reasons may be responsible for a weak coupling. When in addition to a weak coupling, the vibration directly excited in the electronic transition leads to dissociation, then predissociation will occur in a way similar to diatomic molecules. In particular, the broadening of lines will set in rather sharply.

If the two combining electronic states have different symmetries, then a radiationless transition may be caused by non-totally symmetrical vibrations. The larger the amplitude of the corresponding vibration, i.e., the more quanta are excited, the greater is the transition probability. We have seen, on the other hand, that non-totally symmetrical vibrations have a small probability of excitation and are practically never excited with many quanta. Therefore, radiationless transitions will occur with relatively small probability and weak predissociation will be observed.

Even if only totally symmetrical vibrations are excited there is a possibility for predissociation accompanied by a 0-1 transition of a non-totally symmetrical vibration. This change in vibrational quantum number preserves the symmetry of the total wave function  $\psi_{el}\psi_n$ . Predissociation from states in which only totally symmetrical vibrations are excited means in the semi-classical picture that the zero-point amplitude of a non-totally symmetrical vibration is sufficient to cause the radiationless transition. While the strong bands should show only small broadening, the weaker bands which contain also non-totally symmetrical vibrations may show a stronger broadening. This phenomenon can be used to recognize predissociations of the type discussed here.

Another characteristic feature of predissociation in polyatomic spectra is its frequently large

<sup>33</sup> R. de L. Kronig, *Zeits. f. Physik* **50**, 347 (1928); **62**, 300 (1930)

extension over several 100Å as already mentioned. It can be explained<sup>34</sup> by the simultaneous action of several normal vibrations. The potential curves of diatomic molecules have in general to be replaced by  $n$ -dimensional hypersurfaces for polyatomic molecules. The nuclear motion in the molecule can be represented by the motion of a point in such a surface. Dissociation can occur either by passing over a maximum of a surface or by going over to another surface which intersects the first. In either case the point must reach an  $n-1$  dimensional surface lying in the  $n$  dimensional surface. If the excited vibrations together have sufficient energy for dissociation, the separation into fragments can occur only at certain nuclear constellations, and it will take considerable time until this favorable position is reached. Hence this vibrational state will have a long life and the broadening of lines will correspondingly be small. If the energy is increased the  $n-1$  dimensional surface, in which dissociation takes place, becomes accessible for the motion of the point in a larger region. Dissociation can therefore occur within a shorter time and the bands are more diffuse. Thus with increasing oscillation energy the point describing a Lissajous figure needs less time to find the critical region of dissociation. This can also be expressed in quantum-mechanical terms. The wave function extending over the region covered by the Lissajous figure overlaps the region of dissociation. In this overlapping region there exists a perturbation which causes the dissociation. The square of the integral of the wave function taken over this region is proportional to the transition probability. The larger the area of intersection, the greater is this probability and hence the more frequent is predissociation.

The motion of the representative point will be much simpler in highly symmetrical molecules, because they possess a smaller number of totally symmetrical vibrations. In such molecules dissociation processes in which the symmetry is preserved are not probable because they would lead to separation into too many parts (p. 99). On the other hand, totally symmetrical vibrations are most strongly excited in electronic

transitions. Now, since it is improbable that they lead to dissociation one must conclude that non-totally symmetrical vibrations are mostly responsible for dissociation processes in highly symmetrical molecules. This shows that dissociation takes place from a region of the hypersurface which is not reached by totally symmetrical vibrations. But at larger amplitudes, as mentioned before, anharmonic forces become more important and couple totally symmetrical with non-totally symmetrical vibrations which may lead to dissociation. But since this coupling is relatively weak, the molecule will need a long time until it reaches a position advantageous for dissociation.<sup>35</sup> As dissociation takes place from an unsymmetrical configuration, conservation of the symmetry of the electronic wave function need not be discussed here. Again, the weaker bands in which non-totally symmetrical vibrations are excited will be more broadened than those containing only totally symmetrical vibrations. But even in the latter diffuseness will become more pronounced with increasing amplitudes because of the larger influence of anharmonicity.

An increase of broadening in absorption spectra is to be expected with rising temperature. Temperature will be particularly effective by exciting non-totally symmetrical vibrations in the ground state. Then according to the selection rules, they will also be excited in the upper state. As mentioned before, this is in many cases favorable for predissociation.

#### e. Rotational Structure

It has been stated that the rotational structure in spectra of polyatomic molecules does not have the same great practical importance as the rotational structure for diatomic molecules. With the exception of rather simple molecules the resolution of rotational structure is all but impossible. Nevertheless, the careful analysis which has been carried out in the case of a few molecules ( $\text{H}_2\text{CO}$ ,<sup>36</sup>  $\text{CS}_2$ ,<sup>37</sup>  $\text{NO}_2$ ,<sup>38</sup>  $\text{SO}_2$ <sup>39</sup>) makes

<sup>34</sup> See case 3 in J. Franck, H. Sponer and E. Teller, reference 34.

<sup>35</sup> G. H. Dieke and G. B. Kistiakowsky, *Phys. Rev.* **45**, 4 (1934).

<sup>37</sup> L. N. Liebermann, *Phys. Rev.* **58**, 183 (1940); **59**, 106A (1941).

<sup>38</sup> L. Harris and G. W. King, *J. Chem. Phys.* **8**, 775 (1940)

<sup>39</sup> N. Metropolis, *Phys. Rev.* **59**, 106A (1941).

<sup>34</sup> J. Franck, H. Sponer and E. Teller, *Zeits. f. physik. Chemie* **B18**, 88 (1932).



it probable that the rotational structure will eventually yield valuable information about the simpler polyatomic molecules. The great improvement in experimental technique allows better resolution and thus the possibilities of an exact analysis have increased considerably. In the present report we shall restrict ourselves to a qualitative discussion of the rotational structure.

Even such a qualitative procedure may lead to useful results. It yields not only an estimate of the moments of inertia but also gives information about the position of the electric transition moment within the molecule. Thus, if the moments of inertia are very different in different directions ( $\text{H}_2\text{CO}$ ,  $\text{H}_3\text{CI}$ ) or if the molecule is linear, even the rough appearance of "parallel" and "perpendicular" bands may show that the electronic moment is parallel or perpendicular to the axis of smallest moment of inertia.

The rotational energy levels are, of course, those familiar from the theory of rotational structures in the infra-red: the selection rules are also practically identical with rules encountered in infra-red spectra. The only important deviation from the infra-red spectra is that the moments of inertia may be quite different in the initial and final states. Rotational bands with pronounced heads and a shading towards the red or violet side result. Since as a general rule the moments of inertia are greater in the excited state, degradation toward the red is more common. However, the opposite case may occur and it is even possible that some moments of inertia are larger in the upper electronic state and some in the lower. Thus, bands may be expected which are degraded towards both sides. Bands of  $\text{SO}_2$  seem to show this kind of behavior.<sup>39</sup>

#### Linear Molecules

For linear molecules the moments of inertia are similar to those for a diatomic molecule: the moment of inertia about the molecular axis is zero while the two other moments of inertia are equal. The rotational energy levels and selection rules are essentially the same as for diatomic molecules. The energy levels are<sup>40</sup>

<sup>40</sup> This expression is valid for Hund's case *a* where the spin is strongly coupled to the molecular axis. If the spin is coupled to the axis of total angular momentum, *J* has

$(h^2/8\pi^2 I)[J(J+1) - \theta^2]$  where *I* is the moment of inertia about an axis perpendicular to the figure axis, *J* is the total angular momentum and  $\theta$  is the angular momentum about the molecular axis. In diatomic molecules the corresponding quantity  $\Omega$  signifies the electronic angular momentum (spin and orbit) about the axis while in polyatomic molecules  $\theta$  is obtained by adding the vibrational angular momentum to the electronic angular momentum  $\Omega$ . The rotational selection rules are  $\Delta J = 0, \pm 1$ . In addition  $\Delta J = 0$  is forbidden if  $J = 0$  or if the band corresponds to a  $\theta = 0 \rightarrow \theta = 0$  transition. For  $\Delta\theta = 0$ ,  $\theta \neq 0$  the lines  $\Delta J = 0$  are weak, particularly for high *J* values.

There is one essential difference between the rotational structures of diatomic and of linear polyatomic molecules. In the former case as a general rule either all bands of a band system are parallel bands ( $\Delta\Omega = 0$ ) or all are perpendicular bands ( $\Delta\Omega = 1$ ). In polyatomic molecules perpendicular and parallel bands may occur in the same system. This will happen if a transition is forbidden but can be made allowed both by an  $\alpha$  vibration (with angular momentum = 0 about the figure axis) and also by an  $\epsilon$  vibration (with angular momentum =  $\pm 1$  about the same axis). For instance a  ${}^1\Sigma_g - {}^1\Sigma_g$  transition can be made allowed by an  $\alpha_u$  and by an  $\epsilon_u$  vibration. Those bands in which the  $\epsilon_u$  vibration has changed by  $\pm 1$  quantum are perpendicular bands with strong *P*, *Q* and *R* branches while the bands in which an  $\alpha_u$  vibration changes by  $\pm 1$  quantum are parallel bands, in which the *Q* branch is either absent or weak.

Another complication arises if the molecule is linear only in the initial and non-linear in the final state. The rotational structure of some  $\text{CS}_2$  absorption bands seems to indicate such a behavior.<sup>37</sup> This and similar complications for other types of molecules we shall not discuss here.

#### Spherical Top Molecules

Tetrahedral and octahedral molecules should have particularly simple rotational structure

to be replaced by *L* and  $\theta$  by *K*; *L* and *K* contain only contributions from orbital (nuclear + electronic) momenta. *J* is obtained from *L* by adding the spin momentum. If the spin is zero, then  $J = L$  and  $\theta = K$ . It will be in closer accordance with previous practice to use in this case the quantum numbers *L* and *K*.

since their three moments of inertia are equal. The ellipsoid of the moments of inertia then reduces to a sphere and the rotational structure can be described by the model of a spherical top.

The rotational energy for such molecules is  $(h^2/8\pi^2 I)l(l+1)$ . Here  $I$  is the molecular moment of inertia about any axis and  $l$  is the mean value of the angular momentum of the molecular rotation in units of  $h/2\pi$ .  $l$  differs from the total angular momentum  $J$  by the angular momentum of the vibrations and by the orbital plus spin angular momentum of the electrons in the system of fixed nuclei. While  $J$  is, of course, an integer the mean values of the other angular momenta need not be integers. For  $J$  the selection rule  $\Delta J = \pm 1, 0$  holds, but there is no general selection rule for  $\Delta l$ . According to the difference of electronic and vibrational angular momenta in the normal and excited states  $l$  can change by any amount. Furthermore, the possibility of different orientations of the electronic and vibrational angular momenta with regard to the total angular momentum may give rise to a rather great number of rotational branches. It is of interest to note in this connection that a vibration (or an electronic state) may possess an angular momentum only if the symmetrical product of its representation with itself contains the representation of the rotation. (Designated by  $R$  in Table IX.)

As an example we may consider an  ${}^1A_{1g} - {}^1A_{1g}$  transition in a molecule of symmetry  $O_h$ . This transition is forbidden but is made allowed by a  $\varphi_{1u}$  vibration.  $\varphi_{1u}$  may have an angular momentum since the symmetrical product of  $F_{1u}$  with itself contains  $F_{1g}$ , i.e., the representation corresponding to the rotation of the molecule. From the nine branches ( $\Delta J = \pm 1, 0$  and three possible orientations of the  $\varphi_{1u}$  vibration with respect to the rotational axis) which might be expected, only three appear in the  $0 \rightarrow 1$  and  $1 \rightarrow 0$  transition of  $\varphi_{1u}$ . Actually the rotational selection rules are similar to those known in the infra-red spectrum for spherical top molecules.<sup>41</sup> Just as in the infra-red spectra  $l$  may change by 0 or  $\pm f$  where  $f$  is a number between 0 and 1

characteristic of the vibration in question.  $f$  is different for different vibrations and may change with anharmonicity or through interaction with other vibrational levels. Thus the rotational spacings in the bands of the same system may be different.

A further small splitting of the rotational levels should appear because of orientation of the rotational axis within the molecule. This splitting is, however, due to second-order interaction of the rotation with the vibrations and should be in general negligible.

It should be recalled that allowed transitions in tetrahedral and octahedral molecules always involve a threefold degenerate state and that in such a state the symmetrical nuclear configuration is not stable (p. 92). Unless the degenerate electron moves in an orbit which is practically uncoupled with the remainder of the molecule, the nuclear equilibrium positions in one of the combining states will not correspond to a spherical top and the spectrum will be rather complicated.

### Symmetrical Top Molecules

In symmetrical top molecules two moments of inertia are equal, while the third is different (but not equal to zero). Molecules having one threefold or higher axis of symmetry belong to this class. If the two equal moments of inertia are  $I_A$  and the third moment of inertia about the figure axis is called  $I_C$ , then the energy levels are given by

$$\frac{h^2}{8\pi^2 I_A} [J(J+1) - \theta^2] + \frac{h^2}{8\pi^2 I_C} k^2.$$

Here  $J$  is the quantum number of the angular momentum,<sup>42</sup>  $\theta$  is the quantum number of the component parallel to the figure axis,  $k$  is the component of the angular momentum of molecular rotation parallel to the figure axis.  $J$  and  $\theta$  are integers but  $k$  need not be an integer. The selection rules are  $\Delta J = \pm 1, 0$  and  $\Delta \theta = \pm 1, 0$ . The change of  $k$  may have various values. But frequently the changes in  $k$  correspond to changes

<sup>41</sup> E. Teller and L. Tisza, *Zeits. f. Physik* **73**, 791 (1931); E. Teller, *Hand- und Jahrbuch der chemischen Physik*, Vol. 9, No. 2 (1934), p. 125; D. M. Dennison and M. Johnston, *Phys. Rev.* **47**, 93 (1935).

<sup>42</sup> We consider here only the analog of Hund's case *a*. If the spin is coupled to the axis of total angular momentum or if the spin is zero, then again  $J$  and  $\theta$  have to be replaced by  $L$  and  $K$ .

in  $\theta$  so that  $\Delta k = f\Delta\theta$ . The number  $f$  can again have different values for bands within the same system though, apart from effects of anharmonicity and resonance,  $f$  should remain constant in a progression in which only the quantum number of a totally symmetrical vibration changes. The value of  $\Delta\theta$  is connected with the direction of the electronic transition moment within the molecule. If the transition moment is parallel to the figure axis (parallel bands) we have  $\Delta\theta=0$ . If the transition moment is perpendicular to the figure axis (perpendicular bands) we must expect  $\Delta\theta=\pm 1$ . In allowed perpendicular bands at least one of the combining electronic states must be twofold degenerate. Then the equilibrium position would not be, as a rule, symmetrical and the spectrum would become complicated.

In forbidden transitions parallel and perpendicular bands may occur in the same system because the transition moment may be parallel or perpendicular to the figure axis according to the symmetry of the vibration which makes the transition allowed.

Even the simplest rotational structure of symmetrical top molecules will have a fairly complex appearance. The reason for this is that in the spectrum two important quantum numbers,  $J$  and  $\theta$ , can vary independently so that a twofold sequence of lines is obtained. Thus, for parallel bands the  $Q$  branches corresponding to different  $\theta$  values with  $\Delta\theta=0$  are arranged to form further  $P$ ,  $Q$  and  $R$  branches according to  $\Delta J = +1, 0$  and  $-1$ . Similarly, the  $P$  and  $R$  branches ( $\Delta\theta=\pm 1$ ) which we find for perpendicular bands again form  $P$ ,  $Q$  and  $R$  branches according to the behavior of  $J$ . If  $I_C$  is very small then the quantum number  $\theta$  regulates the rough appearance of the spectrum. In this case we call the more closely spaced branches originating from  $\Delta J = 0, \pm 1$  sub-branches. If  $I_A$  and  $I_C$  are of similar magnitude all the different branches intermingle and it becomes difficult to draw direct conclusions from the structure.

#### *Asymmetrical Top Molecules*

In these molecules all three moments of inertia are different. No general formula can be given for the energy levels. For each quantum

number  $J$  there are  $2J+1$  energy levels, not counting possible interaction with spin. On the other hand, interaction with vibrations and electronic orbits will be simpler because the low symmetry of the molecules in question does not produce electronic or vibrational degeneracies.

The simple selection rule  $\Delta J = 0, \pm 1$  holds. A further selection rule is based on a peculiar symmetry of the rotational eigenfunctions. These functions may be symmetrical or antisymmetrical to three twofold axes coinciding with the principal axes of the ellipsoid of inertia. If these axes are determined by the symmetry of the molecule then one may expect them to be the same in the upper and lower electronic states; one may also expect in this case that the electronic transition moment lies in one of the axes. Under these conditions transitions may occur only between rotational states which have the same symmetry with regard to the axis parallel to the transition moment but have opposite symmetries with regard to the other axes. A similar selection rule is well known for infra-red spectra. If the ellipsoid of the moments of inertia is not determined in its orientation by molecular symmetry then the principal axes in the two combining states will differ and the transition moment will point in an arbitrary direction. Then  $\Delta J = 0, \pm 1$  remains the only selection rule.

#### **f. Isotopic Effect**

Change of frequencies caused by isotopic substitution is a very valuable practical help in analyzing electronic spectra. If, for instance, substitution of an atom by a heavier isotope causes a shift of a band towards the red, one concludes that the atom in question vibrates more strongly in the upper than in the lower molecular state. If conversely, a shift toward the violet is observed, a vibration in the lower molecular state must have been excited and the atom must have participated in that vibration. If finally no change is observed, the atom has not changed its vibrational energy during the electronic transition.

In applying the above simple rules one must consider the shifts of the individual bands with respect to the  $0, 0$  band of the system. The  $0, 0$  band itself has a different position in compounds containing different isotopes. This shift is

produced by the zero-point vibrations. As a general rule the 0, 0 band moves to the violet if heavier isotopes are substituted. This is so because the vibrational frequencies are usually higher in the lower of the combining electronic states, and because the substitution of heavier isotopes causes a greater decrease in the energy

of the zero-point vibrations in the lower electronic state.

More detailed statements about the isotopic effect have been made in connection with infrared and Raman spectra.<sup>43</sup> In electronic spectra these rules have not yet become important and therefore we shall not discuss them here.

## Part II. Applications to Observed Spectra

We have looked for examples of spectra of polyatomic molecules where theoretical considerations of the discussed kind have either been used for an analysis or where they can be applied in the hope of leading to further understanding of such spectra. It must be said that the examples of complete analyses of polyatomic spectra are extremely scarce: the reasons for this have been mentioned in the introduction. We shall not confine ourselves to these few examples, but we shall also discuss some cases where an application of the theoretical methods leads to a partial understanding of the spectrum. The discussions will show along which line further experimental research is necessary in order to reach eventually a full interpretation of these spectra.

### a. Linear Molecules

#### *Mercury Halides*

The mercury halides offer the only examples for completely analyzed spectra of linear molecules.<sup>44</sup> They possess absorption spectra in the vacuum region. The bands which are degraded towards the red lie for HgCl<sub>2</sub> at 1670–1730Å, for HgBr<sub>2</sub> at 1813–1861 and for HgI<sub>2</sub> at 2066–2108Å. All three molecules are linear in their normal states. If they have linear configurations also in the excited states, and if the bands belong to an allowed transition, then we will expect that the non-totally symmetrical vibrations will change in even numbers while the totally sym-

metrical vibration can undergo any change. The mercury halides have two non-totally symmetrical vibrations, a deformation and a valence vibration. The analysis of the spectra shows the validity of the mentioned selection rule very nicely for the deformation vibration which changes always by 0 or 2. The antisymmetrical valence vibration ( $\rightarrow \leftarrow \rightarrow$ ) which has the largest frequency of all three vibrations in these molecules has not been found for any of the three halides. The totally symmetrical vibrations occur in any multiples, as it should be. Thus, the analysis is in complete agreement with the selection rules for an allowed transition. The lower (normal) state of all three molecules is presumably a  $^1\Sigma_g$ . The upper state is probably a  $^1\Sigma_u$ . A  $^1\Pi$  state would, according to our previous discussion (p. 94), very likely produce a much more complicated spectrum.

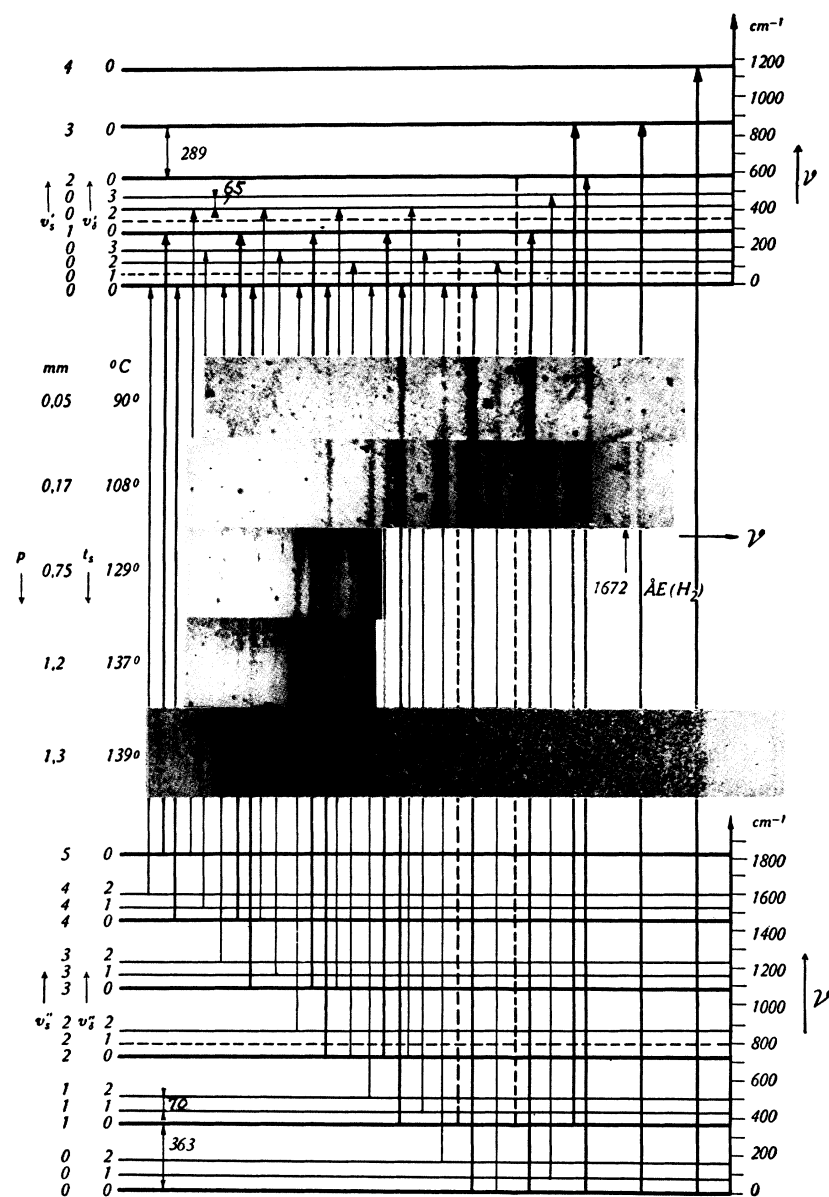
In Fig. 9 the spectrum<sup>45</sup> of HgCl<sub>2</sub> and its analysis is presented. As can be seen, a number of vibrational levels are excited at room temperature. The figure demonstrates that the bands have not very sharp edges and some like the band  $v''_s=2 \rightarrow v'_s=0$ ;  $v''_b=2 \rightarrow v'_b=0$  show no edge at all. In HgBr<sub>2</sub> the bands are much more diffuse as Fig. 10 shows<sup>46</sup> in which also the analysis is included, and in HgI<sub>2</sub> they are extremely diffuse. The broadness of the bands is due to a superposition of a number of vibrational transitions of the small bending vibration,

<sup>43</sup> E. Teller, *Hand- und Jahrbuch der chemischen Physik*, Vol. 9, No. 2 (1934), p. 141; O. Redlich, *Zeits. f. physik. Chemie* **B28**, 371 (1935); J. H. Hibben, *The Raman Effect* (Reinhold Publishing Corporation, 1939), p. 113.

<sup>44</sup> M. Wehrli, *Helv. Phys. Acta* **11**, 339 (1938); H. Spöner and E. Teller, *J. Chem. Phys.* **7**, 382 (1939); M. Wehrli, *Helv. Phys. Acta* **13**, 153 (1940).

<sup>45</sup> We owe the figure to the courtesy of Professor Wehrli. A minor change in the frequency values of the bending vibration has been introduced.

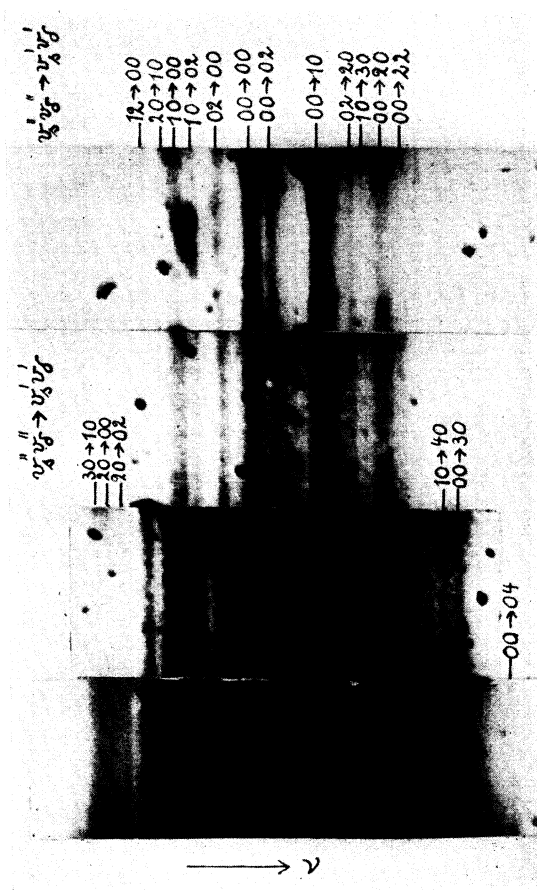
<sup>46</sup> We want to express our sincere thanks to Professor Wehrli for putting the spectrograms of HgBr<sub>2</sub> at our disposal.

FIG. 9. Absorption spectrum of  $\text{HgCl}_2$  and analysis.

so that the 0,0 band for this vibration is in fact a sum of unresolved  $v-v$  transitions. If only the Boltzmann factor is considered, the 0,0 band should be the strongest which would give the unresolved band group the appearance of one band with an edge on the violet side. As mentioned before, this picture fits best for  $\text{HgCl}_2$  but not for the other two halides.

In reality, two further factors have to be considered: firstly, the statistical weight of vibra-

tional states, secondly, matrix elements for the transition as obtained from the Franck-Condon principle. Since the bending vibration is twofold degenerate, the  $v$ th level has the weight  $v+1$ . This increases the intensity of the  $v-v$  transitions as well as that of the  $v \rightarrow v+2$  and  $v+2 \rightarrow v$  transitions by a factor  $v+1$ . The matrix elements for the  $v \rightarrow v+2$  and  $v+2 \rightarrow v$  transitions cause a further increase of  $(v+1)^2$  with increasing  $v$ . At the same time the matrix elements for  $v-v$

FIG. 10. Absorption spectrum of  $\text{HgBr}_2$  and analysis.

transitions decrease but this decrease is relatively small as long as the  $v \rightarrow v+2$  transitions are weak as compared to the  $v \rightarrow v$  transitions. The dependence of the intensity of the  $v \rightarrow v$  transitions upon  $v$  is therefore roughly given by  $(v+1)e^{-h\nu \cdot v/kT}$  where  $\nu$  is the vibrational frequency. The measured edges very probably correspond to the steepest slope<sup>47</sup> on the short wave side in the intensity curve of the  $v \rightarrow v$  groups. The maximum slope occurs for  $v=0$ . Thus, the measured edge actually represents the 0, 0 transition for the bending vibration. The intensities of the  $v \rightarrow v+2$  and  $v+2 \rightarrow v$  transitions depend upon  $v$  as  $(v+1)^3 e^{-h\nu \cdot v/kT}$ . If we set  $h\nu/kT \sim \frac{1}{5}$  for  $\text{HgBr}_2$  the  $v$  value at the greatest slope is then approximately 5. The edges of the band groups designated as 0 $\rightarrow$ 2 and 2 $\rightarrow$ 0 of the deformation vibration in Fig. 10 will be shifted

towards the red from the real 0 $\rightarrow$ 2 and 2 $\rightarrow$ 0 bands by about 5 times the vibrational frequency difference in the upper and lower states.

Inspection of Fig. 10 shows that the distance between 0 $\rightarrow$ 0 and 2 $\rightarrow$ 0 is larger by about 55  $\text{cm}^{-1}$  than the distance between 0 $\rightarrow$ 0 and 0 $\rightarrow$ 2. At first sight one may attribute this to a large change in the frequency of the bending vibrations in the two states. However, already a change of about 5 wave numbers suffices to produce the observed effect. According to the above discussion this will shift the edges of the  $v \rightarrow v+2$  and  $v+2 \rightarrow v$  groups by 25 wave numbers each, which increases the apparent 0 $\rightarrow$ 0 to 0 $\rightarrow$ 2 distance by 25  $\text{cm}^{-1}$  and decreases the 2 $\rightarrow$ 0 to 0 $\rightarrow$ 0 distance by the same amount. With the 5 wave numbers just mentioned the actual distances between 2 $\rightarrow$ 0 to 0 $\rightarrow$ 0 and 0 $\rightarrow$ 0 to 0 $\rightarrow$ 2 bands should differ by 10 wave numbers so that one may expect an observed difference of the edges of about 25+25+10 wave numbers. This is slightly in excess of the reported 55  $\text{cm}^{-1}$ .

Using the corrected values for the location of the different bands one obtains values for the frequencies which are exhibited in Table XI. The unsymmetrical valence vibrations have not been included in the table since they have not been observed in the spectrum. This is in agreement with expectation. The 0 $\rightarrow$ 2 and 2 $\rightarrow$ 0 transitions are too weak for observation for this vibration and the same is true for the corresponding transitions of the bending vibration. Only the small ratio  $h\nu/kT$  for the latter vibration makes temperature excitation of high quanta of this vibration possible and as mentioned before, the  $v \rightarrow v+2$  and  $v+2 \rightarrow v$  transitions become more probable for high values of  $v$ .

### $\text{C}_2\text{N}_2$

A new absorption system of cyanogen gas has recently been found by Woo and Liu<sup>48</sup> in the

TABLE XI. Frequencies found in the ultraviolet spectra of mercury halides.

MOLECULE	$\omega'_s$	$\omega'_s$	$\omega'_\delta$	$\omega'_\delta$
$\text{HgCl}_2$	365	289	70	65
$\text{HgBr}_2$	229	194	41	36
$\text{HgI}_2$	156	126	33	30

<sup>47</sup> According to private communication from Professor Wehrli.

<sup>48</sup> Sho-Chow Woo and Ta-Kong Liu, J. Chem. Phys. 5, 161, 499 (1937).

region 3020–2480Å. The system is very weak. It is well developed with an absorbing path of 1.5 meters and a pressure of one atmosphere. Although the weakness of the bands would suggest a forbidden transition the structure of the system seems to indicate a transition allowed by symmetry. We think it therefore possible that it represents an intercombination which would have the appearance of a permitted spectrum. The interpretation given by Woo and Liu seems to be correct in its main features. They observed two main progressions of regular intensity distribution and fitted them into a general formula  $\nu = 33,293.63 + \omega'_1 v'_1 + x'_{11} v'^2_1 + \omega'_2 v'_2 + x'_{22} v'^2_2 + x'_{12} v'_1 v'_2$  with  $\omega'_1 + x'_{11} = 895.75$ ,  $x'_{12} = -8.00$ ,  $\omega'_2 = 2065.38$ ,  $x'_{22} = -15.13$ . There is no doubt that  $\omega'_2 = 2065$  in the excited state corresponds to the totally symmetrical vibration of  $2336 \text{ cm}^{-1}$  ( $\rightarrow \leftarrow \rightarrow \leftarrow$ ) in the ground state. The difference of  $895 \text{ cm}^{-1}$  corresponds very likely to the other totally symmetrical vibration of  $842 \text{ cm}^{-1}$  in the ground state ( $\rightarrow \rightarrow \leftarrow \leftarrow$ ). Woo and Liu have interpreted only bands with one quantum of 895 but we believe that some of the bands of their Table IV simply represent higher members of this progression. With this assignment the 895 progression can be extended considerably. We see that while the C–N frequency of  $2336 \text{ cm}^{-1}$  in the excited state, the C–C value increases slightly from 842 to  $895 \text{ cm}^{-1}$ . This behavior can be understood according to Woo and Liu if one assumes that the electronic excitation takes place in such a fashion that an electron which in the ground state contributed to the C–N bonding contributes in the excited state more toward the C–C bonding. The interpretation of 33,294 as 0,0 band is probably correct but it may also represent the second or even a higher member, the first ones being too weak on account of the Franck-Condon principle. If one plots the whole spectrum schematically, groups of three bands forming the main progression with distances of about  $2050 \text{ cm}^{-1}$  stand out clearly. (Woo and Liu had considered only doublets.) The member with the shortest wavelength has the largest intensity. We suppose that the two members towards longer waves are caused by  $v-v$  transitions of non-totally symmetrical vibrations. It is suggestive to assign

TABLE XII. Suggested band assignments in  $\text{C}_2\text{N}_2$ .

	33247	25		34172		35045		
	33272			34189	17	35065	20	892 35957
	33294	22	895					
2049	35276	36		36172	33	37047	40	
	35312			36205		37087		
	35343	31	889	36232	27	884 37116	31	
2021	37291	32						
	37323			38200				
	37364	41	880	38244	44	874 39118		
1990				40129	42			
	39299			40171				
	39354	55	871	40225	54			

them to the  $\epsilon_u$  vibration<sup>49</sup> of  $240 \text{ cm}^{-1}$  which can be excited easily by temperature. In order to explain the observed separations one might add to Woo's and Liu's formula a further term  $-\omega''_3 v''_3 + \omega'_3 v'_3 - x'_{23} v'_2 v'_3$  with  $\omega'_3 = 215 \text{ cm}^{-1}$ ,  $x'_{23} = 10$ . Table XII contains the bands for which an interpretation has been suggested. It comprises all observed material with the exception of a few weak bands and one group of stronger bands. This group lying at the ultraviolet end of the system has been assigned by Woo and Liu, because of its appearance and intensity, to another electronic transition.

### $\text{N}_2\text{O}$

Nitrous oxide has continuous spectra in the near ultraviolet and in the Schumann region and several discrete spectra in the Schumann ultraviolet. The first discrete electronic transition occurs<sup>50</sup> below 1550Å. It is according to its intensity an allowed transition consisting of a large number of bands which are fairly narrow at low, and broad at high temperatures. The progression shows a strong convergence; from its limit follows a small dissociation energy. The spacing between the bands is somewhat irregular but this can possibly be attributed to the lack of sharpness of the bands and hence the difficulty in measuring them. The spacing can be represented by a frequency of  $621 \text{ cm}^{-1}$  in the upper state. As already pointed out by Duncan the assignment of this frequency to one of the known

<sup>49</sup> C. R. Bailey and S. C. Carson, J. Chem. Phys. **7**, 859 (1939); S. C. Woo, Zeits. f. physik. Chemie **B37**, 399 (1937).

<sup>50</sup> A. B. F. Duncan, J. Chem. Phys. **4**, 638 (1936).

vibrations of  $N_2O$  encounters ambiguities. It could be a modification of the totally symmetrical vibration 1285 in the ground state and the drop would have to be explained by a considerable decrease of the binding. But perhaps the drop is smaller: since the maximum of intensity lies in the fifth band it is not impossible that all observed bands lead to already vibrating levels and hence the value of 621 is already diminished by anharmonicity. Then the true frequency would be higher. This would make the mentioned explanation more plausible.

Another possible explanation is that the 621 frequency corresponds to the non-totally symmetrical vibration 589. In this latter case the molecule must be bent in the upper state and the frequency would be larger in this state.

There remains also the possibility that the bands should be represented by two separate series each with the spacing of about 1240, which would then correspond to the totally symmetrical vibration. The occurrence of two series may find its explanation by assuming that the upper state is degenerate and is split because of an interaction between electronic and vibrational motion. (p. 90 and 93.)

#### b. Tetrahedral Molecules

##### $OsO_4$

Two extended progressions of bands are found for this molecule in the near ultraviolet spectrum.<sup>51</sup> The weaker progression appears between 31,000 and 38,000  $cm^{-1}$ . In the latter region it is overlapped by the stronger progression which extends to 47,000  $cm^{-1}$ . The intensity distribution suggests that two electronic transitions are involved. The main frequency difference in the weak progression is 811  $cm^{-1}$ , in the stronger progression the difference is about 835  $cm^{-1}$ . This will correspond to a totally symmetrical vibration in the upper electronic states. A strong Raman line at 970 indicates the presence of an analogous vibration in the normal state.

The spectrum of  $OsO_4$  is of interest because it is one of the very few discrete spectra which have been attributed to a tetrahedral molecule. For

<sup>51</sup> J. Lifschitz and E. Rosenbohm, *Zeits. f. physik. Chemie* **97**, 1 (1921); S. Kato, *Sci. Pap. Inst. Phys. Chem. Research* **13**, 248 (1930); A. Langseth and B. Qviller, *Zeits. f. physik. Chemie* **B27**, 79 (1934).

such molecules one should expect for allowed transitions a complicated structure, or more likely a quasi-continuum or continuum (p. 92). There is no definite sign of such a structure in the  $OsO_4$  spectrum. The intensity would also indicate that both progressions belong to forbidden transitions. In this case the observed progression would not start from the 0-0 band but rather from the 0→1 band of the vibration which makes the electronic transition allowed. A corresponding 1→0 band should then be expected. But no frequency difference has been found on the long wave side which could be associated with the vibration that makes the transition allowed.

On the other hand, the evidence for  $OsO_4$  being tetrahedral is not very strong. The probable absence of a dipole moment<sup>51</sup> shows a symmetrical structure, but for instance a plane square configuration would be in as satisfactory agreement with the observations as a tetrahedron. Since the model of the molecule is not definitely known, an analysis of the spectrum should be postponed.

A similar spectrum has been found for  $RuO_4$ .<sup>52</sup>

#### c. Methane Derivatives

We do not start with a consideration of the methane spectrum itself because it is continuous as are all known spectra of tetrahedral molecules.<sup>53</sup> But some derivatives are well investigated experimentally, of which we shall discuss methyl iodide and methylamine.

##### $CH_3I$

Methyl iodide possesses a continuous absorption spectrum with a maximum at about 2500Å. It also has discrete bands<sup>54</sup> which extend from 2100 to 1500Å and furthermore absorption bands in the extreme ultraviolet which form Rydberg series.<sup>55</sup> The temperature dependence<sup>56</sup> has been thoroughly studied for the bands around 2000Å. The high intensity suggests that the transition is allowed. Figure 11 comprises all interesting bands

<sup>52</sup> B. Qviller, *Tidsskr. Kjemi og Bergvesen* **17**, 127 (1937).

<sup>53</sup> See p. 92.

<sup>54</sup> G. Herzberg and G. Scheibe, *Zeits. f. physik. Chemie* **B7**, 390 (1930); A. Henrici, *Zeits. f. Physik* **77**, 35 (1932); G. Scheibe, F. Povenz and C. F. Linström, *Zeits. f. physik. Chemie* **B20**, 283 (1933).

<sup>55</sup> W. C. Price, *J. Chem. Phys.* **4**, 539, 547 (1936).

<sup>56</sup> A. Henrici and H. Grieneisen, *Zeits. f. physik. Chemie* **B30**, 1 (1935).



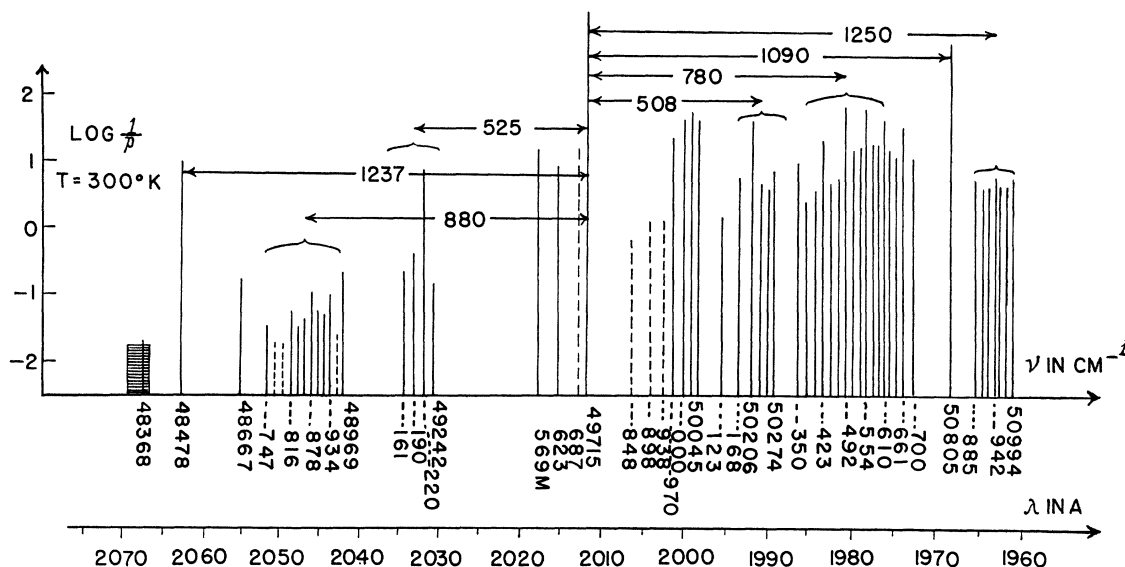


FIG. 11. Schematic representation of the absorption spectrum of  $\text{CH}_3\text{I}$ .  
(Taken from A. Henrici and H. Grieneisen, *Zeits. f. physik. Chemie* **B30**, 20 (1935).)

which appear already at room temperature. The height of the lines corresponds to the logarithm of the intensities. The 0, 0 band lies at  $49,715\text{ cm}^{-1}$ . This can be concluded from the fact that this band and most bands on the violet side show only slight temperature dependence while practically all bands on the red side gain in intensity with increasing temperature. A band displaced by 1237 towards the red from the 0, 0 band corresponds apparently to the  $\text{CH}_3$  deformation vibration in the lower state for which a frequency of  $1250\text{ cm}^{-1}$  is found in infra-red and Raman spectra. A similar vibration occurs in the upper state with the frequency  $1090\text{ cm}^{-1}$ . The intensity ratio of the two bands agrees exactly with what should be expected from the Boltzmann factors. Two more quanta of this vibration have been observed with certainty in the upper state, and in the lower state a second quantum appears weakly at higher temperatures. The totally symmetrical C—I valence vibration  $532\text{ cm}^{-1}$  has also been observed in the lower state (given as  $525\text{ cm}^{-1}$  in Fig. 11). According to its Boltzmann factor it should appear with larger intensity than the 1237 band which, however, is not the case. One has to conclude, therefore, that the corresponding transition probability is lower. The same consideration applies to the excited state where the vibration appears with a frequency 508 in a band

of relatively low intensity. There is no conclusive evidence for a multiple excitation of this vibration.<sup>57</sup> The theory of electronic structures<sup>58</sup> and analogy with other molecules indicate that these bands are due to an excitation of an iodine electron. It is therefore astonishing that the  $\text{CH}_3$  vibration is more strongly excited than the C—I vibration.

From the figure it can be seen that another band appears displaced by 880 from the 0, 0 band to the red which corresponds to a transition  $1 \rightarrow 0$  of one of the non-totally symmetrical bending vibrations of the  $\text{CH}_3\text{I}$  molecule. A corresponding band  $0 \rightarrow 1$  gives a frequency value of  $780\text{ cm}^{-1}$  for this vibration in the excited state. In allowed transitions non-totally symmetrical vibrations should not be excited strongly with one quantum. According to the selection rules they may occur, however, with very small intensity. While the 0, 0 band and the bands in which only totally symmetrical vibrations change are due to a definite electronic transition moment, the excitation of non-totally symmetrical vibrations occurs because of the small change of the transition moment which takes place during the asymmetrical vibration. That is, the whole electronic

<sup>57</sup> The band 48,667 can possibly be explained by a two-fold excitation of 532 but this is not very probable since the corresponding band in the upper state is absent.

<sup>58</sup> R. S. Mulliken, *Phys. Rev.* **47**, 413 (1935).

system is composed of two kinds of bands with two kinds of transition moments: strong and allowed bands, and weak bands in which non-totally symmetrical vibrations change by one quantum and which generally behave as though they belong to a forbidden system. The reported transition probabilities for the bands in question are indeed about 30 times smaller than those for bands with the totally symmetrical  $\text{CH}_3$  bending vibration. Another weak band can be interpreted as originating from the vibrationless ground state and leading to a frequency of  $1250\text{ cm}^{-1}$  in the upper state. This probably corresponds to the other non-totally symmetrical bending vibration of  $1445\text{ cm}^{-1}$  in the ground state.

The direction of the electronic transition moments should be different in the allowed and forbidden bands occurring in the same system. Therefore, different rotational structures are to be expected in allowed and forbidden bands. In fact, the allowed bands have a less extended structure while the forbidden bands consist of a considerable number of equally spaced lines extending over several hundred wave numbers. The equidistant rotational spacing indicates a practically unchanged moment of inertia. The rotational lines show an intensity alternation, every third line being more intense. A similar behavior has been found in the infra-red bands of non-totally symmetrical vibrations. The theoretically predicted intensity ratio for the rotation of three hydrogen atoms with the spin  $\frac{1}{2}$  each about the figure axis is  $2 : 1 : 1 : 2$ . Actually each rotational line represents a  $Q$  branch with  $\Delta J = 0$ , the  $P$  and  $R$  branches with  $\Delta J = \pm 1$  forming a quasi-continuous background. Hence it seems that the allowed bands represent parallel transitions in which the rotational frequency about the figure axis does not appear so that these bands are much narrower. The forbidden bands show the characteristics of perpendicular transitions.

However, closer inspection shows that this simple picture does not explain all details of the band system. The band  $880 \rightarrow 0$  should have the same rotational spacing as the infra-red band at  $880\text{ cm}^{-1}$ , i.e., the distance between successive lines should be  $7.7\text{ cm}^{-1}$ . This spacing is not due to rotation alone, but is influenced by a coupling between rotation and vibration. The same coupling should be found in the electronic band.

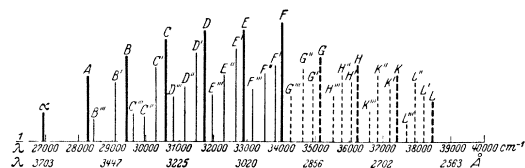


FIG. 12. Schematic representation of the absorption spectrum of  $\text{H}_2\text{CO}$ . (Taken from V. Henri and S. A. Schou, *Zeits. f. Physik* **49**, 781 (1928).)

However, the observed distances are  $20\text{ cm}^{-1}$ , that is, almost 3 times larger than in the infra-red band. The same spacing of  $20\text{ cm}^{-1}$  is also found in the two other perpendicular bands.

It seems that the large spacing cannot be explained unless one assumes an additional electronic angular momentum in the excited state. This would mean, however, that the electronic transition itself is perpendicular and that it leads to a degenerate upper state for which the symmetrical configuration cannot correspond to the equilibrium position. For the equilibrium no trigonal axis must be present although the deviation from the threefold axis may be only slight. With this new interpretation all bands of the system can be regarded as allowed transitions. The detailed structure of the individual bands can probably be explained only by coupling effects between the electronic, vibrational and rotational motions. That this coupling mechanism is not too simple is indicated by bands appearing on the red side close to the  $0,0$  band. They probably cannot be explained as  $1-1$  transitions of low frequencies. Also the width of the  $0,0$  band, although much smaller than that of the "perpendicular" bands, is really too large for an ordinary parallel band. A similar situation holds for the other "parallel" bands.

An absorption group around  $50,000$  wave numbers has been left unexplained. Its intensity decreases strongly with increasing temperature as do a few other narrow bands of the system. The possibility has not been excluded that they are caused by impurities. But it is also possible that the absorption at  $50,000$  is due to peculiar coupling effects of the upper degenerate state.

The most characteristic features of the discussed system are repeated in an electronic transition occurring about  $5000\text{ cm}^{-1}$  toward shorter waves.

Similar bands have been found in  $\text{CH}_3\text{Br}$  and

CH<sub>3</sub>Cl. Here the bands are more diffuse so that a detailed analysis cannot be given. Although the electronic transitions are presumably connected with halogen electrons, the most prominent bands are again due to CH<sub>3</sub> vibrations.

### H<sub>2</sub>CO

Formaldehyde has its first absorption spectrum in the near ultraviolet<sup>59</sup> beginning at about 3570 Å. Because of the small moment of inertia around the figure axis the rotational structure is clearly resolved. From an analysis of some of these bands it has been shown<sup>60</sup> that the electronic transition moment is perpendicular to the figure axis. The weak intensity of the absorption points to a forbidden transition. Figure 12 gives a schematic representation of the spectrum. The height of the lines is a rough measure of the intensities (or more nearly of the logarithms of the intensities). The distance of the main bands called *A*, *B*, *C*, etc.,<sup>61</sup> is 1187 cm<sup>-1</sup>. This has been interpreted as the totally symmetrical C—O vibration. There has, indeed, been found a similar progression in deuterio-formaldehyde<sup>62</sup> with almost unchanged frequency. The corresponding frequency of H<sub>2</sub>CO in the normal state<sup>63</sup> is 1750 cm<sup>-1</sup>. It occurs in a long progression in the fluorescence spectrum.<sup>64</sup> It is remarkable that the C—O frequency drops so much when going from the normal to the excited state. This drop corresponds to a large change in the internuclear distance as shown by the long progression with an intensity maximum in the sixth band (*F* in Fig. 12).

The molecule has the symmetry *C*<sub>2v</sub>. If the transition is forbidden by symmetry then it is probably *A*<sub>1</sub>→*A*<sub>2</sub>. It can be made allowed by either a vibration *β*<sub>1</sub> or *β*<sub>2</sub>. In both cases the

transition moment is perpendicular to the C—O axis. Indeed, it seems plausible that the *α* band represents a 1→0 and the *A* band a 0→1 transition of one of these vibrations. This interpretation would make it necessary that the interacting vibration have a frequency not much higher than half of the distance *α*—*A*. Because of the width of the rotational structure of *α* which has not been analyzed this distance is only approximately known as 1300 cm<sup>-1</sup>. These considerations, if correct, would imply a revision of one of the low bending vibrations. The lowest reported value<sup>65</sup> is 1165 cm<sup>-1</sup> and a lower bending vibration seems difficult to reconcile with existing infra-red data. The measured intensity ratio of *α* : *A* ~ 1 : 15 (rough estimate) and the temperature dependence of this ratio are in agreement with the presence of a vibration 600–700 cm<sup>-1</sup>. The strong decrease of the *α*—*A* distance to about 1000 cm<sup>-1</sup> in D<sub>2</sub>CO is also in agreement with an explanation of this distance as being due to low hydrogen bending vibrations. In view of the evidence from the infra-red against a low bending vibration it would be most desirable to redetermine the temperature dependence of the *α* band intensity.

It has not been possible to find consistent explanations, in spite of many attempts, for the other progressions in Fig. 12 which are denoted by different primes. A disagreeable property of formaldehyde is its tendency to polymerize which may have some bearing on the spectrum. Some authors have also assumed that the system contains more than one electronic transition.

The absorption spectra of formaldehyde in the vacuum ultraviolet<sup>65</sup> consist mainly of two electronic series of strong bands. They converge to a limit, hence forming Rydberg series. Two electronic transitions of the series, the bands 1556 and 1397 Å, show a well-developed vibrational pattern. In the first case companion bands to the violet with frequency differences of 1250 and 1470 cm<sup>-1</sup>, in the second case of 1120 and 1260 cm<sup>-1</sup> have been observed. These frequencies belong in all probability to the totally symmetrical hydrogen bending and the C—O vibration with values 1503 and 1750 in the ground state. Very weak bands distant by ~2900 cm<sup>-1</sup> from the mentioned bands have also been found.

<sup>59</sup> V. Henri and S. A. Schou, Zeits. f. Physik **49**, 774 (1928); S. A. Schou, J. Chim. Phys. **26**, 665 (1929); G. Herzberg, Trans. Faraday Soc. **27**, 378 (1931).

<sup>60</sup> G. H. Dieke and G. B. Kistiakowsky, Phys. Rev. **45**, 4 (1934).

<sup>61</sup> The notation *A*, *B*, *C* . . . for the bands has been introduced by Henri. This notation must not be confused with our *A*<sub>1</sub>, *A*<sub>2</sub>, etc., symbols which signify electronic symmetries. Similarly *α* will be used in the following discussion for a band rather than for vibrational symmetry.

<sup>62</sup> E. S. Ebers, Ph.D. Thesis, Harvard University, 1935.

<sup>63</sup> E. S. Ebers and H. H. Nielsen, J. Chem. Phys. **6**, 311 (1938).

<sup>64</sup> G. Herzberg and K. Franz, Zeits. f. Physik **76**, 720 (1932); S. Gradstein, Zeits. f. physik. Chemie **B22**, 384 (1933).

<sup>65</sup> W. C. Price, J. Chem. Phys. **3**, 256 (1935).

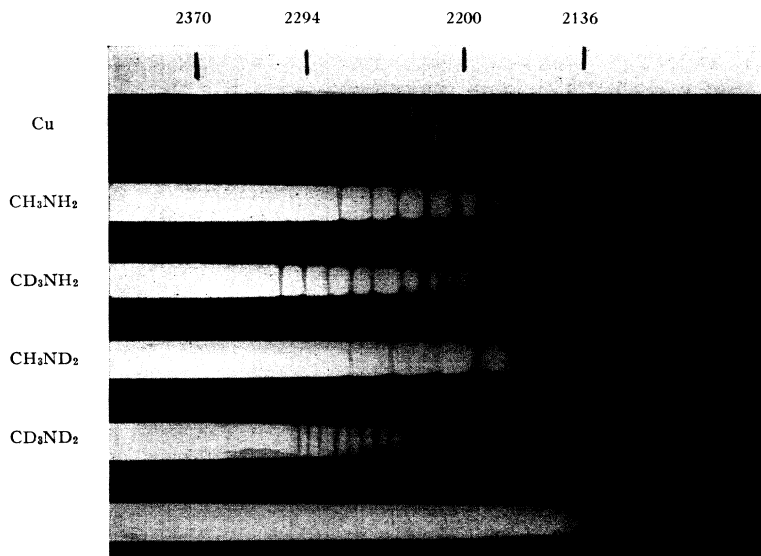
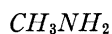


(FIG. 13. Absorption spectrum of  $\text{CH}_3\text{NH}_2$  and deuterated molecules. (Taken from Th. Förster and J. C. Jungers, *Zeits. f. physik. Chemie* **B36**, 390 (1937).)

This frequency represents probably the value of the totally symmetrical hydrogen valence vibration in the upper state.



The known absorption spectrum of methylamine<sup>66</sup> lies in the ultraviolet at 2500–2000 Å. It seems that the spectrum gradually goes over into a continuum at shorter wave-lengths. Although the absorption is not strong, the electronic transition cannot be forbidden by symmetry because of the low symmetry of the methylamine molecule which most likely is  $C_s$  but certainly cannot be higher. Figure 13 represents parts of the absorption spectra of methylamine and its deuterated compounds. The methylamine spectrum gives the appearance of regularly spaced bands. But these bands cannot be explained by a progression with a single frequency, the regularity is rather caused by an accidental rational relation between two frequencies. This can be seen from the changed appearance of the spectrum in the deuterated compounds.<sup>67</sup> With only one frequency involved the spectrum would have a different spacing but would otherwise remain regular. Förster and Jungers have described the

bands by the following formulas:

$$\text{CH}_3\text{NH}_2: \quad \nu = 41,680 + v_1 \times 650 + v_2 \times 1000,$$

$$\text{CD}_3\text{NH}_2: \quad \nu = 41,780 + v_1 \times 600 + v_2 \times 870,$$

$$\text{CH}_3\text{ND}_2: \quad \nu = 42,540 + v_1 \times 515 + v_2 \times 1000,$$

$$\text{CD}_3\text{ND}_2: \quad \nu = 42,580 + v_1 \times 500 + v_2 \times 825.$$

One sees immediately that for  $\text{CH}_3\text{NH}_2$   $3 \times 650 \approx 2 \times 1000$ , and therefore bands with  $v_1 \geq 3$  fall on top of the  $v_2$  bands. The apparent regular distance of about  $330 \text{ cm}^{-1}$  between successive bands is the smallest common denominator of the two frequencies. It follows from the formulas that the 1000 frequency is associated with the  $\text{CH}_3$  group. However, it cannot be called a pure hydrogen vibration because of the relatively small drop in the  $\text{CD}_3$  amines. The 650 frequency is more dependent on the substitution in the amino group. It is most plausible to correlate this frequency with the NH bending vibration  $783 \text{ cm}^{-1}$  in the lower state.<sup>68</sup> This is supported by the observation that ethyl and propyl amine have also a frequency of about  $650 \text{ cm}^{-1}$  in the upper state. According to the progressions of the 650 frequency in the upper state, the 783 should appear on the long wave side of the 0, 0 band of methylamine. Actually a band is observed at  $40,918 \text{ cm}^{-1}$  which has within the

<sup>66</sup> G. Herzberg and R. Kölsch, *Zeits. f. Elektrochemie* **39**, 572 (1933); V. Henri and W. Lasareff, *J. Chim. Phys.* **32**, 353 (1935).

<sup>67</sup> Th. Förster and J. C. Jungers, *Zeits. f. physik. Chemie* **B36**, 387 (1937).

<sup>68</sup> A. P. Cleaves and E. K. Plyler, *J. Chem. Phys.* **7**, 563 (1939); C. R. Bailey, S. C. Carson and E. F. Daly, *Proc. Roy. Soc. London* **A173**, 339 (1939); R. G. Owens and E. F. Barker, *J. Chem. Phys.* **8**, 229 (1940).

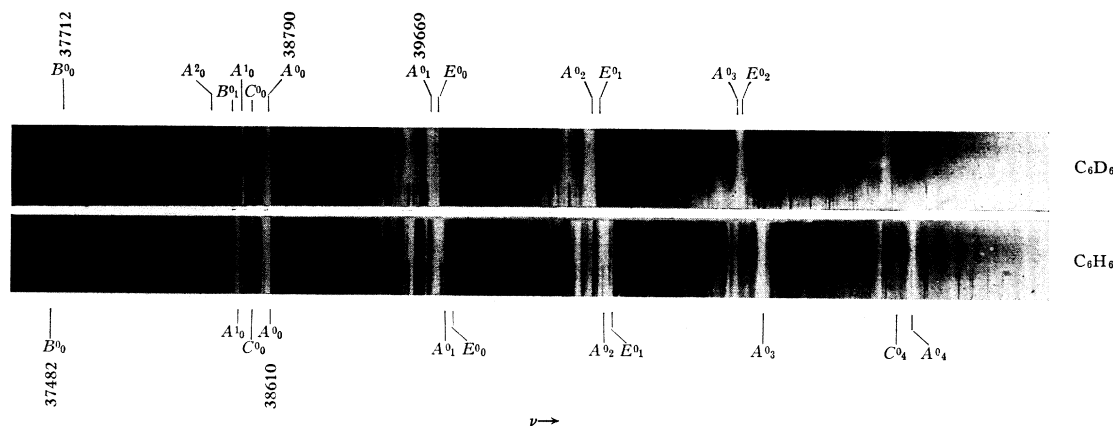


FIG. 14. Absorption spectra of  $C_6H_6$  and  $C_6D_6$ .  
(Taken from H. Sponer, J. Chem. Phys. **8**, 705 (1940).)

limits of error the correct distance from the 0, 0 band. The temperature dependence<sup>69</sup> of this band supports this interpretation. In fact, a whole series of bands with frequencies  $40,918 + \nu_1 \times 650 + \nu_2 \times 1000$  appears at elevated temperatures. Further temperature dependent bands which appear on the long wave side of the 0, 0 band may be correlated with the frequencies 1127, 1426 and  $2 \times 1045 \text{ cm}^{-1}$  in the ground state of methylamine. The band in which the 1045 vibration is excited with one quantum in the lower state is perhaps obscured by the  $1 \rightarrow 0$  transition of the 1127 vibration. Progressions from these bands toward shorter waves are observed in all cases where the higher terms of the progressions are not obscured by stronger superimposed bands. The interpretation of the temperature dependent bands is not as certain as the assignments in the violet end of the spectrum. In order to make unambiguous assignments to the long wave bands it would be necessary to study the deuterated compounds in this region and in the infra-red and Raman spectrum.

#### d. Benzene and Derivatives

##### *The Near Ultraviolet Absorption System of Benzene*

Benzene offers the best example known so far for the vibrational structure of a forbidden transition. The system in question is the near ultraviolet absorption system at 2700–2200 Å. It

has been investigated in light and heavy benzene in absorption<sup>70</sup> and fluorescence<sup>71</sup> and for  $C_6H_6$  absorption spectra have been taken also at temperatures as low<sup>72</sup> as  $-259^\circ\text{C}$ . Moreover, infra-red and Raman spectra are known for the liquid and gaseous phase and a rather complete interpretation was possible with the help of deuterio-substituted benzenes.<sup>73</sup> All these data were necessary in order to interpret the rather involved spectrum of benzene in an unambiguous way.

Benzene belongs to the symmetry class  $D_{6h}$ . (See Tables VII and VIII.) The fundamental state has the symmetry  $A_{1g}$ . For the excited state  $B_{2u}$  has been proposed from calculations of the energy levels.<sup>74</sup> The vibrational analysis<sup>75</sup> confirms the assumption of an  $A_{1g} \rightarrow B_{2u}$  transition. The lower part of Fig. 14 represents this

<sup>70</sup> R. Witte, Zeits. f. wiss. Phot. **14**, 347 (1915); K. Schulz, Zeits. f. wiss. Phot. **20**, 1 (1920); V. Henri, J. de phys. et rad. [6] **3**, 181 (1922); and *Structure des Molécules* (Hermann, Paris, 1925), p. 108 ff.; G. B. Kistiakowsky and A. K. Solomon, J. Chem. Phys. **5**, 609 (1937); A. Ionescu, Comptes Rendus Acad. Roum. **2**, 39 (1937); H. Sponer, J. Chem. Phys. **8**, 705 (1940).

<sup>71</sup> G. B. Kistiakowsky and A. Nelles, Phys. Rev. **41**, 595 (1932); G. R. Cuthbertson and G. B. Kistiakowsky, J. Chem. Phys. **4**, 9 (1936); C. K. Ingold and collaborators, J. Chem. Soc. 912 (1936).

<sup>72</sup> A. Reimann, Ann. d. Physik **80**, 43 (1926); P. Pringsheim and A. Kronenberger, Zeits. f. Physik **40**, 75 (1926); A. Kronenberger, *ibid.* **63**, 494 (1930).

<sup>73</sup> C. K. Ingold and collaborators, J. Chem. Soc. 971 (1936); A. Langseth and R. C. Lord, Det. Kgl. Danske Vidensk. Selskab. Math.-fys. Medd. **16**, No. 6 (1938).

<sup>74</sup> A. L. Sklar, J. Chem. Phys. **5**, 669 (1937).

<sup>75</sup> H. Sponer, G. Nordheim, A. L. Sklar and E. Teller, J. Chem. Phys. **7**, 207 (1939); H. Sponer, J. Chem. Phys. **8**, 705 (1940).

<sup>69</sup> V. Henri and W. Lasareff, J. Chim. Phys. **32**, 353 (1935).

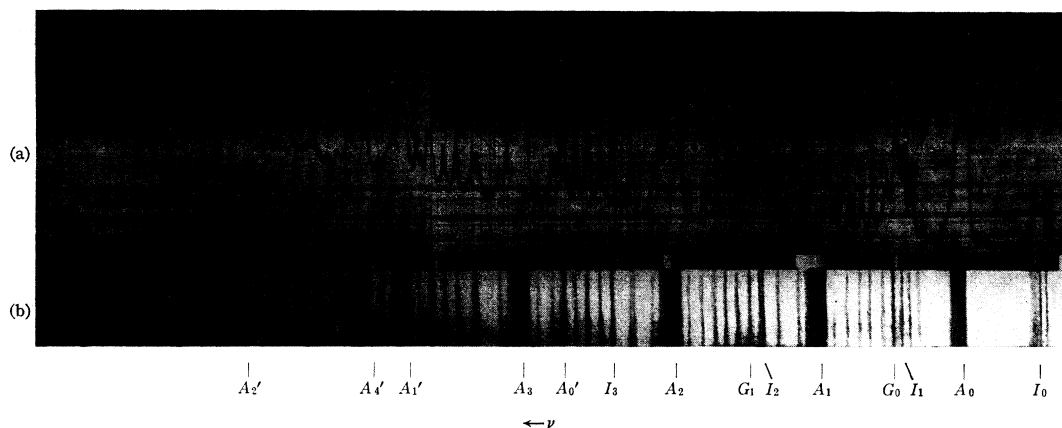


FIG. 15. Absorption spectrum of solid benzene at  $-259^{\circ}\text{C}$ .  
(Taken from A. Kronenberger, *Zeits. f. Physik* **63**, 497 (1930).)

absorption system, the upper gives the same bands for  $\text{C}_6\text{D}_6$ . The characteristic feature of the spectrum is that it consists of a number of groups apart from each other, by  $923\text{ cm}^{-1}$  and  $879\text{ cm}^{-1}$ , respectively. These distances represent the totally symmetrical  $C$  vibrations in the upper state, the values in the lower state are  $992$  and  $946\text{ cm}^{-1}$ . The occurrence of progressions is readily explained by the Franck-Condon principle if the size of the  $C$  hexagon is slightly changed in the upper state. From the degradation of the bands toward the red one must conclude that the hexagon has slightly increased. The strongest member of each group is the one on the violet side. The bands extending toward the red can be explained as  $v-v$  transitions of non-totally symmetrical vibrations whose frequencies are smaller in the upper electronic state. All that has been said applies to an allowed transition as well as to a forbidden one. It is the occurrence and behavior of the weak group lying on the red side of the first strong group that gives conclusive evidence for a forbidden transition. Its temperature dependence<sup>76</sup> shows that it arises from a vibrating ground level. Its separation from the first strong group is  $1126\text{ cm}^{-1}$  ( $1076\text{ cm}^{-1}$  in  $\text{C}_6\text{D}_6$ ) and does not agree with any totally symmetrical vibration in the ground state. From the Boltzmann factor of the temperature dependence one must conclude, moreover, that a

vibration of about  $600\text{ cm}^{-1}$  is excited. Hence the natural conclusion seems to be that we are concerned here with a forbidden transition which is made allowed by the excitation of a non-totally symmetrical vibration. With this assumption the weak group would correspond to a  $1\rightarrow 0$  and the first strong group to a  $0\rightarrow 1$  transition of this particular vibration. (The low  $f$  value  $\sim 10^{-4}$  is in agreement with the assumption of a forbidden transition.)

From Table VIII we can see that  $A_{1g}\rightarrow B_{2u}$  is indeed forbidden for hexagonal symmetry. The only allowed transitions are  $A_{1g}\rightarrow E_u^-$  and  $A_{1g}\rightarrow A_{2u}$ . For the first type the transition moment  $M$  lies in the plane of the ring; for the second type it is perpendicular to it (Table VIII). According to p. 98 a vibration of the symmetry  $A_{1g}B_{2u}M=A_{1g}B_{2u}E_u^-$  or  $A_{1g}B_{2u}A_{2u}$  will make the transition allowed. This is in the first case  $\epsilon_g^+$ , in the second case  $\beta_{1g}$ . Benzene does not have a vibration of the latter symmetry<sup>77</sup> but has 4 vibrations of the  $\epsilon_g^+$  type. Two of them, namely  $606$  and  $1496\text{ cm}^{-1}$ , are  $C$  vibrations. These should be chiefly effective because the transition takes place between  $\pi$  electrons which only involve the C-C bonds. From the foregoing it is clear that the distance of  $1126\text{ cm}^{-1}$  is the sum of the low  $\epsilon_g^+$  vibration in the upper and lower states, thus<sup>78</sup>  $\epsilon_g^{+'} + \epsilon_g^{+''} = 1126\text{ cm}^{-1}$  and  $\epsilon_g^{+'}$  becomes  $520\text{ cm}^{-1}$ . The

<sup>76</sup> G. B. Kistiakowsky and A. K. Solomon, *J. Chem. Phys.* **5**, 609 (1937); W. F. Radle and C. A. Beck, *J. Chem. Phys.* **8**, 507 (1940).

<sup>77</sup> E. B. Wilson, *Phys. Rev.* **45**, 706 (1934).

<sup>78</sup> The primes and double primes refer, as usually, to the upper and lower states, respectively.

corresponding values for  $C_6D_6$  are 1078 and  $498\text{ cm}^{-1}$ . From this the location of the 0,0 bands can be calculated as being 38,089 and  $38,292\text{ cm}^{-1}$  for  $C_6H_6$  and  $C_6D_6$ . According to selection rules the 0,0 band should not appear in the gas. Indeed, the band is absent in  $C_6D_6$  and its presence is doubtful in  $C_6H_6$ . The 0,0 band, however, is fairly strong in the absorption spectrum of  $C_6H_6$  at  $-259^\circ\text{C}$  (Fig. 15). Here the selection rule is violated by the interaction of neighbored molecules in the crystal. The whole spectrum of the solid is shifted by  $280\text{ cm}^{-1}$  towards the red on account of crystal forces and the individual bands are split for the same reason. The spectrum looks different from the vapor spectrum mainly because bands arise only from the vibrationless ground state. In fluorescence the  $0\rightarrow 1$  and  $1\rightarrow 0$  bands of the  $\epsilon_g^+$  vibration appear with inverted intensities according to the Boltzmann factor in the upper state. Progressions of  $992\text{ cm}^{-1}$  ( $C_6H_6$ ) and  $946\text{ cm}^{-1}$  ( $C_6D_6$ ) extend to the long wave-length side. Of the further details of the benzene spectra which have been discussed<sup>75</sup> only the explanation of some  $v-v$  transitions will be mentioned here. In Fig. 14 there appear bands on the long wave-length side from the main bands with distances of 86 and  $160\text{ cm}^{-1}$ . The 86 correspond to transitions  $1\rightarrow 2$  and  $2\rightarrow 1$  of the  $\epsilon_g^+$  vibration. This can

also be expressed as a  $1\rightarrow 1$  transition of  $\epsilon_g^+$  superimposed on the  $0\rightarrow 1$  or  $1\rightarrow 0$  transition of the same vibration. Indeed  $\epsilon_g^{+''} - \epsilon_g^{+'} = 606 - 520 = 86$ . The corresponding values in  $C_6D_6$  give 82 instead of  $86\text{ cm}^{-1}$ . As to the  $160\text{ cm}^{-1}$ , Kistiakowsky and Solomon<sup>76</sup> have shown that this spacing which occurs in long progressions in absorption and fluorescence, is a difference between a frequency of 404 in the ground state and of  $244\text{ cm}^{-1}$  in the excited level. The most probable assignment on the basis of Raman effect observations is an  $\epsilon_u^+$ . The  $160\text{ cm}^{-1}$  drops to  $140\text{ cm}^{-1}$  in heavy benzene.

There occurs predissociation at shorter waves in the discussed system, which has been interpreted as rupture of one C-H bond. It is of interest to note the appearance of the bands belonging to different vibrations. It seems that the weaker bands are more strongly affected than those of greater intensity although this may be an optical illusion due to the intensity itself. The effect, if real, would indicate that in the weak bands in which non-totally symmetrical vibrations are excited, these vibrations facilitate the rupture of one C-H bond. Indeed, such a rupture cannot be produced by totally symmetrical vibrations alone. One can see from Fig. 14 that, for instance, the band  $C_4^0$  in  $C_6H_6$  is more diffuse than other weak bands in the

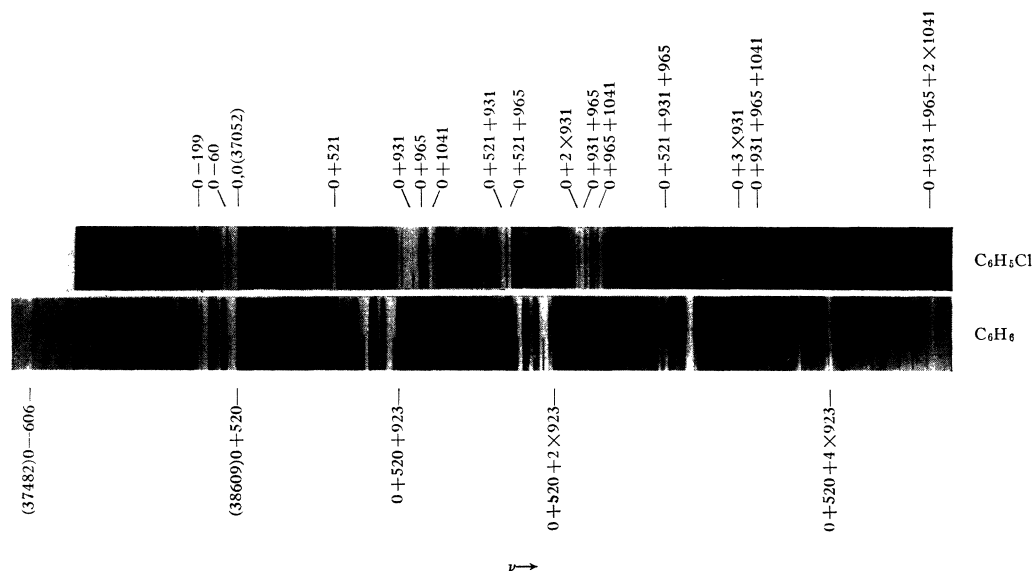


FIG. 16. Absorption spectra of  $C_6H_5Cl$  and  $C_6H_6$

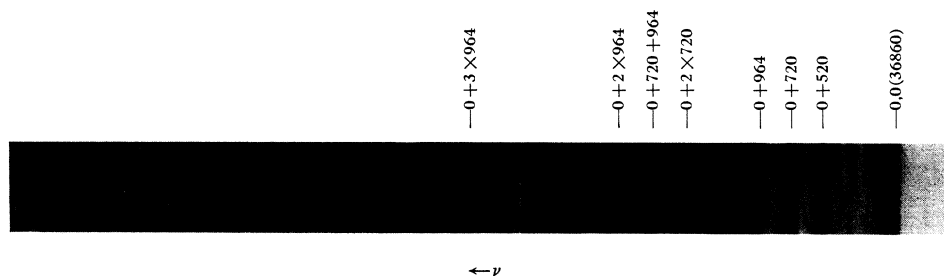


FIG. 17. Absorption spectrum of  $C_6H_5Cl$  at  $-259^\circ C$ .  
(Taken from A. Kronenberger, *Zeits. f. Physik* **63**, 512 (1930).)

neighborhood. In the  $C$  series two quanta of the low  $\epsilon_g^+$  vibrations are excited.

Another, more definite statement can be made from a comparison of the spectra of the two benzenes. The phenomenon of predissociation sets in earlier in  $C_6D_6$  than in  $C_6H_6$ . The band  $A_0^3$  in  $C_6D_6$  is just beginning to look diffuse while the corresponding band in  $C_6H_6$  is still quite sharp, and even  $A_0^4$  looks fairly sharp. This may be explained by an easier transfer of energy between C and D atoms than between C and H atoms corresponding to the smaller C : D mass ratio.

#### *The Near Ultraviolet Absorption System of Substituted Benzenes*

If we substitute in benzene an H atom by a chlorine atom the symmetry  $D_{6h}$  is reduced to  $C_{2v}$ . This group has no degenerate representations; therefore all degenerate benzene vibrations will split. In order to determine the symmetry character of the electronic state corresponding to  $B_{2u}$  in benzene, Tables III and VII should be compared. We must remember, however, that the  $z$  direction in Table VII is the sixfold axis and hence perpendicular to the benzene ring. In Table III the  $z$  direction is the twofold axis and therefore coincides with the C—Cl direction. In order to compare Tables VII and III we replace the  $x, y, z$  axes of the former by the  $x, z, y$  axes of the latter. Columns  $C_2^{(z)}$  and  $\sigma_v^y$  of Table III must be used since we are dealing with a  $C_{2v}$  symmetry. From Table VII we see that  $B_{2u}$  is antisymmetrical to  $C_2^y$  which corresponds in Table III to  $C_2^z$ . Hence  $B_{2u}$  must correspond to  $B_1$  or  $B_2$ . In order to decide now between  $B_1$  and  $B_2$  the behavior with respect to  $\sigma_v^y$  in Table III has to be investigated. This

would correspond to  $\sigma_h$  in Table VII, to which element  $B_{2u}$  is symmetrical. Hence the corresponding term in group  $C_{2v}$  becomes  $B_1$ . Therefore we conclude that the transition  $A_{1g} \rightarrow B_{2u}$  in benzene becomes a transition  $A_1 \rightarrow B_1$  in monochlorobenzene. This transition is allowed in group  $C_{2v}$  and the transition moment lies in the  $x$  direction, that is in the molecular plane in a direction perpendicular to the C—Cl bond.

Figure 16 represents the absorption spectrum<sup>79</sup> of  $C_6H_5Cl$  in the region 2750–2400 Å (with the spectrum of  $C_6H_6$  for comparison) and Fig. 17 gives the same spectrum at  $-259^\circ C$ . In agreement with the assignment to an allowed transition the 0,0 band appears strongly both in the vapor at 37,052 and in the solid at 36,860  $cm^{-1}$ . Since  $C_6H_5Cl$  possesses 11 totally symmetrical vibrations instead of the two in  $C_6H_6$  we shall expect more progressions of totally symmetrical vibrations than in benzene. Accordingly we observe a structure which becomes more complicated towards the violet because of the increasing number of possible combinations of totally symmetrical vibrations. From polarization measurements in the Raman effect<sup>80</sup> one can conclude that there are four totally symmetrical vibrations in the 1000  $cm^{-1}$  region in all of which motions of the carbon atoms will be considerably involved. Indeed, taking degrees of freedom of the carbon atoms alone three vibrations are expected in this region. The bands at 37,983, 38,017, 38,093, and 38,116  $cm^{-1}$  can be interpreted as transitions to the similar vibrations in the upper state.

<sup>79</sup> H. Sponer and S. H. Wollman, to be published soon in *J. Chem. Phys.*

<sup>80</sup> L. Simons, *Soc. Sci. Fennica, Com. Phys.-Math.* **6**, No. 13 (1932).



Although this spectrum of  $\text{C}_6\text{H}_5\text{Cl}$  belongs to an allowed transition its total absorption strength is only two times larger than the corresponding benzene absorption. This is not surprising since the substitution leaves the ring almost unchanged. Therefore the mechanism which brought the benzene spectrum into appearance will remain relatively important.<sup>81</sup> Consequently we should expect  $0 \rightarrow 1$  and  $1 \rightarrow 0$  transitions of the vibrations corresponding to the  $\epsilon^+_{\theta}$  606  $\text{cm}^{-1}$  vibration of benzene. From polarization measurements in the Raman effect<sup>80</sup> one finds a totally symmetrical vibration at 417  $\text{cm}^{-1}$  and a non-totally symmetrical vibration at 608  $\text{cm}^{-1}$  which are reasonably assigned to this  $\epsilon^+_{\theta}$  vibration in benzene. The totally symmetrical vibration is strongly influenced because the carbon attached to the chlorine participates in it while in the non-totally symmetrical vibration the motion of this carbon atom is smaller and perpendicular to the C—Cl bond. It is even possible that the 706  $\text{cm}^{-1}$  (C—Cl) vibration partakes in the properties of the 606 benzene vibration as greatly as the 417  $\text{cm}^{-1}$  vibration. In the totally symmetrical vibration the direction of the transition moment will be the same as for the other totally symmetrical bands, namely perpendicular to the C—Cl direction, while in the non-totally symmetrical vibration it is parallel to the C—Cl bond. In both cases, it is of course in the plane of the ring. As a striking feature of the monochlorobenzene spectrum appears a second group whose strongest band on the violet side lies 521  $\text{cm}^{-1}$  apart from the 0,0 band. It is suggestive to interpret this as the drop of the 608 frequency in the upper state. This interpretation is confirmed by the appearance of a band 617  $\text{cm}^{-1}$  toward the red from the 0,0 band. These bands representing the  $0 \rightarrow 1$  and  $1 \rightarrow 0$  transitions of a non-totally symmetrical vibration occur only because the system has the character of partly an allowed and partly a forbidden transition.

The other vibration related to the mode giving the frequency 606  $\text{cm}^{-1}$  in benzene is the totally symmetrical 417  $\text{cm}^{-1}$  vibration. It gives rise to a  $1 \rightarrow 0$  transition the intensity of which is difficult to estimate. On the other hand, the

$0 \rightarrow 1$  transition leading to a corresponding vibration in the upper state does not stand out clearly enough to be identified in an unambiguous way. The behavior of the C—Cl vibration is similar but more striking. It appears in a  $1 \rightarrow 0$  transition 705  $\text{cm}^{-1}$  apart from the 0,0 band with an intensity comparable to that of the non-totally symmetrical 617  $\text{cm}^{-1}$  vibration. On the other hand, the  $0 \rightarrow 1$  transition appears at best rather faintly if one interprets the band at 37,723 or possibly a band at 37,784  $\text{cm}^{-1}$  as this transition (665  $\text{cm}^{-1}$  or 726  $\text{cm}^{-1}$ ). No stronger band is available in this spectral region. There are two possible reasons for the appearance of these totally symmetrical vibrations: first the equilibrium position in the normal and excited state may be a little different for these vibrations so that both the  $0 \rightarrow 1$  and  $1 \rightarrow 0$  transitions will occur according to the Franck-Condon principle; second, the electronic transition moment may depend upon the normal coordinate of this vibration (see p. 97) and this again will give rise to  $0 \rightarrow 1$  and  $1 \rightarrow 0$  transitions of the vibrations. A relatively high intensity of the  $1 \rightarrow 0$  and the low intensity of the  $0 \rightarrow 1$  transition can be explained by assuming that the two mentioned effects reinforce each other in the first case and tend to cancel in the second case. We designate the wave functions of the four vibrational states concerned as  $\psi'_0, \psi''_0, \psi'_1, \psi''_1$  where the primes indicate, as usually, the electronic states and 0 and 1 refer to the vibrational quantum numbers of the C—Cl vibration. The

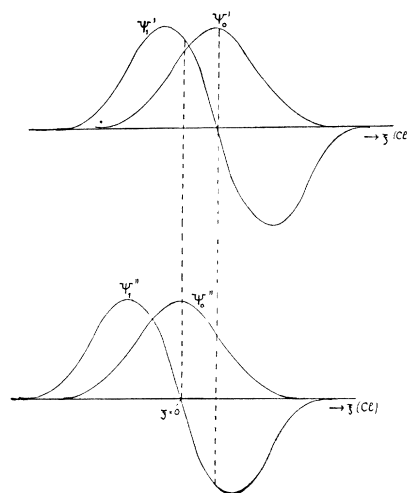


FIG. 18.

<sup>81</sup> H. Spöner and S. H. Wollman, Phys. Rev. **57**, 1078A (1940).

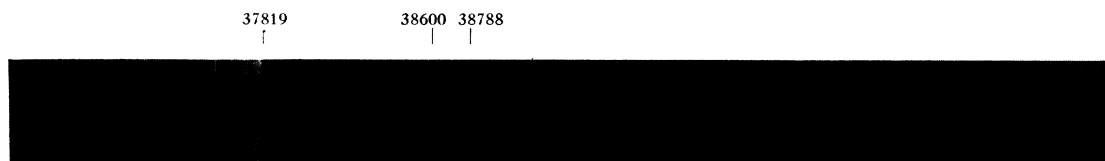
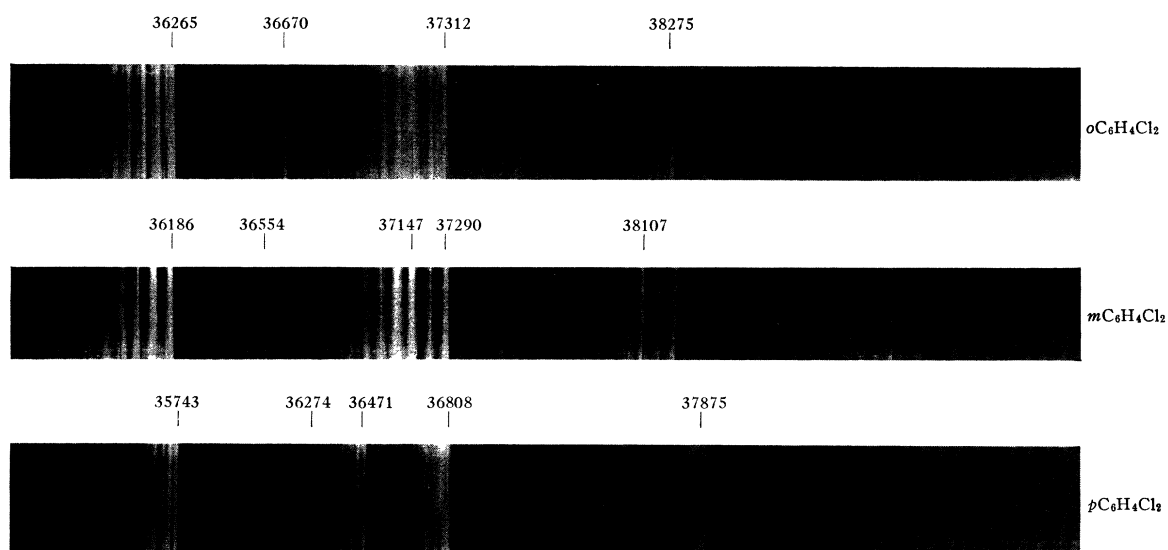
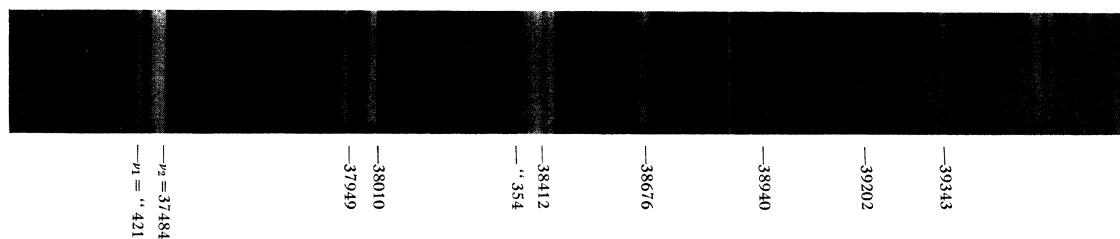
FIG. 19. Absorption spectrum of  $C_6H_5F$ .

FIG. 20. Absorption spectra of dichlorobenzenes.

FIG. 21. Absorption spectrum of toluene. (Taken from J. Savard, Ann. de Chimie **11**, 287 (1929).)FIG. 22. Absorption spectrum of paracresole. (Taken from J. Savard, Ann. de Chimie **11**, 287 (1929).)

normal coordinate of this vibration is called  $\xi$ . If we use of the expansion of the matrix element  $\mathfrak{M}$  into a power series in the displacements only the first two terms (p. 97), these give for the matrix element of the  $1 \rightarrow 0$  transition  $\int \psi'_0 \psi''_1 \mathfrak{M}_0 d\xi + \int \psi'_0 \psi''_1 \mathfrak{M}_1 \xi d\xi$ . The magnitude of the first integral is determined by the shift in equilibrium position and the second contains the change  $\mathfrak{M}_1 \xi$  of the transition moment. The corresponding integrals for the  $0 \rightarrow 1$  transition are  $\int \psi''_0 \psi'_1 \mathfrak{M}_0 d\xi$  and  $\int \psi''_0 \psi'_1 \mathfrak{M}_1 \xi d\xi$ . It can be seen from Fig. 18 that the integrals  $\int \psi'_0 \psi''_1 d\xi$  and  $\int \psi''_0 \psi'_1 d\xi$  have opposite signs since the integrand  $\psi'_0 \psi''_1$  has its maximum in a region where  $\psi''_1$  is negative while the integrand  $\psi''_0 \psi'_1$  attains its maximum value where  $\psi'_1$  is positive. On the other hand, the integrals  $\int \psi'_0 \psi''_1 \xi d\xi$  and  $\int \psi''_0 \psi'_1 \xi d\xi$  have presumably both negative signs, which is the sign they would have if the equilibrium position would be the same in both electronic states. Thus it is quite possible that for a  $1 \rightarrow 0$  transition the matrix elements add up while for a  $0 \rightarrow 1$  transition their main parts cancel. This argument might be used for the  $417 \text{ cm}^{-1}$  vibration as well though the similarity of this vibration and the C—Cl vibration is merely qualitative. It is interesting to note that the  $0 \rightarrow 1$  transition of the C—Cl vibration appears strongly in the spectrum of the solid.<sup>82</sup> This may be explained by assuming that due to the influence of neighbors the shift in the equilibrium distance of the C—Cl vibration is different in the crystal from what it is in the gas. Thus the cancellation of matrix elements may not work in the same way. The frequency  $720 \text{ cm}^{-1}$  is found for the C—Cl vibration in the upper state of the solid. This agrees better with the  $726 \text{ cm}^{-1}$  proposed for the gas. On the other hand,  $665 \text{ cm}^{-1}$  may be the correct value for the gas and the difference in frequency may be due to the influence of the neighbors in the solid.

Weaker bands appearing in the gas on the red side of all main bands with distances of  $62 \text{ cm}^{-1}$ ,  $2 \times 62 \text{ cm}^{-1}$ , and  $199 \text{ cm}^{-1}$  must be ascribed to  $v-v$  transitions.

The characteristic features of the chlorobenzene spectrum are also found in other substituted benzenes. Besides changes in vibrational fre-

quencies strong variations in intensities occur in those bands which correspond to the  $417$ ,  $617$  and  $705$  vibrations (values given for the lower state) of  $\text{C}_6\text{H}_5\text{Cl}$ . This is to be expected since the intensities depend on several terms which may compensate or reinforce each other.

In Figs. 19–22 the spectra of fluorobenzene,<sup>83</sup> *o*-, *m*-, *p*-dichlorobenzene,<sup>84</sup> toluene<sup>85</sup> and paracresole<sup>85</sup> are reproduced. They all have strong 0,0 bands in agreement with the assumption of allowed transitions. In all spectra strong bands appear at a distance of  $1000 \text{ cm}^{-1}$  towards the violet. (In paracresole the distance is only about  $800 \text{ cm}^{-1}$ .) The C—F frequency<sup>86</sup> appears strongly. The C—Cl frequency is very pronounced in *p*-dichlorobenzene while it is weaker in the *m*-, and *o*-compounds. The vibrations corresponding to  $\epsilon_g^+$  in benzene seem to be very marked in toluene and *m*-dichlorobenzene. They are weaker in *o*-dichlorobenzene, and much weaker in fluorobenzene, paracresole and *p*-dichlorobenzene. The 0,0 region and the bands about  $1000 \text{ cm}^{-1}$  to the violet show in *m*- and *o*- $\text{C}_6\text{H}_4\text{Cl}_2$  several edges close to each other. They probably represent low bending vibrations of the chlorine atoms. In fact, the symmetry of these molecules makes totally symmetrical bend-

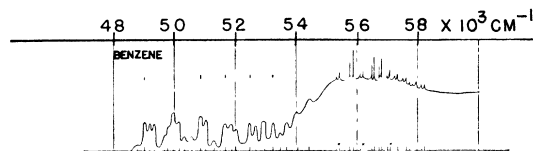


FIG. 23. Schematic representation of benzene absorption in the vacuum region. (Taken from E. P. Carr and H. Stücklen, J. Chem. Phys. **6**, 55 (1938).)

ing vibrations of the chlorine atoms possible. The two para-compounds show a markedly simpler structure in agreement with their higher symmetry and correspondingly smaller number of totally symmetrical vibrations. A closer inspection of all these spectra will probably reveal additional bands which have no analog in chlorobenzene.

<sup>83</sup> S. H. Wollman, unpublished results.

<sup>84</sup> S. H. Wollman, unpublished results.

<sup>85</sup> J. Savard, Ann. de Chimie **11**, 287 (1929).

<sup>86</sup> The numerical value of this frequency does not differ greatly from carbon vibrations so that this vibration will probably contain some contributions from the motion of the other carbon atoms.

<sup>82</sup> See Fig. 17.

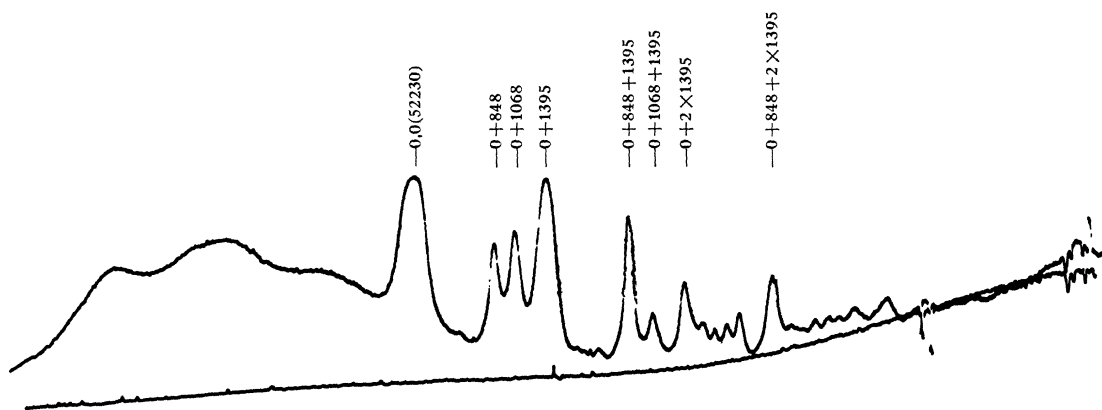


FIG. 24. Microphotometer record of the absorption spectrum of furan.

*Other Absorption Systems of Benzene in the Farther Ultraviolet*

Stronger absorption systems than the discussed one have been observed in benzene from 2050Å towards shorter wave-lengths. The first one extends from 2050 to 1850Å and consists of a number of diffuse broad groups showing some structure. Below 1850Å the bands are overlapped by a still stronger absorption system which has the appearance of a continuous background upon which relatively sharp bands are superimposed. Figure 23 shows the intensities in this region.<sup>87</sup> For the first diffuse system a  ${}^1A_{1g} \rightarrow {}^1B_{1u}$  transition has been suggested.<sup>88</sup> For the bands and continuum below 1850Å transitions  ${}^1A_{1g} \rightarrow {}^1E_u^-$  are assumed.

The transition  $A_{1g} \rightarrow B_{1u}$  is a forbidden one but can be made allowed by vibrations of type  $\epsilon_g^+$  and  $\beta_{2g}$ . The former will be particularly effective since they cause mixing of the  $B_{1u}$  state with the near  $E_u^-$  level which can combine directly with the fundamental state. The proximity of the  $E_u^-$  state is responsible for the higher intensity of the 2000Å system compared to that of the near ultraviolet bands at 2600Å. Indeed, as shown on p. 97 the ratio of the intensities of a forbidden to the allowed transi-

tion is roughly given by

$$\left( \sum_k \frac{Z_k^* e^2 |\xi_{ik}|}{\Delta E r^2} \right)^2.$$

For an  $\epsilon_g^+$  vibration of  $600 \text{ cm}^{-1}$   $\sum_k \xi_{ik} \sim 10^{-9} \text{ cm}$ . With  $Z_k^* = 1$ ,  $r = \text{C}-\text{C distance} = 1.4 \times 10^{-8} \text{ cm}$  and  $\Delta E = 6000 \text{ cm}^{-1}$  (distance between long wave ends of the  $A_{1g} \rightarrow E_u^-$  and  $A_{1g} \rightarrow B_{1u}$  systems) one obtains 0.4 for the ratio of the  $A_{1g} \rightarrow B_{1u}$  and  $A_{1g} \rightarrow E_u^-$  intensities. A similar calculation yields 0.04 for the intensity ratio of the systems  $A_{1g} \rightarrow B_{2u}$  to  $A_{1g} \rightarrow E_u^-$  if  $\Delta E$  is taken as  $17,000 \text{ cm}^{-1}$ . In the  $A_{1g} \rightarrow B_{1u}$  system the occurrence of 965 and 160 progressions has been observed and may be explained in an analogous way as for the near ultraviolet bands. The 965 progression which represents very likely the excitation of the totally symmetrical C-C vibration in the upper state shows unusually strong convergence so that large anharmonicity of this vibration must be assumed. A more detailed analysis of the spectrum seems impossible owing to the diffuseness of the whole system.

The sharp intense bands below 1850Å are interpreted as an allowed  $A_{1g} \rightarrow E_u^-$  transition and are believed to represent the first member of one of the Rydberg series observed<sup>89</sup> between 1550 and 1360Å. The somewhat irregular vibrational structure of this system may be due to a slight change in equilibrium configuration be-

<sup>87</sup> E. P. Carr and H. Stücklen, J. Chem. Phys. **6**, 55 (1938).

<sup>88</sup> M. Goeppert-Mayer and A. L. Sklar, J. Chem. Phys. **6**, 645 (1938); G. Nordheim, H. Sponer and E. Teller, J. Chem. Phys. **8**, 455 (1940).

<sup>89</sup> W. C. Price and R. W. Wood, J. Chem. Phys. **3**, 439 (1935).

cause of the degenerate character of the upper level (p. 90). The continuous absorption underlying this region corresponds perhaps to another electronic transition involving a rupture of one C—H bond. It must have the symmetry  $E^-_u$  or  $A^-_{2u}$  in the vicinity of the equilibrium distance in order to give rise to a strong absorption. If proper intersections of this repulsive surface are assumed with the  $B_{1u}$  potential surface at very low vibrational energies and with the  $B_{2u}$  surface at higher vibrations then the diffuseness of the  $A_{1g} \rightarrow B_{1u}$  system and also the predissociation occurring in the  $A_{1g} \rightarrow B_{2u}$  from about 2400Å to shorter waves may be explained.

### *Furan*

While the high symmetry of benzene imposes a number of limitations on the interpretation of its spectrum and while for the spectra of benzene derivatives analogies to benzene have to be taken into account, such restrictions do not exist for a five ring molecule like  $C_4H_4O$ . Besides some apparently continuous absorption<sup>90</sup> at

<sup>90</sup> Narrow bands have been reported in this region by J. E. Purvis, J. Chem. Soc. **97**, 1648 (1910) and O. V. Fialkowskaja, Acta Physicochim. U. R. S. S. **9**, 215 (1938); but have not been confirmed by other authors.

2500Å and some broad bands in the region of 46,700  $\text{cm}^{-1}$ , sharp and strong bands have been observed<sup>91</sup> between 52,000 and 57,000  $\text{cm}^{-1}$ . These bands are reproduced<sup>92</sup> in Fig. 24. The intensity of the spectrum points to an allowed transition. If we assume  $C_{2v}$  for the symmetry of furan we find there exist eight totally symmetrical vibrations. Four of them represent internal vibrations of the ring which give enough possibilities for the interpretation of the spectrum. The proposed interpretation<sup>91</sup> has been included in the figure. The frequencies 848, 1068 and 1395 in the upper state probably correspond to 986, 1137 and 1483  $\text{cm}^{-1}$  in the ground state. The latter frequencies have been found in the Raman effect with low depolarization factors and therefore must belong to totally symmetrical vibrations.

In conclusion, we wish to acknowledge the facilities placed at our disposal during the writing of this paper by Dr. H. F. Prytherch, Director of the Biological Station of the U. S. Bureau of Fisheries at Beaufort, North Carolina.

<sup>91</sup> L. W. Pickett, J. Chem. Phys. **8**, 293 (1940); there also previous references.

<sup>92</sup> The microphotometer tracing was kindly given to us by Dr. L. W. Pickett.

*Appendix: Table of Electronic Spectra of Polyatomic Molecules\**

Table A. Linear molecules.

MOLECULE	SPECTRAL REGION (Å)	FREQUENCIES† (CM <sup>-1</sup> )	CHARACTERISTICS OF TRANSITION	REMARKS	LIT.
CO <sub>2</sub> carbon dioxide	1390–1250	$\omega' \sim 1225$	Absorption bands	Appear at a few tenths of a mm pressure and 80 cm absorption path. Perhaps two progressions with about 1225 cm <sup>-1</sup> intervals. Diffuse, shaded to the red.	1, 3, 4, 4a
	1150–830		Absorption bands. Transitions ${}^1\Sigma_g^+ \rightarrow$ states converging to lowest ${}^2\Pi_g$ of CO <sub>2</sub> <sup>+</sup>	Appear at 0.01 pressure in 80 cm absorption path. Doublets. Bands form Rydberg series $\nu = 111,250 - R/(n+0.21)^2$ with $n = 2, 3, \dots$ . Ionization potential $13.73 \pm 0.01$ ev in agreement with Mulliken's theoretical predictions. Two weaker series found converging to same limit with different denominators.	
	900–600		Absorption bands	Previously reported by Henning, see 1. Form Rydberg series $\nu = 145,800 - R/(n+0.95)^2$ .	
	6250–3250	$\omega'' \sim 565$	Emission bands	Observed in flames of CO burning in air or oxygen. Narrow headless bands superposed on continuous background. Show doublet separation of about 60 cm <sup>-1</sup> . Besides 565 other possible frequency differences are 2065 and 1500 cm <sup>-1</sup> . CO <sub>2</sub> as emitter considered as most likely (4a), but C <sub>3</sub> O <sub>2</sub> seems not impossible.	
CO <sub>2</sub> <sup>+</sup> carbon dioxide ion	4800–2800	$\omega'_t = 1260$	Two systems of emission bands, ${}^2\Pi_u \rightarrow {}^2\Pi_g$ , ${}^2\Sigma^+_u \rightarrow {}^2\Pi_g$ , ${}^2\Pi_g$ being the ground state. ${}^2\Pi_{3/2} \rightarrow {}^2\Pi_{3/2}$ 0,0 band at 28,532.59 cm <sup>-1</sup> . ${}^2\Pi_{1/2} \rightarrow {}^2\Pi_{1/2}$ 0,0 band at 28,468.51 cm <sup>-1</sup> . Rotational constants: ${}^2\Pi_{3/2g}$ : $B_0 = 0.3795$ ${}^2\Pi_{1/2g}$ : $B_0 = 0.3809$ ${}^2\Pi_{3/2u}$ : $B_0 = 0.3486$ ${}^2\Pi_{1/2u}$ : $B_0 = 0.3501$	Bands are the same as previously reported by Smyth and Schmidt, for references see 1.	1, 4b, 4c
COS carbon oxysulphide	2550–1600		Continuous absorption	At low pressures (i.e., about 0.01 mm with 80 cm path) it breaks into several regions: 2380–2150 Å with maximum at 2250, 2120–2080 Å, 2050–1860, etc., probably leading to dissociations CO + S( <sup>1</sup> D), CO + S( <sup>3</sup> S), CS + O( <sup>1</sup> D), etc. In 5 determination of extinction coefficients.	1, 3, 5
	1565–1410	$\omega'_t \parallel \sim 760$	Absorption bands	Diffuse. Show at about 0.01 mm pressure and 80 cm path.	
	1410–1310	$\omega'_t \parallel \sim 710$ $\omega'_t \parallel \sim 715$ }	Absorption bands	Complex bands, very sharp, weaker than above system. Different intensity distribution in both pro-	

\* These tables have been prepared by H. Sponer. They comprise all accessible work on electronic spectra of polyatomic molecules in the gaseous phase since 1936, thus supplementing the respective tables in *Molekülspektren und ihre Anwendung auf chemische Probleme* by H. Sponer, Vol. I (1935), Tables and Vol. II, p. 480–492 (1936) (Julius Springer, Berlin). Literature references 1 and 2 refer to these books and are added in all cases where molecules have been treated already there.

† Frequencies are generally denoted by  $\omega$ ; for detailed symbols see references 1 and 2.

Table A.—Continued.

MOLECULE	SPECTRAL REGION (Å)	FREQUENCIES† (CM <sup>-1</sup> )	CHARACTERISTICS OF TRANSITION	REMARKS	LIT.
				gressions in this region with frequency differences of $\sim 710$ cm <sup>-1</sup> .	
	1200–1160		Absorption bands	Moderately strong, diffuse. Frequency difference about 700 cm <sup>-1</sup> .	
	below 1110		Absorption bands	Stronger, diffuse.	
CS <sub>2</sub> carbon disulphide	3980–2767	$\omega'' = 401(^2\delta_u \perp)$ $\omega' = 275(^2\delta_u \perp)$	Absorption bands band $\lambda 3501$ type $^1\Sigma^+_u \leftarrow ^1\Sigma^+_g$ with rot. constants. $B' = 0.1122$ , $B'' = 0.1093$ ; band $\lambda 3467$ type $^1\Pi_g \leftarrow ^1\Sigma^+_u$ $B'_{PR} = 0.1044$ , $B'_g = 0.1065$ , $B'' = 0.1016$ band $\lambda 3637$ type $^1\Sigma^+_u \leftarrow ^1\Sigma^+_g$ $B' = 0.1178$ , $B'' = 0.1151$ band $\lambda 3601$ type $^1\Sigma^+_u \leftarrow ^1\Sigma^+_g$ $B' = 0.1120$ , $B'' = 0.1097$	Appear at several cm pressure with 1 m absorbing path. Rotational analysis of four bands. Bands 3501 and 3601 have common upper state with perturbed rotational levels. Molecule possibly bent in upper state of band 3467. Ground state is $^1\Sigma^+_g$ .	1, 6
	3640–3355		Magnetic rotation spectrum	Intense. Doublets with 17 cm <sup>-1</sup> separation. Excellent correlation between sharp, low frequency members of doublets and sharp absorption edges. Conclusion molecule has magnetic moment along figure axis in upper state. Magnetic rotational lines form progressions with about 270 cm <sup>-1</sup> differences.	7
	3250–3125		Magnetic rotation spectrum	Weak. No correlation with absorption edges found.	
	2200–1800	$\omega' \sim 410$	Absorption bands	Bands reach till 2150 Å at 0.5 mm pressure and 1 m path, till 2300 at 40 cm pressure. Each band has several components. In 9 also frequency differences of 656, 1547, 870 observed.	8, 9, 4
	1815		Absorption band	Consists of at least two components. Assigned in 8 to transition between non-bonding atomic orbitals.	
	1950–1650	$\omega' \sim 830$	Absorption bands	Weak. Progression with 830 difference in 8 seems continuation of 803 progression in 9.	
	1612, 1595, 1577, 1553	$\omega''_1 = 650(\nu_t)$ $\omega''_1 = 660$ $\omega'_2 = 1670$	Absorption bands	In 8 group assigned to excitation of non-bonding electron. 1595 strongest bands. All bands show well-resolved structure, degraded to red.	
	1535–1450		Absorption bands	Complex bands without obvious regularities.	
	1450–1230		Absorption bands. Transitions $^1\Sigma^+_g \rightarrow$ states converging to lowest $^2\Pi_g$ of CS <sub>2</sub> <sup>+</sup>	Bands form Rydberg series $\nu = 81,734 - R/(n+0.55)^2$ ; $n = 3, 4, \dots$ with ionization potential $10.083 \pm 0.005$ volts, and $\nu = 81,298 - R/(n+0.55)^2$ ; $n = 3, 4, \dots$ with ionization poten-	

Table A.—Continued.

MOLECULE	SPECTRAL REGION (Å)	FREQUENCIES† (cm <sup>-1</sup> )	CHARACTERISTICS OF TRANSITION	REMARKS	LIT.
				tial 10.027 volts. Difference between two limits corresponds to doublet separation of $^2\Pi_g$ of $\text{CS}_2^+$ . Besides Rydberg series other vibrationless electronic transitions.	
	below 1200		Absorption bands	Diffuse bands with fairly wide vibrational pattern. Diffuseness probably due to pre-ionization. Bands almost certainly due to excitation of $\pi_u$ electron from double bond, converge perhaps to ionization potential of about 13.5 ev.	
$\text{N}_2\text{O}$ nitrous oxide	3000–1760		Continuous absorption	Consists of several regions showing up at different pressures: extremely weak absorption at 5 atmos. and 33 m path with flat maximum at 2900Å, interpreted as forbidden transition leading to normal $\text{N}_2$ and O. Rise of next absorption at about 2820Å. Its long wave limit is at 2750Å in 1 m path and atmos. pressure. With 2 m path and 7.3 mm pressure absorption from 2070–1770Å with center at 1900Å. In these regions different dissociations processes possible: $\text{N}_2(^1\Sigma) + \text{O}(^1D)$ , $\text{NO}(^2\Pi) + \text{N}(^4S)$ , $\text{N}_2(^1\Sigma) + \text{O}(^1S)$ , $\text{NO}(^2\Pi) + \text{N}(^3D)$ . In 12 photometric study of region 2350–2150Å at +20° and –90°C.	1, 10–12
	1520–1425	$\omega' = 621$	Absorption bands	Appear at 0.01 mm pressure with 2 m path. Above 0.1 mm bands merge into continuum whose limits increase with pressure. At 7.3 mm strong absorption till 1700Å. Bands fit formula $\nu = 65,939 + 621.2v - 11.54v^2$ with $v=0, 1, 2, \dots$ . See also p. 109.	
	1280		Maximum of continuous absorption	Appears at 0.002 mm pressure and 2 m path, widens to 1356–1215Å at 0.2 mm.	
	1185–1160 1153, 1144, 1133		Absorption bands	Appear at 0.001 mm pressure in 2 m path. Perhaps two electronic transitions. Origin of 1st group at 84,992 cm <sup>-1</sup> .	
	1096		Maximum of continuous absorption	Appears at 0.01 mm pressure with 2 m path.	
	1056		Absorption band	Appears at 0.004 mm pressure and 2 m path.	
	below 1056		Absorption bands	Appear at 0.004 mm pressure. Fit, together with lowest pressure centers of 1280 and 1096 absorptions, into Rydberg series $\nu = 102,567 - R/(n-0.92)^2$ ; $n=3, 4, 5, \dots$ ; ionization potential 12.66 volts.	
	below 1000		Continuous absorption	Extends to end of the plate, about 850Å.	



Table A.—Continued.

MOLECULE	SPECTRAL REGION (Å)	FREQUENCIES† (cm <sup>-1</sup> )	CHARACTERISTICS OF TRANSITION	REMARKS	LIT.
C <sub>3</sub> O <sub>2</sub> carbon suboxide	3300–2400	$\omega'_t \sim 840$	Absorption bands till 2800Å and overlapping continuum till 2400Å	Absorbing columns 50–100 cm and pressures 200–800 mm. Complicated spectrum. Bands are diffuse. Pairs of 100 cm <sup>-1</sup> and 50–70 cm <sup>-1</sup> interval form progressions with 840 differences according to totally symmetrical C≡C vibration. Other observed frequencies 2160, 640 cm <sup>-1</sup> . Tentative analysis not entirely satisfactory.	1, 13
	below 2200		Continuous absorption	Absorbing columns 20–100 cm, pressures 20–800 mm. At higher pressures this region eventually overlaps former, giving continuous absorption from ca. 3200Å to shorter wavelengths. No visible fluorescence observed by irradiation with lines of Hg lamp.	
HgCl <sub>2</sub> mercuric chloride	1731–1670	$\omega''_s = 365(\nu_t)$ $\omega'_s = 289$ $\omega''_d = 70(^2\delta_u \perp)$ $\omega'_d = 65$	Absorption bands Normal state $^1\Sigma^+_g$ , upper state probably $^1\Sigma_u$ . 0,0 band at 59,016 cm <sup>-1</sup> .	Appear with 4.22 cm path above 0.004 mm pressure, degraded to red. Analysis in agreement with selection rules of Herzberg and Teller for allowed transition. See also p. 106.	1, 14–16
HgBr <sub>2</sub> mercuric bromide	1862–1813	$\omega''_s = 229(\nu_t)$ $\omega'_s = 194$ $\omega''_d = 41(^2\delta_u \perp)$ $\omega'_d = 36$	Absorption bands. Normal state $^1\Sigma^+_g$ , upper state probably $^1\Sigma_u$ . 0,0 band at 54,418 cm <sup>-1</sup> .	Appear with 5.2 cm path above 0.1 mm pressure. Bands are rather diffuse. Analysis as for HgCl <sub>2</sub> . See also p. 106.	1, 14
HgI <sub>2</sub> mercuric iodide	2108–2066	$\omega''_s = 156(\nu_t)$ $\omega'_s = 126$ $\omega''_d = 33(^2\delta_u \perp)$ $\omega'_d = 30$	Absorption bands. Normal state $^1\Sigma^+_g$ , upper state probably $^1\Sigma_u$ . 0,0 band at 47,883 cm <sup>-1</sup> .	Appear with 4.4 cm path above 0.1 mm pressure. Bands are very diffuse. Analysis as for HgCl <sub>2</sub> . See also p. 106.	1, 14
PbBr <sub>2</sub> lead bromide				Upon illumination with 2300–2000Å are observed Br <sub>2</sub> bands at 5600–5050Å, bands at 4950–4433Å ascribed to PbBr, and atomic Pb lines.	1, 17
TeCl <sub>2</sub> tellurium dichloride	7400–4350	$\omega'_1 = 300$ $\omega'_2 = 60$ $\omega'_2 = 125$	Absorption bands	In 18 absorbing paths of 100 cm in visible, of 30 cm in ultraviolet. In 19 absorbing paths of 5 and 60 cm, region of observed spectrum 6500–4700Å is ascribed to same transition. Bands are diffuse, degraded to red at longer waves. Superimposed continuous absorption. In 19 isotopic effect of Cl observed, attempt at analysis made and molecule as linear suggested.	18, 19
	4360–3960		Absorption bands	With 10 cm absorbing column and 500°C transparency was found below and above the bands in contradiction to 18 and 19. Brief note.	20
	3170–2510		Maxima of continuous absorption	Dissociation processes are discussed.	84
	2460		Long wave limit of continuous absorption		

Table A.—Continued.

MOLECULE	SPECTRAL REGION (Å)	FREQUENCIES† (CM <sup>-1</sup> )	CHARACTERISTICS OF TRANSITION	REMARKS	LIT.
TeBr <sub>2</sub> tellurium dibromide	6500–5300		Absorption bands	Absorption path 10 cm. Diffuse bands, degraded to red at longer waves. Superimposed continuum towards shorter waves. Uncertain whether molecule linear.	2, 19
	4730, 3800, 3140, (2280)		Maxima of continuous absorption	Dissociation processes are discussed.	84
C <sub>2</sub> H <sub>2</sub> acetylene	2430–2090	$\omega'_1 \sim 1050$ $\omega'_2 \sim 1000$ $\omega'_3 \sim 580$	Absorption bands	Pressures from a few mm to 1040 mm and absorption cells of 50 and 350 cm. Temperature dependence of bands studied. Bands are double-headed, degraded to the red. Complicated system. Analysis not satisfactory.	1, 2, 21
C <sub>2</sub> N <sub>2</sub> cyanogen	3020–2400	$\omega'_t(\text{CN}) = 2050$ $\omega'_t(\text{C}-\text{C}) = 895$	Absorption bands 0,0 band perhaps at 33,294 cm <sup>-1</sup> .	Absorbing paths of 0.5, 1.5 and 3 m, pressures up to 2 atmos. Bands degraded to red. Two main progressions with spacings of 2050 and 895 cm <sup>-1</sup> ; members appear threefold, the two at longer waves probably being due to $v-v$ transitions of non-totally symmetrical vibrations. Main features of analysis in agreement with selection rules for allowed (by symmetry) transition. Weakness of system suggests intercombination. See also p. 108.	1, 22
	2250–2050		Absorption bands	Original lit. not accessible. According to review in Phys. Ber. 50 bands observed, frequency differences of 766, 2149, 2355 and $2 \times 508$ cm <sup>-1</sup> found.	23
				In 24 observation of CN bands in fluorescence upon illumination of C <sub>2</sub> N <sub>2</sub> with H <sub>2</sub> continuum.	24
BrCN bromo- cyanogen				Fluorescence of CN $^2\Sigma - ^2\Sigma$ bands upon illumination of BrCN with H <sub>2</sub> lamp	1, 25
ICN iodocyano- gen				Fluorescence of CN $^2\Sigma - ^2\Sigma$ bands upon illumination of ICN with H <sub>2</sub> lamp and Al spark. Also I <sub>2</sub> fluorescence observed.	1, 25
C <sub>4</sub> H <sub>2</sub> diacetylene	2970–2650	$\omega' = 690$	Absorption bands	Absorbing paths of 3, 50 and 350 cm, pressures up to 745 mm. Longer wave system appears at high pressures, has many sharp and narrow bands. Satisfactory analysis not yet possible, progression of doublet bands with 690 difference reported.	2, 26
	2650–2000	$\omega'_1 = 2100$ $\omega'_2 = 1900$ $\omega''_3 = 635$	Absorption bands	Shorter wave-lengths bands are diffuse, appear at low pressures. Several progressions found. Frequencies 2100 and 1900 are, respectively, ascribed to totally symmetrical $\nu_t^{(2)}(\text{C}\equiv\text{C})$ and unsymmetrical $\nu_u^{(2)}  $ ( $\text{C}\equiv\text{C}$ ) in excited state. From temperature dependence 635 is regarded as ground state frequency.	

Table B. Bent triatomic molecules.

MOLECULE	SPECTRAL REGION (Å)	FREQUENCIES (CM <sup>-1</sup> )	CHARACTERISTICS OF TRANSITION	REMARKS	LIT.
H <sub>2</sub> O water vapor	below 1240		Absorption bands	Two sets of bands, one starts with doublet band of 170 cm <sup>-1</sup> separation ( <i>A</i> bands), the other has diffuse bands ( <i>B</i> bands). Bands form weak Rydberg series probably related to atomic term series $2p^3(^4S)np$ , $^5,^3P$ of O I. (27)	1, 27-28
	1130-983		Absorption bands	Two sets of bands ( <i>C</i> and <i>D</i> ) whose first members show rotational structure. Mean of <i>C</i> and <i>D</i> bands fit into Rydberg series $\nu = 101,780 - R/(n-1.05)^2$ with $n=4, 5, 6 \dots$ . Limit gives ionization potential of 12.56 volts within probably $\pm 0.02$ volt. Concluded that upper states of Rydberg series are $(2xa_1)(nsa_1)^{3,1}A_1$ (in Mulliken's notation) and that series is related to atomic series $2p^3(^4S)ns$ , $^5,^3S$ of O I. (27)	
H <sub>2</sub> S hydrogen sulphide	1600-1460		Absorption bands	Bands are weaker than those below 1460Å. Shifted from strong band at 1516 by 1250 and 2630 cm <sup>-1</sup> which are ground state frequencies. Hence same electronic jump as 1516-1190 bands. Other bands in this region are transitions to upper vibrational states and from initial vibrational states of the following systems.	1, 2, 27, 29, 30
	1516-1190		Absorption bands	Strong and sharp <i>Q</i> branches, <i>P</i> branches extremely weak compared with <i>R</i> branches. <i>Q</i> branches fit into Rydberg series $\nu = 84,520 - R/(n-1.57)^2$ ; $n=4, 5, 6 \dots$ . Series probably related to atomic series of $(^4S)np$ , $^5,^3P$ of S I.	
	1430-1200		Absorption bands	Two more series leading to limit of following Rydberg series.	
	1391-1190		Absorption bands	Bands have very strong and sharp <i>Q</i> branches accompanied on either side by weaker <i>R</i> and <i>P</i> branches. Little vibrational structure, electronic transition being of non-bonding type. Discussion of rotational structure. Mean of two lower moments of inertia for upper state derived as $2.77 \times 10^{-40}$ gcm <sup>2</sup> . <i>Q</i> branches fit into Rydberg series $\nu = 84,420 - R/(n-2.04)^2$ ; $n=5, 6, 7 \dots$ . Series perhaps related to atomic term series of $(^4S)ns$ , $^5,^3P$ of S I. Mean of both Rydberg series corresponds to ionization potential of $10.420 \pm 0.005$ ev.	
NO <sub>2</sub> nitrogen dioxide	5750-3520		Absorption bands	In 31 table of band heads. In 31a measurement of absorption coefficients from $\lambda 7000$ to $\lambda 4000$ .	1, 31-34
	2600-2270	$\omega'_t = 523$ $\omega'_t = 714$ $\omega''_t = 749?$ $\omega''_t = 1319?$	Absorption bands. Transition parallel to axis of approximate rotational symmetry ( $\sigma$ axis) and perpen-	System consists of sharp bands and diffuse bands. Degradation to red. Absorption lengths from 2 mm to 5 m. Variation of pressure and temperature. Spectra (in 32) taken with medium, large and very large dis-	

Table B.—Continued.

MOLECULE	SPECTRAL REGION (Å)	FREQUENCIES (CM <sup>-1</sup> )	CHARACTERISTICS OF TRANSITION	REMARKS	LIT.
			dicular to molecular axis of symmetry ( $\pi$ axis).	person. Intensity measurements. Vibrational analysis (32) not unambiguous, different explanations discussed.	
			Rotational constants in cm <sup>-1</sup> : $\Delta B_{\sigma}$ (from head spacing) = $-3.78 \pm 0.02$ $\Delta B''_{\sigma}$ (from temperature variation of absorption coefficient) = $20 \pm 5$ . $B'_{\sigma}$ (from $B''_{\sigma} + \Delta B_{\sigma}$ ) = $16 \pm 5$ . $\Delta B_J$ (from intensity of and spacing within sub-bands) = $-0.06 \pm 0.01$ .  $\langle 2B_J \rangle_{Av}$ (from intensity of and spacing within sub-bands) = $0.6 \pm 0.15$ . $B''_J = \frac{1}{2}(\langle 2B_J \rangle_{Av} - \Delta B_J) = 0.33 \pm 0.03$ $B'_J = \frac{1}{2}(\langle 2B_J \rangle_{Av} + \Delta B_J) = 0.27 \pm 0.03$	Sharp and intense sub-band heads. Rotational analysis of $\lambda 2491$ in 33 and 34, given here 34. Sub-band heads in $\lambda 2491$ , $\lambda 2459$ and $\lambda 2576$ are represented by $\nu = \Delta B_{\sigma} K^2 + \text{const.}$ and $\Delta \nu = \Delta B_{\sigma}(2K+1)$ . Rotational levels given by $E_r(J, K) = B_J J(J+1) + B_K K^2 + \dots$ with $ K  \leq J$ ; $B_K = B_{\sigma} - \frac{1}{2}(B_{\sigma} + B_{\perp})$ ; $B_J = \frac{1}{2}(B_{\sigma} + B_{\perp})$ . From rotational constants follows $r''(\text{N-O}) = 1.28 \pm 0.03 \text{ Å}$ ; $r'(\text{N-O}) = 1.41 \pm 0.06 \text{ Å}$ ; $\angle''(\text{O-N-O}) = 154 \pm 4^\circ$ ; $\angle'(\text{O-N-O}) = 154 \pm 6^\circ$ .	
NOCl nitrosyl chloride	6000–2000		Eleven absorption maxima and continuous absorption	Measurement of extinction coefficients in 35 and 36. In the visible two sets of weak diffuse bands, perhaps belonging to same electronic transition. Frequency differences of 380, 690 and 1580 cm <sup>-1</sup> found (35), interpretation not certain. No fine structure found in disagreement with previous work. (See 1.) Broad maxima in the violet and ultraviolet belonging to other transitions.  Molecule is diamagnetic (37).	1, 35–37
SO <sub>2</sub> sulphur dioxide	at 3800	$\omega'_1 = 908(\nu_t   )$ $\omega'_2 = 362(\delta_t   )$	Absorption bands origin at 25,774.6	In 38 vibrational and in 39 rotational analysis, brief abstracts.	1, 38, 39
	3164–2939		Magnetic rotation spectrum	Very weak. Spectrum has regular appearance, its lines may be correlated to absorption band heads.	7
	2440–1750	$\omega'_2 \sim 380(\delta_t   )$	Absorption and emission bands	Degraded to red. Bands show periodic intensity fluctuations. Fine structure of individual bands varies considerably. Short wave-length bands more complex. From temp. variation experiments band 43,100 cm <sup>-1</sup> taken as first member of progression. Transition probably due to a relatively non-bonding electron localized on an oxygen atom. In 40 extension of emission bands.	8, 29, 40
	1573, 1558, 1529		Absorption bands	Weak and diffuse.	8

Table B.—Continued.

MOLECULE	SPECTRAL REGION (Å)	FREQUENCIES (CM <sup>-1</sup> )	CHARACTERISTICS OF TRANSITION	REMARKS	LIT.
	1359–1308 1280–1240 below 1140		Absorption bands	Bands of these electronic transitions very likely belong to a Rydberg series leading to an ionization potential of $12.05 \pm 0.05$ ev.	8
SeO <sub>2</sub> selenium dioxide	4400–3400		Absorption bands	Appear above 290°C, 10 cm absorbing path. Diffuse, some bands show heads, degraded to red. At higher temp. overlapping with next system.	2, 41, 42
	3400–2200		Absorption bands	Appear above 200°C, 10 cm absorbing path. Degraded to red. In 42 and 43 different analyses proposed, both with difficulties involved. Ground state frequencies of about 900 and 1180 cm <sup>-1</sup> probable.	42, 43
	2200–2070		Absorption bands	Appear above 200°C, 10 cm absorbing path. Weak. Degraded to red. Formula for band heads given.	41, 42
TeO <sub>2</sub> tellurium dioxide	5800–4700		Absorption bands	Diffuse, no measurements given. Appear above 1250°C.	42, 44
	4700–3000		Absorption bands	Diffuse, some bands show heads degraded to red. Appear about 720°C. Bands measured between 4030 and 3230 Å. Attempt at analysis made.	
	3000 to vacuum region		Continuous absorption	Appears about 720°C. Absorbing layer of 30 cm used throughout.	
ClO <sub>2</sub> chlorine dioxide	5225–2600	$\omega''_1 = 945(\nu_t   )$ $\omega''_2 = 1105(\nu_\perp)$ $\omega''_3 = 447(\delta_t   )$ $\omega'_1 = 708(\nu_t   )$ $\omega'_2 = 790(\nu_\perp)$ $\omega'_3 = 290(\delta_t   )$	Absorption bands. (000)←(000) band is 21,016 cm <sup>-1</sup>	Degraded to red. Photographs in second order of 30 ft. 30,000 line per inch grating show that each band consists of sub-bands, some with clearly defined rotational series. Analysis in agreement with selection rules.	1, 44a
O <sub>3</sub> ozone	7585–4380		Absorption bands	Measurement of absorption coefficients with absorbing columns between 7 and 26 cm, mean temp. 18°C. In 46 abs. coeff. of atmos. ozone.	1, 45, 46
	4533–3053		Continuum with superimposed emission bands	Table of bands.	47
	3525–2135		Absorption bands	Absorption coeff. in 48. In 49 and 50 table and abs. coeff. of atmos. ozone. In 51 influence of temp. on abs. coeff. Analysis proposed in 52 uncertain, probably not correct. In 53 somewhat strange attempt at interpretation of electronic terms of O <sub>3</sub> .	48–53
SiCl <sub>2</sub> silicon dichloride	4022, 3260 2570, 2450		Maxima of continuous emission	Observed in uncondensed discharge through flowing SiCl <sub>4</sub> vapor at about 0.5 mm pressure. Carrier not certain.	54
	3917–3533	$\omega''_1 = 248$ $\omega''_2 = 540$	Emission bands	Under same conditions but at 0.05 mm pressure. Carrier of both systems is considered to be SiCl <sub>2</sub> because bands appear at lower pressures than SiCl bands and become stronger in condensed discharge where SiCl	
	3482–3158	$\omega'_1 = 201$ $\omega'_2 = 540$ $\omega'_3 = 445$	Emission bands		

Table B.—Continued.

MOLECULE	SPECTRAL REGION (Å)	FREQUENCIES (CM <sup>-1</sup> )	CHARACTERISTICS OF TRANSITION	REMARKS	LIT.
				bands become weaker. SiCl <sub>2</sub> molecule is regarded as bent. This, and analysis, although in agreement with selection rules, seem not absolutely definite.	
SnCl <sub>2</sub> tin dichloride	4500, 3100		Maxima of continuous emission	Obtained in uncondensed discharge through flowing SnCl <sub>2</sub> vapor of about 1 mm pressure.	1, 2, 54
	4800–4500	$\omega''_1 = 122$ $\omega''_2 = 355$	Emission bands	Appear under same conditions, are ascribed to SnCl <sub>2</sub> . Molecule regarded as bent. This, and analysis, although in agreement with selection rules, seem not absolutely definite.	
HClO hypochlo- rous acid	4000–2100 at 3200 and probably about 2100		Cont. absorption. Maxima of cont. absorption	10 m absorbing path. Determination of extinction coefficients. Discussion of dissociation processes and comparison with data in solution.	64

Table C. Miscellaneous simpler inorganic molecules.

MOLECULE	SPECTRAL REGION (Å)	FRE- QUENCIES (CM <sup>-1</sup> )	CHARACTERISTICS OF TRANSITION	REMARKS	LIT.
GaCl <sub>2</sub> gallium dichloride	2275 at 178°C 2130 at 150°C 1990 at 128°C 1735 at 82°C		Maxima of continuous absorption	5 cm absorption path. Temperatures for best development of maxima added. Absorption bands are diffuse, their carriers not yet identified.	55, 56
InCl <sub>2</sub> indium dichloride	2391 at 285°C 2161 at 260°C 1920 at 257°C 1818 at 237°C		Maxima of continuous absorption	Upon illumination of indium halides with light of second and third continua there appear the InCl, InBr and InI systems $A-X^1\Sigma$ and $B-X^1\Sigma$ in fluorescence. Illumination with light of third continuum gives InCl bands $C-X^1\Sigma$ in fluorescence, corresponding InBr and InI systems are continua. (private communication from Dr. Wehrli). Not known whether molecules linear but photochem. behavior, which is similar to mercury halides, suggests linearity.	
	2042, 2002, 1970 at 300°C		Absorption bands		
InBr <sub>2</sub> indium dibromide	2553 at 300°C 2275 at 280°C 2060 at 260°C 1896 at 200°C		Maxima of continuous absorption		
	1864, 1859 1852, 1671, 1655, 1648 at 230°C		Absorption bands		
InI <sub>2</sub> indium diiodide	2640 at 144°C 2465 at 144°C 2115 at 131°C		Maxima of continuous absorption		
SeCl <sub>2</sub> selenium dichloride	6000–4660	$\omega = 350$	Absorption bands	Absorption path 10 cm. Weak, diffuse bands. At higher pressures superimposed continuum. Observed frequency 350 perhaps due to ground state. Uncertain whether molecule linear.	57
SeBr <sub>2</sub> selenium dibromide	5400–4960	$\omega = 240$	Absorption bands	Absorption path 10 cm. Weak, diffuse bands. At higher pressures superimposed continuum. Observed frequency 240 perhaps due to ground state. Uncertain whether molecule linear.	58

Table C.—Continued.

MOLECULE	SPECTRAL REGION (Å)	FRE- QUENCIES (CM <sup>-1</sup> )	CHARACTERISTICS OF TRANSITION	REMARKS	LIT.
FeCl <sub>2</sub> ferrous chloride	2730–2400		Maxima of contin- uous absorption	Various pressures and temperatures (600–1100°C). In far ultraviolet another absorption region (59). Temperatures up to 1000°C in 30 cm silica tube. 800°C correspond to 91 mm pressure, 1010°C to 522 mm pressure. At 100–200 mm pressure appearance of lines and bands which are ascribed to Co <sup>++</sup> and Cl <sub>2</sub> (60).	59, 60
CoCl <sub>2</sub> cobaltous chloride	3000				
NiCl <sub>2</sub> nickelous chloride	3450				
Cu <sub>2</sub> Cl <sub>2</sub> cuprous chloride	2230		Maxima of contin- uous absorption	Absorption dependent upon pressure, extends to 3300Å at 750°C corresponding to 20 mm pressure. All halides show second absorption in Schumann region, appears near 1600Å at 220°C ~0.001 mm pressure and extends with pressure. Upon illumination with wave-lengths from maxima there appear in fluorescence the CuCl, CuBr, CuI bands and Cu resonance lines. Photodissociation processes are discussed.	1, 2, 61
Cu <sub>2</sub> Br <sub>2</sub> cuprous bromide	2300				
Cu <sub>2</sub> I <sub>2</sub> cuprous iodide	2340				
MoCl <sub>3</sub> molybdenum trichloride	6400, 6000, 5300, 4500		Emission continua	Observed in discharge. Carrier not quite certain.	62
MoCl <sub>5</sub> molybdenum pentachloride	4650(4550), 3300(3700), 2800(2900)		Maxima of broad absorption bands	4650 band very intense, 3300 band weak and narrower, 2800 band intense. This spectrum exists at 100–200°C (low pressures). At higher temp. and mean pressures shift of spectrum to positions indicated in brackets. At high pressures both spectra present, from this suggested that shifted spectrum due to polymerized substance.	62
	below 2200 (2300)		Continuous absorption		
F <sub>2</sub> O <sub>2</sub> fluorine dioxide	from 5900 to shorter wave-lengths		Continuous absorption	Absorbing path 15 cm. Absorption increases towards shorter wave-lengths, maximum not yet reached at 2000Å. Curve shows slight step outs. Determination of extinction coeff. Because of thermal decompos. of F <sub>2</sub> O <sub>2</sub> absorption tube was kept below –60°C.	63
H <sub>2</sub> O <sub>2</sub> hydrogen peroxide	2800–2100		Continuous absorption	10 m absorbing path. Determination of extinction coefficients.	1, 2, 64
SO <sub>3</sub> sulphur trioxide	3000–2300		Absorption bands and continuum	Absorption paths of 40, 54 and 346 cm length. Bands are weak and diffuse, continuous background superimposed. Determination of extinction coeff. (65). Photochemical decomposition occurs with light >2760Å, most likely into normal SO <sub>2</sub> and O (66).	1, 65, 66
NO <sub>3</sub>	6640–5000		Absorption bands	Appear in gaseous system N <sub>2</sub> O <sub>5</sub> –O <sub>3</sub> during decomposition of ozone, or in discharge through gaseous NO <sub>2</sub> –O <sub>2</sub> . Determination of extinction coeff.	67–70
N <sub>2</sub> O <sub>5</sub> nitrogen pentoxide	3800–2400		Continuous absorption	Abs. coeff. measured between 3800 and 2850Å. Absorption increases from 3800 to shorter wave-lengths with no maximum as far as λ2400. No absorption found in 4500Å region contrary to previous report. (See ref. 56a in 1.)	1, 67

Table C.—Continued.

MOLECULE	SPECTRAL REGION (Å)	FRE- QUENCIES ( $\text{cm}^{-1}$ )	CHARACTERISTICS OF TRANSITION	REMARKS	LIT.
$\text{P}_4\text{O}_{10}$ phosphorus pentoxide	2530		Long wave limit of continuous absorption	Corresponds to 563°C (melting point) in 10 cm cell. Absorption complete from $\lambda 2400$ .	82
$\text{P}_4\text{Se}_{10}$ phosphorus penta- selenide	3420, 2534 and 2780		Long wave limits and maximum of cont. absorption	80 cm absorption path. Dissociation processes are discussed.	71
$\text{Cl}_2\text{O}_3$	4650–4260 4260–3500		Absorption bands Continuum	Broad bands. 10 cm absorbing layer. Short note.	72
$\text{ClO}_3$ chlorine trioxide	3500–2100		Continuous absorption	54 cm absorption path. Determination of extinction coefficients. Maxima at 2780 and from 2170 Å onwards. Ob- served absorption limited by spectro- graph. Substance polymerizes in liquid phase to $\text{Cl}_2\text{O}_6$ .	73
$\text{Cl}_2\text{O}_6$ chlorine hexoxide	6000–2200		Continuous absorption	Liquid used in very thin layer. Ob- served absorption limited by spectro- graph.	73
$\text{Cl}_2\text{O}_7$ chlorine heptoxide	from 3000 to shorter wave- lengths		Continuous absorption	30 cm absorbing layer. Up to 85 cm pressure substance transparent to 3000 Å. From there on smooth cont. absorpt. with increasing intensity to measured limit of 2000 Å. Determina- tion of extinction coeff.	74
$\text{Se}_2\text{Cl}_2$ selenium monochlo- ride	4100, 3200, 2490 and 3500, 2950, 2370		Long wave limits and maxima of cont. absorption	5 cm cell, 1–3 mm pressure. Dissocia- tion processes discussed.	2, 84
$\text{Se}_2\text{Br}_2$ selenium monobro- mide	4650, 3500, 2880 and 3840, 3220, 2570		Long wave limits and maxima of cont. absorption	10 cm cell, pressure corresponding to 75°C. Dissociation processes discussed.	84
$\text{S}_2\text{O}_5\text{Cl}_2$ pyrosul- phuryl chloride	2460		Long wave limit of continuous absorption	10 cm cell, about 2 mm pressure, room temp.	84
$\text{POCl}_3$ phosphorus oxychloride	2250		Long wave limit of continuous absorption	Corresponds to 3.5 cm pressure in 20 cm cell. Complete absorption from $\lambda 2200$ .	82
$\text{SbOCl}_3$ antimony oxychloride	2460		Long wave limit of continuous absorption	At 100°C in 10 cm cell. Difficult to obtain because substance decomposes easily.	82
$\text{HNO}_2$ nitrous acid	3850–3180	$\omega' \sim 1000$	Absorption bands	Observed in $\text{NO}/\text{NO}_2/\text{H}_2\text{O}$ mixtures. Diffuse. Different interpretations dis- cussed in 75 and 208. In 76 system of very similar bands observed in $\text{NO}/$ $\text{CO}/\text{N}_2\text{O}$ mixtures and suggested as selectively enhanced $\text{NO}_2$ bands. Iden- tity of both systems suggestive but not definitely certain.	75–77, 208
$\text{NaNO}_2$ sodium nitrite	3010–2540 with maximum at 2710		Continuous absorption	80 cm absorption path. Well developed when $\text{NO}$ bands begin to appear at 275°C and $\text{NO}_2$ bands at 380°C.	78
$\text{HNO}_3$ nitric acid	2980–2520 with maximum at 2620		Continuous absorption	10 cm absorption path. Appears at 2 mm pressure and is well developed at 4 mm.	78



Table C.—Continued.

MOLECULE	SPECTRAL REGION (Å)	FRE- QUENCIES (CM <sup>-1</sup> )	CHARACTERISTICS OF TRANSITION	REMARKS	LIT.
KNO <sub>3</sub> potassium nitrate	3080–2520 with maximum at 2670		Continuous absorption	80 cm absorption path. Appears at 360–375°C. Disappears at higher temp. along with appearance of NO <sub>2</sub> bands.	78
AgNO <sub>3</sub> silver nitrate	3010–2510 with maximum at 2630		Continuous absorption	80 cm absorption path. Well developed at 234°C, decomposition rapid above 250°C.	78
Mg(NO <sub>3</sub> ) <sub>2</sub> magnesium nitrate	2940–2570 with maximum at 2700		Continuous absorption	80 cm absorption path. Well developed at 280°C, decomposition above 170°C.	78
Pb(NO <sub>3</sub> ) <sub>2</sub> lead nitrate	2920–2520 with maximum at 2680		Continuous absorption	80 cm absorption path. Appears at 240°C. NO bands appear above 290°, NO <sub>2</sub> bands above 370°C.	78
NH <sub>4</sub> NO <sub>3</sub> ammonium nitrate	2990–2520 with maximum at 2620		Continuous absorption	80 cm absorption path. Appears at 110°C, well developed at 240°C. Decomposition with appearance of NO <sub>2</sub> bands begins at 200°C, becomes rapid at 280°C.	78
H <sub>2</sub> SO <sub>4</sub> sulphuric acid	2850–2540 with maximum at 2620		Continuous absorption	80 cm absorption path and 2 mm pressure. Probably superposition of SO <sub>2</sub> absorption.	78
K <sub>2</sub> SO <sub>4</sub> potassium sulphate	2930–2540 with maximum at 2580		Continuous absorption	80 cm absorption path. Well developed at 800°C. Probably superposition of SO <sub>2</sub> absorption.	78
Ag <sub>2</sub> SO <sub>4</sub> silver sulphate	3000–2500 with maximum at 2650		Continuous absorption	80 cm absorption path. Appears at 160°C, SO <sub>2</sub> bands appear from 180° on.	78
ZnSO <sub>4</sub> zinc sulphate	2940–2420 with maximum at 2690		Continuous absorption	80 cm absorption path. Appears above 600°C together with traces of SO <sub>2</sub> at longer wave-lengths.	78

Table D. Pyramidal and tetrahedral molecules.

MOLECULE	SPECTRAL REGION (Å)	FREQUENCIES (CM <sup>-1</sup> )	CHARACTERISTICS OF TRANSITION	REMARKS	LIT.
NH <sub>3</sub> ammonia	1620–1450		Absorption, 0, 2 till 0, 8 bands of second electronic state above normal	Pressures of 0.017 to 0.09 mm. 6 m normal incidence vacuum spectrogr. used as absorpt. tube. Each band has <i>P</i> and <i>R</i> branch and broad intense line as <i>Q</i> branch. From rotational analysis concluded $I_A'$ only slightly larger than $I_A''$ and $I_c' \approx I_c''$ ( $I_c$ moment of inertia about symmetry axis). In 80 a discussion is given of a possible Rydberg series in ammonia.	1, 2, 79
ND <sub>3</sub> , ND <sub>2</sub> H, NDH <sub>2</sub> deutero- ammonias	2167–1675		Absorption bands Origin taken as 46,167 ± 30 cm <sup>-1</sup>	Diffuse bands because of pre-dissociation. ND <sub>3</sub> pressures from 0.014 to 0.70 mm. (80) ND <sub>2</sub> H and NDH <sub>2</sub> present as formed contaminations.	2, 80, 81
	1664–1412	$\omega'_{\text{ND}_3} = 721(\delta_t   )$ $\omega'_{\text{ND}_2\text{H}} = 804(\delta_t   )$ $\omega_{\text{NDH}_2} = 872(\delta_t   )$	Absorption bands	Less intense than first transition. Bands are sharp, show heads on ultraviolet side. Fit formulas:	

Table D.—Continued.

MOLECULE	SPECTRAL REGION (Å)	FREQUENCIES (CM <sup>-1</sup> )	CHARACTERISTICS OF TRANSITION	REMARKS	LIT.
				$\nu_{\text{ND}_3} = 60,071 + 721v + 3.3v^2$ $\nu_{\text{ND}_2\text{H}} = 60,083 + 804v + 4.64v^2$ $\nu_{\text{NDH}_2} = 60,133 + 872v + 6.48v^2$ $v = 0, 1, 2, \dots$	
	1433–1248	$\omega'_{\text{ND}_3} = 686(\delta_i)$ $\omega'_{\text{ND}_2\text{H}} = 775(\delta_i)$ $\omega'_{\text{NDH}_2} = 837(\delta_i)$	Absorption bands	Sharp, more intense than preceding bands. Fit formulas: $\nu_{\text{ND}_3} = 69,791 + 686v + 7.50v^2$ $\nu_{\text{ND}_2\text{H}} = 69,764 + 775v + 7.32v^2$ $\nu_{\text{NDH}_2} = 69,786 + 837v + 9.50v^2$ , NDH <sub>2</sub> bands stronger than ND <sub>2</sub> H bands, the latter being stronger than ND <sub>3</sub> bands.	
	below 1220 below 1150		Absorption bands Continuous absorption	Bands overlap.	
PCl <sub>3</sub> phosphorus trichloride	2815		Long wave limit of continuous absorption	Corresponds to 8 mm pressure in 10 cm cell. No maximum observed, absorption complete below $\lambda 2440$ .	1, 82
PBr <sub>3</sub> phosphorus tribromide	3083, 2635 and about 2440 2695, 2495		Long wave limits of cont. absorption. Flat maxima of cont. absorption	At 4 mm pressure in 1 cm tube, complete absorption from $\lambda 2360$ .	82
AsCl <sub>3</sub> arsenic trichloride	2687, 2475 and 2547		Long wave limits and maximum of cont. absorption	Corresponds to 2 mm pressure in 10 cm cell. Complete absorption from $\lambda 2390$ .	1, 82
SbCl <sub>3</sub> antimony trichloride	2837, 2694 2475 and 2745, 2551		Long wave limits and maxima of cont. absorption	10 cm cell, 0.5–12 mm pressures. At 3 mm pressure complete absorption from $\lambda 2410$ . First maximum very flat, second one high.	1, 82
BiCl <sub>3</sub> bismuth trichloride	3350, 2660 and 2800		Long wave limits and maximum of cont. absorption	10 cm cell, pressures according to temperatures of 90°–335°C. Discussion of dissociation processes of the last 5 halides (82).	1, 82
PCl <sub>5</sub> phosphorus pentachloride	2625, 2240 and 2310		Long wave limits and maximum of cont. absorption	Taken at 10 mm pressure. Molecule trigonal bipyramid according to electron diffraction (83).	1, 82, 83
PBr <sub>5</sub> phosphorus pentabromide	3146, 2688 and 2744		Long wave limits and maximum of cont. absorption	With 4 mm pressure and 10 cm cell.	82
SOBr <sub>2</sub> thionyl bromide	3780, 2180, 2450 and 3270, 2650		Long wave limits and maxima of cont. absorption	First figure 3780 belongs to spectrum taken in 10 cm cell with 0.5 mm pressure, at higher pressures shift of limit to longer waves. Dissociation processes of SOBr <sub>2</sub> and SeOCl <sub>2</sub> discussed in 84.	84, 85
SeOCl <sub>2</sub> selenium oxychloride	3150, 2500 and 2660		Long wave limits and maximum of cont. absorption	Since SOCl <sub>2</sub> and SOBr <sub>2</sub> are pyramidal (86, 85 electron diffraction), SeOCl <sub>2</sub> and TeOCl <sub>2</sub> have been included in this table for analogy reasons.	84–86
TeOCl <sub>2</sub> tellurium oxychloride	5750–5000		Absorption bands	Carrier does not seem definitely established, very brief note.	20

Table D.—Continued.

MOLECULE	SPECTRAL REGION (Å)	FREQUENCIES (CM <sup>-1</sup> )	CHARACTERISTICS OF TRANSITION	REMARKS	LIT.
CH <sub>4</sub> methane				Photodecomposition of CH <sub>4</sub> upon illumination with Xe lines λ1470 and λ1295, in 88 H <sub>2</sub> continuum used. Dissociation into CH <sub>3</sub> +H most probable.	87, 88
SiH <sub>4</sub> monosilane				10 cm cell. No absorption down to 1850Å at 75 mm pressure.	89
CCl <sub>4</sub> carbon tetra-chloride	4600, 3348, 3070, 2580, 2430, 2300		Maxima of continuous emission bands	Appear in uncondensed discharge through flowing CCl <sub>4</sub> vapor at 0.2–0.3 mm pressure. Carrier not identified.	1, 90
CBr <sub>4</sub> carbon tetra-bromide	2932, 2453 and 2525		Long wave limits and maximum of cont. absorption	Exact conditions not given.	1, 91
CI <sub>4</sub> carbon tetra-iodide	3930, 3177, 2795 and 3449, 3010, 2700		Long wave limits and maxima of cont. absorption	Obtained by heating absorption tube up to 60°C with warm air.	91
SiBr <sub>4</sub> silicon tetra-bromide	4220–2370		10 maxima of continuous emission bands	Appear in condensed and uncondensed discharge through flowing SiBr <sub>4</sub> vapor at pressures above 0.5 mm. Carrier not identified.	1, 92
SnCl <sub>4</sub> tin tetra-chloride	below 2500		Continuous absorption	10 cm cell and 1–10 mm pressure.	1, 91
SnBr <sub>4</sub> tin tetra-bromide	3471, 2915, 2442 and 3063, 2728		Long wave limits and maxima of cont. absorption	1 cm cell, pressure indicated as low. Discussion of photodissociation processes of carbon and tin tetrachlorides in 91.	1, 91
SnI <sub>4</sub> tin tetra-iodide	3570, 2800, 2450 below 2300		Maxima of cont. absorption Cont. absorption	Absorption path 1.5 m. Dissociation processes are discussed.	93
SeCl <sub>4</sub> selenium tetra-chloride	4150, 3010, 2500 and 3250, 2750 2400		Long wave limits and maxima of cont. absorption	Pressures according to temperatures up to 100°C.	84
SeBr <sub>4</sub> selenium tetra-bromide	5800, 5300, 3500, 2500 and 4900, 4270, 2620		Long wave limits and maxima of cont. absorption	Dissociation processes of selenium and tellurium tetrahalides discussed in 84. Similarity between spectra of Se tetra- and monohalides, and of Te tetra- and dihalides pointed out. Electron diffraction shows (94) that TeCl <sub>4</sub> has most likely a distorted trigonal bipyramidal configuration, the same may be assumed for the other three tetrahalides.	84, 94
TeCl <sub>4</sub> tellurium tetra-chloride	4800, 2720 and 3240, 2470		Long wave limits and maxima of cont. absorption		
TeBr <sub>4</sub> tellurium tetra-bromide	5250, 2960 2490, and 4650, (4000), 2650		Long wave limits and maxima of cont. absorption		
RuO <sub>4</sub> ruthenium tetroxide	4500–2800 from 2850	ω~780 ω~895	Absorption bands Cont. absorption	Spectrum is similar to that of OsO <sub>4</sub> (see reference 67a in 1) but more diffuse. Several electronic transitions are suggested. Brief preliminary note. Not known whether	95, 96

Table D.—Continued.

MOLECULE	SPECTRAL REGION (Å)	FREQUENCIES ( $\text{cm}^{-1}$ )	CHARACTERISTICS OF TRANSITION	REMARKS	LIT.
				molecule strictly tetrahedral. (96) was not accessible, re- viewed in Phys. Ber. 1938.	
$\text{C}_2\text{H}_6$ ethane				Determination of extinction coeff. for Xe lines $\lambda 1470$ and $\lambda 1295$ . Photodissociation into two methyl radicals concluded from photochemical study.	97
$\text{B}_2\text{H}_6$ diborane	2200–1550 with maximum at 1820		Continuous absorption	15 cm cell in ordinary ultra- violet, 20 cm cell in Schumann region. Atmospheric pressure. Rough determination of ab- sorption coeff. down to $\lambda 1550$ . After minimum at about 1700 Å second steeper rise of absorpt. Discussion of possible elec- tronic config. of the two ex- cited states.	98
$\text{Si}_2\text{H}_6$ disilane	below 2020		Continuous absorption	10 cm cell, 65 mm pressure.	89
$\text{Si}_3\text{H}_8$ trisilane	below 2190		Continuous absorption	10 cm cell, 60 mm pressure.	89

Table E. Hydrocarbons.

MOLECULE	SPECTRAL REGION (Å)	FREQUENCIES ( $\text{cm}^{-1}$ )	CHARACTERISTICS OF TRANSITION	REMARKS	LIT.
$\text{C}_2\text{H}_2$ $\text{C}_4\text{H}_2$ $\text{CH}_4$ $\text{C}_2\text{H}_6$ aromatic hydrocarbons				See Table A. See Table A. See Table D. See Table D. See Table G.	
$\text{C}_2\text{H}_4$ ethylene	1745–1600	$\omega'_{\text{C}_2\text{H}_4} \sim 1370(\nu_t^1)$ $\omega'_{\text{C}_2\text{D}_4} \sim 1290(\nu_t^1)$ $\omega'_{\text{C}_2\text{D}_3\text{H}} \sim 1350(\nu_t^1)$	Absorption bands	Appear at 0.01 mm in path of 2m. Degraded to red, perhaps double-headed. Belong to dif- ferent electronic transitions whose zero bands fit Rydberg formula	1, 2, 99– 101
$\text{C}_2\text{D}_4$ , $\text{C}_2\text{H}_3\text{D}$ deutero- ethylenes	1390–1320	$\omega'_{\text{C}_2\text{H}_4} \sim 1450(\nu_t^1)$ $\omega'_{\text{C}_2\text{D}_4} \sim 1360(\nu_t^1)$	Absorption bands	$\nu = 84,750 - R/(n+0.91)^2$ $\text{C}_2\text{H}_4$ with $n = 2, 3, 4 \dots$ $\nu = 84,850 - R/(n+0.92)^2$ $\text{C}_2\text{D}_4$ . Ionization potential from limit $10.45 \pm 0.03$ ev, for $\text{C}_2\text{D}_4$ about 0.01 volt higher. Bands inter- preted as arising from exci- tation of a double band $\pi$ electron. Bands appear in pairs with $470 \text{ cm}^{-1}$ separation in $\text{C}_2\text{H}_4$ and $290 \text{ cm}^{-1}$ in $\text{C}_2\text{D}_4$ . (415 in $\text{C}_2\text{H}_3\text{D}$ .) In 1700 region both components equally strong, in 1390 and subsequent systems long wave component much weaker than short wave one. No satisfactory explana- tion of this pair phenomenon yet given. In $\text{C}_2\text{D}_4$ also bands observed in 1700 region with separation of about $730 \text{ cm}^{-1}$ from main bands. Shift of zero	
	1290–1225	$\omega'_{\text{C}_2\text{D}_4} \sim 1330(\nu_t^1)$	Absorption bands		

Table E.—Continued.

MOLECULE	SPECTRAL REGION (Å)	FREQUENCIES (CM <sup>-1</sup> )	CHARACTERISTICS OF TRANSITION	REMARKS	LIT.
	at 1630		Maximum of cont. absorption	band in 1750 system of C <sub>2</sub> D <sub>4</sub> 280 cm <sup>-1</sup> to short waves com- pared to C <sub>2</sub> H <sub>4</sub> . Superimposed on Rydberg bands in this region.	
	1518-1220		Absorption bands	Two other much weaker sys- tems going to same ionization potential but with changed de- nominators in Rydberg for- mula. In 101 irradiation of ethylene at pressure 1 mm with H <sub>2</sub> lamp and discussion of pos- sible mechanisms for occurring reaction.	
$\begin{array}{c} \text{H} & & \text{H} \\ & \diagdown & / \\ & \text{C}=\text{C} \\ & / & \diagdown \\ \text{H} & & \text{CH}_3 \end{array}$ propylene	1850-1580 with maxi- mum at 1730		Diffuse absorp- tion	Pressure low but not given. Absorption extends with pres- sure. In 102 absorpt. observed below 2400Å in 1.5 cm cell with gas at 26-27°C and pres- sures of 910 and 2910 mm; de- termination of extinction coeff. till 1860Å.	99, 102
	below 1500		Absorption bands	Diffuse. If the two sets of bands are consecutive Rydberg series numbers, then ionization po- tential of about 9.6 volts.	
	below 1400		Absorption bands		
$\begin{array}{c} \text{H} & & \text{H} \\ & \diagdown & / \\ & \text{C}=\text{C} \\ & / & \diagdown \\ \text{H} & & \text{C}_2\text{H}_5 \end{array}$ butene-1	1875, 1819		Maxima of dif- fuse absorption bands	60 cm absorbing path. Pres- sures from less than 0.1 mm to about 50 mm. Vapor kept flow- ing through absorption cell. These conditions apply to hy- drocarbons, reference 103.	1, 103,
	1750-1730		Maximum of broad absorption band	Propylene and the following four molecules of this group are of type $\begin{array}{c} \text{H} & \text{H} \\   &   \\ \text{H}-\text{C}=\text{C}-\text{R} \end{array}$ one H of ethylene substituted by alkyl group. The next groups have two and more hy- drogens substituted by alkyls. Substitution produces progres- sive shift toward visible of whole set of bands, while dif- ferent alkyl groups as substit- uents have negligible effect. The long wave-length shift of the spectra parallels diminution in heat of hydrogenation with alkyl substitution (104). This diminution and long wave-length shifts partly due to conjugation between satu- rated groups and double bonds. (Called hyperconjugation by Mulliken (112, 113).)	104, 112, 113
$\begin{array}{c} \text{H} & & \text{H} \\ & \diagdown & / \\ & \text{C}=\text{C} \\ & / & \diagdown \\ \text{H} & & \text{C}_3\text{H}_7 \end{array}$ pentene-1	1884, 1830		Maxima of dif- fuse absorption bands		
	1750-1730		Maximum of broad absorption band		
$\begin{array}{c} \text{H} & & \text{H} \\ & \diagdown & / \\ & \text{C}=\text{C} \\ & / & \diagdown \\ \text{H} & & \text{C}_5\text{H}_{11} \end{array}$ heptene-1	1886, 1831		Maxima of dif- fuse absorption bands		
	1750-1730		Maximum of broad absorption band		
$\begin{array}{c} \text{H} & & \text{H} \\ & \diagdown & / \\ & \text{C}=\text{C} \\ & / & \diagdown \\ \text{H} & & \text{C}_3\text{H}_7 \end{array}$ isopropyl- ethylene	1895, 1865 1813		Maxima of dif- fuse absorption bands		
	1750-1730		Maximum of broad absorption band	As in ethylene, electronic ex- citation of ethylene derivatives arises from excitation of a double bond $\pi$ electron.	

Table E.—Continued.

MOLECULE	SPECTRAL REGION (Å)	FREQUENCIES (CM <sup>-1</sup> )	CHARACTERISTICS OF TRANSITION	REMARKS	LIT.
$\begin{array}{c} \text{H} & & \text{H} \\ & \diagdown & / \\ & \text{C}=\text{C} \\ & / & \diagdown \\ \text{H}_3\text{C} & & \text{CH}_3 \end{array}$ <i>cis</i> -butene-2	2080–1860 1750–1730		Absorption bands Maximum of broad absorption band	Show structure, have average breadth of 90 cm <sup>-1</sup> .	103, 105
$\begin{array}{c} \text{H} & & \text{CH}_3 \\ & \diagdown & / \\ & \text{C}=\text{C} \\ & / & \diagdown \\ \text{H}_3\text{C} & & \text{H} \end{array}$ <i>trans</i> -butene-2	2040–1890 1750–1730 below 1700		Absorption bands Maximum of broad absorption band Diffuse abs. bands	Bands show structure, have average breadth of 40 cm <sup>-1</sup> .	99, 103, 105
$\begin{array}{c} \text{H} & & \text{H} \\ & \diagdown & / \\ & \text{C}=\text{C} \\ & / & \diagdown \\ \text{H}_3\text{C} & & \text{C}_2\text{H}_5 \end{array}$ pentene-2	2060–1850 ~1760		Absorption bands Maximum of broad absorption band	<i>Cis</i> and <i>trans</i> forms have slightly different spectra (105). Bands are diffuse and narrow.	1, 103– 105
$\begin{array}{c} \text{H} & & \text{H} \\ & \diagdown & / \\ & \text{C}=\text{C} \\ & / & \diagdown \\ \text{H}_5\text{C}_2 & & \text{C}_2\text{H}_5 \end{array}$ hexene	2040–1700		Absorption bands	Diffuse and narrow.	103
$\begin{array}{c} \text{H} & & \text{H} \\ & \diagdown & / \\ & \text{C}=\text{C} \\ & / & \diagdown \\ \text{H}_5\text{C}_2 & & \text{C}_3\text{H}_7 \end{array}$ heptene-3	2040–1950 1750–1720 below 1530		Absorption bands Maximum of broad absorption band Broad absorption band.	Diffuse and narrow. Molecules from butene-2 to heptene-3 are of type $\begin{array}{c} \text{H} & \text{H} \\ & \diagdown & / \\ & \text{R}-\text{C}=\text{C}-\text{R} \end{array}$ and $\begin{array}{c} \text{H} & \text{H} \\ & \diagdown & / \\ \text{R}_1-\text{C}=\text{C}-\text{R}_2 \end{array}$ , see remark for preceding group with one substitution.	103, 106
$\begin{array}{c} \text{H} & & \text{CH}_3 \\ & \diagdown & / \\ & \text{C}=\text{C} \\ & / & \diagdown \\ \text{H} & & \text{CH}_3 \end{array}$ isobutene	2020–1830 1800–1670		Absorption bands	First bands in second set show structure.	103
$\begin{array}{c} \text{H} & & \text{CH}_3 \\ & \diagdown & / \\ & \text{C}=\text{C} \\ & / & \diagdown \\ \text{H} & & \text{C}_2\text{H}_5 \end{array}$ unsym. methyl-ethylethylene	2010–1820 1790–1650		Absorption bands	First group more intense than second, diffuse bands.	103
$\begin{array}{c} \text{H} & & \text{CH}_3 \\ & \diagdown & / \\ & \text{C}=\text{C} \\ & / & \diagdown \\ \text{H} & & \text{C}_6\text{H}_{11} \end{array}$ diisobutylene I	2040–1860 below 1700		Absorption bands New rise of abs.	Diffuse. Last three molecules are of type $\begin{array}{c} \text{H} & & \text{R}_1 \\ & \diagdown & / \\ & \text{C}=\text{C} \\ & / & \diagdown \\ \text{H} & & \text{R}_2 \end{array}$ .	103
$\begin{array}{c} \text{H} & & \text{CH}_3 \\ & \diagdown & / \\ & \text{C}=\text{C} \\ & / & \diagdown \\ \text{H}_3\text{C} & & \text{CH}_3 \end{array}$ trimethylethylene	2200–1690 below 1600 below 1360		Absorption bands Absorption bands Absorption bands	Diffuse, first band shows three-fold splitting.	1, 99, 103, 104, 107

Table E.—Continued.

MOLECULE	SPECTRAL REGION (Å)	FREQUENCIES (CM <sup>-1</sup> )	CHARACTERISTICS OF TRANSITION	REMARKS	LIT.
$\begin{array}{c} \text{H} \quad \text{C}_2\text{H}_5 \\ \diagdown \quad \diagup \\ \text{C}=\text{C} \\ \diagup \quad \diagdown \\ \text{H}_3\text{C} \quad \text{C}_2\text{H}_5 \\ \text{diethylmethyl-} \\ \text{ethylene} \end{array}$	2160–1650		Absorption bands	Diffuse and fairly narrow.	103
$\begin{array}{c} \text{H} \quad \text{CH}_3 \\ \diagdown \quad \diagup \\ \text{C}=\text{C} \\ \diagup \quad \diagdown \\ \text{H}_3\text{C}_4 \quad \text{CH}_3 \\ \text{diisobutylene II} \end{array}$	2160–1930 1727		Absorption bands Maximum of broad absorption band	Diffuse. The last three molecules belong to type $\begin{array}{c} \text{H} \quad \text{R}_1 \\   \quad   \\ \text{R}_2-\text{C}=\text{C}-\text{R}_3, \end{array}$ hence further shift to red.	103
$\begin{array}{c} \text{H}_3\text{C} \quad \text{CH}_3 \\ \diagdown \quad \diagup \\ \text{C}=\text{C} \\ \diagup \quad \diagdown \\ \text{H}_3\text{C} \quad \text{CH}_3 \\ \text{tetramethylethylene} \end{array}$	2320–2150 2100–1780 with maximum at 1870 below 1700 below 1500		Absorption bands Absorption bands New rise of abs. Absorption bands	Diffuse and narrow. Diffuse. According to complete substitution of hydrogens $\begin{array}{c} \text{R} \quad \text{R}' \\   \quad   \\ \text{R}-\text{C}=\text{C}-\text{R}' \end{array}$ , largest shift to red in olefin spectra, see remark in butene group.	99, 103, 104, 106
(CH <sub>2</sub> ) <sub>3</sub> cyclopropane	below 1950		Continuous absorption	Transmission from 5000 to 1950Å. Determination of extinction coeff. down to 1860Å.	102
$\begin{array}{c} \text{CH}-\text{CH}_2 \\    \quad \diagup \\ \text{CH}-\text{CH}_2 \\ \text{cyclopentene} \end{array}$	2100–2000 2000–1895 1880–1795		Absorption bands Absorption bands Absorption bands	60 cm cell through which vapor was kept flowing. Pressures from 0.1 to 40 mm. Bands almost equally spaced with average separation of 130 cm <sup>-1</sup> , breadth of bands 40–50 cm <sup>-1</sup> . This system due to presence of cyclopentadiene. Intensity of the different band systems increases towards shorter waves.	108
$\begin{array}{c} \text{CH}=\text{CH} \\ \diagdown \quad \diagup \\ \text{CH}_2 \quad \text{CH}_2 \\ \diagup \quad \diagdown \\ \text{CH}_2-\text{CH}_2 \\ \text{cyclohexene} \end{array}$	2110–1970 1960–1800 1800–1720 1700–1620 below 1540	$\omega' \sim 1485$	Absorption bands Absorption bands Absorption bands	Experimental conditions as for cyclopentene (108). Breadth of bands about 100 cm <sup>-1</sup> . Separation of 1485 corresponds to C=C vibration. Bands are doublets with separation of components of about 130 cm <sup>-1</sup> . Diffuse.	99, 107, 108
$\begin{array}{c} \text{CH}=\text{CH} \\   \quad \diagup \\ \text{CH}=\text{CH} \\ \text{cyclopentadiene} \end{array}$	2630–2100 1990–1860	$\omega' = 770$ $\omega' = 770$ $\omega' = 930$	Broad absorption band with many maxima Groups of sharply defined	0.02 to 80 mm pressures in 5 cm tube. Less than 0.1 mm pressure in 60 cm tube. Two band sets	109

Table E.—Continued.

MOLECULE	SPECTRAL REGION (Å)	FREQUENCIES (CM <sup>-1</sup> )	CHARACTERISTICS OF TRANSITION	REMARKS	LIT.
		$\omega' = 1050$ $\omega' = 1410$	absorption bands	displaced by 455 cm <sup>-1</sup> , each showing 4 vibrational frequencies, of which 1410 is most prominent.	
	1860–1750		Absorption bands	Possibly a continuation of former group, weaker than preceding bands.	
$  \begin{array}{c}  \text{CH} - \text{CH} \\  \diagdown \quad \diagup \\  \text{CH} \quad \text{CH} \\  \diagup \quad \diagdown \\  \text{CH}_2 - \text{CH}_2  \end{array}  $ 1, 3-cyclohexadiene	2860–2220	$\omega' \sim 1640$	Absorption band with five maxima	0.02–50 mm pressures in tubes of 5 and 50 cm. Separations of different maxima about 1640 cm <sup>-1</sup> (probably C=C vibration) and 380 cm <sup>-1</sup> . Values of oscillator strength obtained from measurements in vapor and in hexane solution, agree well with each other if Lorenz-Lorentz correction for solvent is not applied (111).	108, 110– 113
	2100–2030 with maximum at 2050	$\omega' \sim 1400$	Two groups of absorption bands	Experimental conditions as for cyclopentene. Groups show marked intensity rise to a maximum followed by a decrease and minimum. Separation between maxima of different groups about 1400 cm <sup>-1</sup> , corresponding to sym. C=C vibration.	
	2030–1960 with maximum at 2000				
	1960–1820		Three more groups	Less intense and much less pronounced intensity course (108).	
	1730–1710		Absorption bands	For theoretical discussion of spectra and their intensities, particularly in comparison to open-chain conjugated dienes, see 112.	
CH <sub>2</sub> —CH—CH—CH <sub>2</sub> butadiene	2170–1975	$\omega' \sim 1440$	Four absorption bands	Diffuse, broad. Separation of 1440 cm <sup>-1</sup> corresponds to sym. C=C vibration.	1, 114– 117
	1960–1760		Absorption bands	Strong individual bands and pairs of bands with about 350 cm <sup>-1</sup> separation between components.	
	1750–1630	$\omega' \sim 1560$	Absorption bands	Diffuse, extend with pressure to long and short waves. Separation of 1560 cm <sup>-1</sup> belongs to sym. C=C vibration. Background of contin. absorption.	
	below 1520		Absorption bands	Bands have no vibrational structure. Fit into Rydberg series: $\nu = 73,115 - R/(n+0.90)^2$ ; $n = 2, 3$ , etc. $\nu = 73,066 - R/(0+0.50)^2$ ; $n = 3, 4$ , etc. giving ionization potential of $9.022 \pm 0.01$ volts. Members of series are multiplets with quickly diminishing separations.	



Table E.—Continued.

MOLECULE	SPECTRAL REGION (Å)	FREQUENCIES (CM <sup>-1</sup> )	CHARACTERISTICS OF TRANSITION	REMARKS	LIT.
	below 1370		Absorption bands	Show a maximum about 1280Å. Spectral evidence that molecule has <i>trans</i> form. For theoretical interpretation of electronic states of dienes and intensity relations, see 115–117. All spectra produced by excitation of double bond $\pi$ electrons.	
$\text{CH}_2=\text{C}-\text{CH}=\text{CH}_2$ $\quad\quad\quad $ $\quad\quad\quad\text{CH}_3$ isoprene	2210–2090	$\omega' \sim 1470$	Three absorption bands	Diffuse, broad. Separation of 1470 cm <sup>-1</sup> corresponds to sym. C=C vibration.	114–117
	1909 and 1892		Absorption bands	Pair of bands without vibrational structure.	
	1800–1700	$\omega' \sim 1640$	Absorption bands	Diffuse, rather weak. Separation of 1640 probably corresponds to sym. C=C vibration.	
	below 1600		Absorption bands	Have no vibrational structure. Form Rydberg series, strongest are $\nu = 71,353 - R/(n+0.90)^2$ ; $\quad\quad\quad\quad\quad\quad n = 3, 4, \text{etc.}$ $\nu = 71,321 - R/(n+0.50)^2$ ; $\quad\quad\quad\quad\quad\quad n = 2, 3, \text{etc.}$ giving ionization potential of 8.805 $\pm$ 0.01 ev.	
	below 1400		Absorption bands	Diffuse. Probably from C—H and C—C bonds.	
$\text{CH}_2=\text{C}-\text{C}=\text{CH}_2$ $\quad\quad\quad  \quad  $ $\quad\quad\quad\text{CH}_3 \text{CH}_3$ $\beta\gamma$ -dimethyl- butadiene	2285–2150	$\omega' \sim 1400$	Three absorption bands	Diffuse, broad. Separation of 1400 corresponds to sym. C=C vibration.	114–117
	1920 and 1860		Absorption bands	Pair of bands.	
	1810–1700	$\omega' \sim 1650$	Absorption bands	Diffuse, with separation of about 1650 cm <sup>-1</sup> corresponding to sym. C=C vibration.	
	below 1600		Absorption bands	Have no vibrational structure. Fit into Rydberg series, strongest are $\nu = 70,240 - R/(n+0.90)^2$ ; $\quad\quad\quad\quad\quad\quad n = 3, 4, \text{etc.}$ $\nu = 70,241 - R/(n+0.50)^2$ ; $\quad\quad\quad\quad\quad\quad n = 3, 4, \text{etc.}$ leading to ionization potential of 8.668 volts. Diminution in ionization potential with alkyl substitution interpreted as simple inductive effect.	
$\text{CH}_2=\text{C}-\text{CH}=\text{CH}_2$ $\quad\quad\quad $ $\quad\quad\quad\text{Cl}$ chloroprene	2220–2100	$\omega' \sim 1230$	Absorption bands	Included in this table because of analogy with isoprene. Diffuse, broad. Separation of 1230 probably corresponds to sym. C=C vibration.	114–117
	at 1750		Absorption bands	Diffuse	

Table E.—Continued.

MOLECULE	SPECTRAL REGION (Å)	FREQUENCIES (CM <sup>-1</sup> )	CHARACTERISTICS OF TRANSITION	REMARKS	LIT.
	below 1600		Absorption bands	Form Rydberg series, strongest are: $\nu = 71,215 - R/(n+1.10)^2$ ; $n=3, 4$ , etc. $\nu = 71,190 - R/(n+0.50)^2$ ; $n=3, 4$ , etc. leading to ionization potential of $8.787 \pm 0.01$ ev.	
	below 1430		Absorption bands	Fairly strong, have no analog in spectra of alkyl substituted butadienes. From comparison with alkyl halides concluded bands arise from non-bonding $p\pi$ electron from chlorine atom.	

Table F. Halogen derivatives of hydrocarbons.

MOLECULE	SPECTRAL REGION (Å)	FREQUENCIES (CM <sup>-1</sup> )	CHARACTERISTICS OF TRANSITION	REMARKS	LIT.
CH <sub>3</sub> Cl methyl chloride	1610–1540	$\omega' \sim 1100(\delta_i  )$	Absorption bands	Extremely diffuse.	1, 118, 119
	1400–1320	$\omega' = 1320(\delta_i  )$	Absorption bands	Start with strong doublet $\Delta\nu = 650$ cm <sup>-1</sup> accompanied by weaker bands on short wave-length side.	
	below 1320		Absorption bands	Another doublet with same separation as above.	
	1230–1100		Absorption bands	Doublet bands with $\Delta\nu = 650$ cm <sup>-1</sup> . Difficult to observe because of superposition of continuous absorption from C–H bonds. The doublet bands are represented by Rydberg formulas: $\nu = 90,500 - R/(n+0.50)^2$ ; $n=2, 3, 4 \dots$ $\nu = 91,180 - R/(n+0.50)^2$ ; $n=2, 3, 4 \dots$ leading to ionization potentials of 11.17 and 11.25 ev with $\pm 0.01$ volt error. Separation of 650 cm <sup>-1</sup> agrees well with Mulliken's predicted value for doublet state of CH <sub>3</sub> Cl <sup>+</sup> (119). Many other weak bands probably due to vibrational structure accompanying main electronic transitions.	
CH <sub>3</sub> Br methyl bromide	2880–1920 with maximum at 2040		Continuous absorption	Determination of extinction coeff. and calculation from them of position of upper potential curve (repulsive). Absorbing columns of 1, 8, 55 and 3355 cm (120).	1, 120
	from 1800 to shorter wave- lengths	$\omega' \sim 1100(\delta_i  )$ $\omega' = 1260(\delta_i  )$	Absorption bands	Longest wave-length bands probably due to excitation of a bromine $d\pi$ electron. Most bands form two main electronic Rydberg series: $\nu = 85,020 - R/(n+0.90)^2$ ; $n=3, 4, 5 \dots$ $\nu = 87,560 - R/(n+0.90)^2$ ; $n=3, 4, 5 \dots$	118, 119

Table F.—Continued.

MOLECULE	SPECTRAL REGION (Å)	FREQUENCIES (CM <sup>-1</sup> )	CHARACTERISTICS OF TRANSITION	REMARKS	LIT.
				giving ionization potentials of 10.488 and 10.803 ev with $\pm 0.003$ volt error. Separation of 0.315 volt = 2540 cm <sup>-1</sup> occurs with slight variation throughout spectrum and agrees with Mulliken's predicted doublet separation of CH <sub>3</sub> Br <sup>+</sup> . Two weaker series with changed denominators go to same limits.	
CH <sub>3</sub> I methyl iodide	3600–2270 with maximum at 2577 followed by minimum at 2110		Continuous absorption	Determination of extinction coeff. and calculation from them of position of upper potential curve (repulsive). Proposed that continuum contains two electronic transitions leading to CH <sub>3</sub> +I( <sup>2</sup> P <sub>3/2</sub> ) and CH <sub>3</sub> +I( <sup>2</sup> P <sub>1/2</sub> ) (121, 122).	1, 2, 118, 119, 121, 122
	2110–1600		Absorption bands	New discussion of longest wavelength bands see p. 110. Strong predissociation sets in at 1650Å and diminishes to shorter wave-lengths, at 1400Å bands become sharp again.	
	1400–1215		Absorption bands	Form Rydberg series: $\nu = 76,930 - R/(n+0.75)^2$ ; $n = 6, 7, 8 \dots$ $\nu = 81,990 - R/(n+0.80)^2$ ; $n = 6, 7, 8 \dots$ Limits correspond to ionization potentials of 9.490 and 10.115 ev with $\pm 0.003$ volt error. Only bands from $n=7$ to $n=14$ represented really well; lower members, particularly between 1400–1600Å, very broad and diffuse due to predissociation and also deviate from simple Rydberg formula. Separation of series limits 0.625 volt agrees with Mulliken's prediction for doublet state of CH <sub>3</sub> I <sup>+</sup> . Other bands obey formulas with same limits and changed denominators.	
C <sub>2</sub> H <sub>5</sub> Cl ethyl chloride	1600–1540		Absorption bands	Extremely diffuse.	1, 2, 123
	1465–1400		Absorption bands	Main electronic doublet of 0.08 ev = 650 cm <sup>-1</sup> separation as in CH <sub>3</sub> Cl, but bands shifted to red by 60Å. Lowering of ionization potential of $\sim 0.3$ volt expected.	
	below 1350		Continuous absorption		
C <sub>2</sub> H <sub>5</sub> Br ethyl bromide	2850–1900		Continuous absorption	Determination of extinction coefficients and theoretical discussion of absorption curve (121).	1, 2, 121, 123
	below 1770		Absorption bands	Bands show a one to one correspondence to those of CH <sub>3</sub> Br, although some are shifted slightly to the violet and others to the red. As a whole, bands very diffuse compared with those of CH <sub>3</sub> Br. Ionization potentials of C <sub>2</sub> H <sub>5</sub> Br are 10.24 and 10.56 ev with a probable error of about 0.02 volt. Continuous absorp-	

Table F.—Continued.

MOLECULE	SPECTRAL REGION (Å)	FREQUENCIES ( $\text{cm}^{-1}$ )	CHARACTERISTICS OF TRANSITION	REMARKS	LIT.
				tion from C—C and C—H bonds weakens background and makes observation of higher bands difficult (123).	
$\text{C}_2\text{H}_5\text{I}$ ethyl iodide	3600–2100		Continuous absorption	Determination of extinction coefficients, and theoretical discussion of absorption curve (121, 122).	1, 2, 121, 122
	2085–1770 region particularly studied 2085–2014	$\omega'' = 261$ } $\omega' = 217$ } $\omega''(\text{C—I}) = 503$ } $\omega'(\text{C—I}) = 424$ } $\omega'' = 1202$ } $\omega' = 1161$ }	Absorption bands  0,0 band proposed at $49,970 \text{ cm}^{-1}$	As in $\text{CH}_3\text{I}$ bands due to excitation of iodine electron. Study of temp. dependence. Conclusion that bands belong to two separate electronic transitions is not certain. Bands appear in groups, small separations between individual bands perhaps partly due to $v-v$ transitions, partly to coupling effects between electronic, vibrational and rotational motions. Some details of analysis uncertain (124).	124
	below 1750		Absorption bands	Some bands are diffuse, others are sharp.	123
	below 1420		Absorption bands	Form Rydberg series: $\nu = 75,380 - R/(n+0.80)^2$ ; $n = 4, 5, 6 \dots$ $\nu = 80,080 - R/(n+0.80)^2$ ; $n = 4, 5, 6 \dots$ Limits correspond to ionization potentials of 9.299 and 9.883 volts with about $\pm 0.005$ volt error. Separation of 0.58 volt of limits almost same as in $\text{CH}_3\text{I}$ .	
propyl, iso-propyl and several varieties of butyl, amyl and allyl chlorides	1600–1500		Absorption bands	No details given. Bands become increasingly diffuse with increase in molecular weight and contin. absorp- tion from C—C and C—H correspondingly increases. Little difference between <i>n</i> , <i>iso</i> , secondary, tertiary, etc., varieties.	1, 123
	from about 1480–1400		Absorption bands		
	below 1350		Continuous absorption		
$n\text{C}_4\text{H}_9\text{Br}$ <i>n</i> -butyl bromide	2850–1900		Continuous absorption	Determination of extinction coefficients and theoretical discussion of absorption curve (121).	1, 121, 123
	below 1770		Absorption bands	Bands are similar to those of $\text{C}_2\text{H}_5\text{Br}$ . Details not given. Strong contin. absorpt. from C—C bonds makes estimate of ionization potentials impossible, but expected are values only slightly smaller than for $\text{C}_2\text{H}_5\text{Br}$ .	
$n\text{C}_3\text{H}_7\text{I}$ <i>n</i> -propyl iodide	2120–1950	$\omega'' = 1184$ } $\omega' = 1091$ } $\omega'' = 760$ } $\omega' = 675$ } $\omega'' = 590$ } $\omega' = 535$ } $\omega''(\text{C—I}) = 503$ } $\omega'(\text{C—I}) = 431$ } $\omega'' = 285$ } $\omega' = 264$ } $\omega'' = 198$ }	Absorption bands. 0,0 band proposed at $49,709 \text{ cm}^{-1}$	Broader and more diffuse than corresponding bands of methyl and ethyl iodide. System due to excitation of iodine electron. Analysis attempted using mentioned frequencies.	1, 125, 126

Table F.—Continued.

MOLECULE	SPECTRAL REGION (Å)	FREQUENCIES (CM <sup>-1</sup> )	CHARACTERISTICS OF TRANSITION	REMARKS	LIT.
(CH <sub>3</sub> ) <sub>2</sub> CHI isopropyl iodide	2120–1950	$\omega'' = 1195$ } $\omega' = 1072$ } $\omega''(\text{C-I}) = 489$ } $\omega'(\text{C-I}) = 447$ } $\omega'' = 400$ } $\omega' = 350$ } $\omega'' = 264$ } $\omega' = 184$ }	Absorption bands. 0,0 band proposed at 49,733 cm <sup>-1</sup>	Same remarks as for <i>n</i> -propyl iodide, but not all frequencies which have been used, are mentioned here.	1, 125, 127
	below 1770		Absorption bands	No details given. Diffuseness of bands and contin. absorption from C–C bonds prevents determination of ionization potentials, but values only slightly less than for ethyl iodide expected.	123
<i>n</i> C <sub>4</sub> H <sub>9</sub> I <i>n</i> -butyl iodide	2120–1950	$\omega'' = 1190$ } $\omega' = 1088$ } $\omega'' = 727$ } $\omega' = 670$ } $\omega'' = 595$ } $\omega' = 540$ } $\omega''(\text{C-I}) = 505$ } $\omega'(\text{C-I}) = 431$ } $\omega'' = 250$ } $\omega' = 190?$ }	Absorption bands. 0,0 band proposed at 49,711 cm <sup>-1</sup>	Same remarks as for <i>n</i> -propyl iodide.	1, 125, 126
	below 1770		Absorption bands	Same remarks as for isopropyl iodide.	123
(CH <sub>3</sub> ) <sub>3</sub> CI tert-butyl iodide	2120–1950	$\omega'' = 1229$ } $\omega' = 1016$ } $\omega''(\text{C-I}) = 490$ } $\omega'(\text{C-I}) = 436$ } $\omega'' = 395$ } $\omega' = 357$ } $\omega'' = 257$ } $\omega' = 187$ }	Absorption bands. 0,0 band proposed at 49,077 cm <sup>-1</sup>	Bands somewhat sharper than those of <i>n</i> -butyl and the propyl iodides. Appearance of groups perhaps partly due to <i>v-v</i> transitions. Analysis at- tempted, but not all frequencies which have been used, are men- tioned here.	1, 125, 127
	below 1770		Absorption bands	Same remarks as for isopropyl iodide.	123
CH <sub>2</sub> I <sub>2</sub> methylene iodide	3499, 2640, 2365 and 2955, 2474 2220		Long wave limits and maxima of continuous absorption	Because of difficulty to obtain all three maxima in the vapor, abs. curve was taken for CH <sub>2</sub> I <sub>2</sub> dissolved in ether.	1, 91
CHCl <sub>3</sub> chloroform	below 2200		Continuous absorption	Conditions not stated.	1, 91
CHBr <sub>3</sub> bromoform	2750, 2497 2195? and 2559, 2275		Long wave limits and maxima of continuous absorption	Condition not stated.	1, 91
CHI <sub>3</sub> iodoform	4230, 3229, 2872 and 3429, 3029, 2828		Long wave limits and maxima of continuous absorption	Obtained by heating absorption tube with warm air.	1, 91
benzene derivatives				See Table G.	

Table G. Aromatic molecules.

MOLECULE	SPECTRAL REGION (Å)	FREQUENCIES (CM <sup>-1</sup> )	CHARACTERISTICS OF TRANSITION	REMARKS	LIT.
C <sub>6</sub> H <sub>6</sub> benzene	2800-2200	Vibrational frequencies of following types: $\alpha_{1g}: \omega''_1(\text{C}-\text{C}) = 992$ $\alpha_{1g}: \omega'_1(\text{C}-\text{C}) = 923$ $\alpha_{1g}: \nu'(\text{C}-\text{H}) = 2565$ $\epsilon^+_{2g}: \omega''_4(\text{C}-\text{C}) = 606.4$ $\epsilon^+_{2g}: \omega'_4(\text{C}-\text{C}) = 520$ $\epsilon^+_{2g}: \omega'_5(\text{C}-\text{C}) = 1596$ $\epsilon^+_{2g}: \omega'_6(\text{C}-\text{C}) = 1480$ $\epsilon^+_{2u}: \gamma''(\text{C}-\text{C}) = 400$ $\epsilon^+_{2u}: \gamma'(\text{C}-\text{C}) = 240$ $\omega$ and $\gamma$ refer to vibra- tions of the ring, $\nu$ to valence C-H vibra- tions	Absorption and fluorescence bands $^1A_{1g} \rightarrow ^1B_{2u}$ 0,0 band (calcu- lated) at 38,089 cm <sup>-1</sup> $^1A_{1g}$ ground state.	In 10 to 75 cm absorption tubes pressures from 0.2 to 100 mm. Transition is for- bidden according to selection rules (139), becomes allowed by excitation of type $\epsilon^+_{2g}$ vibrations. Analysis yielded following series (138). <i>A</i> series $\nu = 38089 + 520 + \nu'_1 \times 923$ $- \nu''_1 \times 992 + \nu'_2 \times 2565$ $- \nu_3 \times (400 - 240)$ 160 <i>B</i> series $\nu = 38089 - 606.4 + \nu'_1 \times 923$ $- \nu''_1 \times 992 + \nu'_2 \times 2565$ $- \nu_3 \times 160$ <i>C</i> series $\nu = 38089 + 2 \times 520 - 606.4$ $+ \nu'_1 \times 923 + \nu'_2 \times 2565$ $- \nu_3 \times 160$ <i>D</i> series $\nu = 38089 + 520 - 2 \times 606.4$ $+ \nu'_1 \times 923 - \nu_3 \times 160$ <i>E</i> series $\nu = 38089 + 1480 + \nu'_1 \times 923$ <i>F</i> series $\nu = 38089 - 1596 - \nu_3 \times 160$ <i>G</i> series $\nu = 38089 + 520 + 2 \times 240$ $+ \nu'_1 \times 923 - \nu_3 \times 160$ <i>H</i> series $\nu = 38089 - \nu_3 \times 160$ with $\nu'_1 = 0, 1, 2 \dots$ ; $\nu''_1 =$ $0, 1, 2$ ; $\nu'_2 = 0, 1$ ; $\nu_3 = 0, 1 \dots$ . Analysis in agreement with measurements of temperature dependence (134) and theo- retical selection rules, see p. 115. Analysis explains also main features of spectrum of solid benzene. Illumination with spark lines of $\lambda < 2100\text{Å}$ causes dissociation into C <sub>6</sub> H <sub>5</sub> + H (142, 143).	1, 2, 128- 145, 108
	2050-1850	$\alpha_{1g}: \omega'_1(\text{C}-\text{C}) = 965$	Absorption bands. $^1A_{1g} \rightarrow ^1B_{1u}$ is proposed	Diffuse broad groups showing some structure, occurrence of 965 and 160 progressions. Transition is forbidden, be- comes allowed by excitation of vibrations of type $\epsilon^+_{2g}$ and $\beta_{2g}$ . Intensity much stronger than bands at 2800-2200Å because of closeness to al- lowed system at 1770Å (108, 145). See p. 122.	

Table G.—Continued.

MOLECULE	SPECTRAL REGION (Å)	FREQUENCIES (CM <sup>-1</sup> )	CHARACTERISTICS OF TRANSITION	REMARKS	LIT.
	1850–1650		Absorption bands. Proposed transition ${}^1A_{1g} \rightarrow {}^1E^-_u$	Sharp very intense bands superimposed on continuous background. Allowed transition. Somewhat irregular vibrational structure. Underlying continuum corresponds perhaps to another electronic transition involving rupture of one C–H bond. Bands believed to represent first member of one of Rydberg series reported in 2.	
	1600–1360		Absorption bands forming Rydberg series	Both Rydberg series may be assigned to allowed transitions of symmetry ${}^1A_{1g} \rightarrow {}^1E^-_u$ (145).	
C <sub>6</sub> D <sub>6</sub> hexadeutero- benzene	2700–2300	Vibrational frequencies of following types $\alpha_{1g}: \omega''_1(\text{C–C}) = 940$ $\alpha_{1g}: \omega'_1(\text{C–C}) = 879$ $\epsilon^+_{\theta}: \omega''_4(\text{C–C}) = 579.5$ $\epsilon^+_{\theta}: \omega'_4(\text{C–C}) = 498.5$ $\epsilon^+_{\theta}: \omega'_5(\text{C–C}) \leq 1410$ $\epsilon^+_{\theta}: \gamma''(\text{C–C}) - \gamma'(\text{C–C}) = 140$ with possibly $\gamma'(\text{C–C}) = 207$	Absorption and fluorescence bands ${}^1A_{1g} \rightarrow {}^1B_{2u}$ 0,0 band (calculated) at 38,292 cm <sup>-1</sup>	75 cm absorption path, pressures from 0.2 to 100 mm. As in benzene forbidden transition becomes allowed by interacting $\epsilon^+_{\theta}$ vibrations. Analysis yielded series corresponding to those in benzene. Discussion of some bands for which interpretation is not unambiguous (146).	129, 130, 136– 138, 146
C <sub>6</sub> H <sub>5</sub> Cl monochloro- benzene	2750–2400	Vibrational frequencies of following types $\alpha_1: \omega''_1(\text{C–C}) = 1001$ $\alpha_1: \omega'_1(\text{C–C}) = 931$ $\alpha_1: \omega'_2(\text{C–C}) = 965$ $\alpha_1: \omega'_3(\text{C–C}) = 1041$ $\beta_1: \omega''_4(\text{C–C}) = 615$ $\beta_1: \omega'_4(\text{C–C}) = 521$ $\alpha_1: \omega'_6(\text{C–C}) = 417$ $\alpha_1: \omega''_7(\text{C–Cl}) = 706$	Absorption band $A_1 \rightarrow B_1$ . 0,0 band at 37,052 cm <sup>-1</sup>	15 and 75 cm absorption tubes, pressures from 0.4 to 500 mm. Total intensity of spectrum only about twice that of corresponding benzene spectrum. In agreement with this the system has character of partly an allowed and partly a forbidden transition; strong 0,0 band according to allowed transition and appearance of one quantum of $\beta_1 = 615$ according to forbidden transition. Peculiarities observed in intensities of totally sym. vibrations 417 and 706 cm <sup>-1</sup> . See discussion, p. 118. Frequency differences of 62 and 199 cm <sup>-1</sup> interpreted as resulting from $v-v$ transitions.	1, 147, 148, 226
C <sub>6</sub> H <sub>5</sub> Br bromobenzene	2760–2400	$\beta_1: \omega''_4(\text{C–C}) = 608$ $\alpha_1: \omega''_6(\text{C–C}) = 315$ $\alpha_1: \omega''_7(\text{C–Br}) = 668$	Absorption bands. 0,0 band at 36,996 cm <sup>-1</sup>	Identification of some vibrational frequencies in the ground state.	1, 148
C <sub>6</sub> H <sub>5</sub> CH <sub>3</sub> toluene	2740–2300	$\omega''_4(\text{C–C}) = 623$ $\omega''_6(\text{C–C}) = 517$ $\omega''_7(\text{C–CH}_3) = 781$	Absorption bands. 0,0 band at 37,484 cm <sup>-1</sup>	Identification of some vibrational frequencies in the ground state.	1, 148, 227, 231
C <sub>6</sub> H <sub>5</sub> OH phenol	2800–2480	$\omega''_4(\text{C–C}) = 604$ $\omega''_6(\text{C–C}) = 528$ $\omega''_7(\text{C–O}) = 820$	Absorption bands. 0,0 band at 36,350 cm <sup>-1</sup>	Identification of some vibrational frequencies in the ground state (148).	1, 148
	2420–2080		Absorption bands	In 149 attributed to O–H group. Consists of two regions: first showing faint and broad diffuse band, second	149

Table G.—Continued.

MOLECULE	SPECTRAL REGION (Å)	FREQUENCIES (CM <sup>-1</sup> )	CHARACTERISTICS OF TRANSITION	REMARKS	LIT.
				three successive strong bands with separation of about 850 cm <sup>-1</sup> .	
C <sub>6</sub> H <sub>5</sub> OCH <sub>3</sub> anisol	2840–2600		Absorption bands	Absorption due to the ring $\pi$ electrons. Frequency differences of 800, 953 and 403 reported.	156
	2415–2120		Absorption bands	In 149 attributed to OCH <sub>3</sub> group. Consists of two regions, first has broad and diffuse absorption, second has strong bands with separation of about 800 cm <sup>-1</sup> .	149
C <sub>6</sub> H <sub>5</sub> NH <sub>2</sub> aniline	2800–2450	$\omega''_1(\text{C}-\text{C}) = 991$ $\omega''_2(\text{C}-\text{C}) = 1032$ $\omega''_6(\text{C}-\text{C}) = 529$ $\omega''_7(\text{C}-\text{N}) = 821$ ( $\omega'' = 422$ )	Absorption and fluorescence bands 0,0 band at 34,034 cm <sup>-1</sup>	Fluorescence spectrum consists at low pressures of two parts, a discrete one excited by $\lambda 2937$ and a continuous one, excited by $\lambda 2800$ . Temperature effect studied. (153 abstracted from Phys. Ber. 21, 1956 (1940).) In 151–153 interesting quenching experiments of fluorescence by H <sub>2</sub> , O <sub>2</sub> , N <sub>2</sub> , CO, NH <sub>3</sub> , H <sub>2</sub> O, cyclohexane, of which only O <sub>2</sub> gives appreciable effect. Other gases cause selective enhancement of aniline bands. In 154 observation of sensitized fluorescence in mixture aniline-benzene vapor.	1, 148, 150– 154, 159a
	2420–2030	$\omega' \sim 550$	Absorption bands	Absorbing paths from 2 to 50 cm. Bands due to absorption of amino group (150). Three progressions with frequency differences of about 550 cm <sup>-1</sup> ; first progression consists of 8 broad diffuse bands, second has 5 sharp bands, third extends further to violet.	
	below 1900		Continuous absorption		
C <sub>6</sub> H <sub>5</sub> CN benzonitrile	2790–2440	$\omega''_1(\text{C}-\text{C}) = 1009$ $\omega''_4(\text{C}-\text{C}) = 616$ $\omega''_6(\text{C}-\text{C}) = 547$	Absorption bands. 0,0 band at 36,516 cm <sup>-1</sup>	Identification of some vibrational frequencies in the ground state.	1, 148
C <sub>6</sub> H <sub>5</sub> CHO benzaldehyde	2960–2600	$\omega''_1(\text{C}-\text{C}) = 1007$ $\omega''_4(\text{C}-\text{C}) = 615$ $\omega'' = 866$ $\omega'' = 418-464$ (from a diffuse band) $\omega'' = 757$ $\omega'' = 650$	Absorption bands. 0,0 band at 35,194 cm <sup>-1</sup>	Identification of some vibrational frequencies in the ground state.	1, 148
C <sub>6</sub> H <sub>5</sub> CH <sub>2</sub> OH benzylalcohol	below 2100		Continuous absorption	Same apparatus used as in previous papers, for reference see 1. Pressures up to 6 mm.	155
C <sub>6</sub> H <sub>5</sub> CH <sub>2</sub> Cl benzylchloride	below 2200		Continuous absorption	Pressures up to 2.5 mm, limit reached at 1 mm.	155
C <sub>6</sub> H <sub>5</sub> CH <sub>2</sub> Br benzylbromide	below 2380		Continuous absorption	Pressures up to 5 mm.	155



Table G.—Continued.

MOLECULE	SPECTRAL REGION (Å)	FREQUENCIES (CM <sup>-1</sup> )	CHARACTERISTICS OF TRANSITION	REMARKS	LIT.
C <sub>6</sub> H <sub>5</sub> CH <sub>2</sub> CN benzylcyanide	below 2250		Continuous absorption	Pressures up to 12 mm.	155
C <sub>6</sub> H <sub>5</sub> CH <sub>2</sub> CH <sub>2</sub> OH phenylethyl alcohol	below 1990		Continuous absorption	Pressures up to 1 mm, limit practically constant.	155
C <sub>6</sub> H <sub>5</sub> CH <sub>2</sub> CH <sub>2</sub> CH <sub>2</sub> OH phenylpropyl alcohol	below 1990		Continuous absorption		155
C <sub>6</sub> H <sub>4</sub> (C <sub>3</sub> H <sub>7</sub> )CH <sub>2</sub> OH propylbenzyl alcohol	below 2140		Continuous absorption		155
C <sub>6</sub> H <sub>5</sub> OCOCH <sub>3</sub> phenyl acetate	2670–2500		Absorption bands	Due to ring $\pi$ electrons. Very diffuse broad structure.	156
	2370–2010		Absorption bands	Consists of three regions, the first two being very diffuse and attributed to single bonded O electron, while the third is attributed to the oxygen in the C=O group.	
C <sub>6</sub> H <sub>5</sub> COCH <sub>3</sub> acetophenone	2830–2600		Absorption bands	Long wave systems due to ring $\pi$ electrons. Frequency differences of 800 and 100 cm <sup>-1</sup> reported.	156
	2390–1960		Absorption bands		
C <sub>6</sub> H <sub>5</sub> CO <sub>2</sub> CH <sub>3</sub> methyl benzoate	2780–2600		Absorption bands	Short wave systems consist of two regions of diffuse bands, systems are attributed to oxygen from C=O group.	
	2290–2045		Absorption bands		
C <sub>6</sub> H <sub>5</sub> NCS phenyl iso-thiocyanate	2900		Long wave limits of continuous absorption	In 1.5 m absorption path pressures up to saturated vapor at room temp. With 3.5 m absorption path temp. of 32°C. Absorption limits correspond to 3.5 m cell, first limit at 0.5 mm, second at lower pressures.	210
	2310				
	2820, 2780, 2750, 2720		Absorption bands	Weak and diffuse, due to excitation in benzene ring.	
C <sub>6</sub> H <sub>4</sub> CH <sub>3</sub> F <i>p</i> -fluorotoluene	2800–2350	$\omega' = 1191$	Absorption bands 0,0 band at 36,866 cm <sup>-1</sup>	Absorption path 1m. Many bands measured, but wavelengths only of few main bands given.	157
		$\omega' = 799$ $\omega' = 1230$ $\omega' = 706$			
<i>o</i> -fluorotoluene			0,0 band at 37,566 cm <sup>-1</sup>		
C <sub>6</sub> H <sub>4</sub> CH <sub>3</sub> Cl <i>p</i> -chlorotoluene <i>o</i> -chlorotoluene	2840–2470	$\omega' = 1055$ $\omega' = 763$ $\omega' = 1070$ $\omega' = 481$	Absorption bands. 0,0 band at 36,297 cm <sup>-1</sup>		
C <sub>6</sub> H <sub>4</sub> CH <sub>3</sub> Br <i>p</i> -bromotoluene <i>o</i> -bromotoluene	2770–2470	$\omega' = 1016$ $\omega' = 755$ $\omega' = 1016$ $\omega' = 479$	Absorption bands. 0,0 band at 36,173 cm <sup>-1</sup>		
C <sub>6</sub> H <sub>4</sub> OHCOOH salicylic acid	3057		Broad absorption band	Minimum of absorption at 2607Å. Brief note.	158
	2386, 2350, 2317		Absorption bands		
	below 2257		Continuous absorption		

Table G.—Continued.

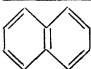
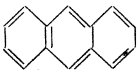


MOLECULE	SPECTRAL REGION (Å)	FREQUENCIES ( $\text{cm}^{-1}$ )	CHARACTERISTICS OF TRANSITION	REMARKS	L IT.
$\text{C}_6\text{H}_4\text{OHCOH}$ salicylic aldehyde	below 2170		Continuous ab- sorption		155
$\text{C}_6\text{H}_4\text{OHCOOLi}$ lithium salicylate	3048		Broad absorption band	Minimum of absorption masked by phenol bands. Decomposition above $130^\circ\text{C}$ with appearance of phenol bands. Brief note.	158
	2385, 2349, 2317		Absorption bands		
	below 2280		Continuous ab- sorption		
 naphthalene	3190–2800 2800–2495		Absorption bands	Long wave bands show struc- ture, appear at higher pres- sures than second group. Frequency difference of $450\text{ cm}^{-1}$ observed. Continuous background with region of transmission from 2500– 2250Å beyond which again absorption. Absorbing path 75 cm. Absorption similar in different states of aggrega- tion but shift toward the red when going from vapor over solution to crystal. Last two remarks apply to all com- pounds investigated in 159 and 162.	1, 159
 anthracene	3700–3100 2960–2300	$\omega' \sim 1420$	Absorption bands	Also frequency difference of $400\text{ cm}^{-1}$ found. Very weak contin. background in first region, stronger in second region continuing to shorter waves (159). First group ap- pears at higher pressures than second. In 160 also fluorescence studied, shows same shift to red for different phases as abs. spectr. If illu- minated with short wave- lengths (i.e., Hg 2537) fluo- rescence becomes continuous. 160 not accessible, abstracted from Phys. Ber. 18, 2526 (1937).	2, 159, 160
 naphthacene	4500–3600 3200–2550	$\omega' \sim 1350$	Absorption bands	Spectrum resembles that of anthracene. Main bands have satellites at intervals of $400\text{ cm}^{-1}$ . First region almost no contin. background, second has pronounced background. Af- ter minimum at $\lambda 2500$ new increase of contin. absorpt. to shorter wave-lengths. Second group appears at lower pres- sures than first.	159
 phenanthrene	3630–3000 2935–2355	$\omega' \sim 1430$	Absorption bands	Cont. abs. superimposed. Also frequency difference of about $400\text{ cm}^{-1}$ found. Shorter wave-length group appears at lower pressures than long wave group.	2, 159

Table G.—Continued.

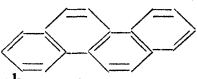
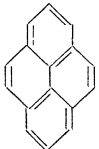
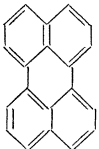
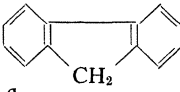
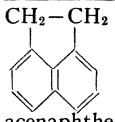
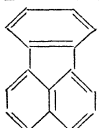
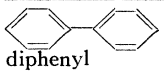
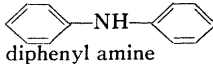
MOLECULE	SPECTRAL REGION (Å)	FREQUENCIES (CM <sup>-1</sup> )	CHARACTERISTICS OF TRANSITION	REMARKS	LIT.
 chrysene (1,2 benzophenanthrene)	3605–2840 2765–2385	$\omega' \sim 1420$	Absorption bands	Spectrum resembles that of phenanthrene. 161 in which chrysene, pyrene and other aromatic hydrocarbons investigated, not accessible; from reviews in Chem. Abstracts and Phys. Ber. not clear, which substances measured in vapor and which in solution.	159, 161
 pyrene	3630–3300 3260–2680 2650–2295	$\omega' \sim 1440$	Absorption bands	Groups develop with pressure starting with the shortest wave-length bands. Cont. background superimposed with minima between groups. Also frequency differences of $\sim 540$ and $380$ cm <sup>-1</sup> observed.	159, 161
 perylene	4245–2800 2695–2330	$\omega' \sim 1440$	Absorption bands	Diffuse bands, particularly in second region which has strong background. Second group appears at lower pressures than first.	159
 fluorene	4780–3870 3675–2460	$\omega' = 1355$	Fluorescence bands Absorption bands	Diffuse, with cont. background. 1 m absorbing path. In 162 bands put in groups with constant frequency differences of 1355, 1025, 840, 545, 395, 260 cm <sup>-1</sup> . Absorpt. spectrum of crystals at $-180^\circ\text{C}$ fairly sharp.	159, 162
 acenaphthene	3190–2755 2725–2520 2490–2300		Absorption bands	Have sharp edges on short wave-length side. Groups develop with pressure starting with short wave bands. Continuous background. Frequency difference of $\sim 460$ cm <sup>-1</sup> .	159
 fluoranthene (benzo-acenaphthene)	3510–2920 2860–2415	$\omega' \sim 1440$	Absorption bands	Spectr. resembles that of fluorene, but has more bands. Continuous background.	159
 diphenyl	2080–1840 below 1785		Absorption with broad diffuse bands Continuous absorption		103
terphenyl			Continuous absorption	Details not given.	159
 diphenyl amine	4000–2400 with broad max. at 3500 3000–2400		Fluorescence Diffuse absorption bands	Strongest at a pressure corresponding to $100\text{--}110^\circ\text{C}$ . Excited by $\lambda 2900\text{--}2200$ .	159a

Table G.—Continued.

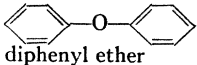
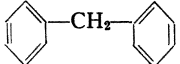
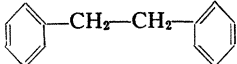
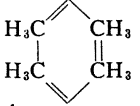
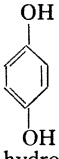
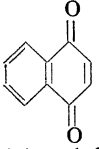
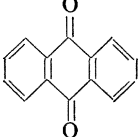
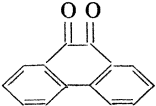
MOLECULE	SPECTRAL REGION (A)	FREQUENCIES (CM <sup>-1</sup> )	CHARACTERISTICS OF TRANSITION	REMARKS	LIT.
	below 2400		Very diffuse absorption	Strong.	
 diphenyl ether	2450–2190		Diffuse absorp- tion	Two regions, first one stronger than second.	149
 diphenyl methane	2670–2495	$\omega' \sim 450$	Absorption bands	Diffuse. Strong continuous background.	159
 diphenyl ethane (dibenzyl)	2690–2460	$\omega' \sim 450$	Absorption bands	Spectr. resembles that of di- phenyl methane.	159
triphenylmethane <i>s</i> -triphenyl benzene			} Continuous absorption	No details given.	159
 durene ( <i>s</i> -tetramethyl- benzene)	2780–2630		Absorption bands		159
hexamethyl- benzene			Continuous absorption	No details given.	159
 hydroquinone	3050–2500 2500–2300	$\omega' \sim 420$	} Absorption bands	75 cm absorbing path. Short wave bands appear at about 100°C, long wave bands at about 130°C, are sharper than second region. Main bands accompanied by com- ponents on either side at intervals of 30 cm <sup>-1</sup> .	163
 1,4 naphthaquinone	3450–3200 2500–2430	$\omega' \sim 46$	} Absorption bands	Second region appears at lower pressures than first.	163
 9,10 anthraquinone	3300–3080 2660–2525	$\omega' \sim 420$	} Absorption bands	Second region appears at lower pressures than first.	163
 9,10 phenanthra- quinone	4100–3820 3300–3100 2675–2615 2465–2410	$\omega' \sim 440$	} Absorption bands	Longest wave-length bands appear at highest pressures, shortest wave-length bands at lowest pressures.	163

Table G.—Continued.

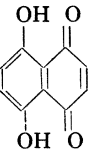
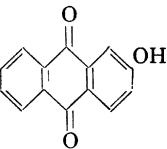
MOLECULE	SPECTRAL REGION (Å)	FREQUENCIES (CM <sup>-1</sup> )	CHARACTERISTICS OF TRANSITION	REMARKS	LIT.
 naphthazarin (dioxynaphthaquinone)	5495–4675		Absorption bands	In the ultraviolet continuous absorption.	163
 hydroxyanthraquinone	3120 2500 2300		} Maxima of } continuous } absorption		163

Table H. Heterocyclic molecules.

MOLECULE	SPECTRAL REGION (Å)	FREQUENCIES (CM <sup>-1</sup> )	CHARACTERISTICS OF TRANSITION	REMARKS	LIT.
C <sub>5</sub> H <sub>5</sub> N pyridine	3100–2500 from 2500	$\alpha_1: \omega''_1(\text{C}-\text{C}) = 990$ $\alpha_1: \omega''_2(\text{C}-\text{C}) = 1030$ $\alpha_1: \omega'_3(\text{C}-\text{C}) = 542$ $\omega''(\text{C}-\text{C}) = 600$	Absorption bands  Continuous absorption	Sharp bands; become diffuse below 2700Å. Absorption paths from 2.5–53 cm. Large pressure range studied. At 30 mm pressure spectr. extends till 2926 toward the visible. With 30 cm path spectr. extends till 2940Å at 38.5 mm pressure, till 2970Å at 72.1 mm, till 3017Å at 400 mm, till 3060Å at 800 mm pressure. Temperature effect studied. Analysis partly correct. No fluorescence observed when illuminated with wave-lengths from 7000–1850Å (166).	1, 2, 164, 166
C <sub>4</sub> H <sub>4</sub> O furan	2650–2480			In this region weak narrow absorption bands reported in 165 and 166, but not confirmed by other authors (167). No fluorescence found (166). In 167 experiments carried out with flowing and nonflowing vapor in 60 cm tube and pressures up to 400 mm. Determination of extinction coefficients. Transmission observed down to 2300Å.	165– 167
	2175–1950		Diffuse absorption	Contains three broad diffuse bands from 2045Å on and at longer waves indications of very shallow maxima (167).	
	1915–1745	$\omega' = 1395$ $\omega' = 1068$ $\omega' = 848$	Absorption bands. 0,0 band at 52,230 cm <sup>-1</sup>	Have sharply defined maxima. Observed frequencies correspond to totally sym. ring vibrations (167). See also p. 123.	
	below 1700		Absorption bands	Intense. Region includes well-defined bands and diffuse absorption.	
C <sub>4</sub> H <sub>4</sub> S thiophene	2522–2246	$\omega' = 980$	Absorption bands	Absorption paths 53 and 100 cm. Pressures from 0.1 to 44 mm Hg. Room temperature. Frequency differences of	2, 166, 168

Table H.—Continued.

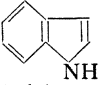
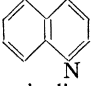
MOLECULE	SPECTRAL REGION (Å)	FREQUENCIES (CM <sup>-1</sup> )	CHARACTERISTICS OF TRANSITION	REMARKS	LIT.
				980,210,1350 reported. Proposed analysis uncertain. No fluorescence observed (166).	
C <sub>4</sub> H <sub>4</sub> NH pyrrole	2880–2540			Existence of absorption bands in this region is very doubtful. In 166 bands were obtained with a Kahlbaum sample; became weaker upon fractional distillation. Sample gave continuous fluorescence from 3300–2700Å. At 2650Å beginning of continuous absorption. With a Schuchardt sample only continuous absorption from 2360Å to shorter waves and no fluorescence observed.	1, 166
 indole	2873–2617		Many narrow absorption bands	Absorbing paths of 35 and 100 mm. In fluorescence a wide diffuse band at 3250–2900Å observed.	166
	2610–2580, 2550–2500		Broad absorption bands	Appear at higher temperatures.	
	below 2300		Continuous absorption		
 quinoline	3156–2790		Broad absorption bands	Absorbing paths of 35 and 100 mm. Continuous absorption begins at about λ2860. Very weak fluorescence observed at 3500–2500Å when heated to 80°C.	166

Table I. Miscellaneous organic molecules.

MOLECULE	SPECTRAL REGION (Å)	FREQUENCIES (CM <sup>-1</sup> )	CHARACTERISTICS OF TRANSITION	REMARKS	LIT
HCOOH formic acid	1550–1100	$\omega'(\text{C}=\text{O})$ ~1450	Absorption bands	Spectrum resembles that of formaldehyde below 1550Å. Most bands form Rydberg series: $\nu = 91,370 - R/(n - 0.40)^2$ ; $n = 2, 3, 4 \dots$ giving an ionization potential of 11.29 ev. Result from excitation of non-bonding 2p-oxygen electron of C=O group. First band group at 1550Å and a group at 1250Å have different character. Besides 1450 other frequency differences of 600 and around 800 and 900 observed.	1, 169
CH <sub>3</sub> COSH thioacetic acid	2960–2820 ~2550		Long wave limit and maximum of cont. absorption	Dissociation processes discussed.	170
CH <sub>3</sub> CSSH dithioacetic acid	3010 2820		Long wave limit and maximum of cont. absorption	Dissociation processes discussed.	170
	2440		Begin of second absorption region		
CH <sub>3</sub> COOCH <sub>3</sub> methylacetate	below 2500		Cont. absorption	50 cm absorbing path.	156

Table I.—Continued.

MOLECULE	SPECTRAL REGION (Å)	FREQUENCIES (CM <sup>-1</sup> )	CHARACTERISTICS OF TRANSITION	REMARKS	LIT.
CH <sub>3</sub> COCH <sub>2</sub> COOC <sub>2</sub> H <sub>5</sub> ethylacetoacetate	2596, 2225 and 2368		Long wave limits and maximum of cont. absorption	Photodissociation processes dis- cussed.	170
CH <sub>2</sub> O formaldehyde				In 171 photodecomposition in Schumann region studied. No evidence found for primary disso- ciation into CH <sub>2</sub> +O. In 172 study of photodissociation with λ3650– λ2537 in presence of iodine. See also discussion of the known 3000Å region on p. 113.	1, 2, 171, 172
CH <sub>3</sub> CHO acetaldehyde	6100–5600, 5100		Broad fluores- cence bands	Fine structure superimposed (173). In 174 photodissociation studied with λ3150 and λ2500– 2600 in presence of iodine. For more complete photochemical literature, also of other aldehydes and ketones, see 175.	1, 2, 173– 175
C <sub>2</sub> H <sub>5</sub> CHO propionaldehyde	5460–4360, maximum 5200		Broad fluores- cence region with maximum	Fluorescence probably due to di- ketone dipropionyl.	1, 2, 173
CH <sub>3</sub> CH=CHCHO crotonaldehyde	3800–2700		Broad absorption region with nar- row discrete bands at longer waves; below 3100 diffuse and finally continuous abs. at shorter waves	Weak absorption, due to C=O group. Theoretical discussion of this transition in aldehydes and ketones in 181–183. Determina- tion of extinction coefficients (176). No photodecomposition in banded region 3800–3130, below that photodecomposition from 150°C on and increasing with temp. and with decreasing wave- lengths (177). No fluorescence be- tween 9000–4000Å (177).	1, 2, 176, 177, 181– 183
	below 2600		Continuous abs.		
CH <sub>2</sub> =CHCHO acrolein	3800–2900, max. at 3450	ω' ~ 1260	Absorption bands	Weak absorption, due to C=O group. Pressures 1–150 mm, ab- sorption paths to 1 m (178). Com- plicated spectrum. Strong pairs of bands with weaker pairs inter- posed between them. At wave- lengths longer than first strong pair many sharp bands which appear to degrade to red and to have fine structure. Bands become diffuse towards shorter waves. No fluorescence observed with irra- diation of 3800–3000Å. Photo- chemical behavior studied (178). Determination of extinction co- efficients in 176. Correlation be- tween photochem. polymerization and abs. spectr. found in 179, large quantum yields.	1, 2, 175, 176, 178, 179, 181– 183
	below 2900		Diffuse absorp- tion, becoming continuous		
	below 1330		Continuous ab- sorption with some narrow dif- fuse bands super- imposed at longer waves with inter- vals of ~300 cm <sup>-1</sup>		
C <sub>2</sub> H <sub>7</sub> CHO <i>n</i> -butyraldehyde isobutyraldehyde	3400–2350		Continuous ab- sorption with diffuse maxima	Photochemical behavior at ordi- nary and elevated temp. studied and different dissociation possi- bilities discussed.	2, 180
OHCCCHO glyoxal	5200–4200		Fluorescence bands	Sharp bands. Strongest bands in the blue-green. Excited by λ4400– 3600Å.	1, 184

Table I.—Continued.

MOLECULE	SPECTRAL REGION (Å)	FREQUENCIES ( $\text{cm}^{-1}$ )	CHARACTERISTICS OF TRANSITION	REMARKS	LIT.
$\text{CH}_3\text{COCH}_3$ acetone	6135, 5610, 5120		Fluorescence bands with fine structure	Green fluorescence of acetone radiated with $\lambda 3130$ is identical with fluorescence of diacetyl radiated with $\lambda 4358, 4047, 3650$ ; does not appear in pure acetone flowing rapidly. Lifetime of fluo- rescence in acetone nearly the same as in diacetyl (186, 194). Also chemical evidence that di- acetyl present in acetone after illumination with 3130 (187, 188). Conclusion diacetyl is emitter (186, 194).	1, 172, 173, 175, 185- 190, 199
	3330-2940	$\omega' \sim 370$ $\omega' \sim 1205$	Absorption bands	1 m absorption path, tempera- tures of $20^\circ$ and $200^\circ\text{C}$ and fairly low pressures. Bands stand out little against surrounding absorp- tion. Spectrum very complex. Frequencies of 394 and $483\text{ cm}^{-1}$ probably belong to the ground state (189). New discussion of absorption regions in vacuum ultraviolet in 199.	
$\text{CH}_3\text{COCOCH}_3$ diacetyl	6135, 5610, 5120		Fluorescence bands with fine structure	Fluorescence produced by absorp- tion within 4600-3600 region. No measurable fluorescence when ir- radiated by $\lambda 3130$ and 2537Å.	1, 173, 191- 196, 201, 230
	4600-3600, max. at about 4150		Absorption bands in longer wave- length region and cont. abs. towards shorter wave- lengths	Fluorescence spectrum independ- ent of pressure (0.1-60 mm), tem- perature ( $10^\circ$ - $100^\circ\text{C}$ ), exciting wave-length and pressure of added gases. $\text{O}_2$ and still more $\text{I}_2$ quench fluorescence strongly (191, 192). Quantum yield of fluore- scence studied (191-193). Mean life of fluorescence determined as $1.6 \times 10^{-8}$ sec., from integrated abs. coeff. lifetime of excited state found $10^{-6}$ sec. (194). Mechanism of fluorescence discussed (193- 195).	
	2000-1883 } 1745-1690 }		Absorption bands, considered as due to two excited electronic states; 0,0 band of first system probably at $50,647\text{ cm}^{-1}$	15 cm absorption path. 0.01-15 mm pressure. Bands have rela- tively sharp red edges. Structure sharpest in longest wave-length region. With increasing pressure appearance of contin. abs. at shorter wave-lengths and grad- ually extending to the red until 2000Å. Frequency difference of 1200 in first region probably cor- responds to upper state (196).	
$\text{CH}_3\text{COC}_2\text{H}_5$ methyl ethyl ketone	3200-2400		Apparently con- tinuous absorp- tion	Absorbing columns of 1 and 10 m with pressures of 3-86 mm used. At highest pressure extension of abs. from 3200 to 2400Å (197). Upon illumination with 3130Å fluorescence bands observed at about 6100, 5600 and 5100Å which are identical with diacetyl fluorescence bands (173). Di- acetyl found during photolysis of methyl ethyl ketone (188, 198). Conclusion diacetyl is emitter of fluorescence.	173, 175, 188, 197, 198



Table I.—Continued.

MOLECULE	SPECTRAL REGION (Å)	FREQUENCIES ( $\text{cm}^{-1}$ )	CHARACTERISTICS OF TRANSITION	REMARKS	LIT.
	1975–1883	$\omega' = 1281$ $\omega' = 575$ $\omega' = 220$	Absorption bands. 0,0 transition triple band at 50,634 50,675 50,728 } $\text{cm}^{-1}$	Long wave-length bands have quite sharp edges. System corresponds to acetone bands at 1960–1800Å. Superposed on bands very weak continuous absorption. 1280 frequency probably belongs to C—O valence vibration (197).	
	1725–1685		Absorption bands. 0,0 band probably at 58,110 $\text{cm}^{-1}$		
	1606–1567		Absorption bands		
	below 1550 down to 780		Continuous absorption	780Å was limit of observation.	
<i>n</i> $\text{CH}_3\text{COC}_3\text{H}_7$ methyl <i>n</i> -propyl ketone	2790		Maximum of cont. absorption	Longest wave-length absorption has been measured in liquid state.	199
	1972–1927	$\omega'_1 = 1190$ $\omega'_4 = 614$	Absorption bands. 0,0 band at 50,699 $\text{cm}^{-1}$	For this and following absorptions pressures of 0.3–2.5 mm in 10 cm cell used and 0.0025–0.5 mm in 4 m path. Applies to all 3 ketones investigated in 199.	
	1718		Absorption band	$\omega'_1$ is probably carbonyl frequency. Discussion of shifts of spectra of ketones with substitution of hydrogens of acetone.	
	1575		Absorption band		
<i>iso</i> $\text{CH}_3\text{COCH}(\text{CH}_3)_2$ methyl isopropyl ketone	2820		Maximum of cont. absorption		
	1982–1920	$\omega'_1 = 1231$ $\omega'_2 = 819$ $\omega'_4 = 388$	Absorption bands. 0,0 band at 50,460 $\text{cm}^{-1}$		
	1737 1586		Absorption band Absorption band		
$\text{C}_2\text{H}_5\text{COC}_2\text{H}_5$ diethylketone	5460–4360, maximum 5200		Broad fluorescence region with maximum	Fluorescence seems identical with that of propionaldehyde (173)	173, 199
	2780		Maximum of cont. absorption		
	1972 1580		Absorption band Absorption band		
$\text{CH}_3\text{COC}_4\text{H}_9$ methyl <i>n</i> -butyl ketone	3200–2500		Continuous absorption	1 m column. Reported extension of abs. corresponds to 40 mm pressure. No fluorescence observed. Photochemical behavior studied.	200
$\text{CH}_3\text{COCH}_2\text{COCH}_3$ acetylacetone	between 3292 and 2935, and 2690		Long wave limit, and maximum of cont. absorption	Photodissociation processes discussed.	170
$\text{CH}_2 = \text{CO}$ ketene	3850–2607		Diffuse absorption bands	1 m absorption path. 110 mm and atmos. pressure used. No fluorescence observed. Photochemical behavior studied (202).	201, 202
	below 2200		Continuous absorption		
$\text{CH}_3\text{COCl}$ acetyl chloride	2875–2725		Broad absorption bands	Frequency differences of 260 and 342 $\text{cm}^{-1}$ found.	1, 2, 203 204

Table I.—Continued.

MOLECULE	SPECTRAL REGION (Å)	FREQUENCIES (CM <sup>-1</sup> )	CHARACTERISTICS OF TRANSITION	REMARKS	LIT
	2750 and 2480, 2150		Mean long wave limit and maxima of continuous ab- sorption	1 m absorption path. Temp. used about 20°C. Long wave-length limits shift with pressure. In 204 determination of abs. coeff.	
CH <sub>2</sub> ClCOCl chloracetyl chloride	2625 and 2350, 2125		Mean long wave limit and maxima of continuous ab- sorption		
CCl <sub>3</sub> COCl trichloroacetyl chloride	2575 and 2350, 2100		Mean long wave limit and maxima of continuous ab- sorption		
C <sub>2</sub> H <sub>5</sub> COCl propionyl chloride	2700		Mean long wave limit of cont. absorption		
C <sub>3</sub> H <sub>7</sub> COCl butyryl chloride	2660		Mean long wave limit of cont. absorption		
CH <sub>2</sub> BrCOBr bromacetyl bromide	2410		Mean long wave limit of cont. absorption		
CH <sub>3</sub> COBr acetyl bromide	below 3100		Cont. absorption with slight indi- cation of a max. at ~2500Å	20 cm absorption tube, 1–70 mm pressures. No visible fluorescence excited by absorption. Photolysis studied with λ2537 and 2652 and mechanism of photodecomposi- tion discussed (205). Determina- tion of abs. coeff. in 204.	204, 205
CH <sub>3</sub> COI acetyl iodide	4000		Long wave limit of cont. absorp- tion	Determination of absorption co- efficient.	204
CH <sub>3</sub> ONO <sub>2</sub> methyl nitrate	below about 3000		Continuous ab- sorption	10–50 cm cell, 10–200 mm pres- sure. Rough qualitative deter- mination of extinction coeffi- cients. Absorption rises towards shorter wave-lengths.	1, 206
C <sub>2</sub> H <sub>5</sub> ONO <sub>2</sub> ethyl nitrate	below about 3000		Continuous ab- sorption		
CH <sub>3</sub> NO <sub>2</sub> nitromethane	below 2900		Continuous ab- sorption	10–50 cm cell. Rough qualit. de- termination of extinction coeff. From 2900 till about 2500Å weak absorption, beyond that increas- ing absorpt.	206
C <sub>2</sub> H <sub>5</sub> NO <sub>2</sub> nitroethane	below about 3000		Continuous ab- sorption with maximum at 2700 and shallow mini- mum at 2450Å	10–50 cm cell. Rough qualit. de- termination of extinction coeff. Absorption increases towards shorter wave-lengths. Indication of faint diffuse structure in longer wave-length part of spectrum found in (207). Photodecomposi- tion studied (207).	1, 206, 207
CH <sub>3</sub> ONO methyl nitrite	4000–2900 below 2900	ω' ~ 1000	Absorption bands Continuous ab- sorption	10–20 cm cell, 10–50 mm pres- sure. Broad, diffuse bands. In- tensity of continuous absorption increases towards shorter wave- lengths, and overlaps band sys- tem at higher pressures. Intensity distribution within individual bands complex. Electronic excita-	1, 206, 208, 209

Table I.—Continued.

MOLECULE	SPECTRAL REGION (Å)	FREQUENCIES (CM <sup>-1</sup> )	CHARACTERISTICS OF TRANSITION	REMARKS	LIT.
C <sub>2</sub> H <sub>5</sub> ONO ethyl nitrite	4000–3000 below 3000	ω' ~ 1000	Absorption bands Continuous absorption	tion suggested in –N=O group. Mechanism for photochemical decomposition discussed (208).	
<i>n</i> C <sub>3</sub> H <sub>7</sub> ONO <i>n</i> -propyl nitrite	4000–3100 below 3100	ω' ~ 1000	Absorption bands Continuous absorption		
<i>iso</i> CH(CH <sub>3</sub> ) <sub>2</sub> ONO iso-propyl nitrite					
<i>sec</i> C <sub>4</sub> H <sub>9</sub> ONO secondary butyl nitrite	4000–3100 below 3100	ω' ~ 1000	Absorption bands Continuous absorption	Degrade to red, have distinct head on short wave-length side.	
<i>tert</i> C(CH <sub>3</sub> ) <sub>3</sub> ONO tertiary butyl nitrite					
<i>iso</i> (CH <sub>3</sub> ) <sub>2</sub> CHCH <sub>2</sub> CH <sub>2</sub> ONO iso amyl nitrite	4000–3100 below 3100	ω' ~ 1000	Absorption bands Continuous absorption		
(CH <sub>3</sub> ) <sub>2</sub> NNO dimethyl nitrosamine	3900–3200 below 3200		Absorption bands Continuous absorption	Spectrum very similar to that of nitrites.	209
(C <sub>2</sub> H <sub>5</sub> ) <sub>2</sub> NNO diethyl nitrosamine	4000–3200 below 3200		Diffuse absorption Continuous absorption	Spectrum similar to that of dimethylnitrosamine except that first region is not clearly resolved.	209
CH <sub>3</sub> NHOCH <sub>3</sub> N methyl O methyl hydroxylamine	below about 2500		Continuous absorption		209
$\begin{array}{c} \text{H}_3\text{C} \quad \text{NO} \\ \quad \diagdown \quad \diagup \\ \quad \text{C} \\ \quad \diagup \quad \diagdown \\ \text{H}_3\text{C} \quad \text{Cl} \end{array}$ nitroschloropropane	7500–5260		Absorption bands		209
	below 2400		Continuous absorption		
CH <sub>3</sub> SCN methyl thiocyanate	2630 2240		Long wave limits of cont. absorption. First limit corresponds to 11 mm pressure in 3.5 m cell	Absorption path 1.5 m and pressures up to saturated vapor at room temp. With experiments at 32°C absorbing column of 3.5 m used. Spectra taken in gaseous state and in solutions of methyl alcohol (for latter 1 mm and 5 mm cells). At pressures given for first long wave limits, the transparent regions between both continua are completely overlapped by extension of both continua, therefore long wave limits of second absorption were taken when overlapping not yet occurred, i.e., at lower pressures than first limits. Process of photodissociation discussed.	210
C <sub>2</sub> H <sub>5</sub> SCN ethyl thiocyanate	2620 2210		Long wave limits of cont. abs. First limit corresponds to 6 mm pressure in 3.5 m cell		
CH <sub>3</sub> NCS methyl isothiocyanate	3010 2130		As above, but first limit corresponds to 19 mm pressure		

Table I.—Continued.

MOLECULE	SPECTRAL REGION (Å)	FREQUENCIES (CM <sup>-1</sup> )	CHARACTERISTICS OF TRANSITION	REMARKS	LIT
C <sub>2</sub> H <sub>5</sub> NCS ethyl isothiocyanate	2860 2120		As above, but first limit corresponds to 11 mm pressure		
CH <sub>2</sub> =CHCH <sub>2</sub> NCS allyl isothiocyanate	2820 2130		As above, but first limit corresponds to 6 mm pressure		
NH <sub>2</sub> CSNH <sub>2</sub> thiourea	between 3300 and 3000, and 2530		Long wave limit and maximum of cont. absorption	Maximum followed by a minimum at 2370Å. Photodissociation processes discussed.	170
Cl <sub>2</sub> CS thiophosgene	5712–3990	$\omega''_1 = 1148$ $\omega'_1 = 914$ $\omega''_2 = 537$ $\omega'_3 = 240$ $\omega'_5 = 400$	Absorption bands	50 and 350 cm absorption paths. Electronic excitation located in C=S bond. $\omega_1$ , $\omega_2$ and $\omega_3$ correspond to totally sym. vibrations. Following formula given: $\nu = 17374 + 914\nu'_1 - 3\nu'^2_1 + 240\nu'_2 + 400\nu'_3 - \nu'^2_3 - 1148\nu''_1 - 537\nu''_2$ . Isotopic effect of Cl was used for analysis. Brief notes, detailed paper must be awaited for confirmation of analysis.	1, 211
CH <sub>3</sub> NH <sub>2</sub> methylamine	2400–2000	$\omega'_1 = 1000$ $\omega'_2 = 650$	Absorption bands 0,0 band at 41,680 cm <sup>-1</sup>	12 cm absorption cell, 0.5–20 mm pressure (212). Frequency $\omega'_1$ associated with CH <sub>3</sub> group, $\omega'_2$ very likely associated with NH bending vibration (783 cm <sup>-1</sup> in ground state of methylamine). Bands are diffuse. Further details on p. 114.	1, 2, 212–214
CD <sub>3</sub> NH <sub>2</sub> trideuteromethylamine	2400–2100	$\omega'_1 = 870$ $\omega'_2 = 690$	0,0 band at 41,780 cm <sup>-1</sup>		
CH <sub>3</sub> ND <sub>2</sub> methyldideuteramine	2360–2100	$\omega'_1 = 1000$ $\omega'_2 = 515$	0,0 band at 42,540 cm <sup>-1</sup>		
CD <sub>3</sub> ND <sub>2</sub> trideuteromethyldideuteramine	2385–2150	$\omega'_1 = 825$ $\omega'_2 = 500$	0,0 band at 42,580 cm <sup>-1</sup>		
C <sub>2</sub> H <sub>5</sub> NH <sub>2</sub> ethylamine	2400–2160	$\omega' \sim 700$	Absorption bands	5 cm abs. tube. Bands arranged in groups with separation of 730 between first members of groups. Width of individual bands 5–8Å. Study of photodecomposition.	1, 213
CH <sub>2</sub> N <sub>2</sub> diazomethane	4710–4250		Absorption bands	20 cm SiO <sub>2</sub> tube. Pressures up to 250 mm. Bands weak and very diffuse.	215
	beyond 4200 with max. at $\sim 3950$		Continuous absorption	After max. intensity decreases till minimum at $\sim 3000$ Å. Determination of extinction coeff. Photochem. decomposition studied with $\lambda 4360$ and $3650$ Å.	
	below 2650		Continuous absorption	Intense.	
CH <sub>3</sub> N=NCH <sub>3</sub> azomethane	4060–2800 with max. at $\sim 3400$ below 2600		Continuous absorption  Continuous absorption	Determination of absorption coefficients.	216


Table I.—Continued.

MOLECULE	SPECTRAL REGION (Å)	FREQUENCIES (CM <sup>-1</sup> )	CHARACTERISTICS OF TRANSITION	REMARKS	LIT.
CH <sub>3</sub> OH methyl alcohol	1607–1565		Three absorption bands	Low pressures down to –70°C of supply bulb containing the liquid. Bands show structure. Width of individual band about 10–12Å. Correlation of wave-lengths of bands with magneto-optical dispersion formulas (217).	1, 217, 218
	1492–1445		Three absorption bands		
	below 700		Further absorption		
C <sub>2</sub> H <sub>5</sub> OH ethyl alcohol	1633–1602		Absorption bands	Extremely faint and narrow.	1, 219
	1518		Center of diffuse abs. band	Correlation of wave-lengths of bands with magneto-optical dispersion formulas (219).	
	below 700		Further absorption		
<i>n</i> C <sub>3</sub> H <sub>7</sub> OH <i>n</i> -propyl-alcohol	1565		Center of diffuse abs. band	Indication of another absorption around 1650Å.	
	below 700		Further absorption		
<i>n</i> C <sub>4</sub> H <sub>9</sub> OH <i>n</i> -butyl-alcohol	1577		Center of diffuse abs. band		
	below 700		Further absorption		
CH <sub>2</sub> =CHCH <sub>2</sub> OH allyl-alcohol	below 2070		Continuous absorption	Limit practically reached at 10 mm pressure.	155,
	1650 } 750 }		Centers of very broad, diffuse abs. bands	Correlation of wave-lengths of bands with magneto-optical dispersion formulas.	217
C <sub>2</sub> H <sub>4</sub> (OH) <sub>2</sub> ethylene glycol	below 2070		Continuous absorption	Same apparatus used as previously, for reference see 1. Probably again 100 cm absorbing layer.	155
CH <sub>2</sub> OHCH <sub>2</sub> CH <sub>2</sub> OH trimethylene glycol	below 2250		Continuous absorption	Pressures up to 5 mm.	
C <sub>3</sub> H <sub>5</sub> (OH) <sub>3</sub> glycerol	below 2120		Continuous absorption		
(C <sub>2</sub> H <sub>5</sub> ) <sub>2</sub> C(OH)CH <sub>3</sub> methyldiethyl carbinol	below 2130		Continuous absorption		
CH <sub>3</sub> SH methylmercaptan	below 2780		Continuous absorption	Pressures up to 280 mm. Absorption limit practically reached at 160 mm.	155
C <sub>2</sub> H <sub>5</sub> SH ethylmercaptan	below 2750		Continuous absorption	Pressures up to 35 mm, limit practically reached at 28 mm.	2, 155,
	below 2100		Several absorption regions	No details given (218).	218
C <sub>3</sub> H <sub>7</sub> SH <i>n</i> -propylmercaptan	below 2600		Continuous absorption	Isomer not stated.	1, 155
C <sub>4</sub> H <sub>9</sub> SH <i>n</i> butylmercaptan	below 2590		Continuous absorption	Pressures up to 40 mm, limit practically reached at 37 mm. Isomer not stated.	155
CH <sub>2</sub> ClCH <sub>2</sub> OH ethylene chlorohydrin	below 2040		Continuous absorption	Pressures up to 6 mm.	155

Table I.—Continued.

MOLECULE	SPECTRAL REGION (Å)	FREQUENCIES (cm <sup>-1</sup> )	CHARACTERISTICS OF TRANSITION	REMARKS	LIT.
CH <sub>2</sub> BrCH <sub>2</sub> OH ethylene bromohydrin	below 2140		Continuous absorption		155
CH <sub>2</sub> ICH <sub>2</sub> OH ethylene iodohydrin	below 2170		Continuous absorption	Pressures up to 4 mm. Second fainter absorption region at longer wave-lengths.	155
CH <sub>2</sub> CNCH <sub>2</sub> OH ethylene cyanohydrin	below 2140		Continuous absorption	Pressures up to 1 mm, limit practically reached at 0.4 mm.	155
CH <sub>3</sub> CCl <sub>2</sub> OH $\alpha\alpha$ dichlorohydrin	below 1990		Continuous absorption		155
Zn(C <sub>2</sub> H <sub>5</sub> ) <sub>2</sub> zinc diethyl	2450–2300  below 2800	$\omega'' = 210$ $\omega' = \begin{cases} 760 \\ 700 \end{cases}$	Absorption bands  Continuous absorption	In addition to previous results (reported in 1) new interpretation of the weaker bands introducing two more frequencies mentioned here. Electronic excitation assumed in metal –C linkages. Discussion of molecular structures, of types of vibration connected with measured frequencies and of photochemical behavior of investigated substances. This applies also to Cd and Hg alkyls.	1, 220
Cd(CH <sub>3</sub> ) <sub>2</sub> cadmium dimethyl	below 2600		Continuous absorption	Limit corresponds to higher pressures, sensitive to pressure changes.	220
Cd(C <sub>2</sub> H <sub>5</sub> ) <sub>2</sub> cadmium diethyl	2300–2100  below 3000	$\omega''_1 = 432$ $\omega'_1 = 340$ $\omega' = 635$ $\omega' = 960$	Absorption bands. 0,0 band taken at 43,573 cm <sup>-1</sup>  Continuous absorption	Diffuse bands, perhaps degraded to red. Analysis proposed similar to zinc diethyl.	220
Hg(CH <sub>3</sub> ) <sub>2</sub> mercury dimethyl	2462–2175  2150–2050  below 2550	$\omega''_1 = 504$ $\omega'_1 = 385$ $\omega' \sim 700$ $\omega'_2 \sim 1065$	Absorption bands  Absorption bands 0,0 band at 47,059 cm <sup>-1</sup>  Continuous absorption	Very weak, diffuse.  Appear at pressure 1 mm in 5 cm column. Degrade to red.  Limit corresponds to higher pressures. Photodecomposition goes evidently via radicals, see 222 and references mentioned there.	2, 220– 222
Hg(C <sub>2</sub> H <sub>5</sub> ) <sub>2</sub> mercury diethyl	2400–2100  below 2500	$\omega' = 690$	Absorption bands  Continuous absorption	Extension of bands, reported in 1, towards ultraviolet. Introduction of another frequency, 690 cm <sup>-1</sup> . Bands appear at 1–2 mm pressures.  Limit corresponds to higher pressures.	2, 220
Hg(C <sub>4</sub> H <sub>9</sub> ) <sub>2</sub> mercury dibutyl	below 2400		Continuous absorption	To observe a continuum between 2400–2000Å 50 cm length at 30 mm pressure necessary.	220
Sn(CH <sub>3</sub> ) <sub>4</sub> tin tetramethyl	below 2200		Continuous absorption	Values for long wave-length limits obtained by extrapolation from the data using pressures in general up to about 1 atmos. Applies to all long wave limits in 220.	220
O(CH <sub>3</sub> ) <sub>2</sub> dimethyl ether	below 2300		Continuous absorption	Weak.	220

Table I.—Continued.

MOLECULE	SPECTRAL REGION (Å)	FREQUENCIES (CM <sup>-1</sup> )	CHARACTERISTICS OF TRANSITION	REMARKS	LIT.
O(C <sub>2</sub> H <sub>5</sub> ) <sub>2</sub> diethyl ether	below 2300		Continuous absorption	Weak.	220
	below 2000		Several absorption regions	Details not given (218).	218
S(CH <sub>3</sub> ) <sub>2</sub> dimethyl sulfide	2300–2100		Absorption bands	Appear in 10 cm absorbing column and pressures of about 3 mm. Bands degrade to red, are diffuse. Frequency differences of 2787 and 1086 cm <sup>-1</sup> observed.	220
	below 2450		Continuous absorption	Limit corresponds to higher pressures.	
S(CH <sub>3</sub> )(C <sub>2</sub> H <sub>5</sub> ) methylethyl sulfide	2280–2140		Absorption bands	Diffuse, degraded to red. Frequency differences of 2787, 705, 311 found. Underlying continuum with maximum at about 2215Å, extends at higher pressures till 2400Å.	220
S(C <sub>2</sub> H <sub>5</sub> ) <sub>2</sub> diethyl sulfide	2290, 2278		Absorption bands with overlapping continuum	Weak bands, 1 mm pressure and 10 cm path. At higher pressures continuum extends till 2400Å.	220
	2200		Max. of narrow continuum		
	below 2100		Several absorption regions	Details not given (218).	218
CH <sub>3</sub> HgBr methyl mercury bromide	} from shortest observable wavelengths to longer waves	}	Continuous absorption	30 cm absorption path. CH <sub>3</sub> I bands observed weakly in absorption as impurity from decomposition. Upon illumination with Al arc visible fluorescence observed identical with fluorescence bands from HgBr <sub>2</sub> and HgI <sub>2</sub> . But spectral range of exciting light, temperature and intensity distribution of fluorescence bands different for methyl mercury halides and mercury halides. Photodissociation CH <sub>3</sub> HgHal + hν = CH <sub>3</sub> + HgHal.	221
CH <sub>3</sub> HgI methyl mercury iodide					
 benzoquinone	4770–4160		Absorption bands	Sharp, show structure. Appear at 85–95°C. 75 cm tube.	163
	3150–2600	} ω' ~ 450	Absorption bands	Appear at 60–70°C, less sharp than first group.	
	2450–2250		Absorption bands	Diffuse. Appear at room temperature.	
C <sub>4</sub> H <sub>4</sub> O <sub>2</sub> · C <sub>6</sub> H <sub>4</sub> (OH) <sub>2</sub> quinhydrone				Observed absorption bands are due partly to benzoquinone and partly to hydroquinone.	163

*Literature References to Appendix Tables A-I***Table A. Linear Molecules**

1. H. Sponer, *Molekülspektren und ihre Anwendung auf chemische Probleme*, Vol. I, Tables (Julius Springer, Berlin, 1935).
2. H. Sponer, *Molekülspektren und ihre Anwendung auf chemische Probleme*, Vol. II (Julius Springer, Berlin, 1936) see supplementary tables p. 480.
3. W. C. Price and D. M. Simpson, Proc. Roy. Soc. London **A169**, 501 (1938). (Vacuum absorption CO<sub>2</sub>, COS.)
4. R. S. Mulliken, J. Chem. Phys. **3**, 720 (1935). (Theory electronic structure of molecules.)
- 4a. A. G. Gaydon, Proc. Roy. Soc. London **A176**, 505 (1940). (Flame spectrum CO.)
- 4b. S. Mrozowski, Phys. Rev. **59**, 923A (1941). (Rotational analysis CO<sub>2</sub><sup>+</sup>.)
- 4c. F. Bueso-Sanllehi, Phys. Rev. **59**, 923A (1941). (Rotational analysis CO<sub>2</sub><sup>+</sup>.)
5. G. S. Forbes and J. E. Cline, J. Am. Chem. Soc. **61**, 151 (1939). (Near ultraviolet absorption and extinction coefficients COS.)
6. L. N. Liebermann, Phys. Rev. **58**, 183 (1940); **59** 106A (1941). (CS<sub>2</sub> rotational analysis.)
7. P. Kusch and F. W. Loomis, Phys. Rev. **55**, 850 (1939). (Magnetic rotation spectrum CS<sub>2</sub>.)
8. W. C. Price and D. M. Simpson, Proc. Roy. Soc. London **A165**, 272 (1938). (Vacuum absorption SO<sub>2</sub>, CS<sub>2</sub>.)
9. E. Hauptman, Acta Physica Polonica **7**, 86 (1938). (Vacuum absorption CS<sub>2</sub>.)
10. A. B. F. Duncan, J. Chem. Phys. **4**, 638 (1936). (Vacuum absorption N<sub>2</sub>O.)
11. H. Sponer and L. G. Bonner, J. Chem. Phys. **8**, 33 (1940). (Near ultraviolet continuous absorption N<sub>2</sub>O.)
12. J. Nicolle and B. Vodar, Comptes Rendus **210**, 142 (1940). (Near ultraviolet continuous absorption N<sub>2</sub>O.)
13. H. W. Thompson and N. Healey, Proc. Roy. Soc. London **A157**, 331 (1936). (Absorption and photochemistry C<sub>3</sub>O<sub>2</sub>.)
14. M. Wehrli, Helv. Phys. Acta **11**, 339 (1938). (Absorption and analysis mercuric halides.)
15. H. Sponer and E. Teller, J. Chem. Phys. **7**, 382 (1939). (Analysis HgCl<sub>2</sub>.)
16. M. Wehrli, Helv. Phys. Acta **13**, 153 (1940). (Absorption and analysis HgCl<sub>2</sub>.)
17. B. Popov, Acta Physicochim. U.R.S.S. **4**, 159 (1936). (Photodissociation PbBr<sub>2</sub>.)
18. J. Larionov, Acta Physicochim. U.R.S.S. **3**, 11 (1935). (Absorption TeCl<sub>2</sub>.)
19. M. Wehrli, Helv. Phys. Acta **9**, 208 (1936); **11** 339 (1938). (Absorption TeCl<sub>2</sub>, TeBr<sub>2</sub>.)
20. M. Kantzer, Comptes Rendus **203**, 163 (1936). (Absorption TeCl<sub>2</sub>, TeOCl<sub>2</sub>.)
21. Sho-Chow Woo, Ta-Kong Liu, T. C. Chu and Wu Chih, J. Chem. Phys. **6**, 240 (1938). (Absorption and analysis C<sub>2</sub>H<sub>2</sub>.)
22. Sho-Chow Woo and Ta-Kong Liu, J. Chem. Phys. **5**, 161, 499 (1937). (Absorption and analysis C<sub>2</sub>N<sub>2</sub>.)

23. A. Ionescu, Comptes Rendus Acad. Roum. **1**, 384 (1937). (Absorption C<sub>2</sub>N<sub>2</sub>.) Reviewed in Phys. Ber. **19**, 1539 (1938).
24. A. V. Jakovleva, Acta Physicochim. U.R.S.S. **10**, 433 (1939). (Photodissociation C<sub>2</sub>N<sub>2</sub>.)
25. A. Jakovleva, Acta Physicochim. U.R.S.S. **9**, 665 (1938). (Photodissociation ICN, BrCN.)
26. Sho-Chow Woo and T. C. Chu, J. Chem. Phys. **5**, 786 (1937). (Absorption and analysis C<sub>4</sub>H<sub>2</sub>.)

**Table B. Bent Triatomic Molecules**

27. W. C. Price, J. Chem. Phys. **4**, 147 (1936). (Vacuum absorption H<sub>2</sub>O and H<sub>2</sub>S.)
- 27a. J. J. Hopfield, Phys. Rev. **53**, 931A (1938). (Vacuum absorption H<sub>2</sub>O.)
28. R. S. Mulliken, J. Chem. Phys. **3**, 506 (1935). (Theory electronic structure of molecules.)
29. L. Bloch, E. Bloch and P. Herreng, Comptes Rendus **203**, 782 (1936). (Vacuum absorption SO<sub>2</sub> and H<sub>2</sub>S.)
30. P. Herreng, Revue d'Optique **15**, 413 (1936). (Vacuum absorption SO<sub>2</sub> and H<sub>2</sub>S.)
31. D. Radulescu and A. Cioara, Bull. Soc. Chim. Romania **19**, 21 (1937). (Common resonators, absorption NO<sub>2</sub>.)
- 31a. F. K. Dixon, J. Chem. Phys. **8**, 157 (1940). (Absorption coefficients NO<sub>2</sub>.)
32. L. Harris, G. W. King, W. L. Benedict and R. W. B. Pearse, J. Chem. Phys. **8**, 765 (1940). (Absorption NO<sub>2</sub>.)
33. L. Harris and G. W. King, J. Chem. Phys. **8**, 775 (1940). (Rotational analysis NO<sub>2</sub>.)
34. A. Ionescu, Comptes Rendus Acad. Roum. **1**, 388 (1937); J. de Phys. et le Rad. **8**, 369 (1938). (Rotational analysis NO<sub>2</sub>.)
35. C. F. Goodeve and S. Katz, Proc. Roy. Soc. London **A172**, 432 (1939). (Absorption NOCl.)
36. G. Natanson, Acta Physicochim. U.R.S.S. **11**, 521 (1939). (Absorption and photochemistry NOCl.)
37. C. M. Beeson and Ch. D. Coryell, J. Chem. Phys. **6**, 656 (1938). (Diamagnetism NOCl.)
38. N. Metropolis and H. Beutler, Phys. Rev. **57**, 1078A (1940). (Absorption SO<sub>2</sub>.)
39. N. Metropolis, Phys. Rev. **59**, 106A (1941). (Rotational analysis SO<sub>2</sub>.)
40. G. Kornfeld, Trans. Faraday Soc. **32**, 1487 (1936). (Emission SO<sub>2</sub>.)
41. Choong Shin-Piaw, Comptes Rendus **203**, 239 (1936). (Absorption SeO<sub>2</sub>, Se<sub>2</sub>, Te<sub>2</sub>.)
42. Choong Shin-Piaw, Ann. de Physique **10**, 173 (1938). (Spectra Se<sub>2</sub>, Te<sub>2</sub>, SeO, TeO, SeO<sub>2</sub>, TeO<sub>2</sub>.)
43. R. K. Asundi, M. Jan-Khan and R. Samuel, Proc. Roy. Soc. London **A157**, 28 (1936). (Absorption SeO and SeO<sub>2</sub>.)
44. Choong Shin-Piaw, Comptes Rendus **202**, 127 (1936). (Absorption TeO<sub>2</sub>, TeO.)
- 44a. J. B. Coon, Phys. Rev. **58**, 926 (1940). (Absorption and analysis ClO<sub>2</sub>.)



45. A. Tournaire-Vassy, *Comptes Rendus* **204**, 1413 (1937); **206**, 1638 (1938). (Absorption coefficients  $O_3$ .)
46. G. Déjardin, A. Arnulf and R. Falgon, *Comptes Rendus* **205**, 1086 (1937). (Absorption coefficients atmos.  $O_3$ .)
47. G. Janin, *Comptes Rendus* **207**, 145 (1938). (Emission  $O_3$ .)
48. Ny Tsi-Zé and Choong Shin-Piaw, *Chinese J. Phys.* **1**, 38 (1933). (Abs. coeff.  $O_3$ .)
49. G. Déjardin and A. Arnulf, *Comptes Rendus* **205**, 1000 (1937). (Absorption  $O_3$ .)
50. G. Déjardin, A. Arnulf and D. Cavissilas, *Comptes Rendus* **205**, 809 (1937). (Abs. coeff. atmos.  $O_3$ .)
51. E. Vassy, *Ann. de Physique* **8**, 679 (1937). (Temp. dependence abs. coeff.  $O_3$ .)
52. A. Jakovlewa and V. Kondratjew, *Physik. Zeits. Sowjetunion* **9**, 106 (1936). (Absorption and analysis  $O_3$ .)
53. L. Herman and R. Herman-Montagne, *Comptes Rendus* **205**, 1056 (1937). (Interpretation electronic terms  $O_3$ .)
54. R. K. Asundi, M. Karim and R. Samuel, *Proc. Phys. Soc.* **50**, 581 (1938). (Emission  $SiCl_2$ ,  $SnCl_2$ .)

#### Table C. Miscellaneous Simpler Inorganic Molecules

55. C. Robert, *Helv. Phys. Acta* **9**, 405 (1936). (Absorption  $InCl_2$ ,  $InBr_2$ .)
56. M. Wehrli and M. Wenk, *Helv. Phys. Acta* **12**, 559 (1940). (Absorption  $GaCl_2$ ,  $InCl_2$ ,  $InBr_2$ ,  $InI_2$ .)
57. M. Wehrli, *Helv. Phys. Acta* **9**, 637 (1936). (Absorption  $SeCl_2$ .)
58. M. Wehrli, *Helv. Phys. Acta* **9**, 329 (1936). (Absorption  $SeBr_2$ .)
59. E. Miescher, *Helv. Phys. Acta* **11**, 463 (1938). (Spectra of halides of iron group.)
60. S. Datta, *Sci. and Cult.* **3**, 495 (1938). (Absorption  $CoCl_2$ .)
61. J. Terrien, *Ann. de Physique* **9**, 477 (1938). (Absorption and fluorescence  $Cu_2Cl_2$ ,  $Cu_2Br_2$ ,  $Cu_2I_2$ .)
62. P. Mesnage, *Comptes Rendus* **208**, 1721 (1939). (Spectra  $MoCl_3$ ,  $MoCl_5$ .)
63. P. H. Brodersen, P. Frisch and H.-J. Schumacher, *Zeits. f. physik. Chemie* **B37**, 25 (1937). (Absorption  $F_2O_2$ .)
64. W. C. Fergusson, L. Slotin and D. W. G. Style, *Trans. Faraday Soc.* **32**, 956 (1936). (Absorption  $HClO$ ,  $H_2O_2$ .)
65. E. Fajans and C. F. Goodeve, *Trans. Faraday Soc.* **32**, 511 (1936). (Absorption  $SO_3$ .)
66. G. Kornfeld, *Trans. Faraday Soc.* **33**, 614 (1937). (Photodissociation  $SO_3$ .)
67. E. J. Jones and O. R. Wulf, *J. Chem. Phys.* **5**, 873 (1937). (Absorption  $N_2O_5$ ,  $NO_3$ .)
68. E. Warburg and G. Leithäuser, *Ann. d. Physik* **20**, 743 (1906); **23** 209, (1907). (Bands  $NO_3$ .)
69. H.-J. Schumacher and G. Sprenger, *Zeits. f. angew. Chemie* **42**, 697 (1929); G. Sprenger, *Zeits. f. Elektrochem.* **37**, 674 (1931). (Kinetics and extinction coeff.  $NO_3$ .)

70. A. F. Klemenc and W. Neumann, *Zeits. f. anorg. u. allgem. Chemie* **232**, 216 (1937). (Formation of  $NO_3$  in discharge.)

71. M. Israrul Haq and R. Samuel, *Proc. Ind. Acad. Sci.* **5**, 423 (1937). (Absorption  $P_4Se_{10}$ .)
72. M. Kantzer, *Comptes Rendus* **202**, 209 (1936). (Absorption  $Cl_2O_3$ .)
73. C. F. Goodeve and F. D. Richardson, *Trans. Faraday Soc.* **33**, 453 (1937). (Absorption  $ClO_3$ ,  $Cl_2O_6$ .)
74. C. F. Goodeve and B. A. M. Windsor, *Trans. Faraday Soc.* **32**, 1518 (1936). (Absorption  $Cl_2O_7$ .)
75. E. H. Melvin and O. R. Wulf, *Phys. Rev.* **38**, 2294 (1931); *J. Chem. Phys.* **3**, 755 (1935). (Absorption  $HNO_2$ .)
76. D. M. Newitt and L. E. Outridge, *J. Chem. Phys.* **6**, 752 (1938). (Absorption  $HNO_2$ .)
77. H. W. Thompson, *J. Chem. Phys.* **7**, 136 (1939). (Absorption  $HNO_2$ .)
78. M. Israrul Haq and R. Samuel, *Proc. Ind. Acad. Sci.* **3**, 487 (1936). (Absorption inorganic nitrates and sulphates.)

#### Table D. Pyramidal and Tetrahedral Molecules

79. A. B. F. Duncan and G. R. Harrison, *Phys. Rev.* **49**, 211 (1936). (Vacuum absorption and rotational analysis  $NH_3$ .)
80. A. B. F. Duncan, *Phys. Rev.* **50**, 700 (1936). (Vacuum absorption  $ND_3$ ,  $ND_2H$ ,  $NDH_2$ .)
81. W. S. Benedict, *Phys. Rev.* **47**, 641A (1936). (Vacuum absorption deuterio-ammonias.)
82. M. Jan-Kkan and R. Samuel, *Proc. Phys. Soc.* **48**, 626 (1936). (Absorption  $PCl_3$ ,  $PBr_3$ ,  $PCl_5$ ,  $PBr_5$ ,  $POCl_3$ ,  $P_4O_{10}$ ,  $AsCl_3$ ,  $SbCl_3$ ,  $SbOCl_3$ ,  $BiCl_3$ .)
83. M. Rouault, *Comptes Rendus* **207**, 620 (1936). (Electron diffraction  $PCl_5$ .)
84. S. L. Hussain and R. Samuel, *Proc. Phys. Soc.* **49**, 679 (1937). (Absorption  $SOBr_2$ ,  $S_2O_5Cl_2$ ,  $SeCl_4$ ,  $SeOCl_2$ ,  $Se_2Cl_2$ ,  $SeBr_4$ ,  $Se_2Br_2$ ,  $TeCl_2$ ,  $TeCl_4$ ,  $TeBr_4$ .)
85. D. P. Stevenson and R. A. Cooley, *J. Am. Chem. Soc.* **62**, 2477 (1940). (Electron diffraction  $SOBr_2$ .)
86. K. J. Palmer, *J. Am. Chem. Soc.* **60**, 2360 (1938). (Electron diffraction of some sulfur, vanadium and chromium compounds.)
87. W. Groth, *Zeits. f. physik. Chemie* **B38**, 366 (1938). (Photodissociation  $CH_4$ .)
88. P. A. Leighton and A. B. Steiner, *J. Am. Chem. Soc.* **58**, 1823 (1936). (Photodissociation  $CH_4$ .)
89. H. J. Emeléus and K. Stewart, *Trans. Faraday Soc.* **32** 1577 (1936). (Absorption  $SiH_4$ ,  $Si_2H_6$ ,  $Si_3H_8$ .)
90. R. K. Asundi and S. M. Karim, *Proc. Ind. Acad. Sci.* **6**, 328 (1937). (Emission  $CCl_4$ .)
91. Y. P. Parti and R. Samuel, *Proc. Phys. Soc.* **49**, 568 (1937). (Absorption carbon and tin halides.)
92. R. K. Asundi and S. M. Karim, *Proc. Ind. Acad. Sci.* **6**, 281 (1937). (Emission  $SiBr_4$ .)
93. A. V. Banov, *Acta Physicochim. U. R. S. S.* **2**, 733 (1935). (Absorption  $SnI_4$ .)
94. D. P. Stevenson and V. Schomaker, *J. Am. Chem. Soc.* **62**, 1267 (1940). (Electron diffraction  $TeCl_4$ .)
95. B. Qviller, Tidssky. Kjemi og Bergvesen **17**, 127 (1937). (Absorption  $RuO_4$ .)

96. S. Je. Krassikow, A. N. Filippow and J. J. Tchern-jajew, *Iswestija Ssektora Platiny i drugih blagorodnyh Platiny* (French title: *Ann. Secteur Platine Mét. préc.*) **13**, 19 (1936). (Absorption  $\text{RuO}_4$ .) Reviewed in *Phys. Ber.* **19**, 453 (1938.)

97. K. Faltings, *Zeits. f. Elektrochem.* **45**, 647 (1939). (Photochemistry  $\text{C}_2\text{H}_6$  in vacuum region.)

98. E. Blum and G. Herzberg, *J. Phys. Chem.* **41**, 91 (1937). (Absorption  $\text{B}_2\text{H}_6$ .)

#### Table E. Hydrocarbons

99. W. C. Price and W. T. Tutte, *Proc. Roy. Soc. London* **A174**, 207 (1940). (Vacuum absorption  $\text{C}_2\text{H}_4$ ,  $\text{C}_2\text{D}_4$ ,  $\text{C}_2\text{H}_3\text{D}$  and alkyl-substituted ethylenes.)

100. R. S. Mulliken, *J. Chem. Phys.* **3**, 517 (1935); **7**, 20, (1939). (Theory electronic spectra polyatomic molecules.)

101. R. D. McDonald and R. G. W. Norrish, *Proc. Roy. Soc. London* **A157**, 480 (1936). (Photochemistry of  $\text{C}_2\text{H}_4$  in vacuum ultraviolet.)

102. A. A. Ashdown, L. Harris and R. T. Armstrong, *J. Am. Chem. Soc.* **58**, 850 (1936). (Absorption propylene, cyclopropane.)

103. E. P. Carr and H. Stücklen, *J. Chem. Phys.* **4**, 760 (1936). (Vacuum absorption alkyl-substituted ethylenes.)

104. G. B. Kistiakowsky, J. R. Ruhoff, H. A. Smith and W. E. Vaughan, *J. Am. Chem. Soc.* **58**, 137 (1936). (Hydrogenation higher olefins.)

105. E. P. Carr and H. Stücklen, *J. Am. Chem. Soc.* **59**, 2138 (1937). (Vacuum absorption butene and pentene.)

106. E. P. Carr and M. K. Walker, *J. Chem. Phys.* **4**, 751, (1936). (Vacuum absorption heptene and tetramethylethylene.)

107. C. P. Snow and C. B. Allsopp, *Trans. Faraday Soc.* **30**, 93 (1934). (Absorption trimethylethylene and cyclohexene.)

108. E. P. Carr and H. Stücklen, *J. Chem. Phys.* **6**, 55 (1938). (Vacuum absorption unsaturated cyclic hydrocarbons.)

109. L. W. Pickett, E. Paddock and E. Sackter, *J. Am. Chem. Soc.* **63**, 1073 (1941).

110. J. Stark, W. Steubing, C. J. Enklaar and P. Lipp, *Jahrbuch d. Rad. u. Elektronik* **10**, 158 (1913); J. Stark and P. Levy, *ibid.* **10**, 179 (1913). (Absorption hydrocarbons.)

111. V. Henri and L. W. Pickett, *J. Chem. Phys.* **7**, 439 (1939). (Absorption 1,3 cyclohexadiene.)

112. R. S. Mulliken, *J. Chem. Phys.* **7**, 339 (1939). (Intensities of electronic transitions in molecular spectra, cyclic dienes.)

113. R. S. Mulliken, C. A. Rieke and W. G. Brown, *J. Am. Chem. Soc.* **65**, 41 (1941). (Hyperconjugation.)

114. W. C. Price and A. D. Walsh, *Proc. Roy. Soc. London* **A174**, 220 (1940). (Vacuum absorption conjugated dienes.)

115. R. S. Mulliken, *J. Chem. Phys.* **7**, 121 (1939). (Intensities of electronic transitions in molecular spectra, conjugated dienes.)

116. E. Hückel, *Zeits. f. Electrochem.* **43**, 752 (1937). (Theory unsaturated and aromatic compounds.)

117. J. E. Lennard-Jones, *Proc. Roy. Soc. London* **A158**, 280 (1937). (Electronic structure of some polyenes and aromatic molecules.)

#### Table F. Halogen Derivatives of Hydrocarbons

118. W. C. Price, *J. Chem. Phys.* **4**, 539 (1936). (Vacuum absorption methyl halides.)

119. R. S. Mulliken, *Phys. Rev.* **47**, 413 (1935). (Theory electronic structure alkyl halides.)

120. P. Fink and C. F. Goodeve, *Proc. Roy. Soc. London* **A163**, 592 (1937). (Continuous absorption  $\text{CH}_3\text{Br}$ .)

121. D. Porret and C. F. Goodeve, *Proc. Roy. Soc. London* **A165**, 31 (1938). (Continuous absorption alkyl iodides and alkyl bromides.)

122. D. Porret and C. F. Goodeve, *Trans. Faraday Soc.* **33**, 690 (1937). (Continuous absorption  $\text{CH}_3\text{I}$ .)

123. W. C. Price, *J. Chem. Phys.* **4**, 547 (1936). (Vacuum absorption alkyl halides.)

124. A. Henrici and G. Milazzo, *Zeits. f. physik. Chemie* **B33**, 201 (1936). (Temperature dependence of absorption of  $\text{C}_2\text{H}_5\text{I}$ .)

125. G. Milazzo, *Zeits. f. physik. Chemie* **B33**, 109 (1936). (Absorption alkyl iodides.)

126. G. Milazzo, *Gazz. Chim. Ital.* **68**, 747 (1938). (Absorption alkyl iodides.)

127. G. Milazzo, *Gazz. Chim. Ital.* **68**, 763 (1938). (Absorption alkyl iodides.)

#### Table G. Aromatic Molecules

128. G. R. Cuthbertson and G. B. Kistiakowsky, *J. Chem. Phys.* **4**, 9 (1936). (Fluorescence benzene.)

129. C. K. Ingold and C. L. Wilson, *J. Chem. Soc.* 941, 955 (1936). (Fluorescence and resonance emission,  $\text{C}_6\text{H}_6$  and  $\text{C}_6\text{D}_6$ .)

130. C. L. Wilson, *J. Chem. Soc.* 1210 (1936). (Fluorescence  $\text{C}_6\text{H}_6$  and  $\text{C}_6\text{D}_6$ .)

131. G. B. Kistiakowsky and A. K. Solomon, *J. Chem. Phys.* **5**, 609 (1937). (Absorption and temperature dependence benzene.)

132. A. Ionescu, *Compt. Rend. Acad. Roum.* **2**, 39 (1937). (Temperature dependence benzene.)

133. M. Aubert and T. D. Georghiu, *Ann. Office Nat. Combustibles Liquides* **30**, 473 (1938). (Temperature dependence benzene.) Reviewed in *Phys. Ber.* **20**, 1086 (1939).

134. W. F. Radle and C. A. Beck, *J. Chem. Phys.* **8**, 507 (1940). (Absorption and temperature dependence benzene.)

135. E. B. Wilson, *Phys. Rev.* **45**, 706 (1934). (Symmetries of benzene vibrations.)

136. C. K. Ingold and collaborators, *J. Chem. Soc.* 971 (1936). (Assignment of  $\text{C}_6\text{H}_6$  and  $\text{C}_6\text{D}_6$  vibrations.)

137. A. Langseth and R. C. Lord, *Det Kgl. Danske Videnskab. Selsk. Math.-fys. Medd.* **16**, No. 6 (1938). (Assignment of  $\text{C}_6\text{H}_6$  and  $\text{C}_6\text{D}_6$  vibrations.)

138. H. Sponer, G. Nordheim, A. L. Sklar and E. Teller, *J. Chem. Phys.* **7**, 207 (1939). (Analysis near ultraviolet benzene spectrum.)

139. A. L. Sklar, *J. Chem. Phys.* **5**, 669 (1937). (Theory electronic transition benzene.)
140. E. Hückel, *Zeits. f. Physik*, **70**, 204 (1931); *Zeits. f. Electrochem.* **43**, 752 (1937). (Theory electronic structure benzene.)
141. L. Pauling and A. Sherman, *J. Chem. Phys.* **1**, 606 679 (1933). (Theory electronic structures.)
142. G. I. Krassina, *Acta Physicochim. U.R.S.S.* **10**, 189 (1939). (Photodecomposition benzene.)
143. N. A. Prileshajewa, *Acta Physicochim. U.R.S.S.* **10**, 193 (1939). (Photodecomposition benzene.)
144. M. Goepfert-Mayer and A. L. Sklar, *J. Chem. Phys.* **6**, 645 (1938). (Theory of electronic levels benzene.)
145. G. Nordheim, H. Sponer and E. Teller, *J. Chem. Phys.* **8**, 455 (1940). (Interpretation of far ultraviolet absorption systems benzene.)
146. H. Sponer, *J. Chem. Phys.* **8**, 705 (1940). (Analysis near ultraviolet spectrum  $C_6D_6$ .)
147. H. Sponer and S. H. Wollman, *Phys. Rev.* **57**, 1078A (1940) and unpublished results. (Absorption spectrum and analysis  $C_6H_5Cl$ .)
148. K. Masaki, *Bull. Chem. Soc. Japan* **11**, 346 (1936). (Assignment of vibrational frequencies from ultraviolet absorption in monosubstituted benzenes.)
149. S. Kato and F. Someno, *Sci. Pap. Inst. Phys. Chem. Research Tokyo* **34**, 905 (1938). (Absorption phenol and derivatives.)
150. S. Kato and F. Someno, *Sci. Pap. Inst. Phys. Chem. Research Tokyo* **33**, 209 (1937). (Absorption aniline.)
151. A. Terenin, A. Vartanian and B. Neporent, *Trans. Faraday Soc.* **35**, 39 (1939). (Fluorescence of aniline and quenching of fluorescence.)
152. A. T. Vartanian, *Russian J. Phys. Chem.* **12**, 308 (1938). (Quenching of aniline fluorescence.)
153. A. Vartanian, *J. Phys. U.S.S.R.* **1**, 213 (1939). (Fluorescence aniline.)
154. N. Prileshajewa and A. Klimowa, *Acta Physicochim. U.R.S.S.* **7**, 163 (1937). (Sensitized fluorescence in aniline-benzene mixture.)
155. Y. Hukamoto, *Sci. Rep. Tôhoku Imp. Univ.* **25**, 1162 (1936). (Continuous absorption polyatomic molecules.)
156. S. Kato and F. Someno, *Sci. Pap. Inst. Phys. Chem. Res. Tokyo* **34**, 912 (1938). (Absorption derivatives of organic acids.)
157. H. Tintea, *Bull. Sect. Sci. Acad. Roum.* **21**, 219 (1939); **22**, 16 (1939). (Absorption monohalides of toluene.)
158. M. Shin-Piaw, *Comptes Rendus* **208**, 1563 (1939). (Absorption salicylic acid and lithium salicylate.)
159. P. K. Seshan, *Proc. Ind. Acad. Sci.* **3**, 148 (1936). (Absorption aromatic compounds in different states of aggregation.)
- 159a. N. Prileshajewa and R. Tschubarow, *Acta physicochim. U.R.S.S.* **1**, 777 (1935). (Fluorescence and absorption aromatic amines.)
160. A. S. Shishlovsky, *Comptes Rendus Acad. Sci. Moscow* **15**, 29 (1937). (Absorption and fluorescence of anthracene in different states of aggregation.) Reviewed in *Phys. Ber.* **18**, 2526 (1937).
161. R. Titeica, *Ann. Office Nat. Combust. Liquides* **11**, 445 (1936); *Bull. Soc. Roum. Phys.* **37**, No. 66, (1936). (Spectroscopy aromatic hydrocarbons.) Reviewed in *Chem. Abs.* **30**, 6644 (1936) and *Phys. Ber.* **18**, 454 (1937).
162. B. Twarowska, *Zeits. f. Physik* **109**, 403 (1938). (Fluorescence and absorption fluorene in different states of aggregation.)
163. P. K. Seshan, *Proc. Ind. Acad. Sci.* **3**, 172 (1936). (Absorption quinones.)

### Table H. Heterocyclic Molecules

164. V. Henri and P. Angenot, *J. chim. Phys.* **33**, 641 (1936). (Absorption and analysis pyridine.)
165. J. E. Purvis, *J. Chem. Soc.* **97**, 1648 (1910). (Absorption heterocyclic compounds.)
166. O. V. Fialkowskaja, *Acta Physicochim. U.R.S.S.* **9**, 215 (1938). (Absorption and fluorescence heterocyclic compounds.)
167. L. W. Pickett, *J. Chem. Phys.* **8**, 293 (1940). (Absorption furan.)
168. J. Godart, *J. chim. Phys.* **34**, 70 (1937). (Absorption thiophene.)

### Table I. Miscellaneous Organic Molecules

169. W. C. Price and W. M. Evans, *Proc. Roy. Soc. London*. **A162**, 110 (1937). (Vacuum absorption  $HCOOH$ .)
170. E. Bergmann and R. Samuel, *J. Org. Chem.* **6**, 1 (1941). (Photodissociation organic molecules.)
171. R. G. W. Norrish and W. A. Noyes, *Proc. Roy. Soc. London* **A163**, 221 (1937). (Photodecomposition  $CH_2O$ .)
172. E. Gorin, *Acta Physicochim. U.R.S.S.* **8**, 513 (1938). (Photodecomposition aldehydes and ketones.)
173. M. S. Matheson and J. W. Zabor, *J. Chem. Phys.* **7**, 536 (1937). (Fluorescence carbonyl compounds.)
174. E. Gorin, *Acta Physicochim. U.R.S.S.* **9**, 681 (1938). (Photolysis acetaldehyde.)
175. *Photochemistry and the Mechanism of Chemical Reactions*, by G. K. Rollefson and M. Burton (Prentice-Hall, Inc., New York, 1939).
176. F. E. Blacet, W. G. Young and J. G. Roof, *J. Am. Chem. Soc.* **59**, 608 (1937). (Absorption crotonaldehyde and acrolein.)
177. F. E. Blacet and J. E. Lu Valle, *J. Am. Chem. Soc.* **61**, 273 (1939). (Photolysis crotonaldehyde.)
178. H. W. Thompson and J. W. Linnett, *J. Chem. Soc.* 1452 (1935). (Absorption, fluorescence, photodecomposition acrolein.)
179. F. E. Blacet, G. H. Fielding and J. G. Roof, *J. Am. Chem. Soc.* **59**, 2375 (1937). (Photolysis acrolein.)
180. Ph. A. Leighton, L. D. Levanas, F. E. Blacet and R. D. Rowe, *J. Am. Chem. Soc.* **59**, 1843 (1937). (Photolysis *n*- and isobutyraldehyde.)
181. H. L. McMurry and R. S. Mulliken, *Proc. Nat. Acad. Sci.* **26**, 312 (1940). (Theory spectra of aldehydes and ketones.)
182. H. L. McMurry, *J. Chem. Phys.* **9**, 231 (1941). (Theory spectra saturated aldehydes and ketones.)

183. H. L. McMurtry, *J. Chem. Phys.* **9**, 241 (1941). (Theory spectra conjugated aldehydes and ketones.)
184. H. W. Thompson, *J. Chem. Phys.* **7**, 855 (1939). (Fluorescence glyoxal.)
185. R. Padmanabhan, *Proc. Ind. Acad. Sci.* **A5**, 594 (1937). (Fluorescence acetone and methyl ethyl ketone.)
186. M. S. Matheson and W. A. Noyes, *J. Am. Chem. Soc.* **60**, 1857 (1938). (Fluorescence acetone.)
187. R. Spence and W. Wild, *J. Chem. Soc.* 352 (1937). (Photodecomposition acetone.)
188. M. Barak and D. G. W. Style, *Nature* **135**, 307 (1935). (Stability acetyl radical.)
189. W. A. Noyes, *Trans. Faraday Soc.* **33**, 1495 (1937). (Absorption acetone.)
190. J. P. Howe and W. A. Noyes, *J. Am. Chem. Soc.* **58**, 1404 (1936). (Photodecomposition acetone.)
191. G. M. Almy, H. Q. Fuller and G. D. Kinzer, *J. Chem. Phys.* **8**, 37 (1940). (Fluorescence diacetyl.)
192. H. Q. Fuller, L. W. Phillips and G. M. Almy, *J. Chem. Phys.* **7**, 973 (1939). (Fluorescence diacetyl.)
193. F. C. Henriques and W. A. Noyes, *J. Am. Chem. Soc.* **62**, 1038 (1940). (Fluorescence diacetyl.)
194. G. M. Almy and S. Anderson, *J. Chem. Phys.* **8**, 805 (1940). (Lifetime fluorescence diacetyl and acetone.)
195. W. A. Noyes and F. C. Henriques, *J. Chem. Phys.* **7**, 767 (1939). (Fluorescence and photochemical kinetics of polyatomic molecules.)
196. V. R. Ells, *J. Am. Chem. Soc.* **60**, 1864 (1938). (Absorption diacetyl.)
197. A. B. F. Duncan, V. R. Ells and W. A. Noyes, *J. Am. Chem. Soc.* **58**, 1454 (1936). (Absorption methyl-ethylketone.)
198. V. R. Ells and W. A. Noyes, *J. Am. Chem. Soc.* **60**, 2031 (1938). (Photodecomposition methylethylketone at 2000–1850 Å.)
199. A. B. F. Duncan, *J. Chem. Phys.* **8**, 444 (1940). (Vacuum absorption aliphatic ketones.)
200. B. M. Bloch and R. G. W. Norrish, *J. Chem. Soc.* 1638 (1935). (Absorption and photolysis methyl *n*-butyl ketone.)
201. G. C. Lardy, *J. chim. Phys.* **21**, 353 (1924). (Absorption ketene, diacetyl.)
202. R. G. W. Norrish, H. G. Crone, and O. D. Saltmarsh, *J. Chem. Soc.* 1533 (1933); *J. Am. Chem. Soc.* **56**, 1644 (1934). (Absorption and photochemistry ketene.)
203. St. Vencov, *Comptes Rendus* **208**, 801 (1939). (Absorption organic molecules.)
204. D. H. Etzler and G. K. Rollefson, *J. Chem. Phys.* **6**, 653 (1938). (Absorption coefficients acetyl halides.)
205. D. H. Etzler and G. K. Rollefson, *J. Am. Chem. Soc.* **61**, 800 (1939). (Photolysis acetylbromide.)
206. H. W. Thompson and C. H. Purkis, *Trans. Faraday Soc.* **32**, 674 (1936). (Absorption nitrates, nitrites and nitro-compounds.)
207. E. Hirschlaff and R. G. W. Norrish, *J. Chem. Soc.* 1580 (1936). (Photodecomposition nitromethane and nitroethane.)
208. H. W. Thompson and F. S. Dainton, *Trans. Faraday Soc.* **33**, 1546 (1937). (Photochemistry alkyl nitrites.)
209. H. W. Thompson and C. H. Purkis, *Trans. Faraday Soc.* **32**, 1466 (1936). (Photochemistry nitrates, nitrites and nitro-compounds.)
210. Sho-Chow Woo and T. C. Chu, *J. Chinese Chem. Soc.* **5**, 162 (1937). (Absorption alkyl thiocyanates.)
211. V. Henri and J. Duchesne, *Nature* **143**, 28 (1939); *Bull. Soc. Roy. Sci. Liège* **8**, 19 (1939). (Absorption thiophosgene.)
212. Th. Förster and J. C. Jungers, *Zeits. f. physik. Chemie* **B36**, 387 (1937). (Absorption deuterio-substituted methylamines.)
213. H. J. Emeléus and L. J. Jolley, *J. Chem. Soc.* 1612 (1935). (Absorption methyl- and ethylamine.)
214. H. J. Emeléus and H. V. A. Briscoe, *J. Chem. Soc.* 127 (1937). (Absorption  $\text{CH}_3\text{ND}_2$ .)
215. F. W. Kirkbride and R. G. W. Norrish, *J. Chem. Soc.* 119 (1933). (Absorption and photodecomposition diazomethane.)
216. H. C. Ramsperger, *J. Am. Chem. Soc.* **50**, 123 (1928). (Absorption and photodecomposition azomethane.)
217. W. J. G. Beynon and E. J. Evans, *Phil. Mag.* **25**, 376 (1938). (Vacuum absorption methyl and allyl alcohols in relation to magneto-optical dispersion.)
218. W. C. Price, *J. Chem. Phys.* **3**, 256 (1935). (Vacuum absorption alkyl derivatives of  $\text{H}_2\text{O}$  and  $\text{H}_2\text{S}$ .)
219. W. J. G. Beynon, *Phil. Mag.* **25**, 443 (1928). (Vacuum absorption alkyl alcohols in relation to magneto-optical dispersion.)
220. H. W. Thompson and J. W. Linnett, *Proc. Roy. Soc. London* **A156**, 108 (1936). (Absorption and photochemistry metal alkyls.)
221. A. Terenin and N. Prileshajewa, *Acta Physicochim. U.R.S.S.* **1**, 759 (1935). (Photodissociation organo-metallic compounds.)
222. J. P. Cunningham and H. S. Taylor, *J. Chem. Phys.* **6**, 359 (1938). (Decomposition mercury dimethyl.)

#### References Added in Proof

223. W. C. Price and D. M. Simpson, *Trans. Faraday Soc.* **37**, 106 (1941). (Vacuum absorption  $\text{NO}_2$ ,  $\text{O}_3$  and  $\text{NOCl}$ .)
224. N. Metropolis, *Phys. Rev.* **59**, 923A (1941). (Vibrational analysis absorption  $\text{SO}_2$ .)
225. J. M. Tolmatschew, *Russian J. phys. Chem.* **14**, 10 (1940). (Absorption  $\text{N}_3\text{H}$ .)
226. K. Asagoe and Y. Ikemoto, *Proc. Phys.-Math. Soc. Japan* **22**, 677, 864 (1940). (Absorption and analysis monochlorobenzene.)
227. K. Asagoe and Y. Ikemoto, *Proc. Phys.-Math. Soc. Japan* **22**, 685, 864 (1940). (Absorption and analysis monobromobenzene.)
228. G. A. Dima and H. Tintea, *Bull. Sect. Sci. Acad. Roum.* **23**, 34 (1940). (Absorption dihalogen derivatives of benzene.)
229. F. M. Uber and R. Winters, *J. Am. Chem. Soc.* **63**, 137 (1941). (Absorption chloropyrimidines.)
230. J. G. Roof and F. E. Blacet, *J. Am. Chem. Soc.* **63**, 1123 (1941). (Photolysis diacetyl near ultraviolet.)
231. I. Walerstein, *Phys. Rev.* **59**, 924A (1941). (Absorption monobromobenzene.)

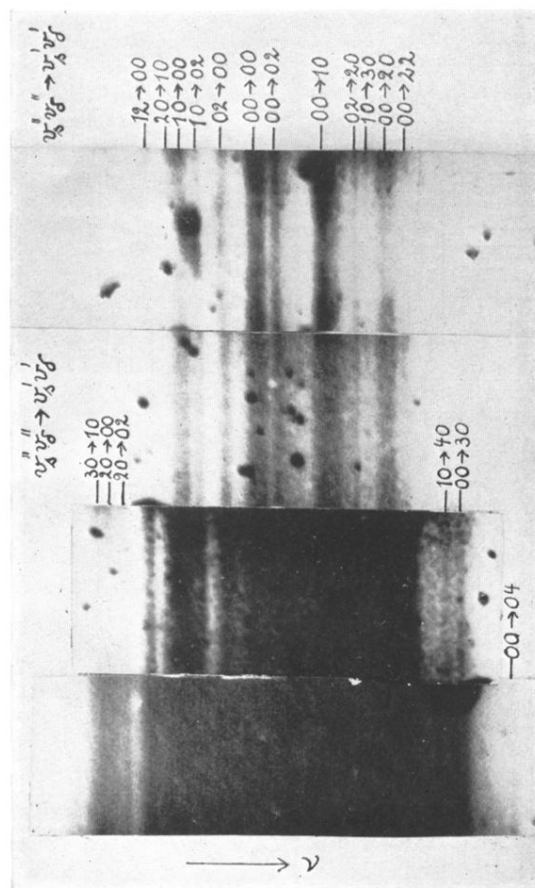
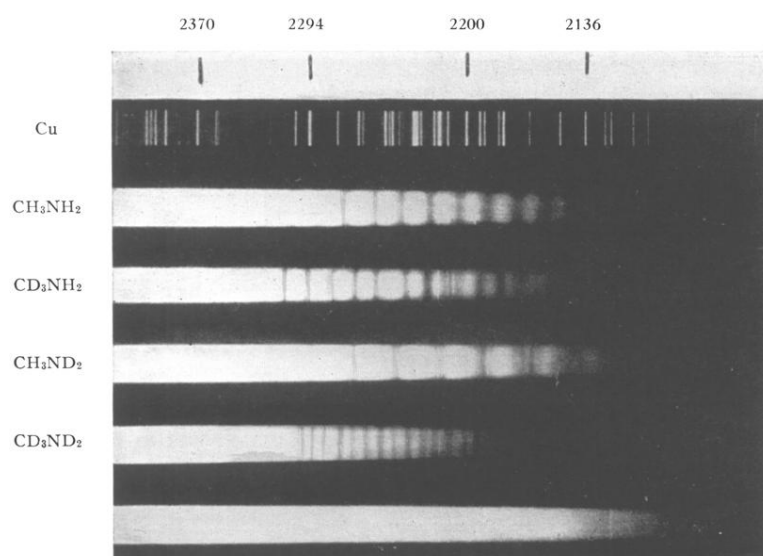


FIG. 10. Absorption spectrum of  $\text{HgBr}_2$  and analysis.



(FIG. 13. Absorption spectrum of  $\text{CH}_3\text{NH}_2$  and deuterated molecules. (Taken from Th. Förster and J. C. Jungers, Zeits. f. physik. Chemie **B36**, 390 (1937).)

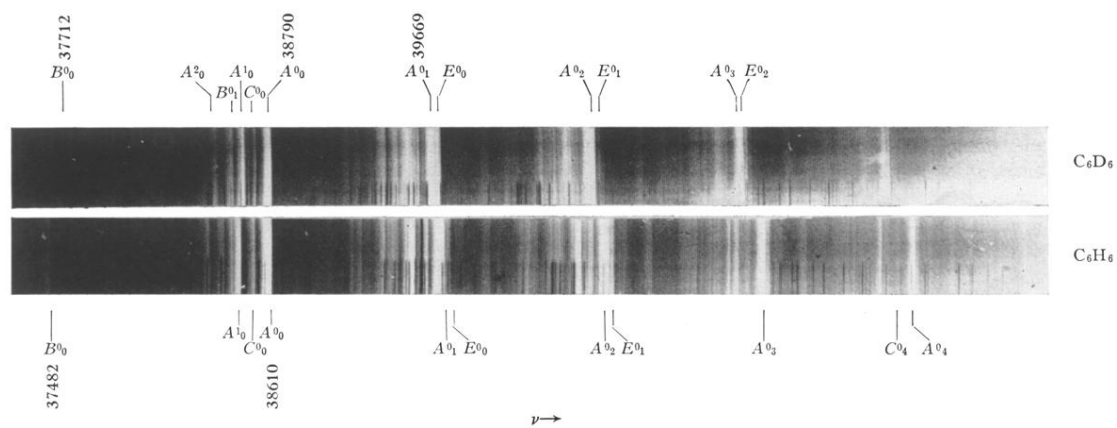


FIG. 14. Absorption spectra of  $C_6H_6$  and  $C_6D_6$ .  
(Taken from H. Sponer, J. Chem. Phys. **8**, 705 (1940).)

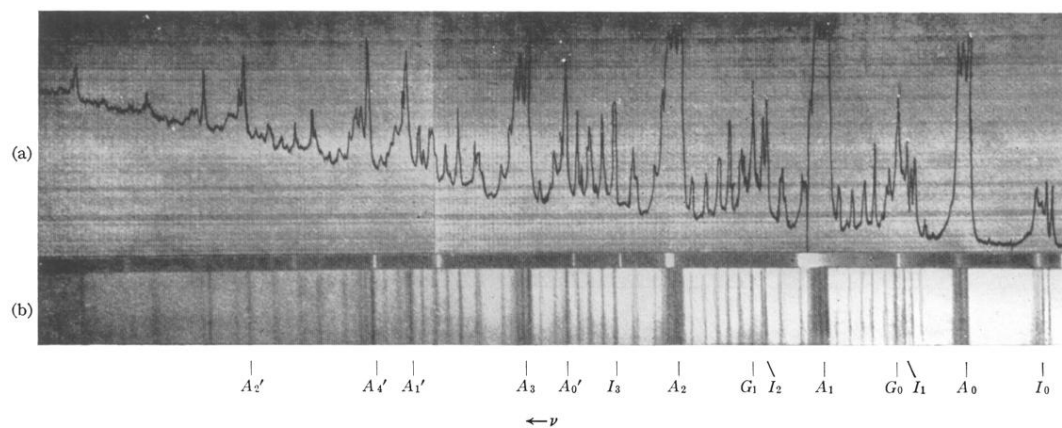


FIG. 15. Absorption spectrum of solid benzene at  $-259^\circ\text{C}$ .  
(Taken from A. Kronenberger, *Zeits. f. Physik* **63**, 497 (1930).)



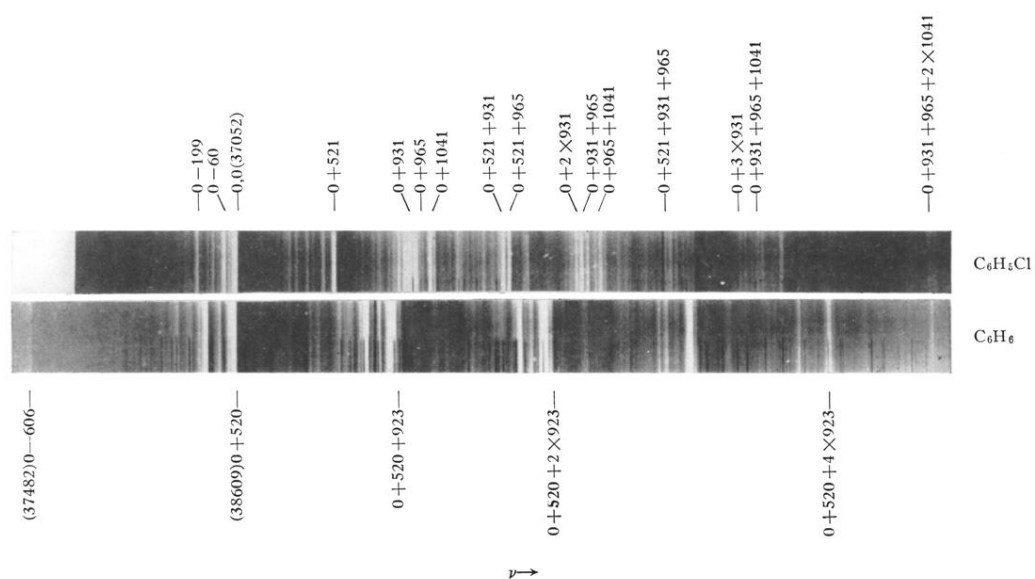


FIG. 16. Absorption spectra of  $C_6H_5Cl$  and  $C_6H_6$

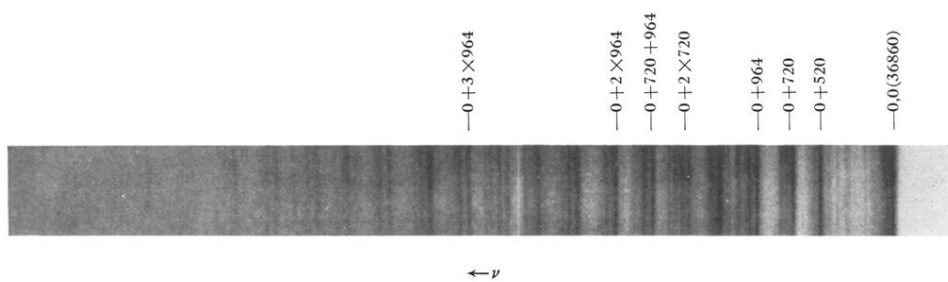


FIG. 17. Absorption spectrum of  $\text{C}_6\text{H}_5\text{Cl}$  at  $-259^\circ\text{C}$ .  
 (Taken from A. Kronenberger, *Zeits. f. Physik* **63**, 512 (1930).)

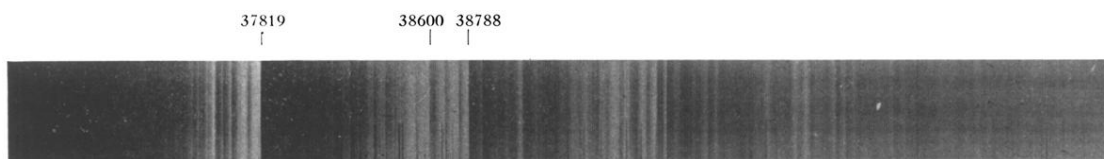


FIG. 19. Absorption spectrum of C<sub>6</sub>H<sub>5</sub>F.

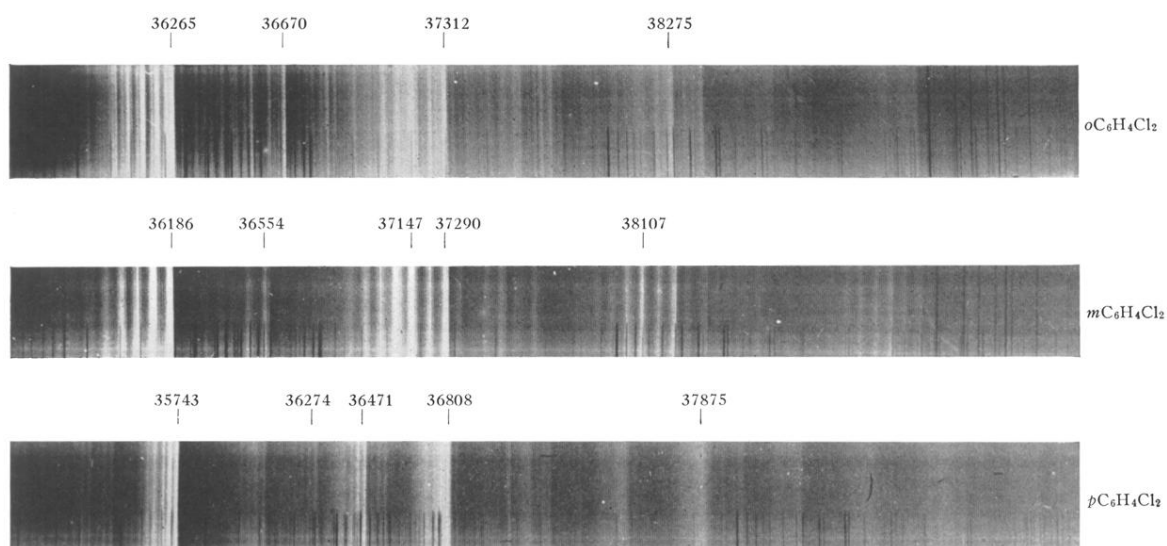


FIG. 20. Absorption spectra of dichlorobenzenes.

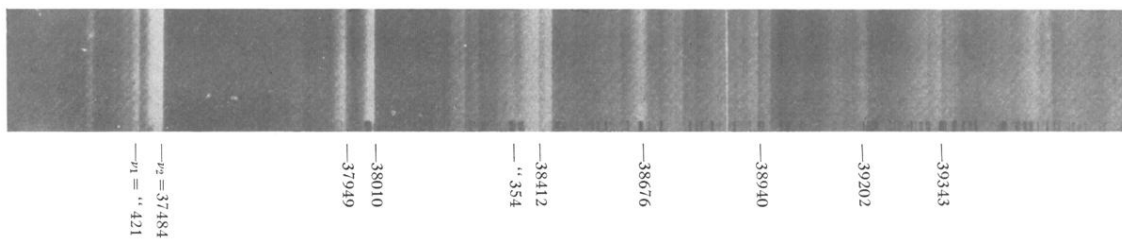


FIG. 21. Absorption spectrum of toluene. (Taken from J. Savard, *Ann. de Chimie* **11**, 287 (1929).)



FIG. 22. Absorption spectrum of paracresole. (Taken from J. Savard, *Ann. de Chimie* **11**, 287 (1929).)

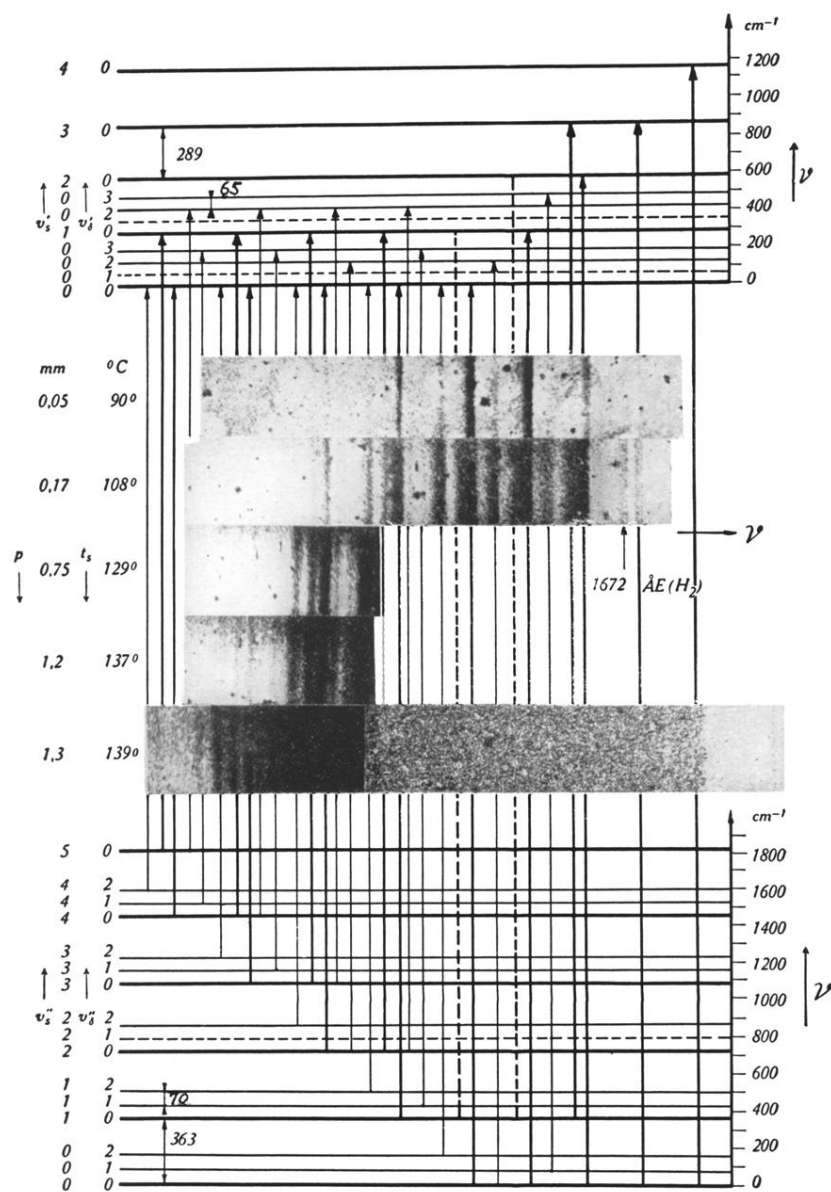


FIG. 9. Absorption spectrum of  $\text{HgCl}_2$  and analysis.